R-05-50

Studies of buffers behaviour in KBS-3H concept

Work during 2002–2004

Lennart Börgesson, Torbjörn Sandén, Billy Fälth
Mattias Åkesson, Clay Technology AB

Erik Lindgren, Svensk Kärnbränslehantering AB

August 2005

Svensk Kärnbränslehantering AB
Swedish Nuclear Fuel
and Waste Management Co
Box 5864
SE-102 40 Stockholm Sweden
Tel 08-459 84 00
+46 8 459 84 00
Fax 08-661 57 19
+46 8 661 57 19

ISSN 1402-3091
SKB Rapport R-05-50

Studies of buffers behaviour in KBS-3H concept

Work during 2002–2004

Lennart Börgesson, Torbjörn Sandén, Billy Fälth
Mattias Åkesson, Clay Technology AB

Erik Lindgren, Svensk Kärnbränslehantering AB

August 2005

Summary

The function of the buffer in the KBS-3H concept has been investigated by laboratory tests in small and full scale, by modeling and by scenario analyses. These investigations have yielded that the concept is feasible but also that there still are some critical questions that need to be further investigated.

The studies and the results and conclusions reached will be presented in this report. The report should be considered a state of the art report at the mid 2004. The studies are planned to continue during the coming years.

The following studies and conclusions have been made:

Scale test

A scale test simulating the saturation and maturation of two canister sections in scale 1:10 have been made and have showed that the interaction between the buffer and the perforated container is complicated but acceptable from a safety point. The following main observations were done:

- The bentonite had swelled through the holes of the container and between the container and the simulated rock and covered the entire gap.
- The measured swelling pressure outside the container and the measured average buffer density were in the same range as the expected without container.
- The axial hydraulic conductivity of the buffer in the gap outside the container was measured and found to be about 10^{-12} m/s, higher than expected from the density and swelling pressure measurements, but still low enough to fulfilling the demands on the buffer.
- The perforated container was expanded by the inside swelling of the buffer and ruptured at a few locations near the end parts.
- The expansion of the container is believed to be the reason for the high swelling pressure and density outside the container.
- The increased hydraulic conductivity in the gap outside the container is judged to be caused by the uneven swelling between the container and the simulated rock as shown by the theoretical calculations.

Big Bertha large scale test

A large scale test has been planned but was postponed, since the equipment was used for testing the function of the distance blocks, and is planned to be started in 2005.

Basic sealing tests

A large number of basic sealing tests have been performed in the laboratory, which revealed problems for bentonite to seal flowing water and show how vulnerable the buffer is when the water pressure is rapidly increased after sealing. The tests lead to the following observations:

- Sealing is hindered even at very low water pressure and permanent piping and erosion occurs at constant water pressure (2–4 kPa).
- Very little water flow is required to hinder sealing and to cause permanent piping and erosion (less than 0.001 l/min) when the water pressure increase rate after sealing is high.
- The processes are complicated with many variables and dependent variables.
- The length of the piping channel is one parameter that influences. The longer the better ability to seal.
- Salt in the ground water improves the possibility for the bentonite to seal but increases the erosion rate strongly.
- The values 2–4 kPa and 0.001 l/min are probably conservative since they are combined with either high water flow rate or high water pressure.
- The hydraulic function of the rock is very important

After a long time the sealing is helped from other wetting parts and is expected to tighten all leaks if the swelling pressure is higher than the water pressure. The distance plug is thus expected to function if the water flow is not so high that the erosion reduces the density but it may take a long time for it to seal. One conclusion from these tests is also that more realistic flow and pressure regulations should be used in further testing and that the complexity of included parameters calls for scenario simulations.

Reference scenario

The following reference scenario has been settled for the subsequent sealing tests in scale 1:10 and 1:1 in order to simulate natural conditions:

- A water inflow rate of 0.1 l/min per canister section.
- A rate of water pressure increase of 100 kPa/hour.

Most tests of the sealing function of the distance block were done with these refernce values but other cases were tested as well.

Tests in scale 1:10 of the function of the distance block

The complex process and geometry called for scale tests with simulation of mainly the basic scenario for further understanding of the processes and for development of the technique for making the distance block function properly. The following main conclusions were drawn from tests of the distance block in scale 1:10:

- The filling rate and the water pressure increase rate are very important for the sealing ability. With the basic inflow scenario the distance plug seems to seal in the scale 1:10 when the annular gap between the rock and the plug is 2–4 mm but not for larger gaps.
- If the distance block seals and prevents leakage the water pressure built up behind the block must be taken by the block.

- A supporting ring that captures part of the water pressure behind the distance block is required.
- The sealing of the distance block works very well for the reference case with the suggested solution.
- The sealing did not work for higher water pressure.
- The water pressure reaches 15–50 mm radially into the block at the applied scale and geometry.
- The sealing function worked well during at least 90 days although the force was doubled during the first 60 days and then remained constant.
- A gap between the container and distance block should be avoided as far as possible since it increases the force on the ring although the sealing ability works well also in radial direction if the gap is not too wide.

Full scale tests of the function of the distance block

Since some design parameters could not be properly tested in the scale 1:10 and since the effect of the scale might be important, several tests were performed in almost full scale in the test equipment designed for the Big Bertha experiment.

The conclusions of the full scale sealing tests were the following:

- The scale effects are strong.
- It is possible to seal according to the desires for the reference scenario if engineering solutions with a supporting ring and either pellets in the annular gap or a very small gap of a few mm is used.
- The measured total force caused by a high water pressure inside the distance block was not very high since the radial distance from the rock surface that the water pressure acted on was only 10–15 mm.
- The results also show that it is important to avoid a slot between the bentonite blocks and between a bentonite block and the container although a slot of 7 mm could be handled as shown in the scale tests.

Modelling

A lot of modelling work for simulation and prediction of different processes has also been performed, analytical, numerical as well as conceptual. The following modelling studies were done:

The swelling of the bentonite through and behind the perforated container has been modelled analytically. The model describes the state after full maturation. The results yielded that the optimal hole diameter is 10 cm when the present container design is used and that the loss in swelling pressure behind the container furthest away from the holes is about 60%.

The hydro-mechanical evolution of the scale test has been predicted by FE-modelling of the test. The model was simplified in the sense that the perforated container was not included. Comparison with measured results showed that the general behaviour was fairly well predicted but also that the measured wetting was considerably slower than predicted, partly due to the influence of the container and partly due to some general shortcomings in the late stage of the water saturation phase.

An imaginary KBS-3H repository has also been modelled both regarding the temperature evolution for design purpose and the saturation rate for safety assessment. The saturation modelling showed that the time until complete water saturation is about 10 years if the rock has an average hydraulic conductivity higher than 10^{-11} m/s while the hydraulic conductivity of the rock determines the hydration rate if it is lower than 10^{-12} m/s. The time to full saturation is e.g. according to these calculations 100 years if $K = 10^{-13}$ m/s.

Scenario analyses of the tight distance block concept

The investigations have mainly concerned the alternative with a distance block that is supposed to seal and prevent all water flow past the block during the installation phase. A scenario analysis of this concept called the tight distance block concept has also been done.

The conclusions from this scenario analyses in combination with other investigations were that the bolted ring can work as intended for the reference scenario and prevent piping and displacement of the distance block with one of the suggested designs. The ring must be fixed to the rock surface with bolts that are so strong and undeformable that the total force can be resisted without deformation. The real danger consists of a sudden small displacement of the block so that the water pressure is applied on the entire cross section area of the tunnel.

The scenario description mainly refers to the base case. The consequence of higher water pressure (up to 5 MPa), faster pressure build-up (up to 1,000 kPa/h) and faster water inflow rate (up to 1.0 l/min) has also been investigated. The results indicate that 5 MPa and 1,000 kPa/h and 1.0 l/min inflow cannot be accepted. 0.2 l/min inflow was barely handled in a scale test (together with 1,000 kPa/h and 5 MPa).

The length of the distance blocks is probably influencing the function in a positive way. If the reference case is considered unacceptable additional large scale tests for investigation of this effect should be done in order to extend the limits. The following additional tests are thus suggested:

- Tests of the consequences of a sudden displacement of the supporting ring.
- Tests in large scale to look at the influence of the length of the distance blocks.

Scenario analyses of the open tunnel concept

An alternative solution is to keep the tunnel open by leaving a gap between the distance block and the rock surface so that the water can pass the block without interference. A scenario analysis was performed and although the analyses and calculations done are very rough the conclusions was that the open tunnel concept does not work unless the bentonite is protected during installation. The swelling of the buffer due to the high RH in the air and the dripping of water on the buffer leads to degradation and erosion of the buffer. The use of degradable plastic cover or other protection materials should therefore be further investigated.

Contents

1 Introduction

1.1 General information about this study

KBS-3H and KBS-3V are very similar with respect to the behaviour of the bentonite buffer. However, there are some differences that require special attention. An early survey of the differences yielded that there are a number of processes and functions that needed to be investigated for evaluating the feasibility of the concept:

1. The function of the distance block. Scenario analyses of different concepts for design and installation of the distance blocks for finding critical issues.
2. Sealing ability of the distance plugs during water inflow.
3. Influence of rapid increase of water pressure inside the distance blocks.
4. Piping and erosion phenomena of the swelling bentonite during the installation phase and during the water saturation phase.
5. Mechanical interaction between the container and the buffer during the homogenisation of the bentonite and breakage of the container.
6. Near field thermal and hydraulic evolution.

These processes have been studied by Clay Technology in a number of tests and analyses during 2002 to 2004. The studies can be structured in the following way:

1. Test scaled 1:10 of a simulated part of a deposition tunnel with two canisters.
2. Design and planning of a large-scale test of the interaction between the bentonite and the perforated deposition container and manufacturing of components (Big Bertha).
3. Investigation of sealing/piping/erosion phenomena during wetting of the buffer material.
   a) Basic laboratory tests.
   b) Study of processes and scenarios in the scale 1:10.
   c) Study of processes and scenarios in full scale.
   4. Investigation of the effect of rapid water pressure increase inside the distance blocks by model tests in the scale 1:10 and in full scale.
4. Modelling
   a) Modelling of the interaction between the bentonite and the perforated deposition container.
   b) Modelling of temperature conditions for design and safety analysis purpose.
   c) Modelling of the water saturation phase and the influence of the hydraulic properties of the rock.
   d) Modelling of the wetting of the test scaled 1:10.
   e) Scenario analyses and conceptual modelling of the function of different distance block concepts.

These studies and the results and conclusions reached will be presented in this report. The report should be considered a state of the art report at the end of 2004. The studies are planned to continue during the coming years.

1.2 General information about KBS-3H

In the KBS-3H concept, the deposition tunnels are replace by horizontal 300-m long circular deposition drifts which are excavated from a niche in the transport tunnel, Figure 1-1. About 40 disposal containers will be deposited in each drift.

In order to make the deposition process easier the buffer material and one copper canister are assembled in a steel disposal container, which then is pushed into the deposition drift. The disposal container consists of a perforated steel cylinder in which the buffer material and one copper canister are assembled, Figure 1-2. Distance blocks of bentonite are placed between each disposal container.

The purpose of the distance blocks is to seal off each canister position from the other and to prevent transport of water and bentonite along the drift. The distance blocks also separate one canister from the other in order to get the right temperature of the canister. The total thickness of the distance blocks between the disposal containers is mainly determined by the thermal conductivity of the rock and is expected to be in the range of 3–6 m.

The main objective for the KBS-3H concept is that the method provides a more efficient way of depositing the canisters in the rock. The reason is that the deposition tunnels of the KBS-3V concept are not needed and the reduction of rock excavation is therefore about 50 percent.

This leads to a lower environmental impact during the construction of the repository but also to a reduced disturbance on the hydro-geological situation in the rock mass. Furthermore, the reduction in rock excavation leads to a significant cost saving for the excavation phase and backfilling of the repository.

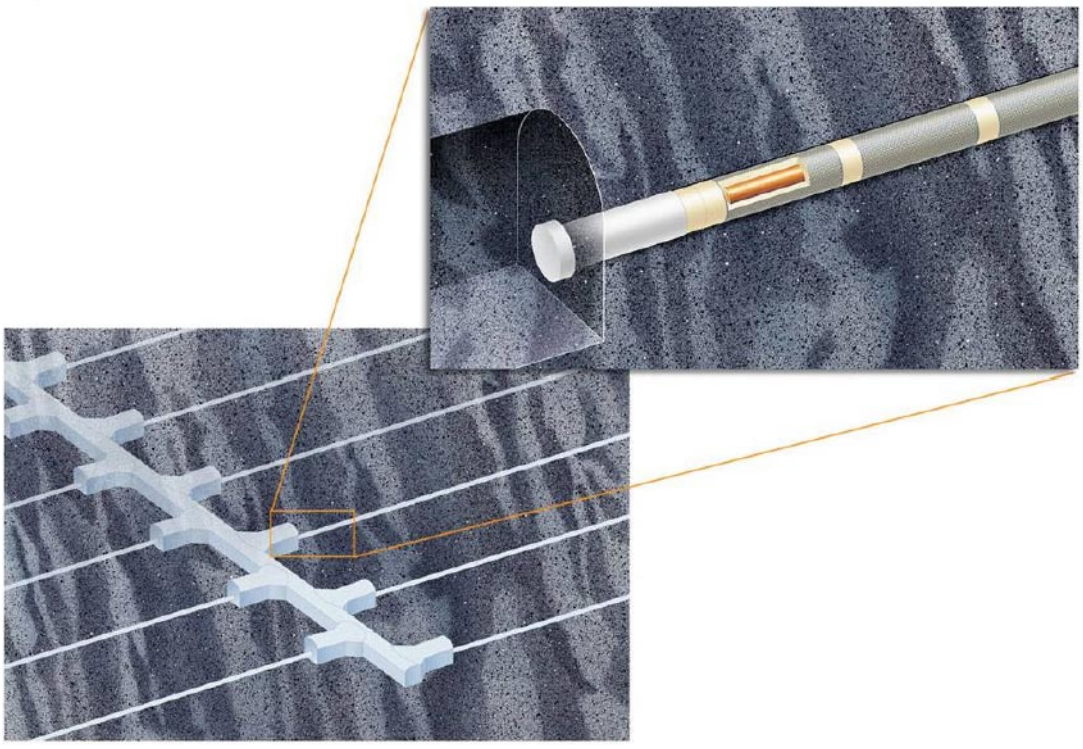

Figure 1-1. *Illustration of a transport tunnel with deposition drifts in KBS-3H.*

The fact that the canister and the buffer material will be assembled in a prefabricated disposal container enables easier quality control of the canister nearzone. Since there are no deposition tunnels, which have to be backfilled in the KBS-3H concept, the requirement on the performance of the backfill of the transport tunnels may be lower than in the KBS-3V concept.

The layout for the KBS-3H reference case is similar to the KBS-3V, but the deposition tunnels and deposition holes are replaced by a 300 m long deposition drift which is excavated from a niche in the transport tunnel. A total of around 45,000 m of deposition drifts are needed with a total volume for deposition drifts being around 120,000 m^3

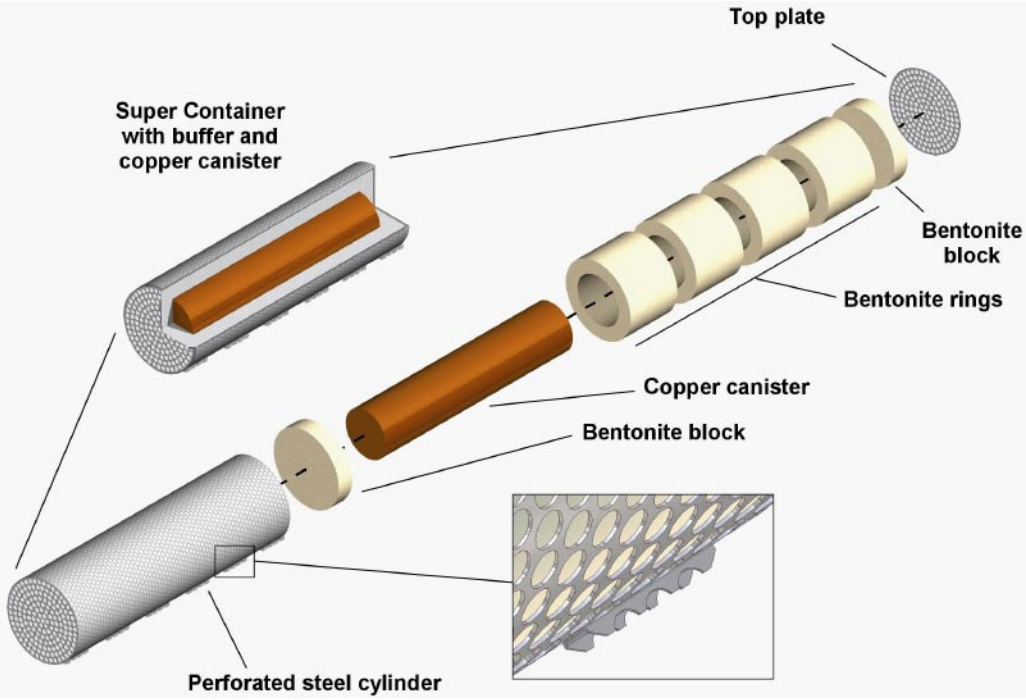

Figure 1-2. *Super container.*

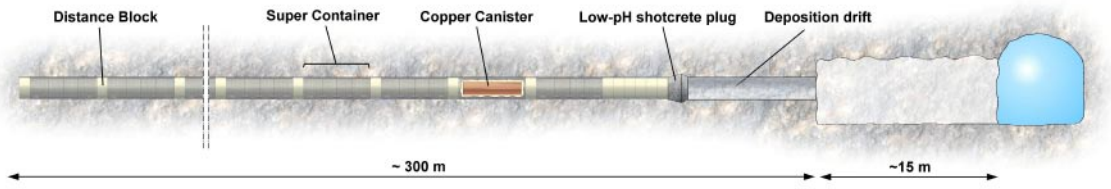

Figure 1-3. *Deposition drift.*

2 Concepts designed to handle the water inflow during the installation phase

2.1 General

A main problem during the installation phase that needs to be treated is the inflow of water. When water comes in contact with the bentonite blocks the bentonite starts to swell instantaneously by at first forming a gel, which keeps swelling until it is either transported away by erosion or prevented from swelling by geometrical reasons. In the latter case the continuous water uptake by the bentonite makes the swelling go deeper into the bentonite, which results in a compression of the gel and an increase in density and swelling pressure with time.

Two main principles regarding the intended function of the distance block during the installation phase can be discerned. The inflowing water can either be intentionally stopped by the distance blocks by filling the entire annular gap between the blocks and the rock surface with bentonite or it can be left with a remaining gap in order to let the water flow freely below the blocks. Those two concepts and the expected scenarios are described in this chapter as well as the assumptions regarding the water inflow.

2.2 Tight distance block

2.2.1 Introduction

A solution for handling the water inflow into the deposition drift in the KBS-3H concept is to make the distance block come in contact with the water, swell and thereby seal the annular gap between the block and the rock surface. The distance blocks are intended to stop the water flow from inside the blocks and also withstand the water pressure that can be developed. This concept with a tight distance block is briefly described.

2.2.2 Preliminary design

The two proposed designs of a distance block section with distance blocks that are intended to prevent water from passing the blocks during installation are shown in Figure 2-1. The annular gap between the block and the rock must either be very small (a few mm) or filled with sealing material (bentonite pellets is proposed) in order to prevent water from passing and to prevent piping when the water pressure increases. According to investigations performed in both scale 1:10 and 1:1 the distance blocks need to be supported by a ring fixed to the rock wall for both alternatives (see Chapter 8).

The perforated container is placed on feet centrally in the tunnel, yielding a gap between the container and the rock averaging 42.5 mm. The first distance block is placed in contact with the lid of the container. The distance block can either be made with a very tight fit to the tunnel or with a annular gap of 15–42.5 mm that is filled with bentonite pellets. In the latter case the distance block is also centered with feet as shown in the figure. In order to keep the pellets in the distance block section in place, a thin perforated steel ring may be attached to the container. Outside the distance block a rather strong steel ring attached to the rock is needed in order to keep the pellets and the block in place, to minimize the risk of piping and to prevent axial displacement of the distance blocks, which may be caused by the swelling buffer and (in particular) the water pressure that may arise inside the block.

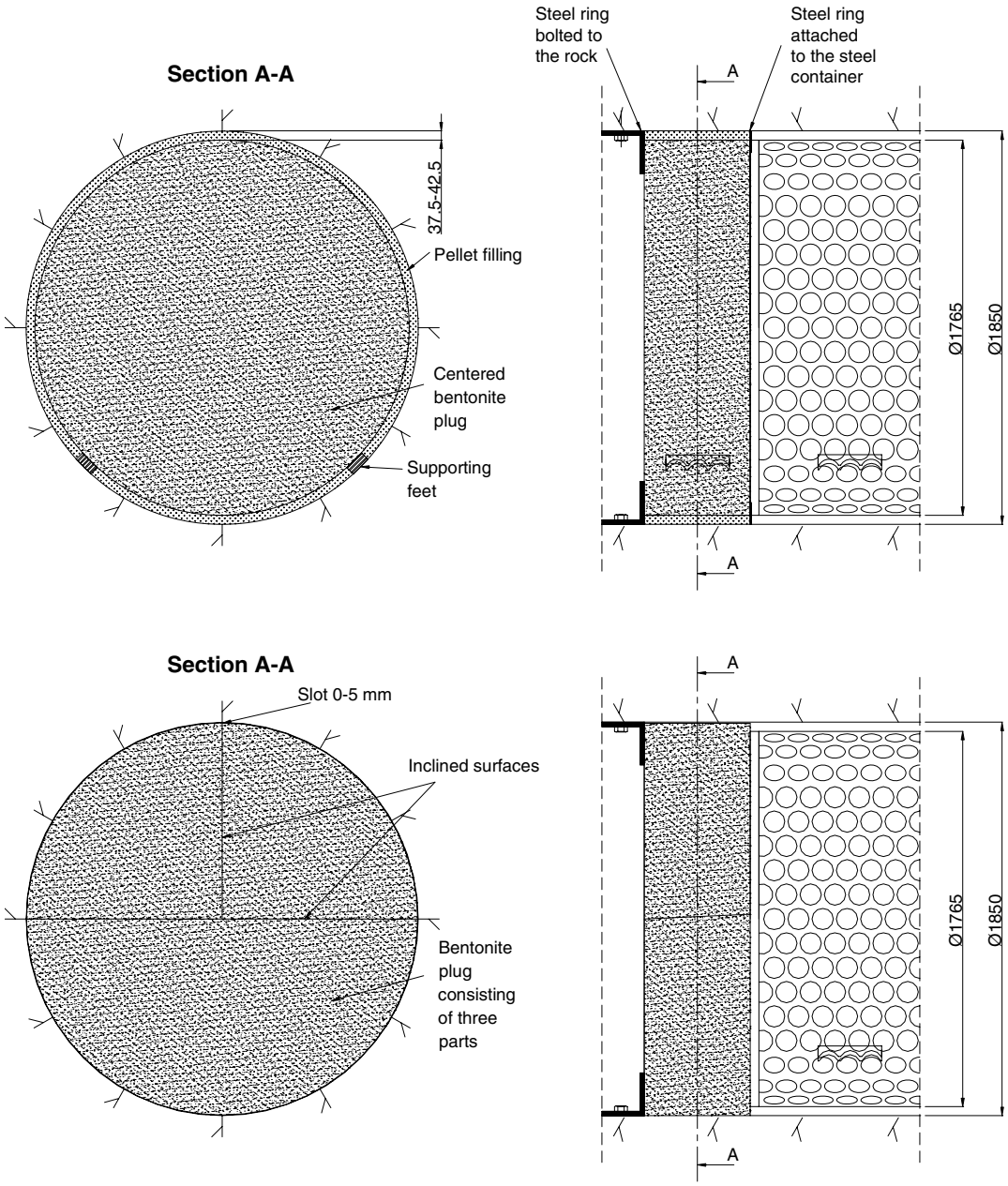

Figure 2-1. *Tight distance block concept. Centered distance block with pellets-filled annular gap (upper) and well fitted distance block standing directly on the floor (dimensions in mm). The thickness of the distance block is drawn to fit the compaction technique available at present (0.5 m) but will probably be larger. The total thickness will be 3–6 m.*

The other design alternative is to make the distance block so well fitted to the diameter of the tunnel that pellets are not needed. In this case the blocks can rest directly on the floor and the blocks probably need to be split into three parts in order to be able to transport it through the tunnel. A supporting ring is needed for this design as well.

2.3 Open tunnel

2.3.1 Introduction

Another solution for handling the water inflow into the deposition drift in the KBS-3H concept is to leave an annular gap also around the distance blocks and let the water flow freely on the tunnel floor. The concept of an open tunnel is briefly described in this chapter.

2.3.2 Presumptions and design

The layout of the concept with open tunnel is shown in Figure 2-2. Both the perforated container and the distance blocks are centred in the tunnel and placed on feet. The annular gap between the rock and both parts are the same (37.5 mm–42.5 mm). No supporting ring is needed in the concept since the distance blocks are not supposed to function until after plugging and sealing the entire tunnel with the end-plug.

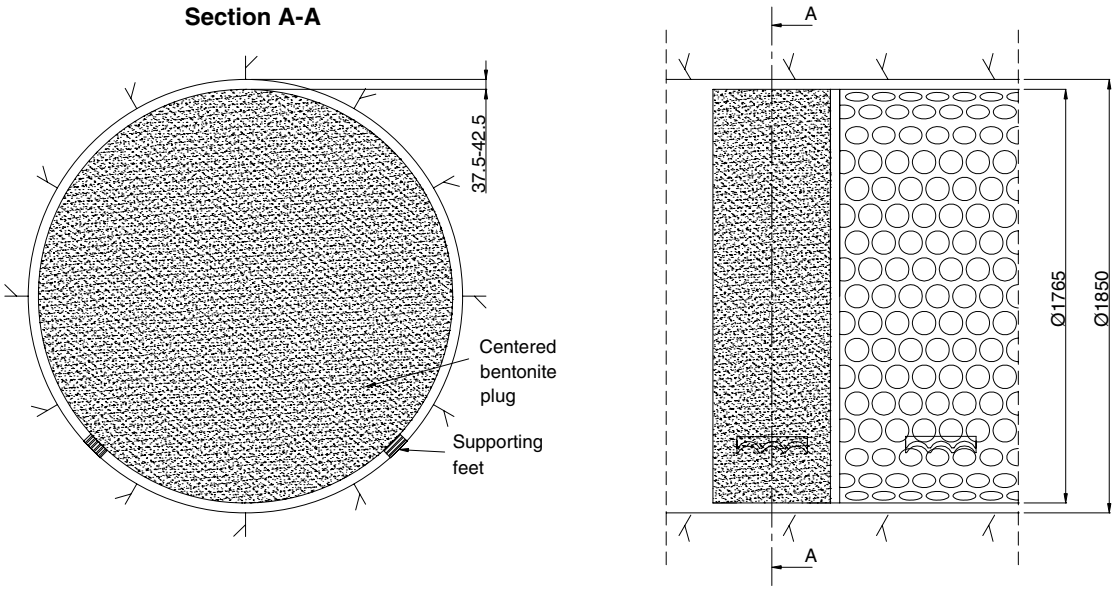

Figure 2-2. *Open tunnel concept. Centered distance block with an open annular gap between the block and the rock (dimensions in mm). The thickness of the distance block is drawn to fit the compaction technique available at present (0.5 m) but will probably be larger. The total thickness will be 3–6 m.*

3 Description of the buffer material in KBS-3H

3.1 Introduction

The buffer material for KBS-3H is intended to be the same as the buffer material for KBS-3V, i.e. sodium bentonite MX-80 from Wyoming. However, while the reference buffer KBS-3V is made of bentonite blocks with an initial water content of 17% the water content of the blocks in KBS-3H is planned to have an initial water content of about 10% (corresponding to the natural water content of the commercial bentonite). The reason for the difference is mainly that the geometrical configuration in KBS-3H requires a higher dry density of the block and 10% yields higher dry density than 17% at the same compaction pressure.

The main purpose of this chapter is to design the geometry and density of the three different types of blocks with the goal to reach an average density after full saturation and swelling of 2,000 kg/m^3.

3.2 Bentonite blocks

The bentonite for the buffer can be produced in many ways. The technique used for the large scale experiments at Äspö, is uniaxial compaction of large blocks. An alternative to uniaxial compaction is isostatic compaction. This technique implies a large press which is not available at this stage.

For the calculation of the final density of the buffer in different sections inside the container and in the plug (see Section 3.3) it is assumed that three different type of blocks are used, one type around the canister, one type in sections outside the canister and one type for the distance blocks. The calculations are independent of the fabrication method of the blocks. Figure 3-1 illustrates the void ratio (which can be recalculated to dry density) reached at mainly uniaxial compaction of MX-80 with the compaction pressure 50–150 MPa. This relation and other experiences from block compaction have been used for optimizing the block geometry.

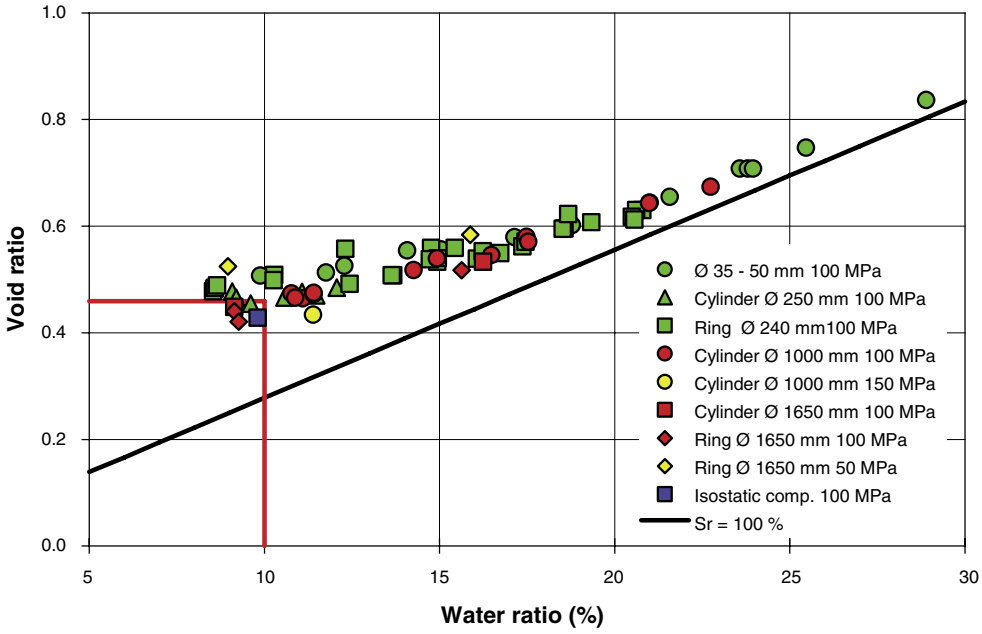

Figure 3-1. *Results of compaction of MX-80 blocks at different water ratio, compaction pressure and block geometry. All tests except one are made with uniaxial compression.*

3.3 Optimization of block geometry and density

Type 1: Ring shaped blocks around the canister

In Figure 3-2 the final density at saturation for the buffer around the canister in the container is plotted as a function of the diameter of the block. The calculations are made with the assumptions shown in the figure concerning the layout of the container, density and water ratio of the compacted blocks and the diameter of the tunnel. Three curves are plotted in which different assumptions about the final volume of the corroded container are used.

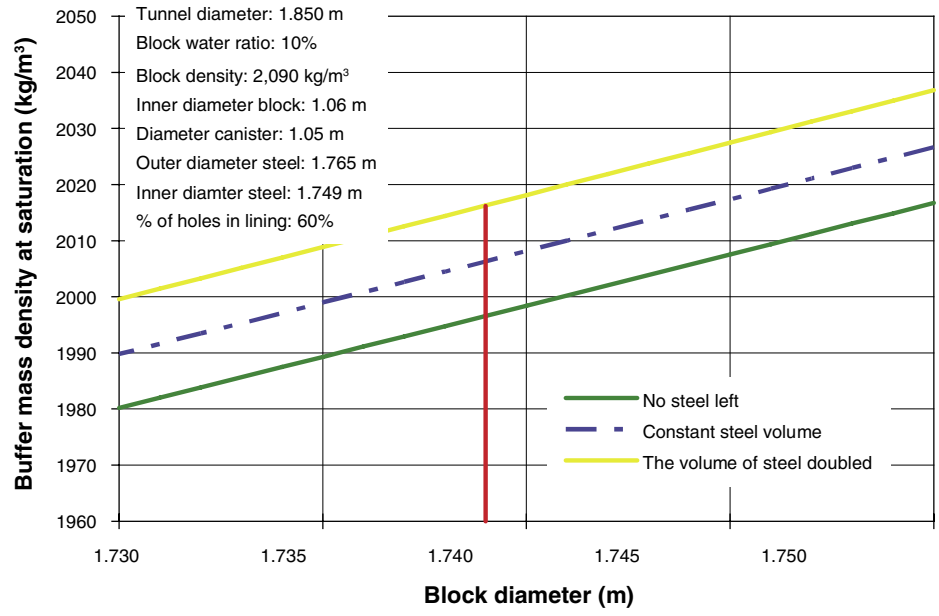

Figure 3-2. *Blocks of type 1. The final buffer density at saturation as a function of the block diameter for the ring shaped blocks inside the container.*

The figure shows that the block diameter should be between 1,730 mm and 1,740 mm in order to yield a density after full saturation and swelling of about 2,000 kg/m^3. The vertical line in the plot corresponds to an outer diameter of the block of 1,739 mm. Depending on the volume of the corroded container the density at saturation for the buffer varies between 1,995–2,015 kg/m^3 at this diameter.

Type 2: Blocks between the lid of the container and the lid of the canister

The corresponding figure for the buffer lying inside the container but in a section without canister (solid blocks) is shown in Figure 3-3. For this case the calculations are made with two different assumptions about the density of the blocks. Since these blocks contain more bentonite the block density must be lower (~ 1,950 kg/m^3) to yield similar swelling pressure if the block diameter is the same.

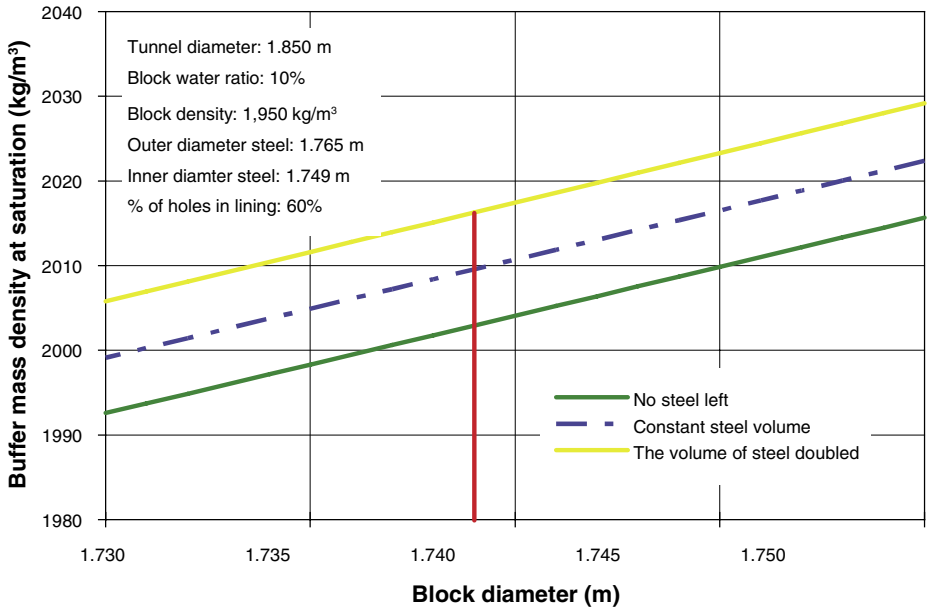

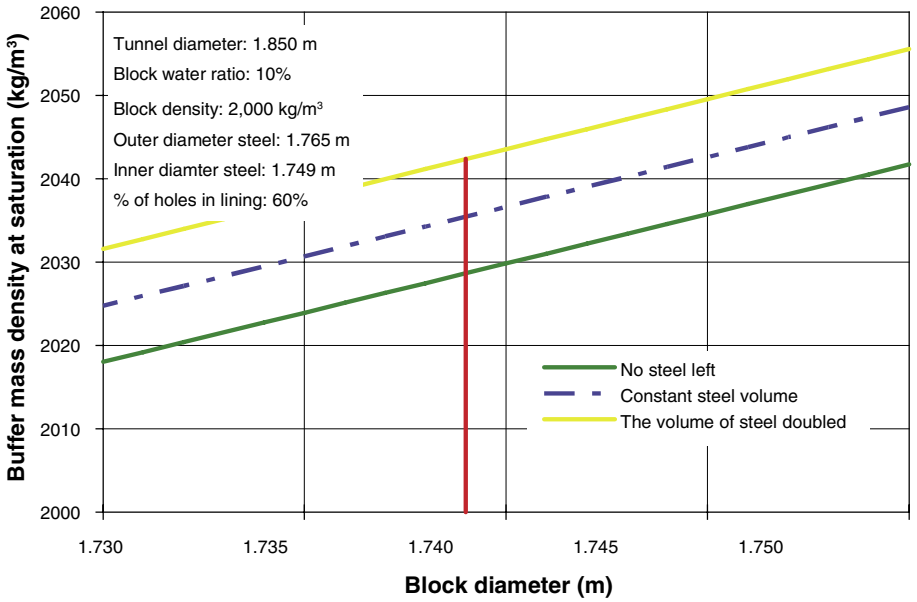

Figure 3-3. *Blocks of type 2. The final buffer density at saturation as a function of the block diameter for the blocks between the container lid and the canister lid inside the container for two different block densities.*

Type 3: Distance blocks between the containers

The plots for the distance blocks placed outside the container are shown in Figure 3-4. For this section calculations are also made with two different densities of the blocks. In this case the vertical lines correspond to a block diameter of 1,765 mm, which is the same as the outer diameter of the container. This diameter yields a final density about 2,030 kg/m^3 even for the low block density, which is higher than the target density but within the requested limits (1,950 kg/m^3–2,050 kg/m^3).

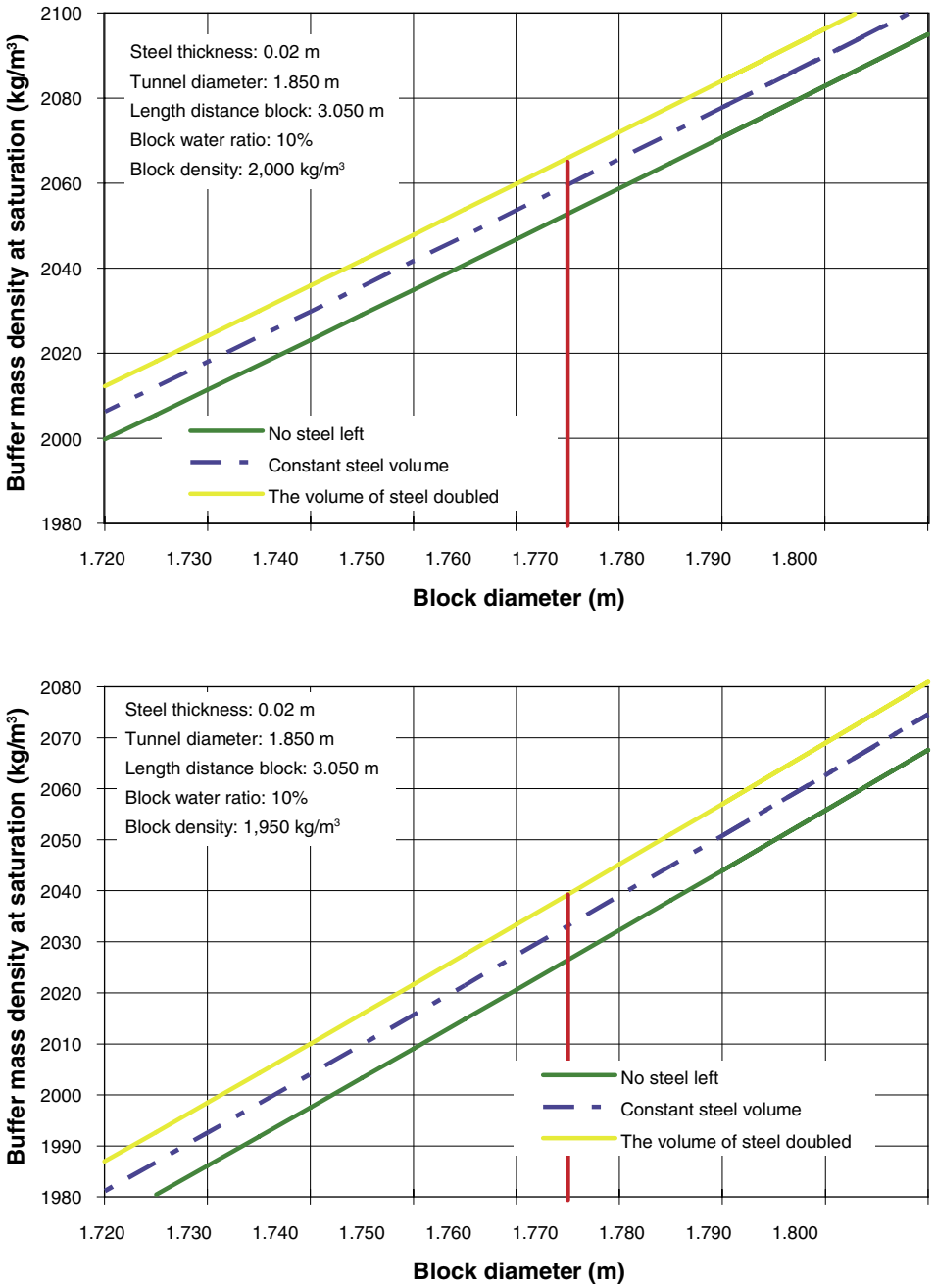

Figure 3-4. *Blocks of type 3. The final buffer density at saturation as a function of the block diameter for the distance blocks between the containers for two different block densities.*

The calculations show that the lowest final density after swelling and saturation is reached around the canister (block of type 1) although the block with the highest density is used (2,090 kg/m^3). The calculations also show that the final density of the parts with the other two block types will be rather high even with a density of the block of 1,950 kg/m^3, which is considered a minimum density since blocks of lower density has not yet been made. An alternative design in order to decrease the final density in these parts would be to use blocks with smaller diameters or/and use a buffer material with higher initial water ratio. If on the other hand the concept of well fitted tight distance blocks is considered the density of the blocks must be considerably lower than 1,950 kg/m^3. The possibility to make such blocks and if they can be handled must thus be investigated.

4 Test scaled 1:10 of the concept

4.1 Test design

The test was scaled 1:10 in order to save time and money, but some parts of the tunnel are planned to be simulated in almost full scale (the Big Bertha test) in order to verify that the processes are scalable. This scale test (in contrary to the sealing tests) is focused on the properties of the fully water saturated system. Although the path to the final stage is different it is most probable that the end stage is scalable since force equilibrium determines the end stage and force equilibrium is scalable. The length of the distance block is not correctly scaled, which is conservative.

The purpose of the test was to study the wetting, swelling and homogenization of the bentonite in the concept and to measure the hydraulic properties of the distance block and the bentonite that has swelled into the gap between the simulated rock and the perforated container. A schematic view of the test is shown in Figure 4-1. The test is scaled 1:10 of the exact geometry proposed for the concept in the beginning of 2002. The equipment consisted of an outer steel tube with lids in the end parts, two perforated steel containers with welded end plates, two canisters and bentonite blocks. The steel containers and the bentonite blocks were placed on the bottom due to gravity so the annular gaps were 0 at the bottom and 3 mm respectively 2 mm in "roof". The bentonite was saturated artificially by filters placed in the periphery of the outer tube, simulating a permeable rock. Total pressure, pore water pressure and relative humidity were measured in several points on the outer tube and on one of the canisters. The equipment was designed to withstand an inner total pressure of 10 MPa.

Outer tube

The length of the test equipment was set in order to contain two pre-assembled test parcels ("super containers"). A distance plug was separating the two containers. The tube was divided in two parts in order to facilitate the mounting and dismantling (see Figure 4-2). Two water inlets were connected to each filter.

The two test parcels were assembled in advance and then placed in the outer tube. Each test parcel was designed with an outer perforated metal sheet with covers in the ends simulating the perforated containers. Inside each test parcel, a canister was placed surrounded by highly compacted bentonite blocks. The test parcels were separated by a distance block with the thickness 38 mm.

Perforated steel containers

The perforations of the steel containers have been made with two different geometries, circular holes and oblong holes. The holes are distributed according to Figure 4-3. A picture of one of the tubes is shown in Figure 4-4. The degree of perforation is 60% for all configurations. The thickness of the perforated steel tubes was 1 mm while the thickness of the steel ends was 3 in one end and 9 mm in the other end.

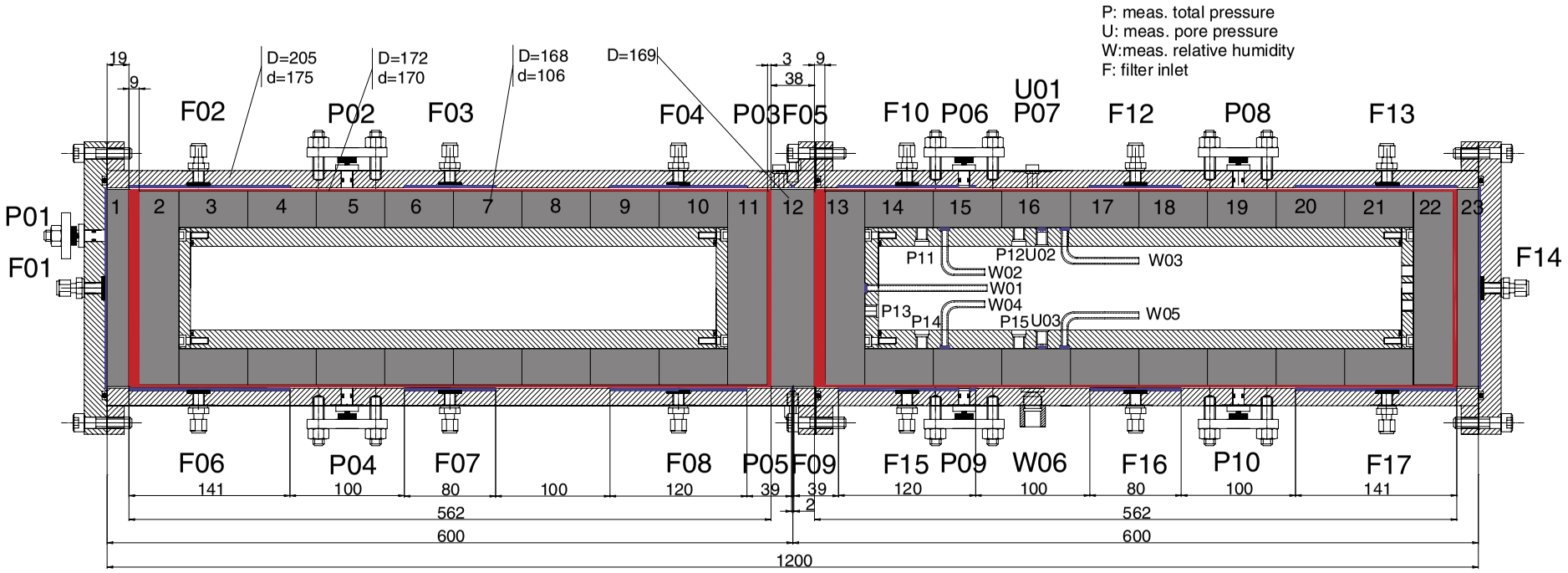

Figure 4-1. *Longitudinal section of the test. F denotes filter inlets, P denotes total pressure gauges, U denotes pore water pressure gauges and W denotes water content gauges (RH-transducers). The filters are blue and the perforated containers are red. D and d represent outside and inside diameters, respectively. Dimensions in mm.*

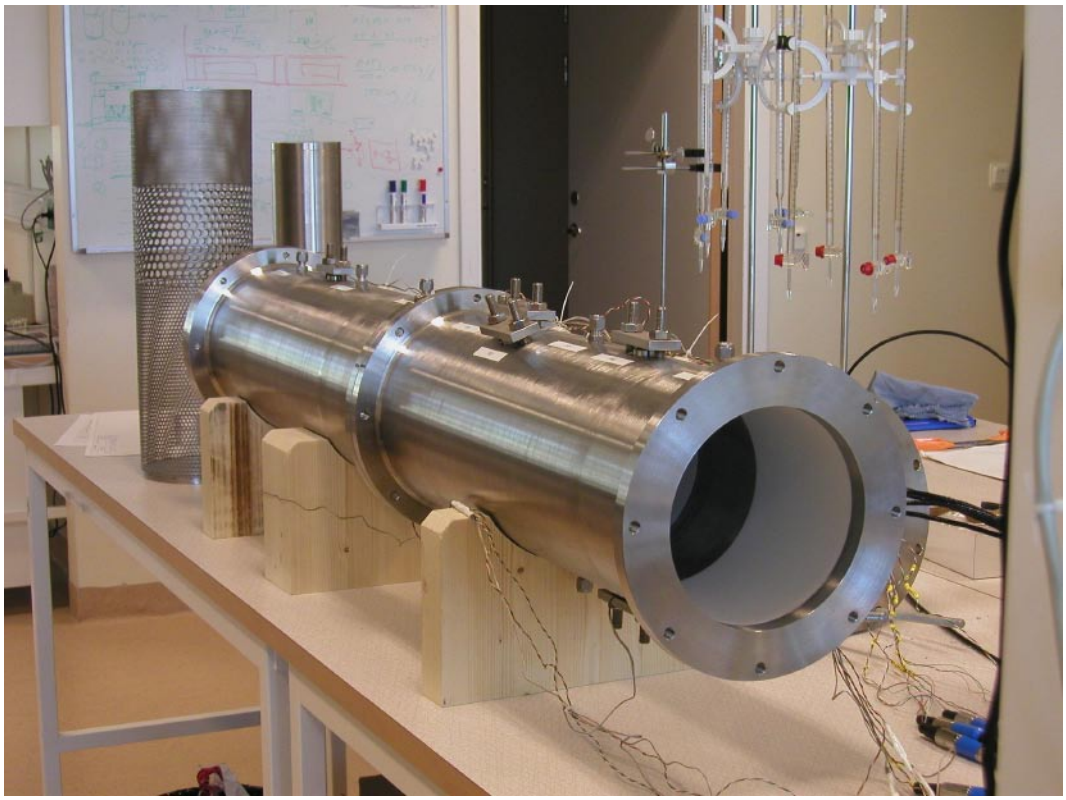

Figure 4-2. *Picture showing the outer tube. The tube is equipped with different sensors and with inner filters.*

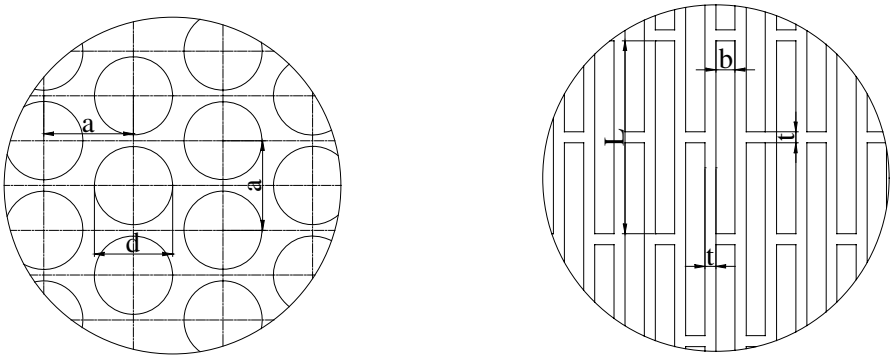

1. Circular holes. d=5 mm a=5.725 mm 2. Oblong holes L=17.5 mm b=1.75 mm t=1.0 mm	1. Circular holes. d=10 mm a=11.45 mm 2. Oblong holes L=35 mm b=3.5 mm t=2.0 mm	1. Circular holes. d=2 mm a=2.3 mm 2. Oblong holes L=7 mm b=0.7 mm t=0.4 mm

Figure 4-3. *Schematic view of the layout of the perforated steel containers. Three different hole dimensions were used for each container.*

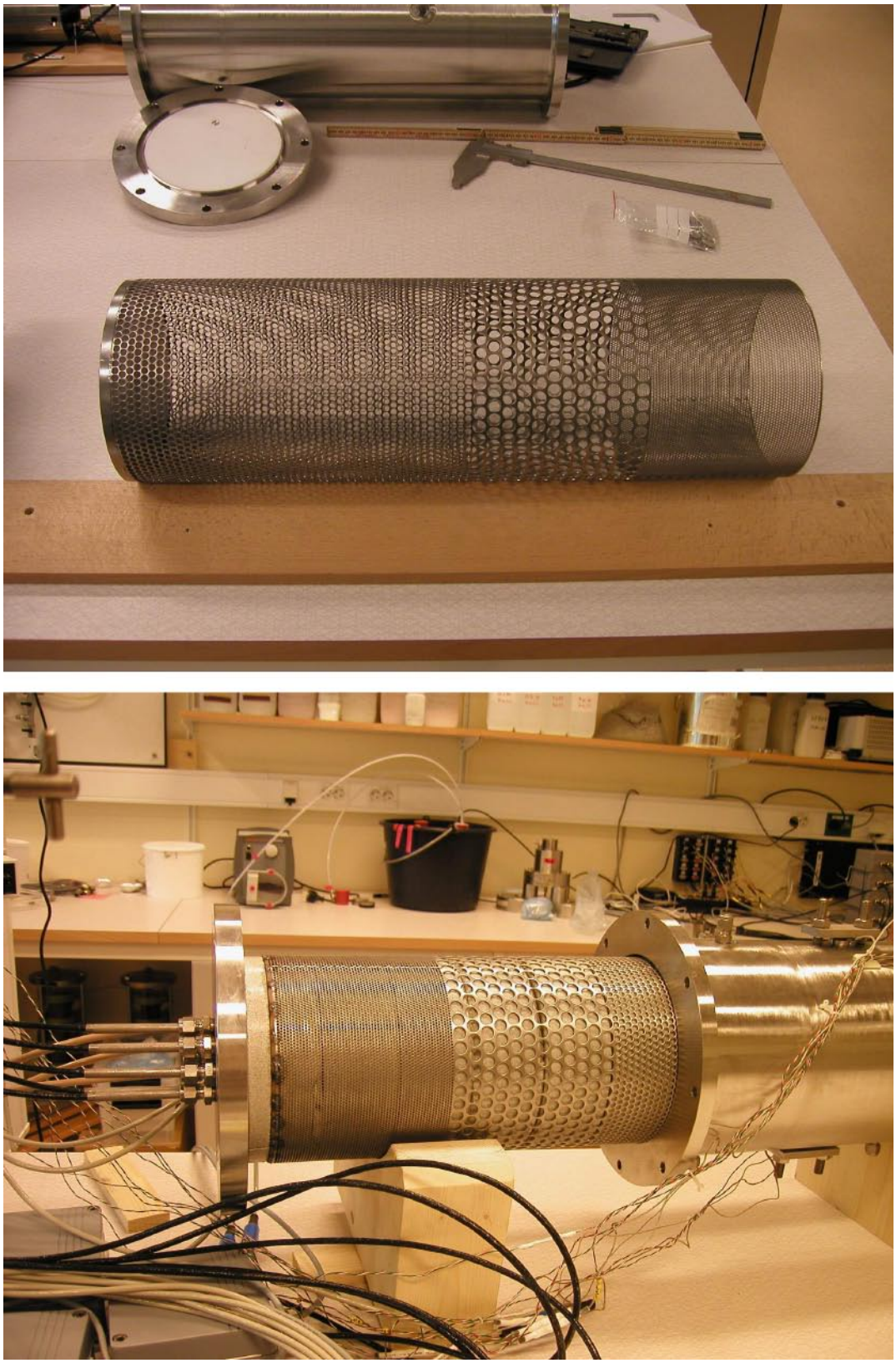

Figure 4-4. *Pictures showing the perforated steel tube equipped with circular holes.*

Canisters

The test included two simulated canisters, one with instruments and one without. The outer diameter was 105 mm. No heating of the canisters was applied. Figure 4-5 shows a picture of one of the canisters before mounting.

Instrumentation

The experiment was equipped with the following devices and instruments for water supply and measurement of HM-processes (see also Figure 4-1):

- 10 total pressure sensors.
- 6 RH-sensors for measuring relative humidity.
- Pore water pressure sensors.
- 17 water inlets for supplying the filter mats with water.
- GDS-instruments for pressurisation and volume measurement of the saturating water and for measurement of the axial hydraulic conductivity.

Figure 4-5. *Picture showing the instrumented canister during calibration of the RH-sensors. The black cables going from the canister to the small vessels are the RH sensors, which are calibrated in the vessels before test start.*

4.2 Bentonite buffer

4.2.1 Quality

The material used in the test was SKB's reference buffer material MX-80. A standard quality control was performed and the liquid limit was determined to be 460%. The natural water content of the bentonite (w = 10–11%) was used for the blocks.

4.2.2 Block production

The technique for producing bentonite blocks has been developed during the last ten years and blocks with different dimensions have been manufactured for many full and small scale tests, for example the Prototype Test, the Canister Retrieval Test and the LOT test. A special compaction device was constructed for the manufacturing of the bentonite blocks to the KBS-3H test scaled 1:10 (see Figure 4-6). The same equipment could be used for both ring shaped and cylindrical blocks.

Figure 4-6. *Device for bentonite block production*

4.2.3 Density of installed buffer material

In order to get the same final density at saturation in the test parcels two types of bentonite blocks were compacted with different pressures. The ring shaped blocks surrounding the canisters were compacted with 100 MPa to an average bulk density of 2.076 kg/m³. The cylindrical blocks were compacted with 40 MPa to an average bulk density of 1.94 kg/m³ (see Table 4-1). The outer diameter of the blocks was also adjusted after the manufacturing in order to reach the intended density. The final saturated density in the test parcel was calculated in two ways:

1. Before test start. Looking on every block type as a section, with only radial swelling, calculations gave saturated densities between 2.041 and 2.048 kg/m³ (see Table 4-1).
2. After test start. All installed bentonite was weighed. Dividing the total solid mass of the bentonite with the actual volume of the saturated bentonite gave an average density of the bentonite. The dry density was calculated to be 1.622 kg/m³ and the saturated density to be 2.040 kg/m³ (see Table 4-2).

At installation every bentonite block was measured and weighed. Looking at every block as a section with only radial swelling, the final density for every block section could be calculated (see Table 4-3). This calculation yields information about the homogeneity of the saturated bentonite. Some of the blocks have a lower density than the average. This depends on the fact that they have been machined, i.e. with drilling and cutting, in order to lead tubes through or to fit at the ends.

Table 4-1. Table showing calculated densities derived by considering each block type as a section with only radial swelling.

Block type	Bulk density of block kg/m³	Outer dia of blocks mm	Dry density of installed bentonite kg/m³	Saturated density of installed bentonite kg/m³	Void ratio
Ring shaped	2,076	168.1	1,623	2,041	0.719
Cylindrical shaped, placed inside the perforated tube	1,940	168.1	1,629	2,044	0.713
Cylindrical shaped, placed outside the perforated tube	1,940	169.1	1,633	2,048	0.708

Table 4-2. Table showing calculated densities derived by dividing the total solid mass of the installed bentonite with the actual volume of the saturated bentonite.

Solid mass of bentonite emplaced kg	Bentonite volume m³	Dry density of installed bentonite kg/m³	Saturated density of installed bentonite kg/m³	Void ratio
31.878	0.019657	1,622	2,040	0.720

Table 4-3. Table showing calculated densities when considering each installed bentonite block as a section with only radial swelling. The height of each block has been measured at three positions (h1–h3). Ms stands for the weight of the dry mass.

Block no	m g	Outer d mm	Inner d mm	h1 mm	h2 mm	h3 mm	ms g	Dry density g/cm³	Sat density g/cm³	e
Block 1	868.96	169.1	0	21.0	21.3	20.8	783.55	1.551	1.995	0.799
Block 2	1,449.92	168.1	0	34.5	34.5	34.5	1,307.41	1.590	2.020	0.755
Block 3	1,653.24	168.1	106.4	58.9	59.8	59.5	1,490.75	1.653	2.061	0.687
Block 4	1,654.60	168.1	106.4	59.5	59.8	59.8	1,491.97	1.646	2.056	0.695
Block 5	1,648.25	168.1	106.4	60.0	59.5	59.5	1,486.25	1.641	2.053	0.700
Block 6	1,635.02	168.1	106.4	60.5	60.1	59.9	1,474.32	1.614	2.036	0.728
Block 7	1,649.08	168.1	106.4	59.6	59.8	60.3	1,487.00	1.635	2.049	0.706
Block 8	1,654.95	168.1	106.4	60.0	59.9	59.5	1,492.29	1.644	2.055	0.697
Block 9	1,651.47	168.1	106.4	60.3	59.9	60.0	1,489.15	1.633	2.048	0.708
Block 10	1,679.72	168.1	106.4	60.5	60.4	60.4	1,514.63	1.651	2.059	0.690
Block 11	1,396.08	168.1	0	34.9	34.8	34.9	1,258.86	1.515	1.972	0.842
Block 12	1,642.90	169.1	0	38.2	38.1	38.2	1,481.42	1.614	2.035	0.729
Block 13	1,496.74	168.1	0	35.2	35.2	35.2	1,349.63	1.608	2.032	0.735
Block 14	1,638.99	168.1	106.4	59.5	60.0	60.4	1,477.90	1.624	2.042	0.718
Block 15	1,652.10	168.1	106.4	60.5	59.8	60.1	1,489.72	1.632	2.047	0.709
Block 16	1,642.32	168.1	106.4	59.8	60.2	59.9	1,480.90	1.627	2.044	0.715
Block 17	1,647.49	168.1	106.4	60.4	60.5	60.1	1,485.56	1.622	2.041	0.720
Block 18	1,650.28	168.1	106.4	60.0	60.5	60.5	1,488.08	1.625	2.043	0.717
Block 19	1,635.05	168.1	106.4	60.4	60.2	60.0	1,474.35	1.613	2.035	0.729
Block 20	1,650.50	168.1	106.4	59.8	59.9	60.4	1,488.28	1.633	2.048	0.708
Block 21	1,652.80	168.1	106.4	60.0	60.0	60.5	1,490.35	1.632	2.047	0.710
Block 22	1,309.09	168.1	0	35.2	35.2	35.2	1,180.42	1.407	1.903	0.983
Block 23	793.21	169.1	0	18.9	19.0	19.0	715.25	1.568	2.006	0.780
Average								1.608	2.032	0.737
Sum	35,352.76						31,878.05			

4.3 Test period

4.3.1 Start of test and water saturation

When the mounting of the test parcel was ready, i.e. the test parcel was completely mounted and the acquisition of data had started, the water saturation could begin. A picture of the test set up is shown in Figure 4-7.

At first the filters and inner space were filled with water by letting the water flow into the lower inlets to the filters. The filters were filled up until water came out from the upper outlets of the filters. The tubes from these connections (inlets/outlets) to the filters were then connected to burettes, one to each filter. With this arrangement, it was possible to measure the total amount of water taken up by the bentonite. Figure 4-8 shows the water inflow as function of time. A problem with this method of filling up water is that air will, after the filling, still be present in parts of the apparatus, disturbing the future water uptake, but on the other hand that will also be the case in a real repository.

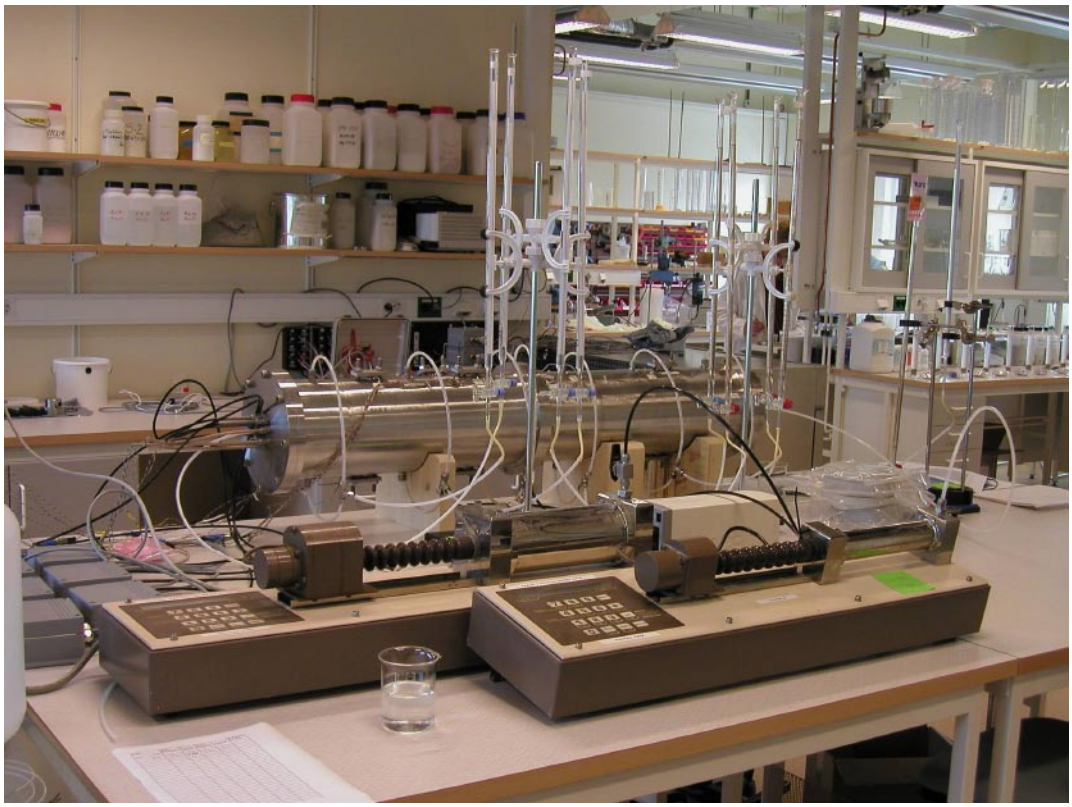

Figure 4-7. *Picture of the experimental set-up in the laboratory.*

Vacuum suction before wetting would probably result in that the sensors measuring relative humidity had been filled with water and destroyed immediately. In order to facilitate the water saturation and ensure homogeneous wetting, the filters were later de-aired a number of times during the saturation period, both by vacuum suction and water flushing.

During the first about 80 days the applied constant water pressure was only 10 kPa and the inflowing water volume was measured manually with burettes. Then all tubes connected to the different filters were collected into one and a water pressure of 1 MPa was applied by use of so called GDS equipment. With this equipment a constant water pressure can be applied and the injected water volume measured.

4.4 Measurements during the test period

4.4.1 Water inflow

Figure 4-8 shows the measured water inflow as function of time until start of the flow tests. The total volume of empty space (including the bentonite porosity) that could be filled with water was 5,208 cm^3. The figure shows that more water was filled than originally calculated. This discrepancy can mostly be explained by leakage, but even after compensation of estimated leakage there is a slight net over volume of filled water. This phenomenon has been observed in other projects and may be explained by changes in water density, but more plausible explanations are additional leakage that has not been detected and loss during filter flushing.

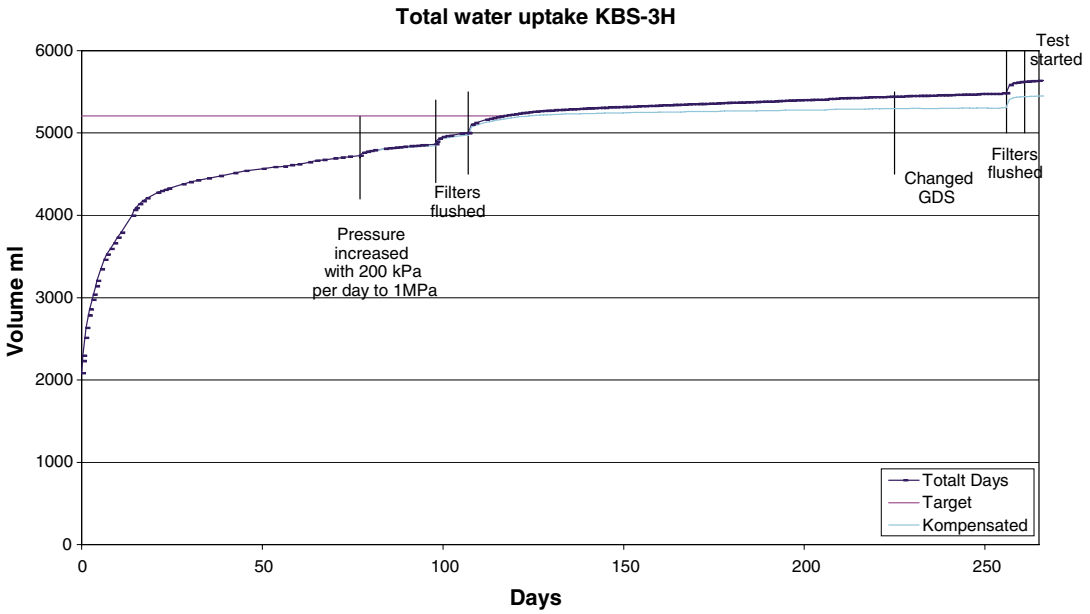

Figure 4-8. *Diagram showing the water uptake in the different filters. The total amount of water needed to saturate the bentonite was calculated to be 5,208 cm³.*

4.4.2 Relative humidity

Relative humidity (RH) was measured at one point on the periphery of the bentonite and at 5 points on the surface of the instrumented canister (see Figure 4-1). Vaisala RH-transducers was used for all measurements. Figure 4-9 shows the measured RH as a function of time. The outer sensor, W06, was not installed until after 62 days in order not to risk initial wetting and destruction. After about 120 days when the relative humidity in this point exceeded 95%, the sensor was exchanged to a Wescor psychrometer, which can give more exact information in the range RH = 95–100%. The five inner sensors never exceeded 96%. Sensor W01 stopped working after 220 days. The remaining sensors were recalibrated after the test, which showed that transducer W04 was malfunctioning and that the other three did not differ from the initial calibration.

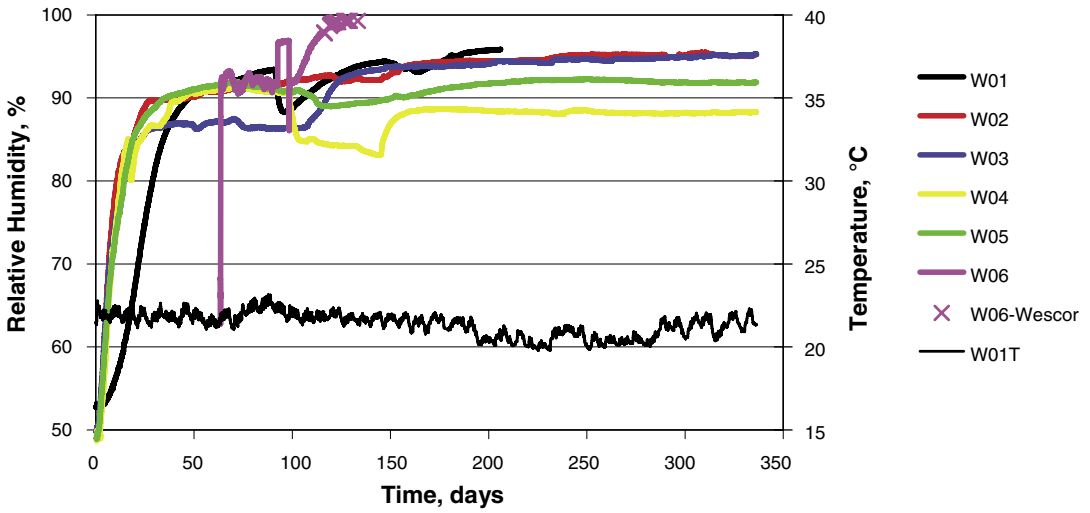

Figure 4-9. *Measured relative humidity and temperature (W01T) as a function of time. W06 is located on the "rock" surface the other transducers are located on the canister. W06 was changed from Vaisala to Wescor after about 120 days. The instrument positions are shown in Figure 4-1.*

4.4.3 Total pressure

Total pressure was measured in 9 points on the outside of the steel tube and in 5 points on the surface of the instrumented canister (see Figure 4-1). The results are shown in Figures 4-10 to 4-12. The final measured total pressure varied between 5 and 14 MPa, which was a rather high scatter. The average void ratio is 0.72 which according to swelling pressure measurements should yield a swelling pressure of 10 MPa /Börgesson et al. 1995/. The measured average swelling pressure agrees very well with this expected value but the scatter is difficult to explain. Especially the pressure outside the perforated steel tube varied a lot, which may be explained by the influence of the steel tube. Recalibration of the transducers after the test showed a small offset of at most a few hundred kPa.

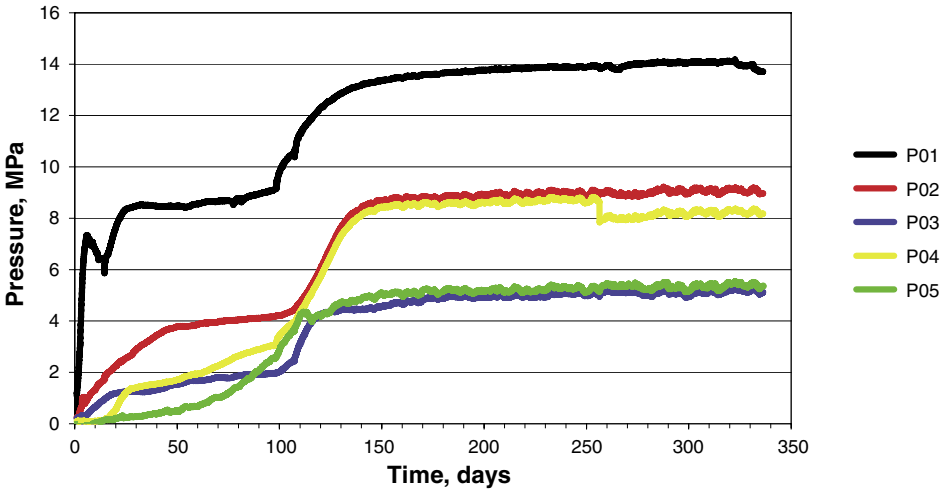

Figure 4-10. *Measured total pressure on the simulated rock surface as a function of time. The instrument positions are shown in Figure 4-1.*

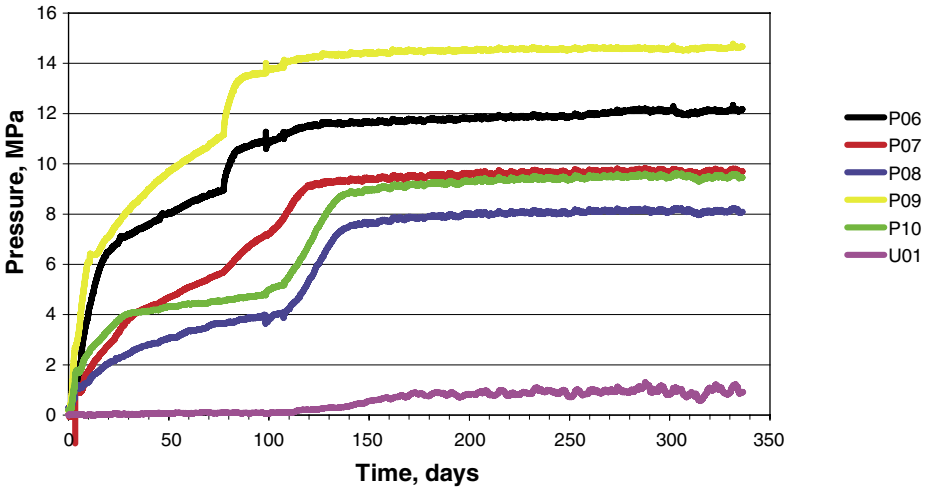

Figure 4-11. *Measured total pressure and pore pressure on the simulated rock surface as a function of time. The instrument positions are shown in Figure 4-1.*

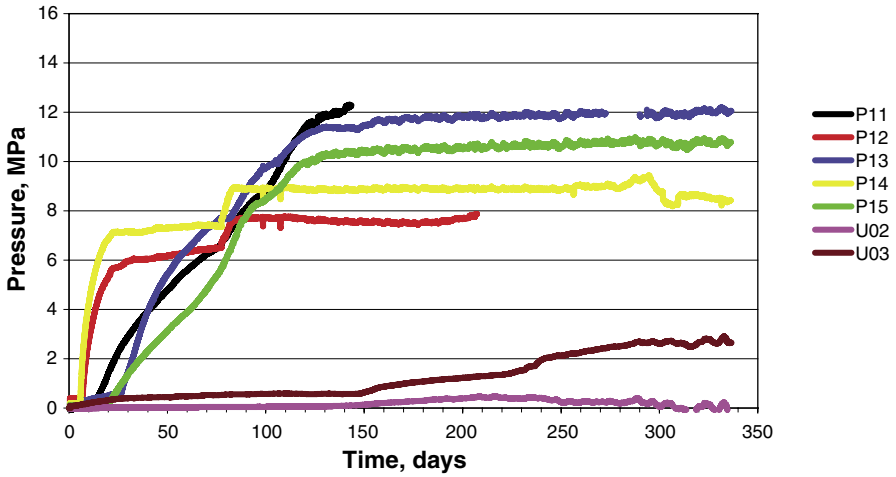

Figure 4-12. *Measured total pressure and pore pressure on the canister as a function of time. The instrument positions are shown in Figure 4-1.*

An explanation could in fact be the scatter in density of the installed blocks. As shown in Table 4-3 the calculated void ratio after swelling varies between 0.69 and 0.84 (with exception of block 22 at the entrance of the cables), which corresponds to a variation in expected swelling pressure of between 4 and 14 MPa. On the other hand, the correlation between high measured swelling pressure and low void ratio is not strong if one compares the location of the transducers and the location of the blocks.

Transducers P06 and P09 show increased pressure with 1 MPa immediately after increasing the water pressure in the filters, which is logical since the transducers are located at a filter. It is however not clear why P01, which also is located at a filter did not react immediately.

4.4.4 Pore pressure

Pore pressure was measured in 1 point on the outside and 2 on the canister surface. These results are shown in the same diagram as the total pressure. It is interesting to see the high pressure on the canister in point U03. This pressure is most likely caused by a gas pressure and not a water pressure. Such a gas pressure can result from shut-in air that has been compressed by the swelling pressure of the buffer. This may also partly explain why RH never came up to 100% on the canister surface.

4.5 Flow tests

In order to test the hydraulic conductivity of the buffer at the periphery a number of flow tests were carried out. By lowering the water pressure in a filter and measure the water flow from the neighbouring filters the hydraulic conductivity of the bentonite zone between the perforated steel container and the “rock” could be evaluated.

The conductivity was calculated according to Equation 4-1 using Darcy’s law and the assumption that all flow takes place in a 1.5 mm thick zone between the container and the “rock”.

$$q = KiA \quad (4\text{-}1)$$

q is the water flow, i is the pressure gradient and A is the area perpendicular to the flow. The flow was measured with a GDS digital controller until a stable flow was established. This normally took about a week. A pressure difference (drop) of 500 kPa was applied.

The test sequence was the following:

- the tested filter was connected to a second GDS controller and a pressure of 1 MPa was established by both GDS controllers,
- the pressure was left at 1 MPa until stabilisation had occurred,
- the pressure in the tested filter was then lowered to 500 kPa,
- after completion of the test the pressure in the tested filter was raised to 1 MPa.

This sequence was repeated for each filter. The hydraulic conductivity was evaluated according to Equation 4-1, taking into account that the flow into the filters came from both neighbouring filters. The hydraulic conductivity of the distance block was evaluated in the same way, i.e. the water was assumed to flow in a 1.5 mm thick zone, which probably is conservative. The results are shown in Table 4-4:

The measurements in filters F05 and F12 were difficult to evaluate since the water flow direction changed from outflow to inflow during the measuring period. The conclusion is though that since the flow is much "lower" than in the other measurements the hydraulic conductivity is lower and thus below 10^{-12} m/s. Filter F01 covers the entire end face of the distance block. The evaluation according to Table 4-4 is thus conservative since the flow also goes through the block and the area A in Equation 4-1 higher.

The conclusion is that the sealing of the space behind the perforated container is rather good although the hydraulic conductivity is about 10 times higher than expected considering the density and swelling pressure. The distance blocks have as expected efficiently sealed the flow paths between the containers.

Table 4-4. Results from the flow testing.

Filter with reduced pressure	Outflow q (mm³/s)	Distance (mm)	K (m/s)
F01 (dist block)	0.721×10^{-3}	19	$< 1.7\times10^{-13}$ (*)
F02	3.191×10^{-3}	100	3.90×10^{-12}
F03	1.935×10^{-3}	100	2.35×10^{-12}
F04	6.443×10^{-3}	100	7.80×10^{-12}
F05 (dist block)	–	–	$< 10^{-12}$
F10	1.673×10^{-3}	100	2.03×10^{-12}
F12	–	–	$< 10^{-12}$

(*) Conservative assumptions.

4.6 Dismantling and sampling

After about one year when the flow tests had been finished, the experiment was terminated, the installation dismantled and a lot of samples taken and analysed.

Figures 4-13 to 4-15 show pictures taken during dismantling. The outside of the perforated steel container was visually completely covered with bentonite. The container was ruptured at some parts as shown in Figure 4-13.

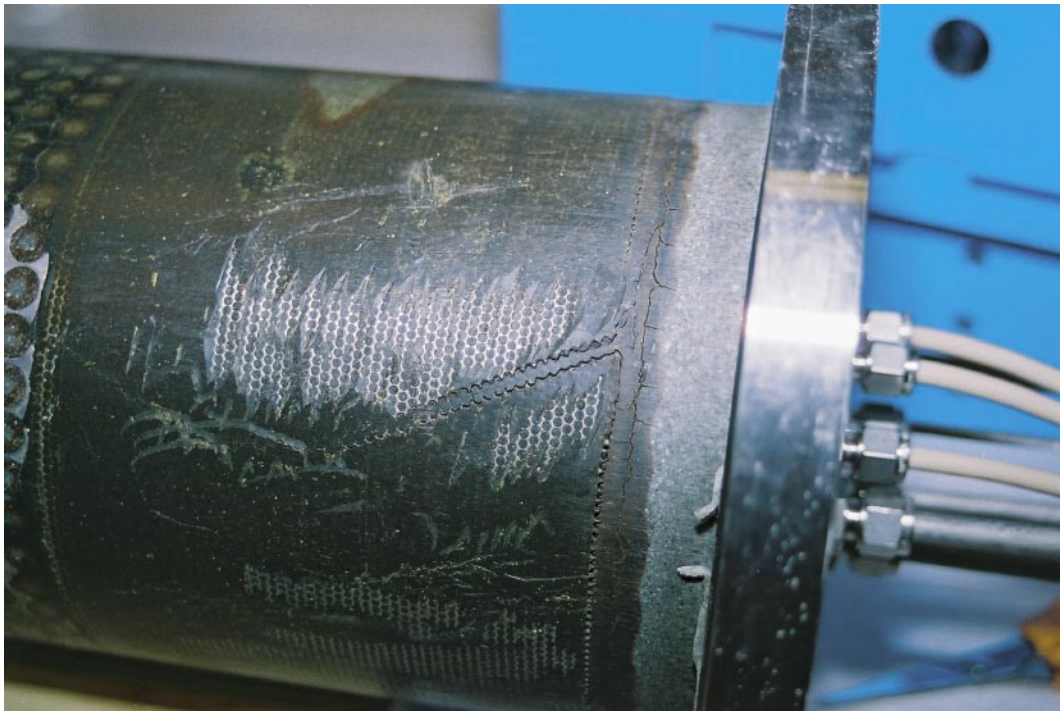

Figure 4-13. *Picture of one of the perforated steel tubes after dismantling. Note the rupture of the perforated steel container. The container is uncovered due to sampling at some parts.*

Figure 4-14. *Picture of the buffer after "unrolling" the perforated steel container.*

Figure 4-15. *Picture taken during removal of the buffer.*

The water ratio of the bentonite outside and in the holes of the perforated steel tubes was determined in a large number of places. A compilation of the results is shown in Figure 4-16 and 4-17. The diagrams show that the water ratio varies between 20 and 30%. The water ratio is generally slightly lower in the holes than on the outside, which is logical (see Chapter 10.2). Other general differences are that the water ratio is higher in the sections covered with filter mats and lowest in the central parts where the largest holes were located. The container appeared to be centered although it was placed on the bottom of the tube before wetting. No differences in thickness or water ratio of the bentonite layer outside the perforated container were observed.

Extensive sampling of the distance blocks and of the buffer inside the perforated container was also made and the density and water ratio determined. The results are shown in Figures 4-18 to 4-21. There is some scatter in the results. Most diagrams also show a decreasing void ratio with increasing distance from the outer periphery, which is caused by friction in the bentonite that restrains the homogenization during swelling. The diagrams also show that the degree of saturation is seldom 100% but usually between 96% and 98%, which is judged to be a combined effect of entrapped air and swelling after dismantling.

The conclusion from the sampling is that the bentonite has swelled and homogenized very well also outside the perforated container although there are still some differences in void ratio. The buffer is close to water saturation although a few percent less probably due to enclosed air and swelling at dismantling. The average void ratio measured outside the perforated container is lower than expected according to the modeling shown in Chapter 10. The reason is probably that the perforated container has been deformed and ruptured and the gap thus decreased by the expansion of the buffer inside the container. The high swelling pressure measured confirms this observation.

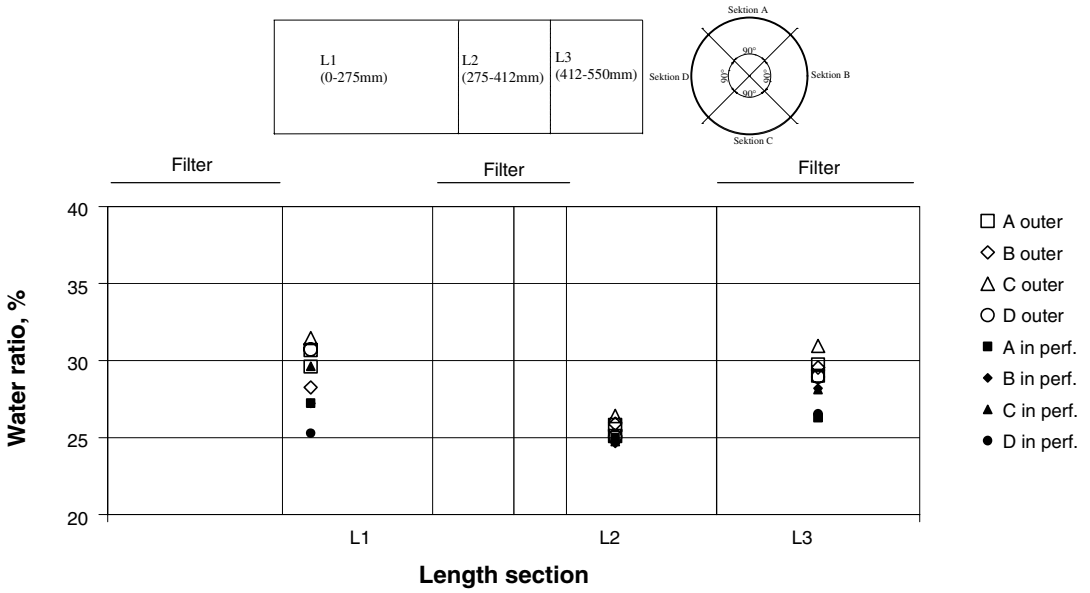

Figure 4-16. *The water ratio of the bentonite determined outside the perforated steel container (termed "outer") and in the perforated holes (named "in perf") in the un-instrumented section (oblong holes).*

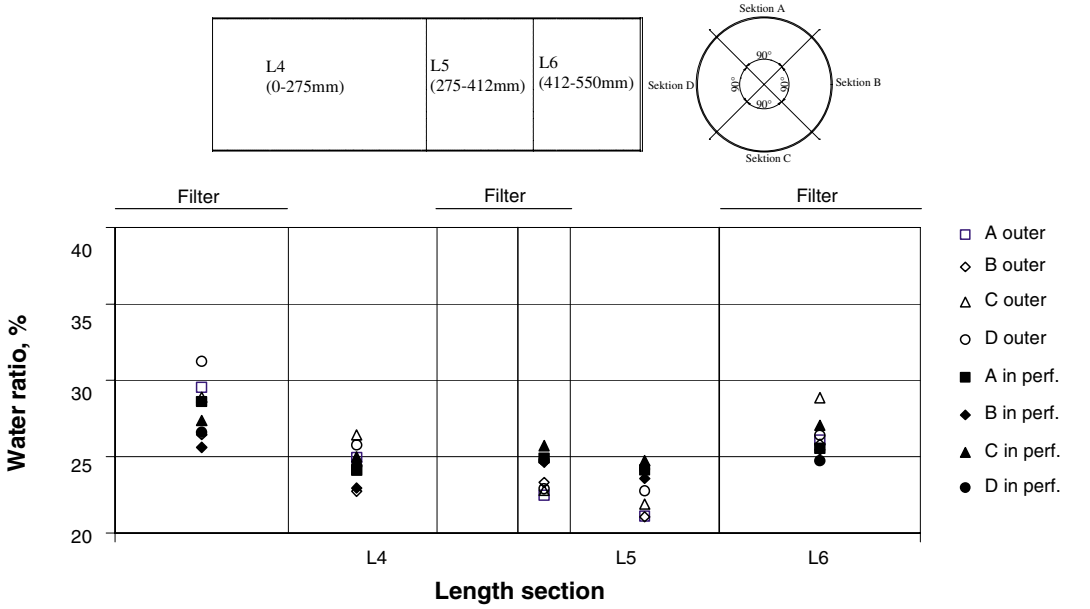

Figure 4-17. *The water ratio of the bentonite determined outside the perforated steel container (termed "outer") and in the perforated holes (named "in perf") in the instrumented section (circular holes).*

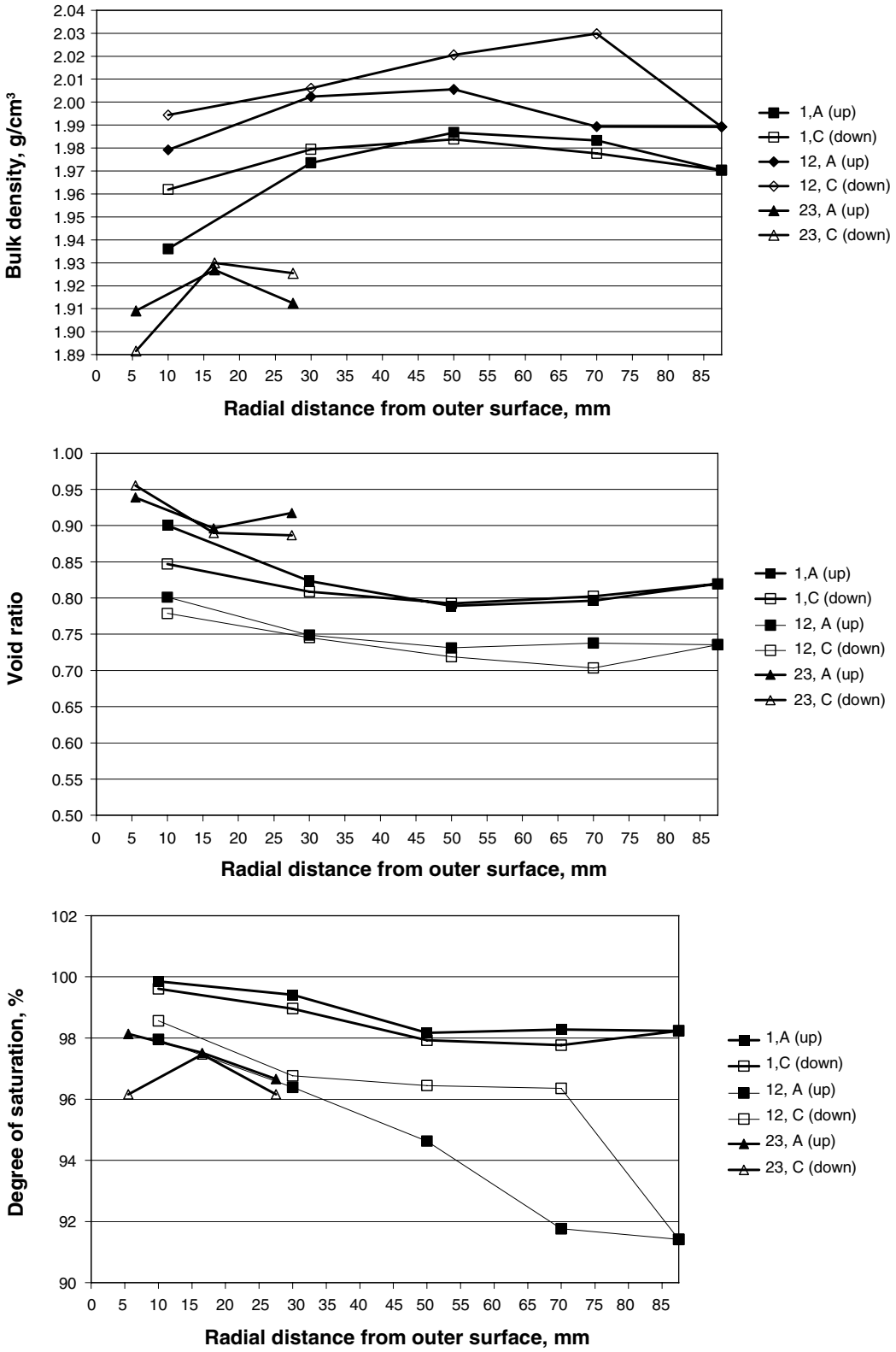

Figure 4-18. *Diagrams showing the results of sampling of the three distance blocks (1, 12 and 23), which were positioned as plugs in the test arrangement. See also Figure 2-1.*

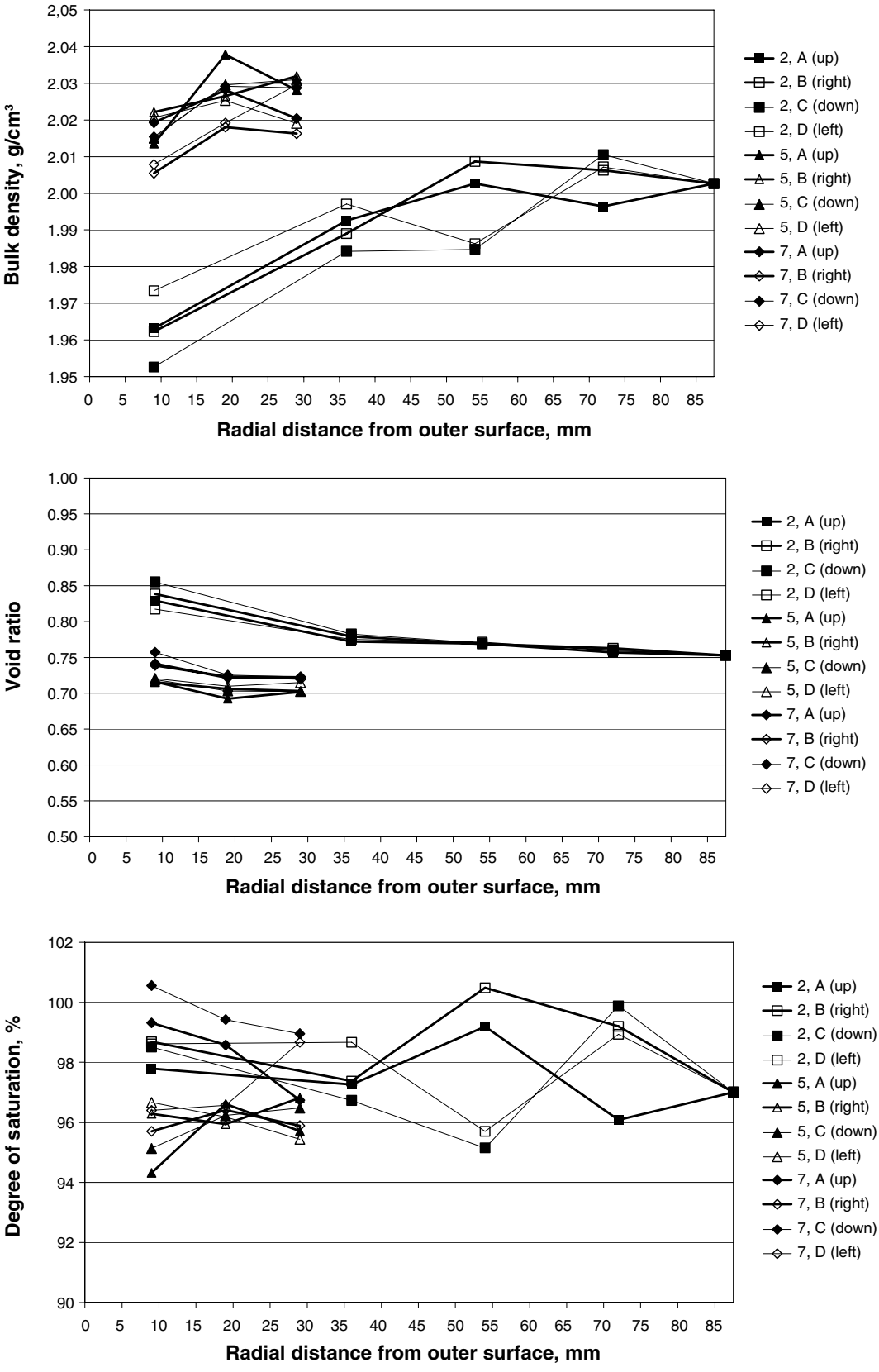

Figure 4-19. *Diagrams showing the results of sampling of two blocks and one ring (2, 5 and 7), which were positioned inside the perforated container in the un-instrumented part. See also Figure 4-1.*

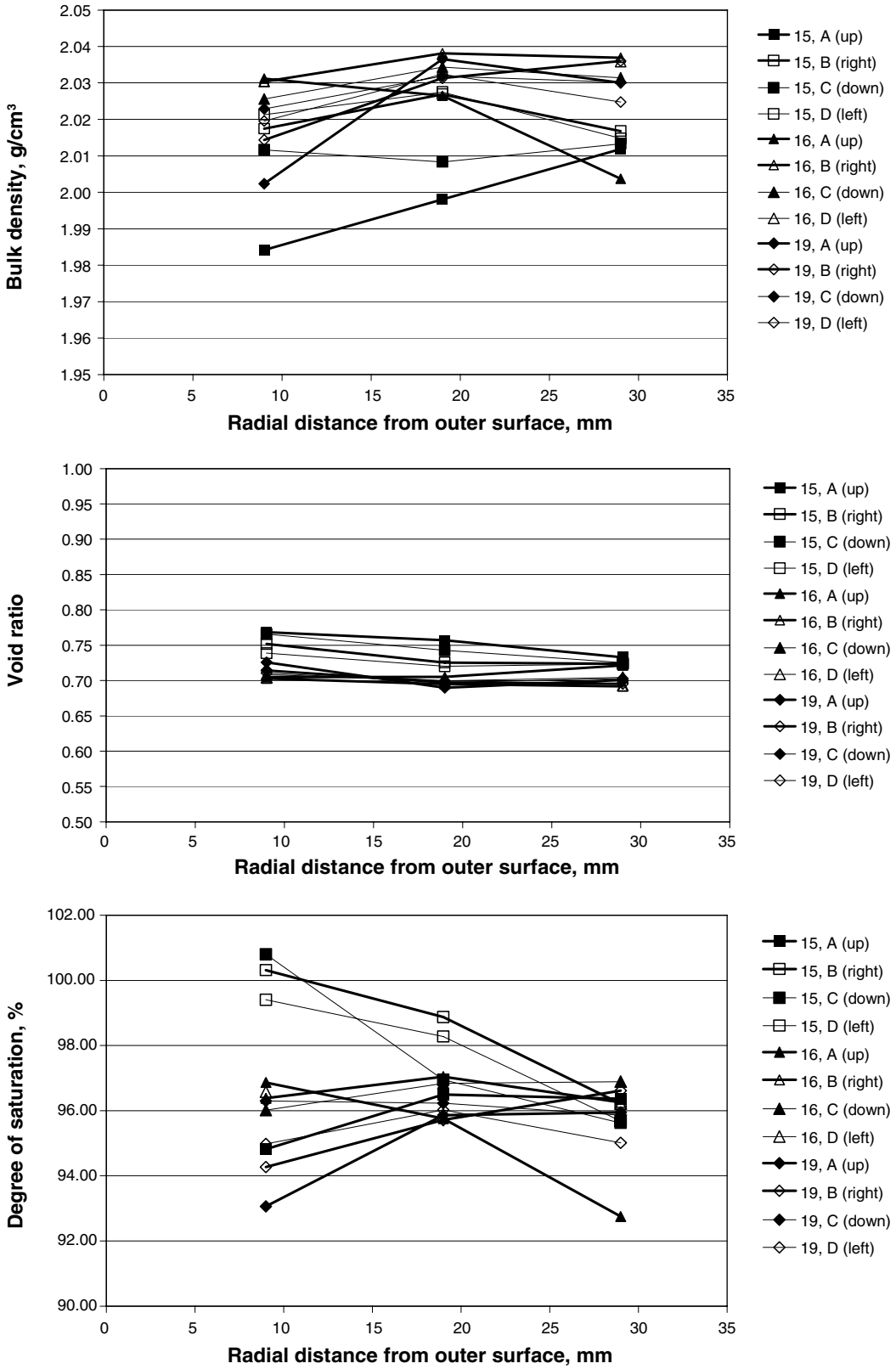

Figure 4-20. *Diagrams showing the results of sampling of three rings (15, 16 and 19), which were positioned inside the perforated container in the instrumented part. See also Figure 2-1.*

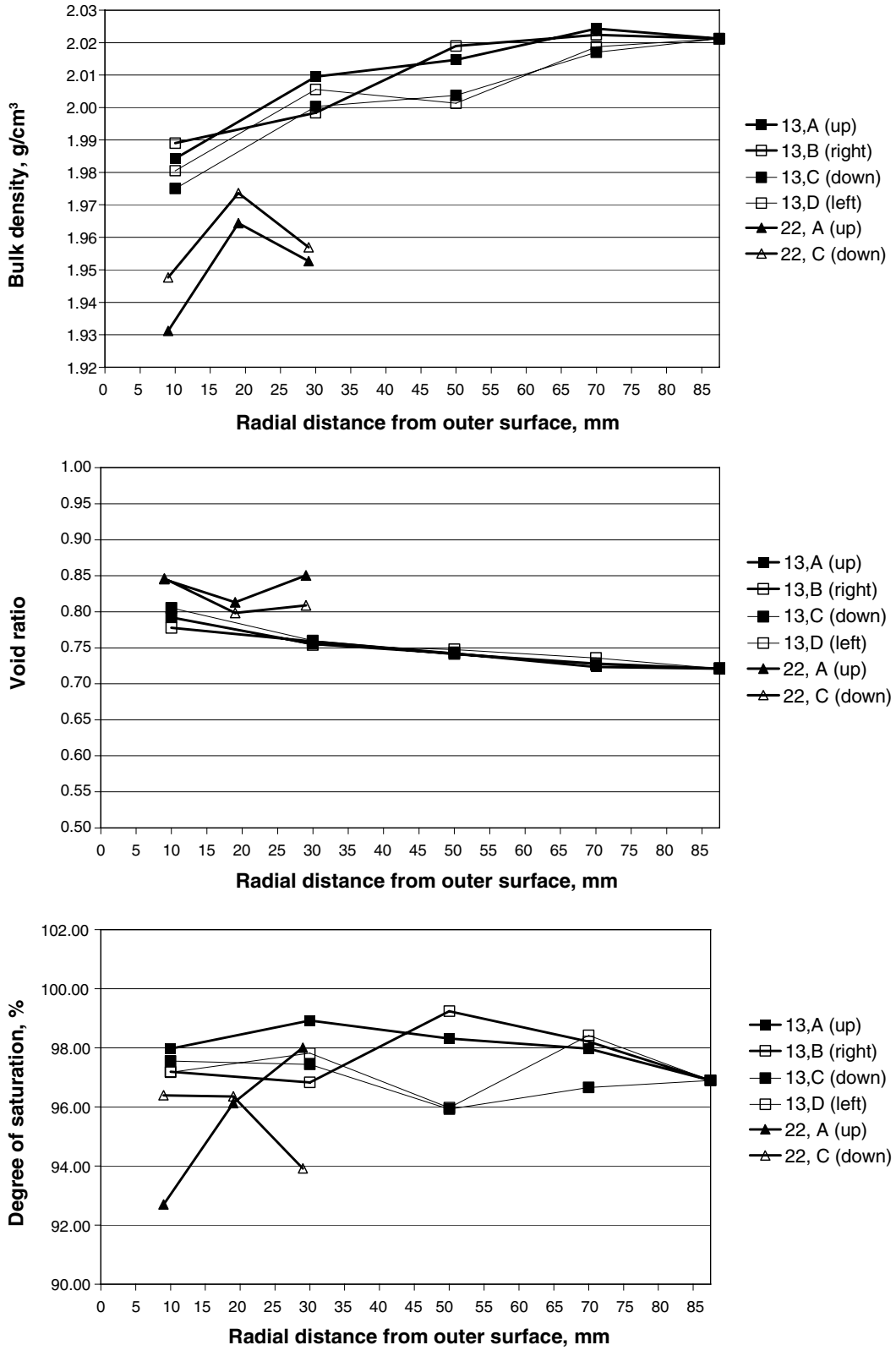

Figure 4-21. *Diagrams showing the results of sampling of two blocks (13 and 22), which were positioned inside the perforated container in the instrumented part. See also Figure 2-1.*

5 Large scale test of buffer/container/distance block interaction (Big Bertha)

In order to test some critical functions in full scale a large-scale model of a part of the perforated steel container and the distance block is planned. A test with the following ingredients will be performed

- Perforated container, buffer thickness and all gaps in full scale but no canister.
- Up-scaling of a part of the test scaled 1:10.
- Flow testing in the same way as for test scaled 1:10.
- Dismantling and sampling after finished test.

The duration of the test is preliminarily intended to be about 2 years but may be prolonged since the test will be far from completely water saturated after that time.

The design of the test equipment and test set up is shown in Figure 5-1.

The test was originally planned to start in 2003 but has been intentionally postponed since the equipment has been used for testing piping and erosion scenarios (see Chapter 7).

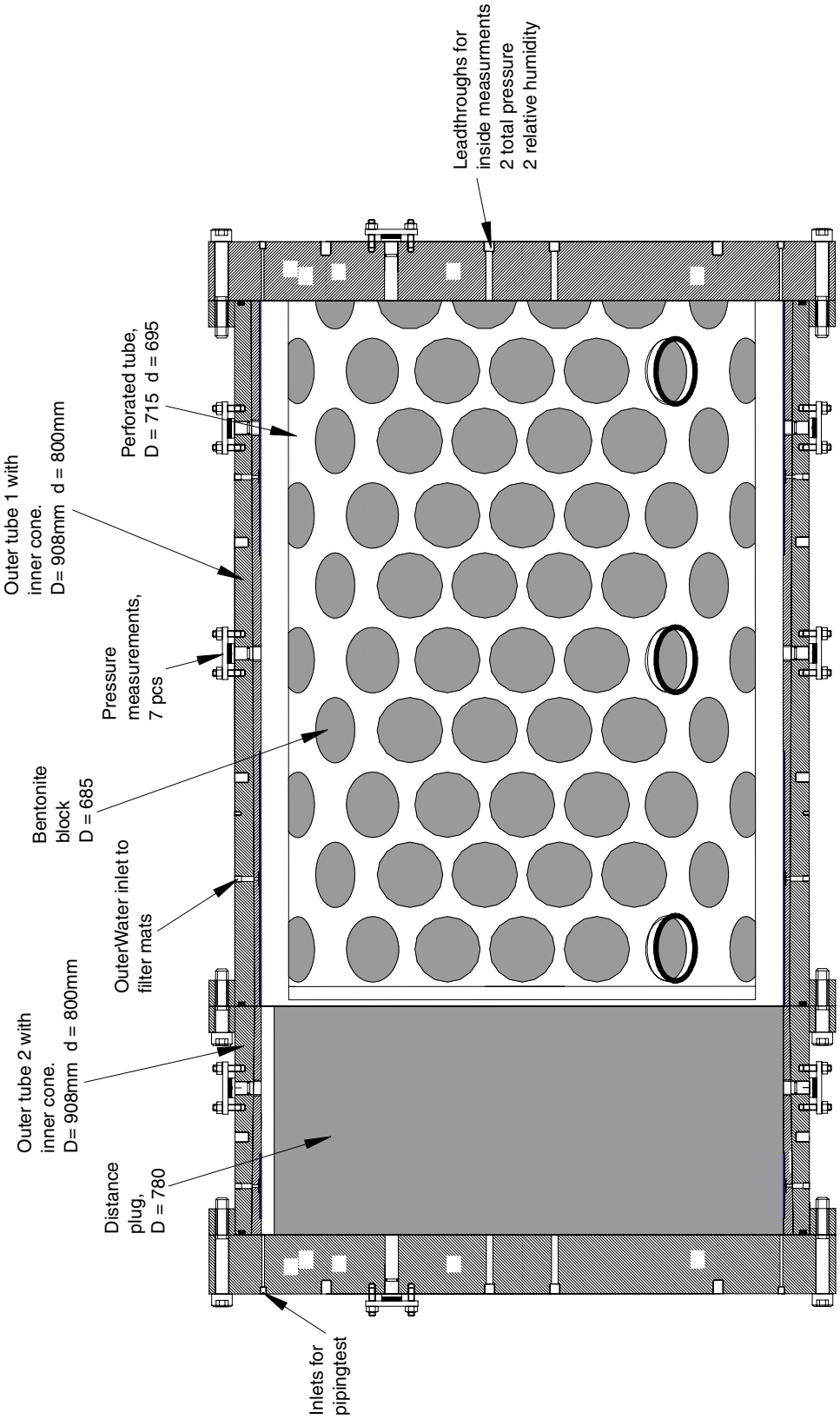

Figure 5-1. *Design of the test "Big Bertha". The total length of the test section is 120 cm.*

6 Investigation of the sealing/piping/erosion phenomena during wetting of the buffer – basic laboratory tests

6.1 Introduction

Water inflow into the deposition tunnel will take place and will contribute to the wetting of the buffer. However, if the inflow is localized to fractures that carry more water that the swelling bentonite can adsorb, there will be a water pressure in the fracture acting on the buffer. Since the swelling bentonite is initially a gel, which increases its density with time as the water goes deeper into the bentonite, the gel may be too soft to stop the water inflow. The results may be piping in the bentonite and a continuing water flow and erosion of soft bentonite gel. There will be a competition between the swelling rate of the bentonite and the flow and erosion rate of the buffer.

In order to investigate this phenomenon a series of tests have been performed, starting with basic laboratory tests, described in this chapter and continuing with scenario studies and scale tests of sealing techniques, described in Chapter 7.

The basic laboratory tests have been performed with the view to understand and quantify the swelling and sealing capability of bentonite against water inflow. The work was mainly concentrated to understand the process in which the swelling in the bentonite is competing with the eroding water. The tests aimed at finding the levels of water pressure and water flow at which the bentonite is sealed and the water flow is stopped.

The tests are divided into two main types, flow-controlled and pressure-controlled. In the flow-controlled tests, the water flow was held at a constant level by use of a GDS. In the pressure-controlled tests, the water pressure was held at a constant level by use of gravity.

6.2 Test design and test data

The first preliminary tests used a design according to Figure 6-1. A bentonite block with 49 mm diameter was put into a container with 50 mm diameter so that a 0.5 mm annular gap was formed between bentonite and container. The block had a height of 120 mm. The water was let in through a hole at the bottom of the container and was let out through a slot at the top. The swelling pressure was in these tests measured at the mid height of the block. In the flow-controlled tests, the water pressure was measured at the inlet side. In the pressure-controlled tests, the water flow was measured by regularly weighing the outgoing water.

Three pressure-controlled tests were done with this geometry, and for each test, the water pressure was reduced until the flow was stopped. In the same way, eight flow-controlled tests were done with decreasing flow rate until stop was achieved. Figure 6-2 shows an unsealed piping of a sample after dismantling.

Since this test configuration gave some uncertainty about the repeatability of the tests, the test design was modified in order to better control the parameters. Instead, the water was led through a hole drilled in the centre of the bentonite sample, which had the same dimensions as in the first design. In this case there was also a possibility to vary the diameter of the drilled hole in order to make parametric studies. The new geometry is shown in Figure 6-3.

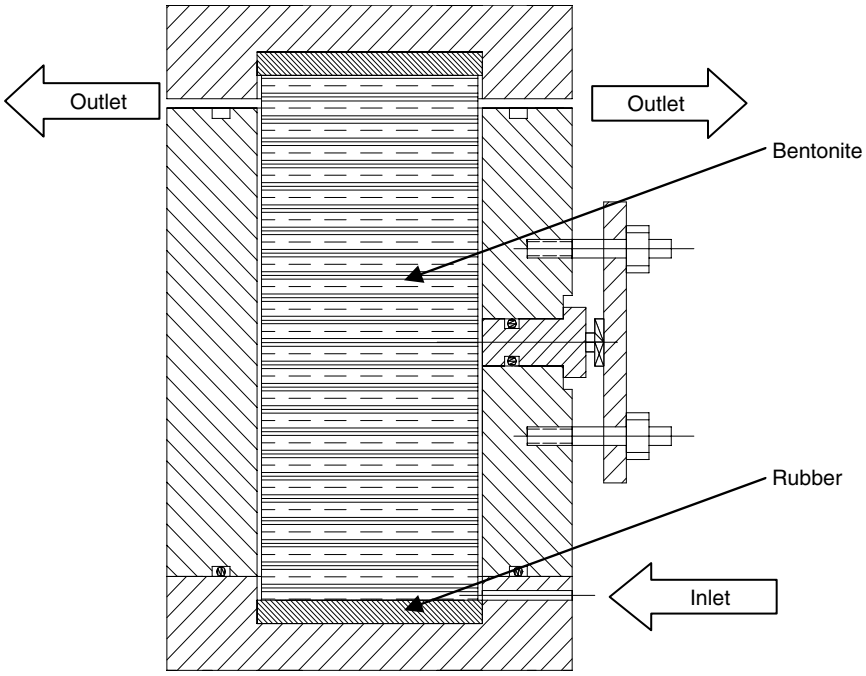

Figure 6-1. *First test design with water inlet through a 2 mm hole at the bottom and outlet through a slot at the top of the bentonite sample.*

Figure 6-2. *Picture of a sample where the piping did not seal.*

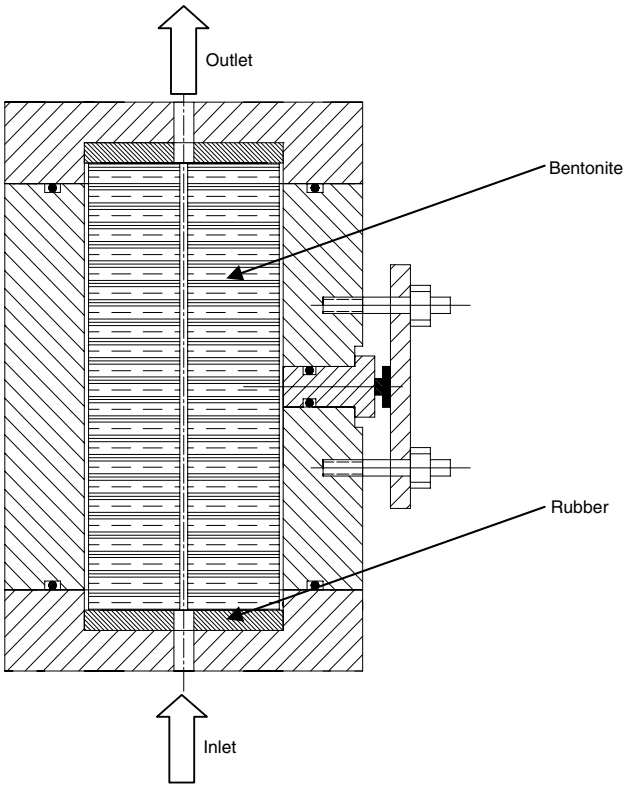

Figure 6-3. *Second test design with a central hole drilled through the bentonite block.*

Three alternatives of the new geometry in Figure 6-3 were used.

1. 2 mm drilled hole and height 120 mm.
2. 4 mm drilled hole and height 120 mm.
3. 2 mm drilled hole and height 20 mm.

For alternatives 1 and 2, a number of pressure-controlled and flow-controlled tests were performed with the aim to find the pressure- and flow levels where the water flow was stopped. Some flow-controlled tests with salt water were also performed. For alternative 3, two pressure-controlled tests were run. In the flow-controlled tests, the water pressure was measured at the inlet side. In the pressure-controlled tests, the water flow was measured by regularly weighing the outgoing water.

The bentonite blocks had a density of 2,000 kg/m^3 and a water ratio of 17.5%. In the flow-controlled tests and in some of the pressure-controlled tests, deionised water was used. With an exception for the tests with salt water (1.1% salt), tap water was used in the remaining of the pressure-controlled tests.

6.3 Results

The test data and test results are compiled in Table 6-1. The water pressure is given for the tests with constant water pressure and the flow rate is given for the tests with constant flow rate. The tests that did not go to piping are marked in bold and marked stop. For most of the tests with constant flow rate the erosion was measured by weighing the outlet water, drying it at 105°C and weighing the dry material. The dry weight and the resulting water ratio (weight of water divided to the dry weight) are included in the table.

Table 6-1. Data of the basic piping tests. The tests that yielded stop are marked in bold.

Test data Test id	Date	Inlet (mm)	Outlet (mm)	u (kPa)	Flow (l/min)	Water	Water ratio	Density (kg/m³)	Result	Erosion (gr)	Water ratio of eroded material w	Remarks
Test 1	19/2-2002	2	Gap	9.7	–	Deionized	0.183	1,995	No stop			
Test 2	20/2-2002	2	Gap	4.8	–	Deionized	0.183	2,000	No stop			
Test 3	**22/2-2002**	**2**	**Gap**	**2.4**	**–**	**Deionized**	**0.183**	**1,999**	**stop**			
Test 4	25/2-2002	2	Gap	–	0.02	Deionized	0.183	1,994	No stop			
Test 5	4/3-2002	2	Gap	–	0.01	Deionized	0.168	1,995	No stop			
Test 6	5/3-2002	2	Gap	–	0.005	Deionized	0.168	1,996	No stop			
Test 7	6/3-2002	2	Gap	–	2.50E–03	Deionized	0.168	1,998	No stop			
Test 8	**7/3-2002**	**2**	**Gap**	**–**	**6.25E–04**	**Deionized**	**0.168**	**2,011**	**Stop**			
Test 9	7/3-2002	2	Gap	–	1.25E–03	Deionized	0.168	2,002	No stop			
Test 10	**12/3-2002**	**2**	**Gap**	**–**	**6.25E–04**	**Deionized**	**0.168**	**1,983**	**Stop**			
Test 11	**14/3-2002**	**2**	**Gap**	**–**	**3.13E–04**	**Deionized**	**0.170**	**2,005**	**Stop**			
New geometry												
Test 12	**11/4-2002**	**2**	**2**	**2.8**	**–**	**Deionized**	**0.170**	**1,996**	**Stop**			
Test 13	**12/4-2002**	**2**	**2**	**4.3**	**–**	**Deionized**	**0.170**	**2,031**	**Stop**			
Test 14	12/4-2002	2	2	5.5		Deionized	0.170	2,007	No stop			
Test 15	22/4-2002	2	2	5.5		Deionized	0.170	2,006	No stop			
Test 16	25/4-2002	2	2	–	2.50E–03	Deionized	0.166	2,010	No stop	0.703	427	
Test 17	29/4-2002	2	2	–	1.25E–03	Deionized	0.166	2,015	No stop	0.637	235	
Test 18	30/4-2002	2	2	–	6.25E–04	Deionized	0.166	2,009	No stop	0.475	158	
Test 19	**3/5-2002**	**2**	**2**	**–**	**3.06E–04**	**Deionized**	**0.164**	**2,010**	**Stop**	**0.01**	**1,346**	
Test 20	16/5-2002	2	2	–	6.25E–04	Deionized	0.164	2,005	No stop	3,54	124	
Test 21	21/5-2002	2	2	–	2.00E–02	Deionized	0.169	2,011	No stop	0.52	1,346	
Test 22	**23/5-2002**	**2**	**2**	**–**	**2.00E–04**	**Deionized**	**0.169**	**1,986**	**Stop**	**–**	**–**	
Test 23	24/5-2002	2	2	13.5	–	Tap water	0.169	2,010	No stop	–	–	1)
Test 24	27/5-2002	2	2	9.5	–	Tap water	0.169	2,009	No stop	–	–	1)
Test 25	30/5-2002	2	2	–	5.00E–03	Deionized	0.169	2,006	No stop	1.01	594	
Test 26	10/6-2002	2	2	8.8	–	Tap water	0.169	1,999	No stop	–	–	1), 2)
Test 27	13/6-2002	2	2	13	–	Tap water	0.169	2,000	No stop	–	–	1), 2)
Test 28	**17/6-2002**	**2**	**2**	**5.8**	**–**	**Tap water**	**0.169**	**1,993**	**Stop**	**–**	**–**	**2)**
Test 29	24/6-2002	4	4	–	2.50E–03	Deionized	0.180	1,993	No stop	0.5	600	
Test 30	25/6-2002	4	4	–	1.25E–03	Deionized	0.180	2,019	No stop	0.37	405	
Test 31	**17/7-2002**	**4**	**4**	**1.4**	**–**	**Tap water**	**0.180**	**1,993**	**Stop**	**–**	**–**	
Test 32	**18/7-2002**	**4**	**4**	**2**	**–**	**Tap water**	**0.180**	**1,997**	**Stop**	**–**	**–**	
Test 33	**19/7-2002**	**4**	**4**	**2.35**	**–**	**Tap water**	**0.180**	**2,020**	**Stop**	**–**	**–**	
Test 34	**22/7-2002**	**4**	**4**	**3.05**	**–**	**Tap water**	**0.180**	**2,019**	**Stop**	**–**	**–**	
Test 35	22/7-2002	4	4	4.3	–	Tap water	0.180	2,014	No stop	–	–	
Test 36	24/7-2002	4	4	–	6.00E–04	Deionized	0.180	2,012	No stop	0.53	108	
Test 37	**25/7-2002**	**2**	**2**	**4.3**	**–**	**Tap water**	**0.180**	**2,021**	**Stop**	**–**	**–**	
Test 38	**30/7-2002**	**2**	**2**	**–**	**3.06E–04**	**Salt water**	**0.190**	**2,031**	**Stop**	**–**	**–**	
Test 39	**30/7-2002**	**2**	**2**	**–**	**6.12E–04**	**Salt water**	**0.190**	**2,031**	**Stop**	**–**	**–**	
Test 40	30/7-2002	2	2	–	2.50E–03	Salt water	0.190	2,034	No stop	5.6884	53	
Test 41	21/8-2002	2	2	3.3	–	Tap water	0.190	2,064	No stop	–	–	3)
Test 42	21/8-2002	2	2	1.7	–	Tap water	0.190	2,050	No stop	–	–	3)

Figures 6-4 and 6-5 show examples of the results of flow-controlled tests. Water pressure is plotted as a function of time. In Figure 6-4 the flow rate was 2×10^{-4} l/min The test resulted in stop at the water pressure 1 MPa after 30 minutes. The figure shows that the flow continued without stopping and without an increase in pressure for 20 minutes. After 20 minutes the gel stopped further water inflow and this resulted in an increase in water pressure. The increase rate is rather high, corresponding to 600 kPa in 5 minutes (see Chapter 7). This pressure increase rate is controlled by the properties of the GDS apparatus. Figure 6-5 shows an example of the same type of test but with a higher flow rate that did not result in sealing

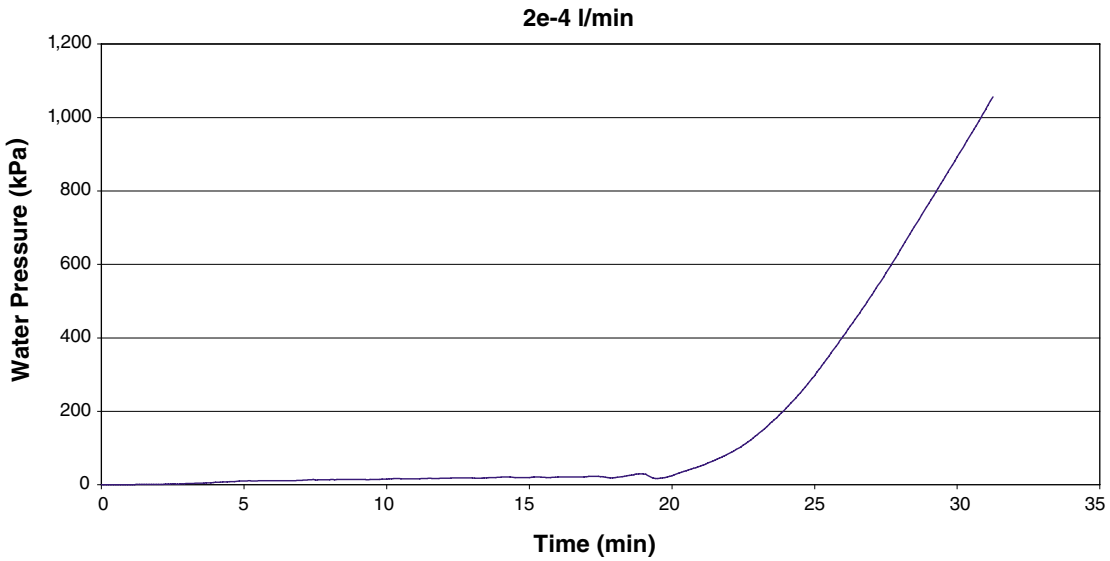

Figure 6-4. *Example of a flow controlled piping test that resulted in sealing. Flow rate 2×10^{-4} l/min The test was stopped after 30 minutes at the water pressure 1 MPa.*

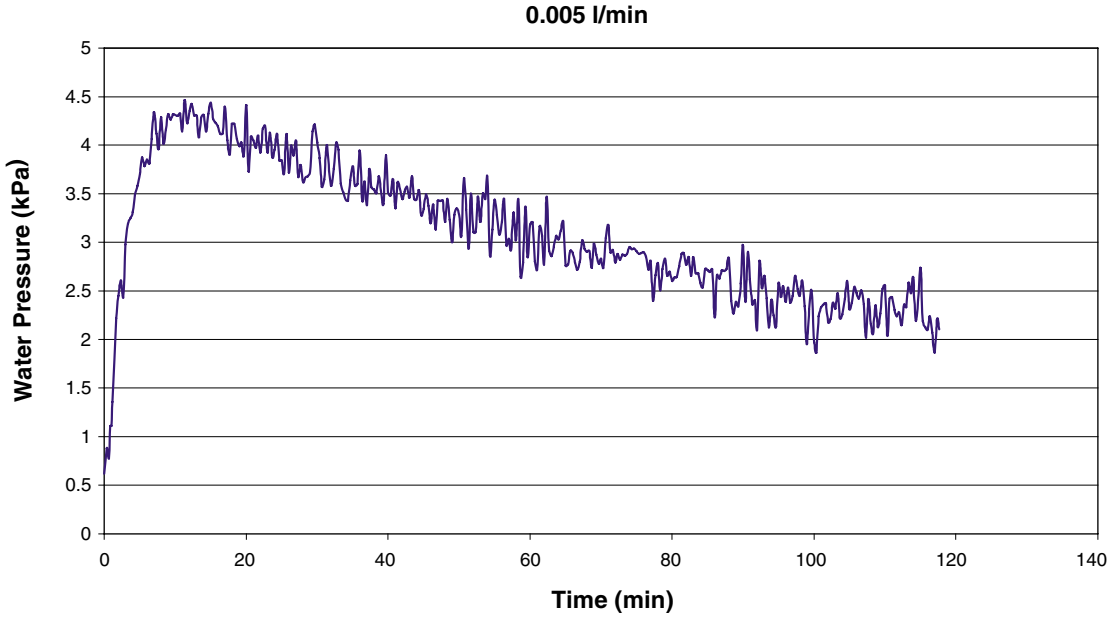

Figure 6-5. *Example of a flow controlled piping test that did not result in sealing. Flow rate 5×10^{-3} l/min.*

Figure 6-6 shows an example of a test with constant water pressure that did not result in sealing. Water flow is plotted against time.

The results of the tests with a central hole are shown in three diagrams with plots of the water velocity, channel diameter and water pressure, all plotted versus water flow. The channel diameter and the resulting water velocity can be calculated from the measured water flow since the water pressure is measured (or applied) assuming laminar flow in a pipe. In the diagrams, each test is represented by just one point or a line connecting two points. The first point in each test represents time = 0 and the second represents time = 30 min after test start. Thus, the tests, which are represented by only one point, did not run for 30 min because the flow was stopped by bentonite swelling (successful tests). In the flow-controlled tests, "stop" is defined by a measured pressure on the inlet side of 1 MPa.

In Figure 6-7, the water velocity data are shown. One should notice that the flow rates for the pressure-controlled tests are several orders of magnitudes larger than for the flow- controlled tests. This is because the flow-controlled tests were run with a very fast increase in pressure as shown in Figure 6-4. If there is a tendency to stop, the water pressure increases rapidly and the channel becomes free again. Thus, the flow rate must be very low if the swelling bentonite is to stop the flow.

It is not directly clear if the velocities have increased or decreased in the flow-controlled tests. However, a study of Figure 6-8 shows that they must have increased since all the diameters have decreased and the flow is held constant. Figure 6-9 shows that the water flow rate must be less than about 10^{-3} l/min if the flow is controlled and the water pressure must be lower than 2–4 kPa if the water pressure is controlled. In Figure 6-9 all tests with flow rate lower than 0.03 l/min are flow controlled and all tests with higher flow rate are pressure controlled. The flow rate is thus rather high for all pressure controlled tests, due to the large initial diameter of 2–4 mm.

The results of the erosion measurements are shown in Figure 6-10.

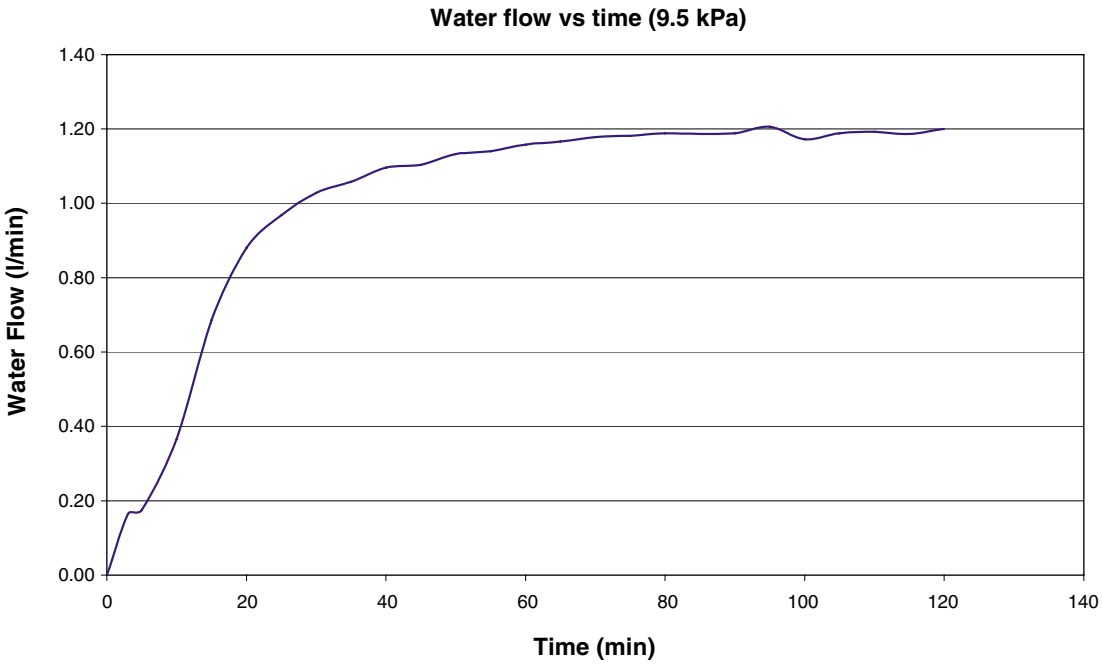

Figure 6-6. *Example of a pressure controlled piping test with the constant water pressure 9.5 kPa that did not result in sealing.*

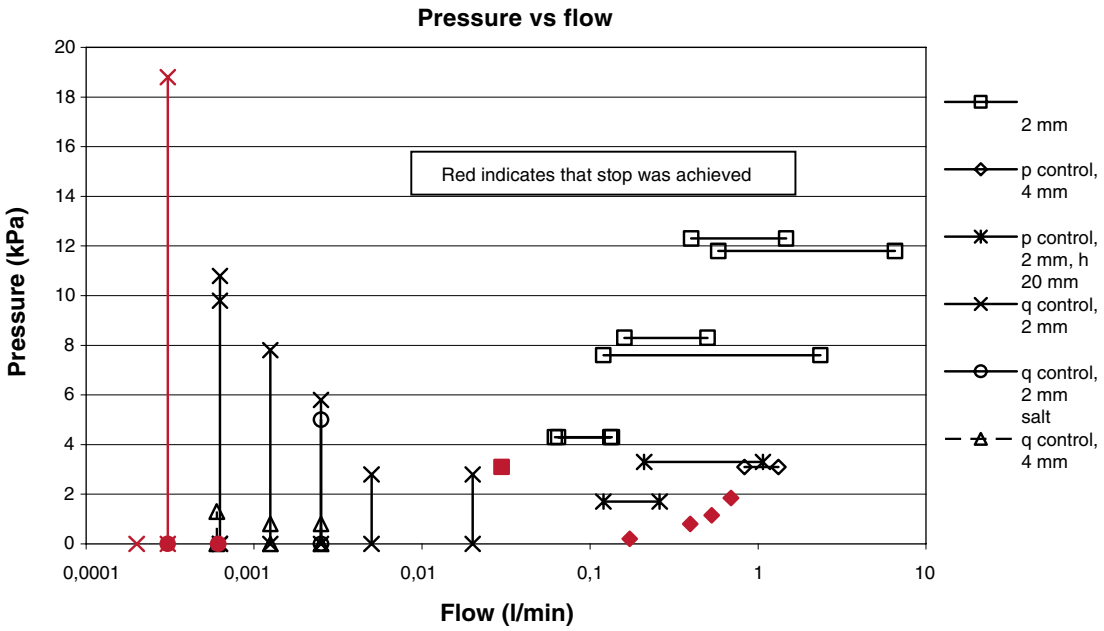

Figure 6-7. *Water pressure versus water flow. Red colour denotes stop.*

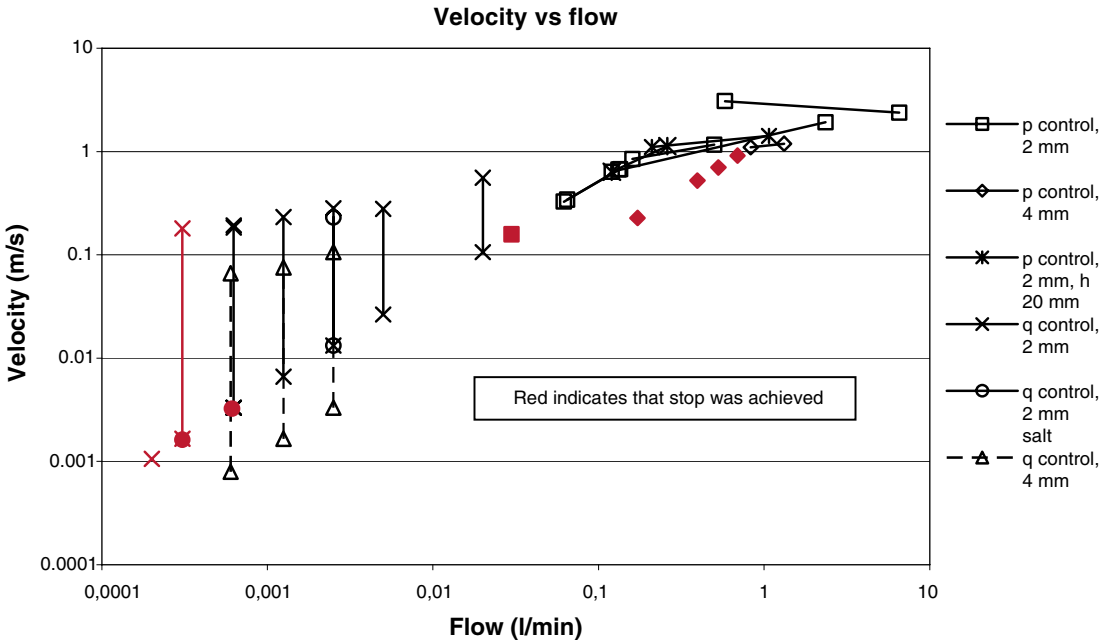

Figure 6-8. *Water velocity versus water flow. Red colour denotes stop.*

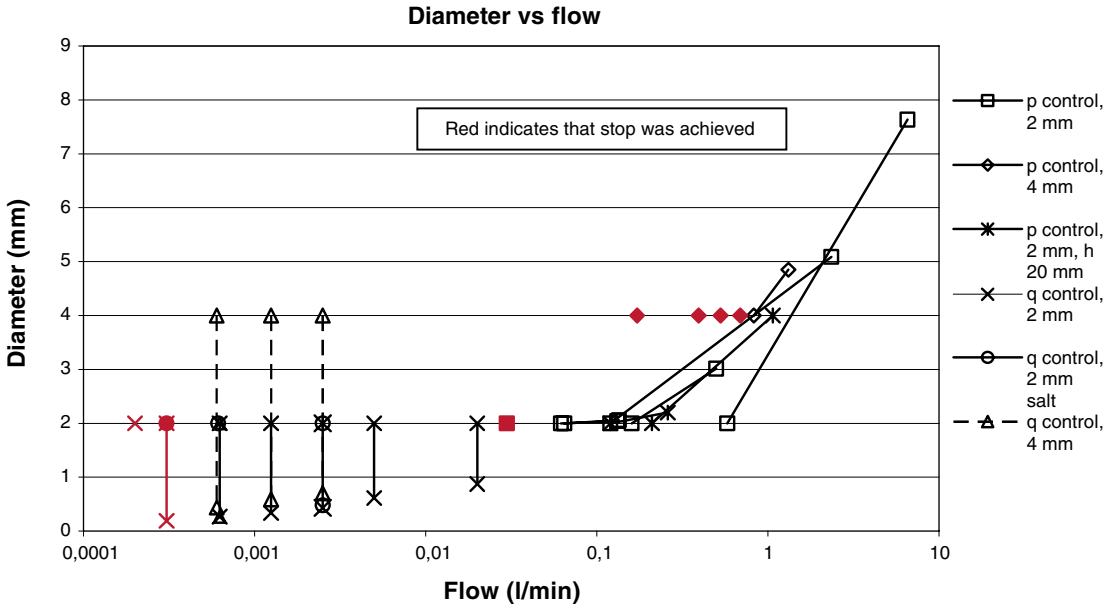

Figure 6-9. *Water velocity versus water flow. Red colour denotes stop.*

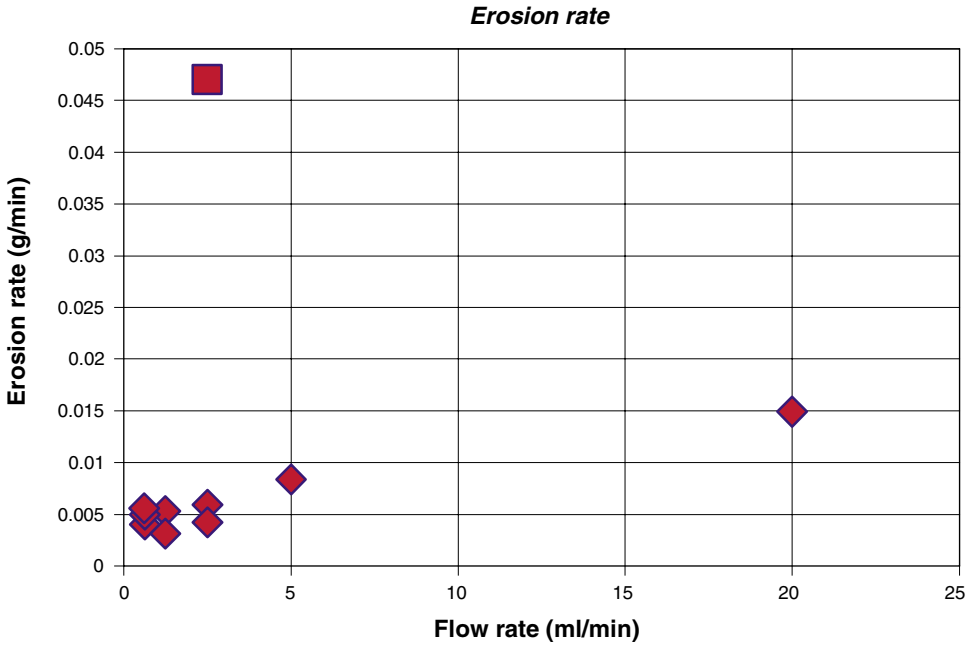

Figure 6-10. *Erosion rate plotted as a function of the flow rate. All tests are made with tap water except the test with high erosion rate that was made with 1.1% salt in the water.*

6.4 Preliminary conclusions

Conclusions and comments derived from the results of the laboratory tests:

- Very low water pressure is sufficient to cause piping and erosion at constant water pressure (2–4 kPa)
- Very little water flow is sufficient to cause piping and erosion at constant water flow (less than 0.001 l/min)
- The processes are complicated with many variables and dependent variables
- The length of the piping channel is one parameter that influences. The longer the channel the better the ability to seal
- Salt in the ground water improves the possibility for the bentonite to seal but increases the erosion rate strongly
- The values 2–4 kPa and 0.001 l/min are probably conservative since they are combined with either high water pressure or high water flow rate
- The hydraulic function of the rock is very important since it determines the flow rate and the pressure increase rate.
- After a long time the sealing is helped from other wetting parts and is expected to tighten all leaks if the swelling pressure is higher than the water pressure
- The distance block is thus expected to function if the water flow is not so high that the erosion reduces the density but it may take years for it to seal

One conclusion from these tests is also that more realistic flow and pressure control should be used in further testing and that the complexity of included parameters calls for scenario simulations.

7 Investigations of the sealing function of the distance blocks

7.1 Introduction

As shown in Chapter 6 the sealing and piping/erosion phenomena are very complex with many parameters and need to be tested in realistic environment since the theoretical understanding is not enough today. The sealing/piping/erosion phenomena of the distance blocks have therefore been further investigated in three studies with the following ingredients:

- Modelling of inflow and piping scenarios both conceptually and in the laboratory.
- Performing tests with realistic inflow properties.
- Simulating the function of the distance plugs for preventing piping.
- Examining the effect of water pressure build-up behind the distance block after sealing.
- Development of an engineering solution for handling the problems.
- Large scale tests of the solutions.

The tests have been divided into three different series:

1. Test series I in scale 1:10 for testing the piping scenario.
2. Test series II in scale 1:10 for testing the effect of water pressure build-up behind the distance block.
3. Test series III in full scale for testing the scale effect.

Only the concept with a distance block that is intended to seal every container section and not let water pass the block (“tight distance block concept”) has been investigated in these test series. This concept is described in Chapter 2.2 and Chapter 9.

7.2 Conceptual model

The following example of a conceptual model of the inflow and piping scenario has been the base for the tests:

Inflow takes place in one point above and in the centre of the package with the perforated steel container and the buffer and canister with the inflow rate 0.1 l/min. Water pressure builds up to 2,000 kPa in the fracture if water inflow is stopped. The rate of water pressure increase is 100 kPa/h when the inflow through a fracture is stopped.

The rate of water pressure increase is taken from hydro-geological considerations (Rehn, pers comm. 2003).

This inflow yields the following scenario for one section:

After 1 day	4 m^2 of the floor is filled with water and gel
After 2 days	The gel reaches the distance block
After 3 days	The entire bottom is filled (to 2 m width). The water or gel level will rise 0.2–0.4 mm/min either on one side at a time or simultaneously
After ~ 10 days	The entire gap is filled with gel and water

The maximum amount of water absorbed by the buffer periphery is ~ 0.01 l/min.

The last part to be sealed is thus the top of the plug. At the same time the water pressure will rise and

1) if there is no unfilled space left to reduce the water pressure increase and the rate of water pressure increase is too high for sealing there will be piping. Once piping has occurred there is a big risk that the water flow rate is too high for sealing to occur as seen in Chapter 4,
2) if the rate of water pressure increase is low enough in combination with the geometrical factors there may not be piping or the initial piping may heal,
3) if there is no piping the water pressure in the fracture and in parts of the gel filled gap will rise to 2,000 kPa in 20 hours.

The scenario is likely to be the same in spite of where the inflow takes place or if it takes place in many spots instead of in one spot. The main parameters that are important are the inflow rate and the rate of water pressure increase. The further testing has therefore been concentrated on this scenario and the following basic inflow properties (reference case)

- Inflow rate: 0.1 l/minute.
- Water pressure increase rate: 100 kPa/h.

but the sensitivity and upper limits are also checked by testing also other values.

7.3 Sealing tests in the scale 1:10, series I

In the first test series the sealing and piping properties of the distance block was tested. Half the dismantled test equipment for the test scaled 1:10 described in Chapter 4 was used for testing the sealing scenarios. In order to simplify the test the entire perforated steel container package was replaced by a dummy container of PVC. Only the distance block was simulated with bentonite. Figure 7-1 shows the test equipment.

Water was filled in one point above the container. The rate of filling is difficult to scale. 0.01 l/min was chosen for most of the tests in this series. This is 10 times lower than the basic scenario but the scale yields that the theoretical time to fill up the slot was only 2 hours compared to 10 days for the full scale. However, there was initial some leakage leading to an actual filling time until start testing of between 5 and 10 hours. The filling rate is thus a compromise between the inflow rate 0.1 l/min and the filling time 10 days. It is probably more relevant to model the correct filling time, which means that the tests are conservative in this respect.

Outside the distance block the next container was simulated with the lid of the test tube and a slot at the periphery of the lid. Eight outlet channels were leading the water from the slot out to a vessel where the out flowing water was collected.

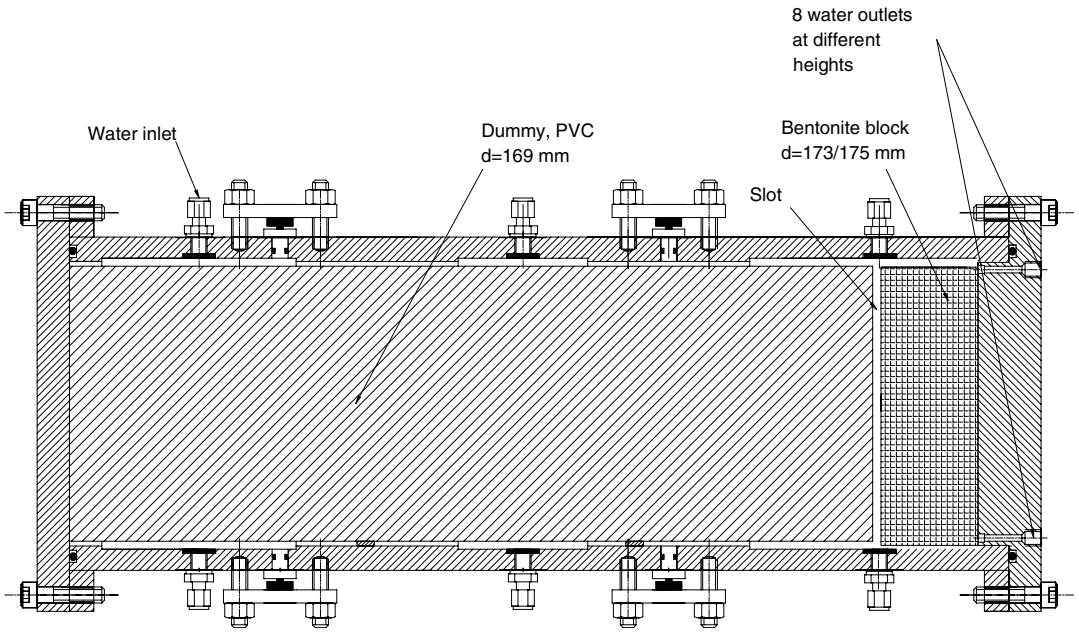

Figure 7-1. *Layout of the sealing tests in scale 1:10, series I.*

The basic conditions for the tests were the following (but other conditions were also tested):

- Bentonite plug with ρ = 2,076 kg/m^3 and w = 10.6%.
- Annular gap at the plug: 4 mm for the entire diameter.
- Filling rate 0.01 l/min with the water pressure 10 kPa.
- Total slot space 1.2 l.
- Pressure increased to 1,500 kPa if possible.

The tests started with water filling until no more water entered. The water filling was in all tests followed by a leakage through the plug. The leakage was generally several liters. When the leakage and the water inflow stopped the pressure increase was started. Seven tests have been performed with mainly different rate of water pressure increase but also different geometry.

Figures 7-2 and 7-3 show examples of two results. Figure 7-2 shows test 4 where the pressure increase rate was 250 kPa/h. The water pressure and volume are shown as function of time after start pressure increase. The figure shows that the water pressure was increased to 1,100 kPa during a water inflow of totally 0.1 l. The inflow is caused partly by water uptake of the bentonite and partly by compression of entrapped air. After about 4 hours, when the pressure reached 1,100 kPa piping occurred resulting in a pressure drop and a water flow until the GDS apparatus was emptied. The piping in this test was rather dramatic, since the gel that sealed the gap was shot out of the equipment and stuck on the wall several meters away. Compressed air inside the distance block made it work like an air-gun.

Figure 7-3 shows test 5 where the pressure increase rate was 50 kPa/h. The water pressure could be increased to 1,500 kPa without piping and the water inflow was about the same as for test 4. Due to the slower pressure increase rate the test took about 1.5 days.

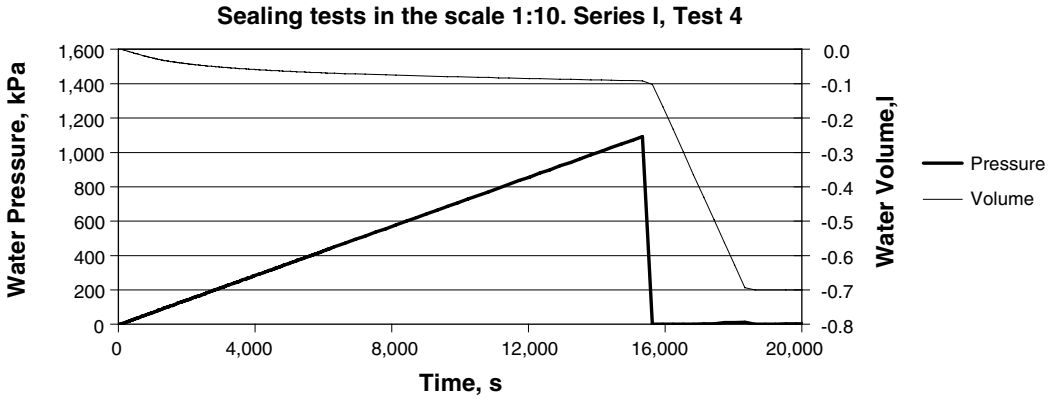

Figure 7-2. *Water pressure and water inflow as function of time for test 4.*

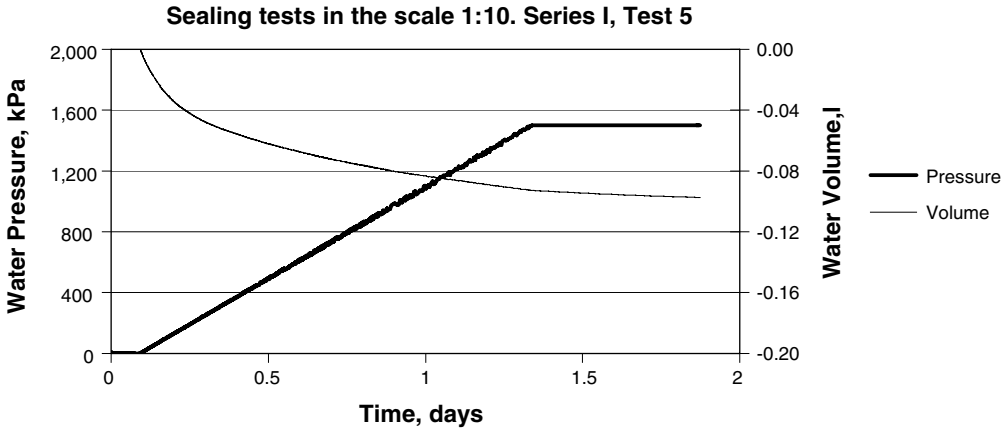

Figure 7-3. *Water pressure and water inflow as function of time for test 5.*

The results of all 7 tests are described in Appendix 4 with the same type of figures. All results are compiled in Table 7-1. The table shows that 500 and 250 kPa/h yield piping although the limit seems to be not too far from 250 kPa/h. 50 kPa/h work for all test cases. 250 kPa also works if the filling rate is reduced as shown by test 7. Test 1 was left for 2.5 days before being tested and could therefore withstand a very fast pressure increase.

The table also shows that all tests yielded a rather large leakage before the plug sealed, except for at the very slow filling of test 7.

The conclusions from these tests were that the filling rate and the water pressure increase rate are very important for the sealing ability. With the basic inflow scenario 0.1 l/h and 100 kPa/h the distance plug seems to work in the scale 1:10, i.e. when the gap between the rock and the plug is 2–4 mm.

Figure 7-4 shows the plug after dismantling of test 5. The wetting of the periphery and the unaffected larger part of the block is clearly seen.

Table 7-1. Compilation of the most important prerequisites and results of the piping tests in scale 1:10, Series I. See also Appendix 4.

Test no	Time until stop leakage (h)	Leakage before test start (l)	Water pressure increase rate (kPa/h)	Pressure at breakthrough (kPa)	Comments
1a	10	3.5	–	No breakthrough	10 kPa water pressure
1b	–	–	9,300	No breakthrough	Left 62 hours before test
2a	6.3	1.1	500	Breakthrough at 22 kPa	
2b	–	–	50	No breakthrough	Left 20 min before test
3	4.5	2.0	50	No breakthrough	
4	6.7	1.8	250	Breakthrough at 1,100 kPa	Shootout!
5	5.3	2.0	50	No breakthrough	
6	6.2	2.5	50	No breakthrough	No axial slot
7	26.3	0.1	250	No breakthrough	Filling rate 0.001 l/min

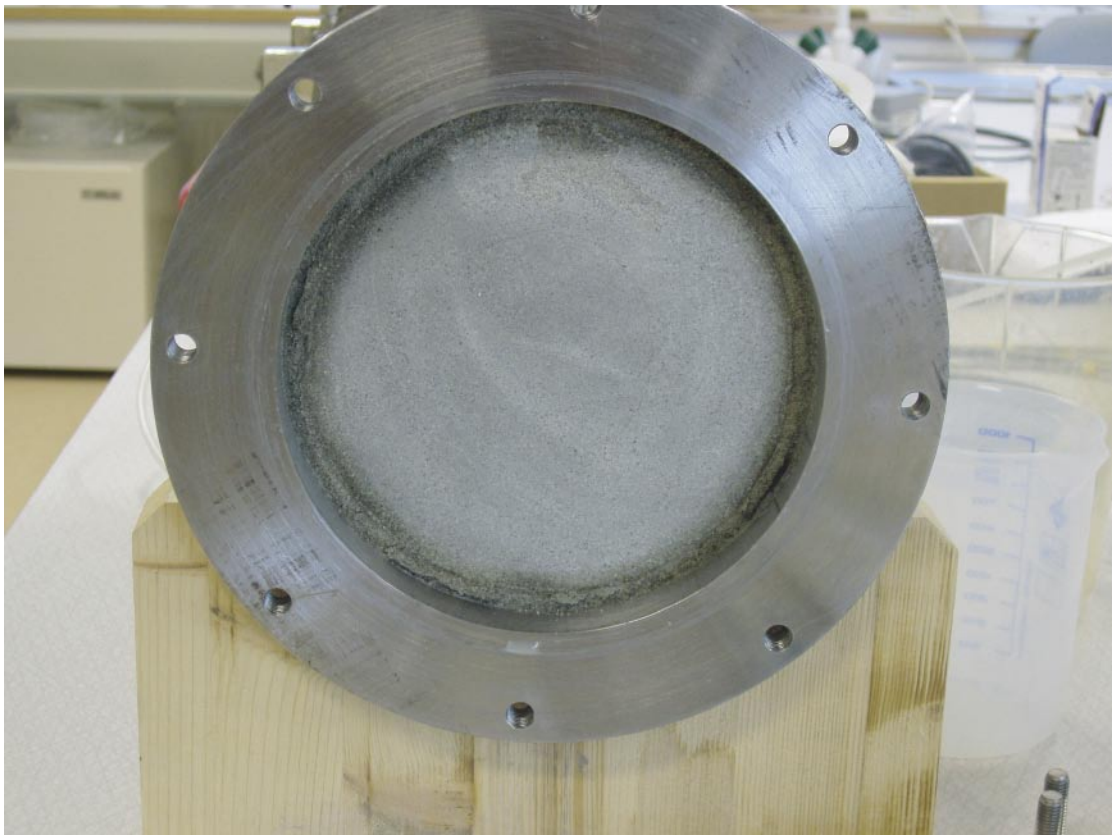

Figure 7-4. *Picture of the plug taken after dismantling of test 5.*

7.4 Sealing tests in the scale 1:10, series II

7.4.1 Test set-up

In the second test series the need for support of the distance block and the forces built up by the swelling and water pressure on the plug were tested. For these tests the equipment used in series I was modified in order to measure displacement or forces on the plug during the water filling. Figure 7-5 shows the test equipment.

Water was filled in one point above the container. The rate of filling was reduced 20 to 100 times compared to series I yielding a filling rate of between 1.5 and 6 days (except for the first test). In the first two tests the block was free to move axially and the displacements of the block were measured. The test showed that the block moved early and that the block thus needed to be fixed. In test 1 no ring was used and in test 2 a “leaking” steel ring was placed outside the distance block and used for the remaining tests. The axial displacement of the bentonite plug was measured in tests 1 and 2 and the axial load was measured in tests 3 to 9 by sensors positioned against the steel ring. In addition the radial swelling pressure of the distance block was measured in two directions, upwards and downwards. Water that leaked past the bentonite block was collected in a vessel.

The basic conditions for the tests were the following:

- Bentonite plug with $\rho = 2{,}076$ kg/m^3 and w = 10.6%.
- Annular gap at the plug: 4 mm for the entire diameter.
- Filling rate between 0.0001 l/min up to 0.01 l/min.
- Total gap space 0.92 l.
- Pressure increased up to 2 MPa (5 MPa in Test 6 and 7) if possible.

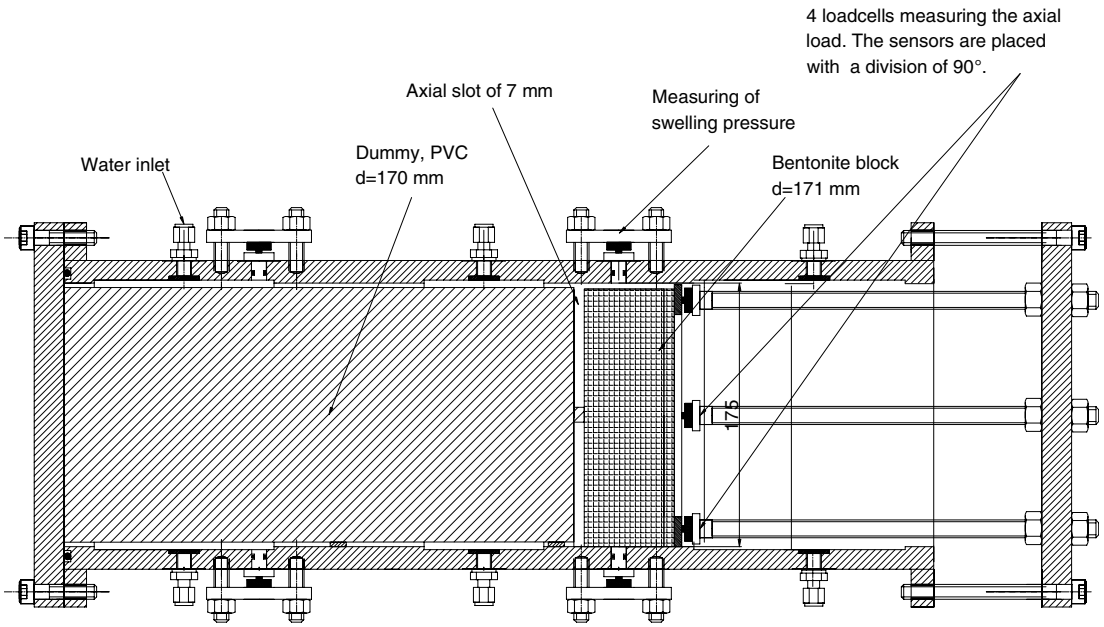

Figure 7-5. *Layout of the sealing tests in scale 1:10, series II. The axial slot was only used in tests 5–9.*

The tests started with water filling at 10 kPa pressure with constant flow until no more water entered. The leakage past the plug was in all tests in this series small or zero except for test 1. When the leakage and the water inflow stopped the pressure increase was started.

Nine tests have been performed with a number of parameters varied:

- In the first two tests, the displacement of the distance plug was measured during the water filling. When large movements of the plug were allowed, it was not possible for the bentonite to seal. In test number 3 to 9 the ring was fixed by exchanging the displacement sensors for load cells. With this test arrangement it was not possible for the plug to move.
- The rate of water filling was varied between 0.0001 l/min and 0.01 l/min, which yielded a filling time between 1 and 144 hours.
- All tests except for two were performed with tap water. In test 4 a solution with 3.5% NaCl was used and in test 9 a solution with 2% NaCl/CaCl was used.
- In tests 5 to 9 the distance block was positioned 7 mm from the container by use of a small plastic disc, mounted on the container, with the purpose to study the consequences of an undesired slot between the blocks or between the block and the container. Such a slot increases the risk of having very high force acting on the block from the water pressure that may be built-up in the slot.

Figure 7-6 shows a picture of the equipment used for test series II.

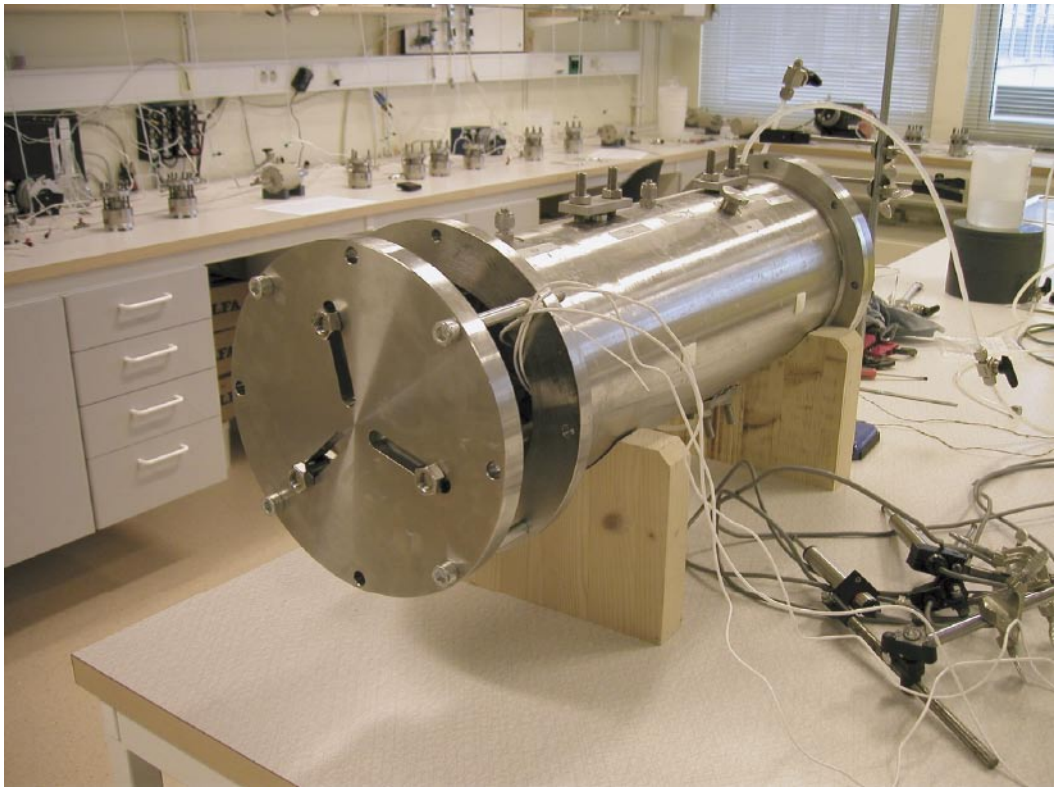

Figure 7-6. *Picture showing the equipment used in test 2 of series II of the scale tests in the laboratory. Three force transducers are placed inside the end plate in this test. The number of force transducers was increased to 4 in the coming tests.*

7.4.2 Test results

Figure 7-7 and 7-8 show examples of results from one of the tests. Figure 7-7 shows that water filling continued for 5 days and that the water pressure increase to 2,000 kPa went on without piping. The water pressure was kept for another 3 days and then the test was dismantled. Figure 7-8 shows as a function of time the axial load measured in 4 locations on the supporting ring and the radial pressure measured in the periphery of the distance block above and below the block. The axial load increase is a direct reflection of the water pressure increase but there is also a continuing increase during the remaining 3 days of the test, despite keeping the water pressure constant. The swelling pressure did not start to increase until two days after the water pressure increase, the reason being mainly that the pressure was measured in the centre of the periphery and that it took some days for the water to reach that part due to the good sealing of the innermost part of the block.

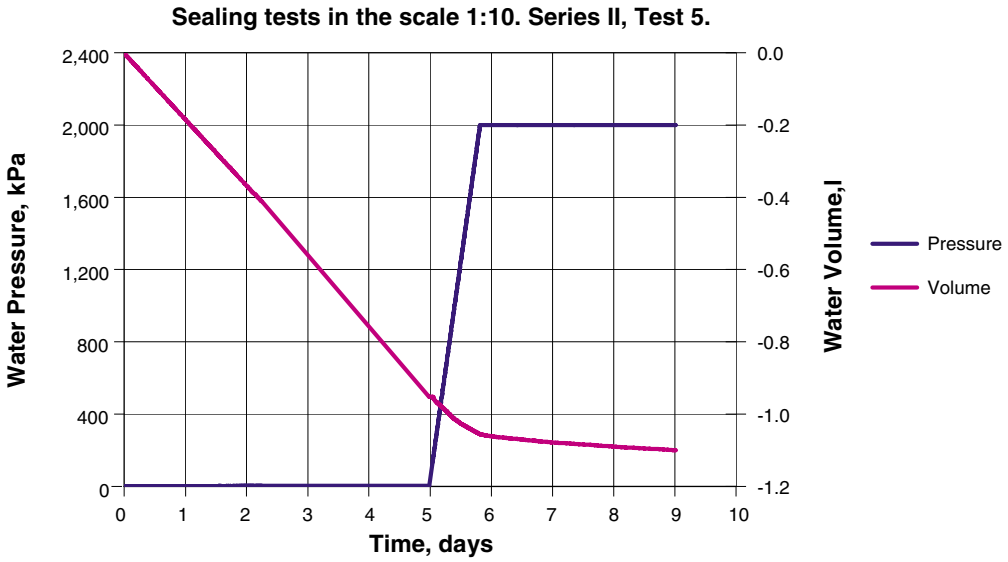

Figure 7-7. *Water pressure and water inflow as function of time for test II-5.*

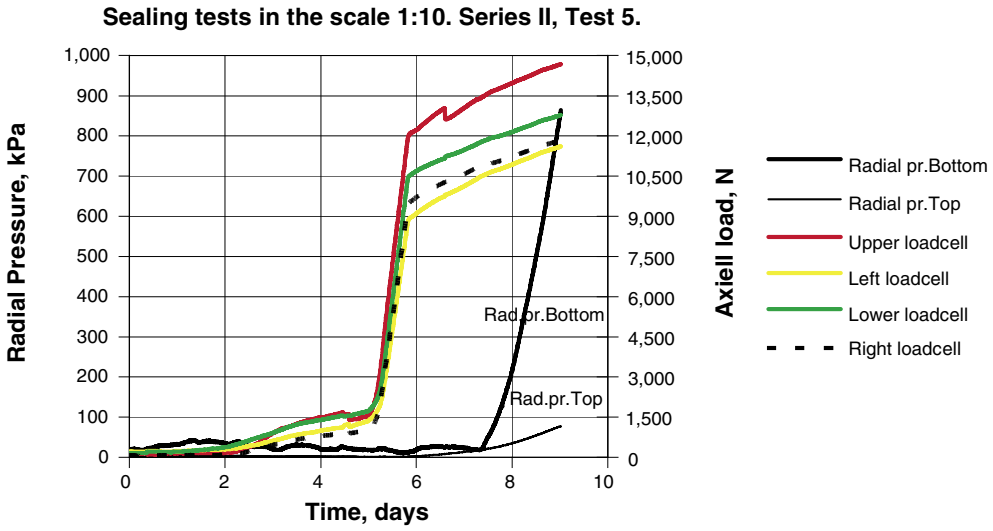

Figure 7-8. *The axial load and the radial swelling pressure as function of time for test II-5.*

All test results from the 9 tests in series II are shown in Appendix 5. The results are compiled in Table 7-2. The table shows that the sealing worked for all tests with a fixed supporting ring but that the sealing could not handle a water pressure higher than 2.5 MPa, since test 7 yielded piping at that pressure in an attempt to test the pressure limits.

One important and interesting issue is how the force from the pressurized water is transferred to the distance block and the supporting ring. Free water or slurry of water and bentonite fills up the space behind the perforated container, when the water pressure starts to rise. It is most likely that this part will exert full pressure towards the distance block and the ring. This means that the minimum force will be the water pressure multiplied with the cross sectional area behind the container. However, the water pressure may also spread radially into the interface between the distance block and the end plate of the container especially if there is a slot between the container and the block as simulated in tests II-5 to II-9. In addition there is a swelling pressure that will be built-up with time.

These phenomena can be studied if the sum of the forces on the supporting ring are recalculated to area by dividing the applied water pressure with the force and further on to a fictive distance from the "rock" surface (see Chapter 9) by assuming that the pressure is axially symmetric. Figure 7-9 shows the results of such calculations for all 7 tests, with the distance from the rock of full water pressure plotted as function of the applied water pressure. The distance between the dummy container and the "rock" is in this test 2.5 mm.

Table 7-2. Compilation of the most important prerequisites and results of the piping tests in the scale 1:10, Series II. See also Appendix 5.

Test no	Type of measurement	Filling rate, l/min	Filling time, h	Leakage during filling	Comments
II-1	Axial deformation	0.01	1.25	All water	Test run for 8 days. **Block did not seal**.
II-2	Axial deformation	0.00017	72	Nothing	Pressure ramp 100 kPa/h. **Block did not seal**.
II-3	Axial load	0.00017	144	Nothing	Pressure ramp 144 kPa/h to 2,000 kPa. **Block sealed**.
II-4	Axial load	0.0001	120	150 cl	3.5% NaCl/$CaCl_2$, pressure ramp 100 kPa/h to 2,000 kPa. **Block sealed**.
II-5	Axial load	0.00013	120	Nothing	Axial slot, pressure ramp 100 kPa/h to 2,000 kPa. **Block sealed**.
II-6	Axial load	0.00064	24 (144)	Nothing	Axial slot, pressure ramp 100 kPa/h to 5,000 kPa. **Block sealed but needed recovery time**[1)].
II-7	Axial load	0.00013	120	A few cl	Axial slot, pressure ramp 100 kPa/h to 5,000 kPa. **Block sealed up to 2.5 MPa then breakthrough**.
II-8	Axial load	0.00032	48	A few cl	Axial slot, pressure ramp 100 kPa/h to 2,000 kPa. **Piping, 2h recovery, Block sealed.**
II-9	Axial load	0.00037	36	A few cl	Long term test (92 days). Two blocks, axial slot, 2% NaCl/CaCl, pressure ramp 100 kPa/h to 2,000 kPa. **Block sealed.**

1) After the fast filling time 24 hours there was no sealing. The test was left for some days corresponding to the total time 144 hours and then the block sealed.

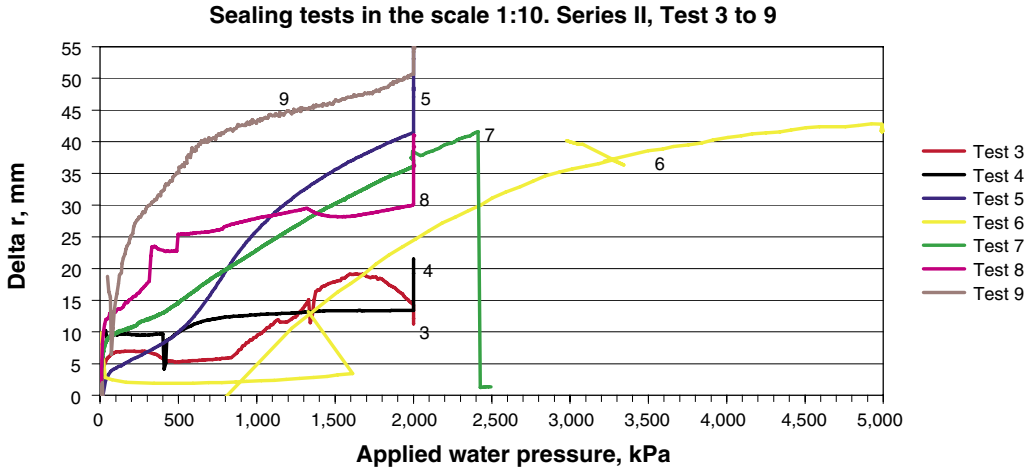

Figure 7-9. *Involved area of full water pressure measured in axial direction (calculated as distance from the "rock") as function of the applied water pressure.*

Figure 7-9 shows that the area (or radial distance) is successively increasing with increasing water pressure. The pressurised distance is substantially larger than the gap width between the container and the "rock" (2.5 mm), which implies that the water pressure is propagated into the block (or between the block and the container) but not all way to the centre (corresponding to 87.5 mm). The pressure continues to increase somewhat also after the water pressure is set to be constant. The influence of a vertical slot of 7 mm between the distance block and the container can also be seen. Tests 3 and 4 (without slot) yield a penetration of 15 mm, while the other tests (with slot) yield a penetration of 40 mm in average.

The distance block thus efficiently prevents the water pressure from propagating radially all the way to the centre, but there is also a pressure build up with time so the long term function for 90 days until closure of the tunnel needs to be investigated. Consequently the last test was left for 90 days after water pressure increase and the resulting forces and swelling pressure studied. Figures 7-10 and 7-11 show the results.

Figure 7-10 shows that there is a slow inflow of water, which is not caused by leakage past the distance blocks but by water uptake in the bentonite. Figure 7-11 shows that there is an increase in force and swelling pressure in the bottom that ceases after about 60 days, while the swelling pressure development in the top of the distance blocks is delayed.

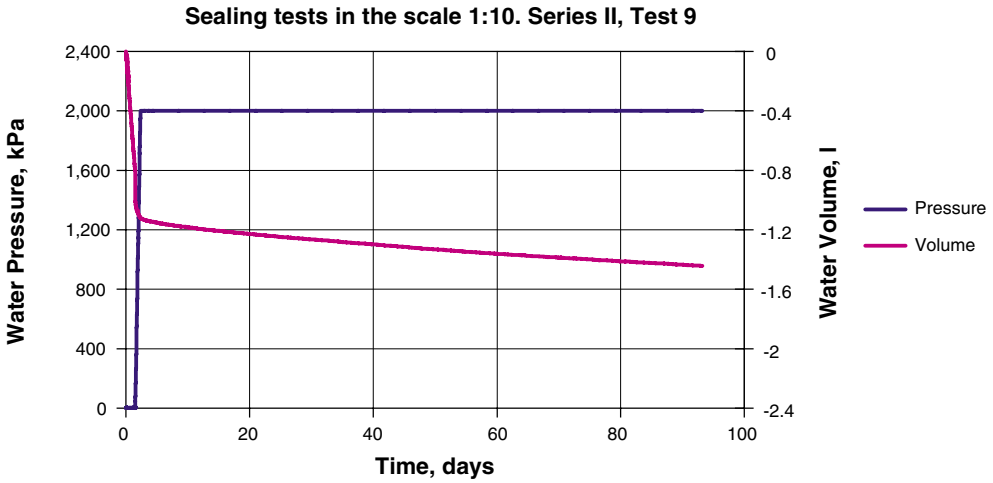

Figure 7-10. *Long term scale test II-9. Water pressure and water inflow as a function of time.*

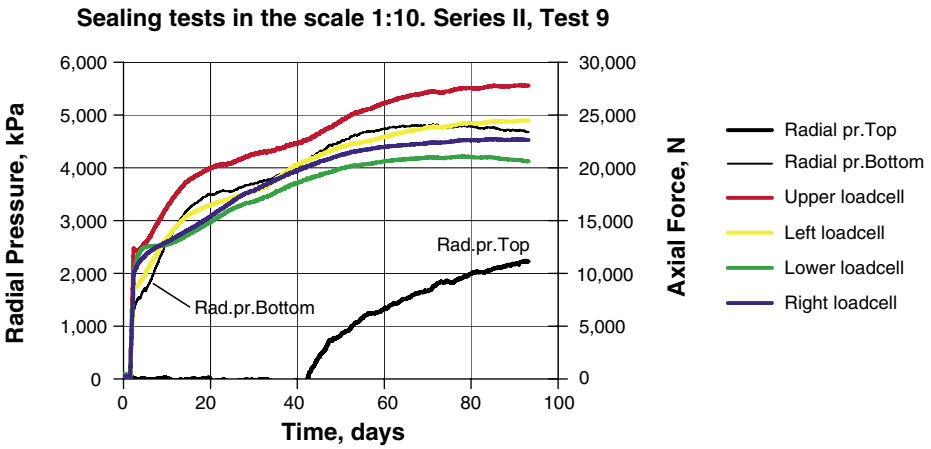

Figure 7-11. *Long term scale test II-9. Axial load and radial swelling pressure as a function of time.*

7.4.3 Dismantling

The test sequence, the test results and the observation during dismantling for all tests are shown in Appendix 5. Some examples will be given in this text.

Figure 7-12 shows a picture taken after dismantling of test 3. The picture shows that only a small triangular part of the block has been involved in the sealing. The wetting and swelling has only reached about 2 cm axially and radially.

Figure 7-13 shows a picture taken after dismantling of test 7. The picture shows that the block has cracked and thus the probable reason for water piping was not the sealing ability but the low strength of the block. The test was interrupted after cracking. It should be noted that the thickness of this block is relatively smaller than the total thickness of the distance blocks in a real concept.

Figure 7-12. *Picture showing a part of the distance block after dismantling of test 3. The left side faced the PVC dummy. The picture shows that only a small part of the block was active in the sealing process.*

Figure 7-13. *Picture from test II-7 showing the outside of the block after removal of the load cells and the steel ring. When the inner water pressure reached 2.5 MPa a central part of the distance block cracked.*

7.4.4 Conclusions

The conclusions of these tests are that

- a supporting ring that captures part of the water pressure inside the distance block is required,
- the sealing of the distance block works very well for the reference case with the suggested solution,
- the sealing did not work for higher water pressure than about 2,000 kPa for the reference conditions,
- the water pressure reaches 15–50 mm radially into the block at the applied scale and geometry,
- the sealing function works well during at least 90 days although the force was doubled during the first 60 days and then remained constant,
- a gap between the container and distance block should be avoided as far as possible since it increases the force on the ring although the sealing ability works well also in radial direction if the gap is not too wide. This is logical since the radial sealing has the same mechanisms as the axial sealing and the smaller the slot the better sealing ability.

7.5 Sealing tests in large scale

7.5.1 Test set-up

The sealing tests in scale 1:10 resulted in the conclusion that the distance blocks work properly for sealing water inflow at the reference case. However, the open annular gap is due to the scale effect only 2–4 mm compared to 2–4 cm in full scale. The gap width is thus unfavorable in full scale. On the other hand the block is 10 times thicker and pellets can be used in the gap if it is larger than 1 cm.

The only way to investigate the scale effect is thus to do full-scale tests. Since the large-scale test (Big Bertha) had not started and the equipment was available, it was decided to postpone the start and use the equipment for some piping tests. For dismantling purpose the Big Bertha cylinder was made in two pieces and the distance block part made with only the length 35 cm. This part and the two end lids have been used for the flow tests. Figure 7-14 shows a photo of the test equipment. Figure 7-15 shows a cross section drawing of the set-up for test BB1.

In all, 7 large scale tests have been performed. The same main equipment was used for all tests, but it was partly modified for the different tests. The holes and recesses that will be used for instrumentation etc. in the actual “Big Bertha test” were plugged.

The bentonite blocks used in the tests were compacted in a mould with the dimensions 105 cm diameter and 35 cm height. The blocks were machined to the exact diameters and heights. All bentonite blocks had a bulk density of 2,180 kg/m^3 and a water ratio of 9.35%.

Figure 7-14. *Photo of the test equipment for the large-scale tests*

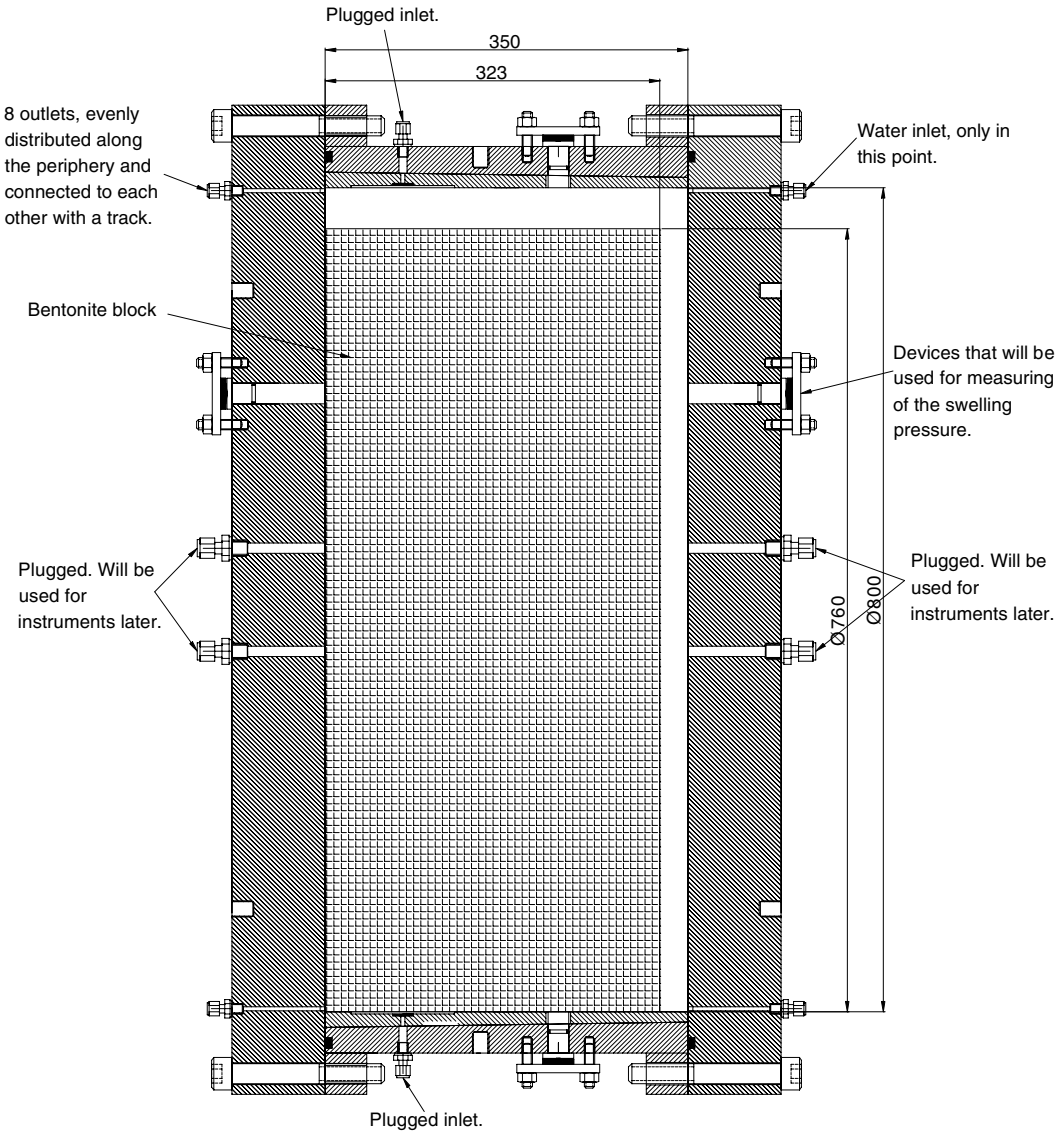

Figure 7-15. *Set-up of test BB1.*

The pellets were produced by roll-compaction at the water ratio of about 13%. The dry density of the individual pellet was about 1,900 kg/m^3. The size of a pellet was about 13x16x8 mm^3 but the pellets were cushion shaped with the maximum thickness 8 mm.

The filling rate was adapted to the empty volume available for water filling in order to fulfill the reference rate 0.1 l/min and yield a filling time of about 10 days except for the first two tests (BB1 and BB2). Also the water pressure increase rate was applied according to the reference case 100 kPa/h except for the first two tests. However, in some tests these rates could not be kept during the entire tests due to different events such us temporary piping. The exact history of all tests are described in Appendix 6.

7.5.2 Test results

The tests prerequisites and results are compiled in Table 7-3. Complete descriptions of all tests with drawings of the geometry, results and photos after dismantling are given in Appendix 6. Two examples will be given in the text namely test BB1, which was done with a gap of 4 cm in the top of the block and test BB6 which was done with pellets in the gap and measurement of axial force with 4 force transducers placed on the supporting ring.

Table 7-3. Compilation of the most important prerequisites and results of the sealing tests in large scale. See also Appendix 6.

Test no	Block diameter (mm)	Block height (mm)	Meas of axial load	Block position centered	Slot volume (l)	Arrangement	Filling rate (l/min)	Water infow /test duration	Remarks
BB1	760	323	No	No	29.4	Axial slot 27 mm. 40 mm gap at the top. Leaking supporting ring.	0.014	29 l/20 days	50 kPa/h not possible. 5 kPa/h caused piping at 1,200 kPa
BB2	760	349	No	Yes	17.6	20 mm gap all round. PVC-ring with O-ring against the “rock”. Sealed supporting ring.	0.004	18 l/6 days	The sample could take 2,000 kPa. Problems with the pressure equipment and with leakages.
BB3	796	348	No	No	2.75	4 mm gap at the top. Leaking supporting ring.	0.0006	4.7 l/8 days	100 kPa/h cause internal piping at 750 kPa. The sample could take 2,000 kPa. The sample had a recovering time of 2 days.
BB4	770	348	No	Yes	6.9	Pellets in the gap. Leaking supporting ring	0.0006	7 l/9 days	Constant flow for 9 days. Could not take the fast pressure increase at constant flow, max 1,600 kPa. With a pressurizing ramp of 100 kPa/h the sample could take 2,000 kPa.
BB5	770	298	No	Yes	10.4	Pellets in the gap. 50 mm thick PVC dummy simulating the next container. Perforated steel plate keeps the pellets in position.	0.0006	11.5 l/14 days	Constant flow for 14 days[1)]. No leakage during the test period. The sample could take 2,000 kPa.
BB6	770	298	Yes	Yes	10.4	Pellets in the gap. 50 mm thick PVC dummy simulated the next container. Perforated steel plate keeps the pellets in position.	0.0006	10.8 l/14 days	Constant flow for 9 days. 0.1 l leakage during the pressure ramp. Internal piping. The sample could take 2,000 kPa.
BB7	796	298	Yes	No	6.9	4 mm gap at the top. 50 mm thick PVC dummy simulated the next container.	0.00048	9.3 l/11 days	Constant flow for 9 days. No leakage. Internal piping. The sample could take 2,000 kPa.

1) Due to technical problems with applying a pressure ramp constant flow was kept for almost 14 days yielding a slower pressure increase than the reference case. See Appendix 6.

Tests BB1–BB5 (no measurement of load)

The two first tests were done with a bentonite block that was 4 cm in diameter smaller than the steel tube. In BB1 the block was placed on the floor and the gap was thus 4 cm in the top, while in test BB2 the block was centered. In addition a supporting ring (such as in Figure 2-1), which is tightly fixed to the rock, was simulated in test 2 since the conclusion of test 1 was that the gap was too wide.

The layout of test BB1 was shown in Figure 7-15. In similarity with the 1:10 scaled test, 8 outlet holes were used for water outflow and a peripheral slot on the lid, connecting the eight holes, was used to simulate the gap on the neighboring perforated container. The design was probably favorable for the sealing since the real gap will be larger than the simulated one and the construction may be regarded to simulate a supporting ring that is not water tight.

The test started and water was filled with a rate that would correspond to a filling time of about a week, which is expected for the reference case. It turned out that the leakage was very strong and the filling rate had to be rather high. After about 8 days no more water could be filled and the pressure increase started. The progress of the test is shown in Figures 7-16 and 7-17.

Figure 7-16 shows that the leakage before no more filling was possible was very high. 110 liters of water had leaked through before the pressure build up test could start. At first the pressure increase rate 50 kPa/h was tried. After about 1.5 days these tests had to be interrupted because piping occurred over and over again. Then the rate was decreased with a factor 10 to 5 kPa/h. This rate worked until after 10 days there was piping at the pressure 1,200 kPa. The test was then interrupted since the conditions were so far from the reference case.

The conclusion from this test was thus that the scale effect was very strong. The gap, which was 10 times larger than the gap at the test in the scale 1:10, could hardly handle the pressure increase rate that was 10 times lower. The distance block thus did not work for the reference case in full scale.

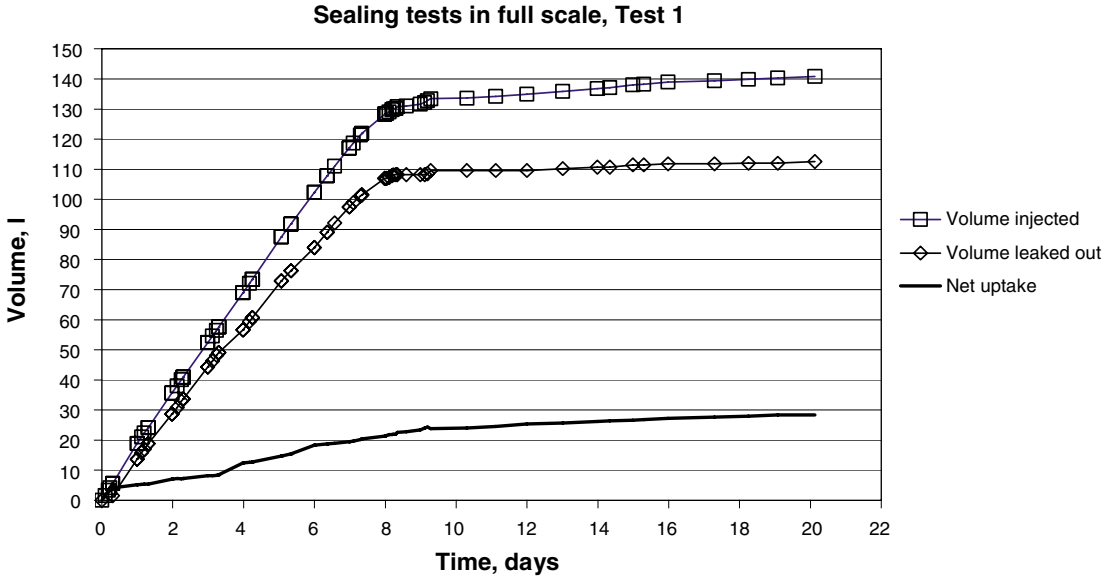

Figure 7-16. *In- and outflow of water as a function of time during the filling and pressure increase of test BB1.*

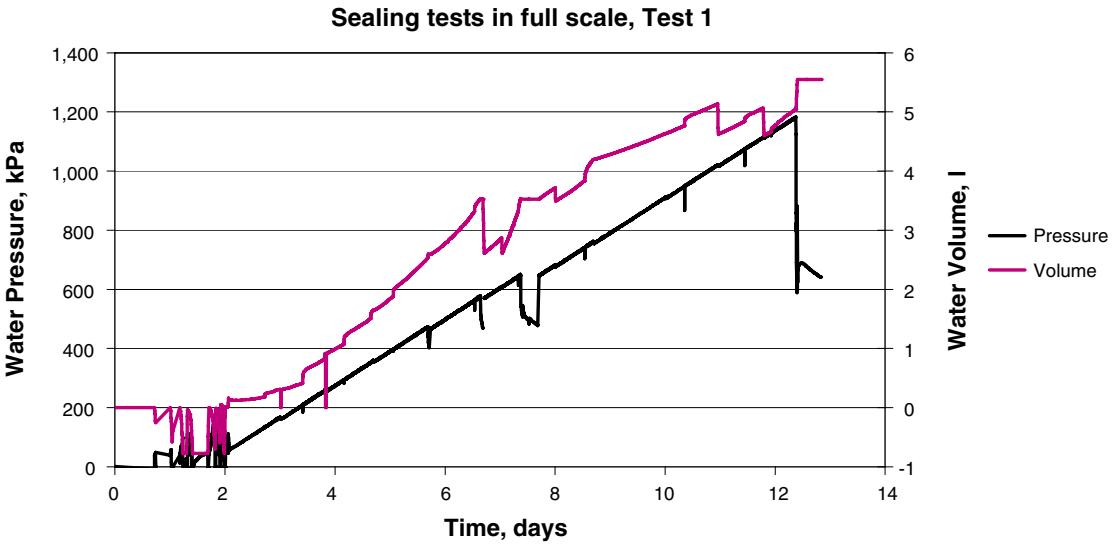

Figure 7-17. *Water pressure increase and inflow volume (read from the GDS) as a function of the dates of test BB1.*

In order to improve the design a supporting ring that was water tight at the rock was simulated (test BB2). This design seemed to work although there were some problems with the equipment during the testing. However, it is probably not easy to make a supporting ring that is water tight at the rock interface so the next tests were done in order to find other solutions.

In test BB3 the gap was reduced to 4 mm at the top of the distance block and in tests BB4 and BB5 pellets were placed in the 1.5 cm gap all around the distance block. These designs seem to work although there were some internal piping and small leakage before the sealing was completed. The tests are described in Appendix 6.

Tests BB6–BB7 (measurement of load)

The large scale tests show that the sealing seems to work for the reference case if a supporting ring that does not need to be water tight at the rock surface is used. In order to study the problem with the pressure on the distance block in large scale two tests with measurement of forces against the supporting ring were performed (BB6 and BB7).

These tests correspond to test series II of the scale tests. The scale tests showed that in spite of the existence of a deliberate slot between the distance block and the container the pressure from the water inside the distance block acted on a ring at the rock surface reaching radially only about 5 cm from the rock surface.

Test BB6 will be shown as example while BB7 is accounted for in Appendix 6. A special frame was constructed in which four load cells were mounted, see Figure 7-18. The lid was mounted outside the steel ring and fixed with bars and the load cells mounted on the lid.

Water was filled up with a constant flow of 0.006 l/min. The theoretical time to fill the pore volume with this flow was about 10 days. After 9 days the system was filled and a pressure ramp of 100 kPa/h applied. Internal piping occured at three different occasions: at 480, at 950 and at 1,300 kPa. At these internal pipings there was a total leakage of about 1 dl. At the fourth pressure ramp the sample could withstand 2 MPa. This pressure was applied for about 48 hours.

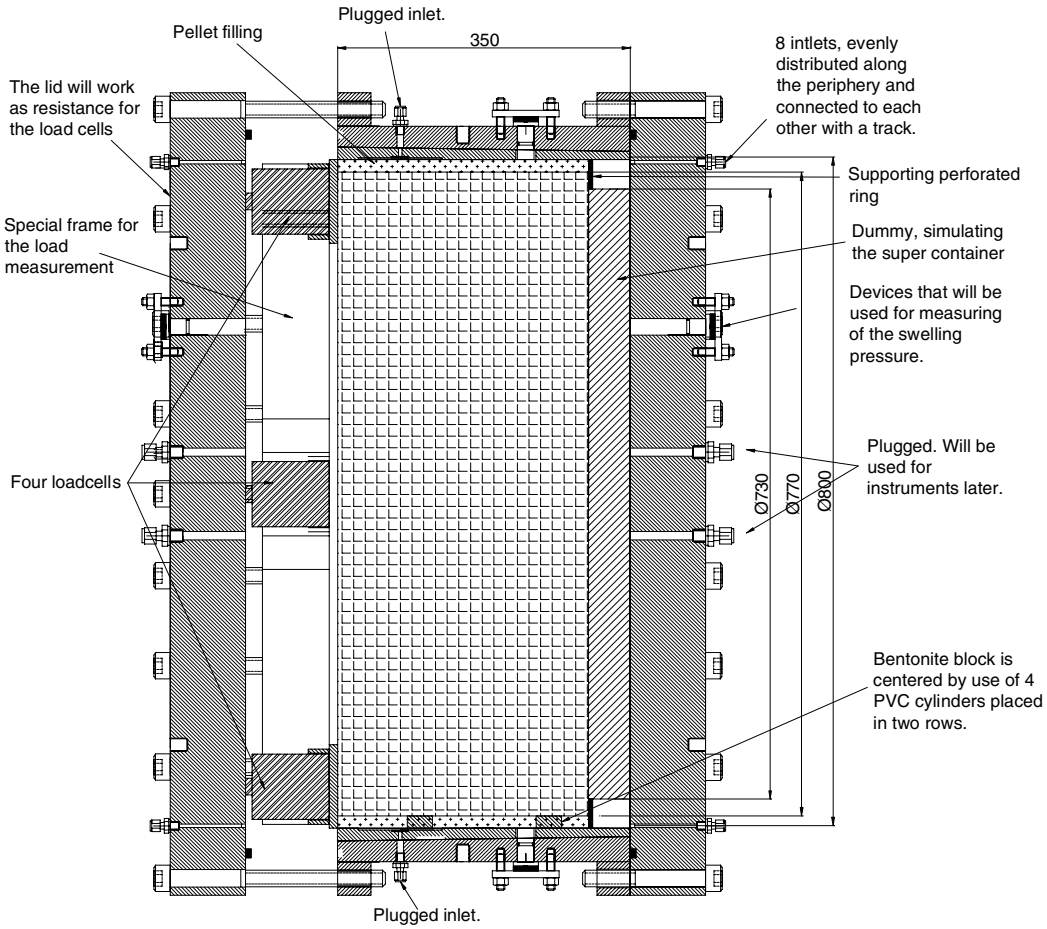

Figure 7-18. *Layout of sealing test BB6. Dimensions in mm.*

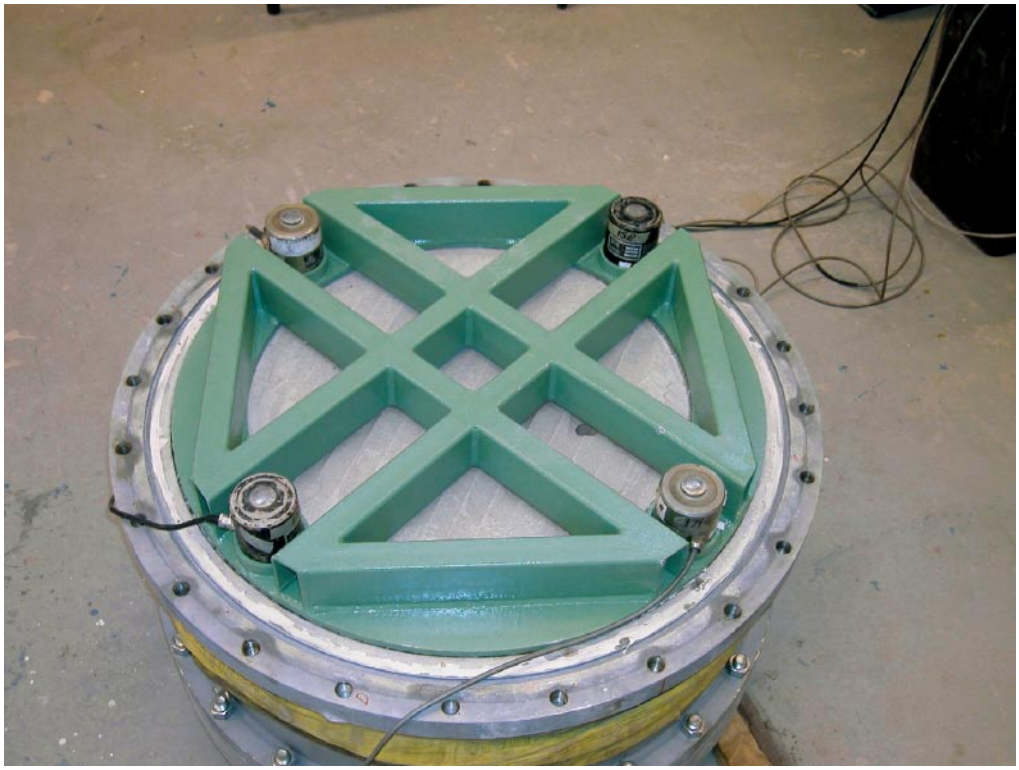

Figure 7-19. *Picture showing the supporting ring with the load cells during mounting. The diagonal framing is made only in order to stiffen the equipment.*

The history plots of applied water pressure and the total volume of inflow water is shown in Figure 7-20 while the forces measured by the four force transducers are shown in Figure 7-21. The results of the sampling after dismantling are shown in Appendix 6.

Test BB7 was intended to be identical to BB6 with the only difference that the distance block was larger, without pellets and the gap only in average 2 mm. The results were similar, showing that a water pressure of 2,000 kPa could be resisted without piping. Unfortunately water penetrated behind the dummy container and the back lid at the water pressure 1,200 kPa so the test had to be interrupted. The test was continued after removal of the force transducers.

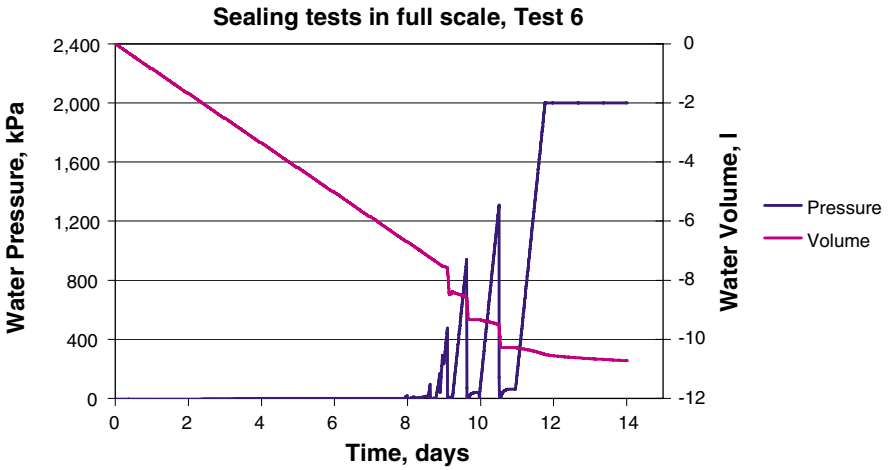

Figure 7-20. *Water pressure increase and inflow volume as a function of time for BB6.*

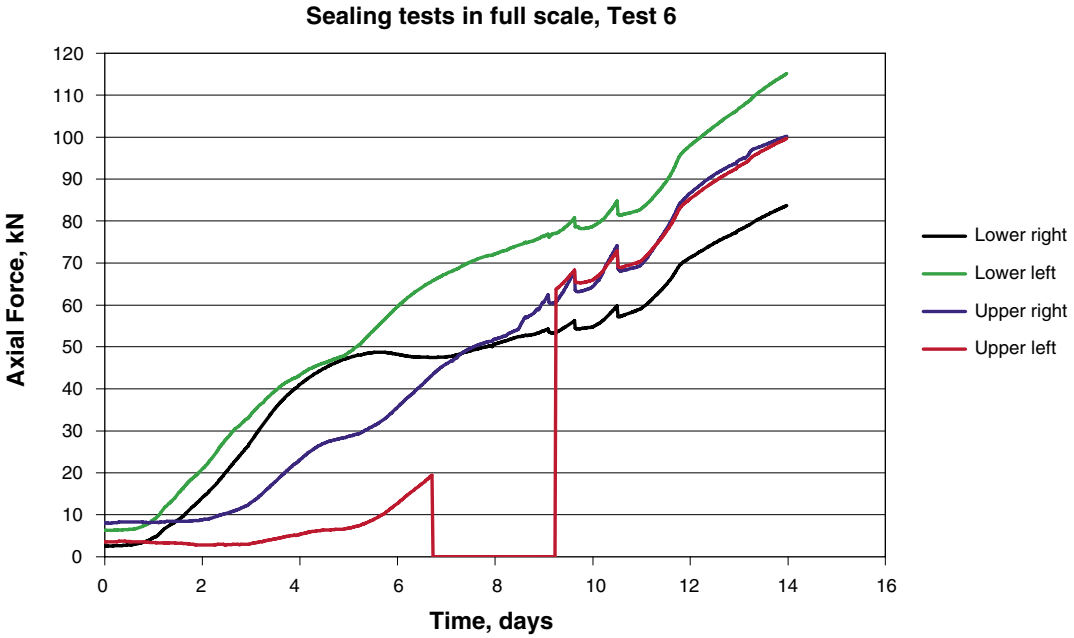

Figure 7-21. *Diagram showing the axial force as a function of time for BB6.*

Figure 7-22 shows the evaluated distance from the simulated rock that the water pressure acted on. The distance is back calculated as the measured total force divided to the area of a ring at the rock surface. The results show that only 10–15 mm is exposed to the full water pressure. This is less than corresponding distance reached in the scale tests in spite of the 10 times larger scale. The reason is probably that the scale tests were done with a 7 mm slot between the distance block and the dummy container while no such slot was used in the full scale tests. Another observation in Figure 7-22 is that test BB7 differs from all other tests by showing an initially large radius which decreases with time, the reason probably being the leakage behind the dummy container (that caused failure later). Figures 7-21 and 7-22 also show that the force on the distance block (and thus also the involved area) increases with time when the water pressure is kept constant. The reason is probably a combination of propagating water pressure and increasing swelling pressure.

7.5.3 Dismantling

Pictures taken during dismantling of the tests are shown in Appendix 6. Sampling and determination of the water ratio were done in all tests and these results are also shown in Appendix 6. Figure 7-23 shows as example the outer part of the distance block after removal of the supporting ring. The picture shows that only parts of the pellets filled gap are wetted.

7.5.4 Conclusions

The conclusions of the full scale sealing tests are that the scale effects are strong but also that it is possible to seal according to the desires for the reference scenario if engineering solutions with a supporting ring and either pellets in the annular gap or a very small gap of a few mm is used. The measured total force caused by a high water pressure inside the distance block was not very high since the radial distance from the rock surface that the water pressure acted on was only 10–15 mm (although increasing with time). The results also show that it is important to avoid a slot between the bentonite blocks and between a bentonite block and the container although a slot of 7 mm could be handled as shown in the scale tests.

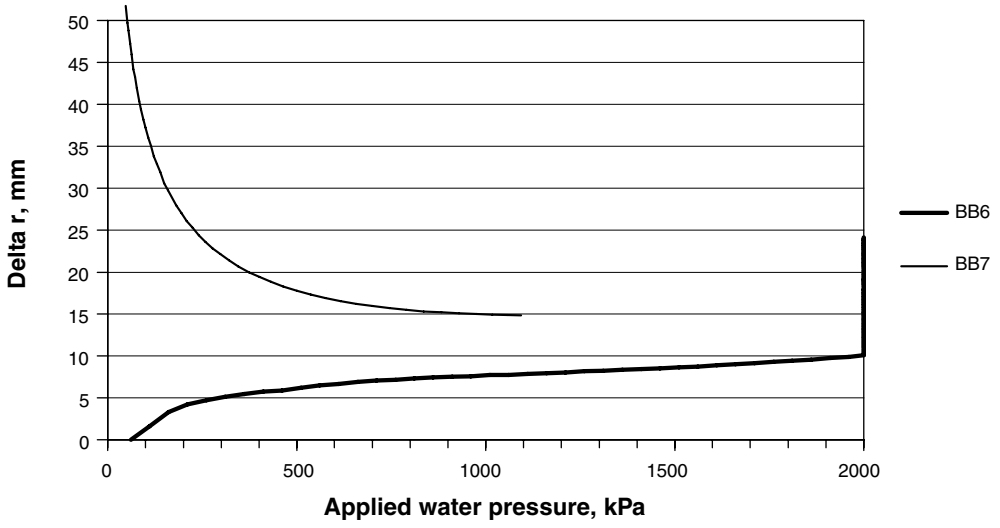

Figure 7-22. *Involved area of full axial water pressure (calculated as distance from the "rock") as function of the applied water pressure.*

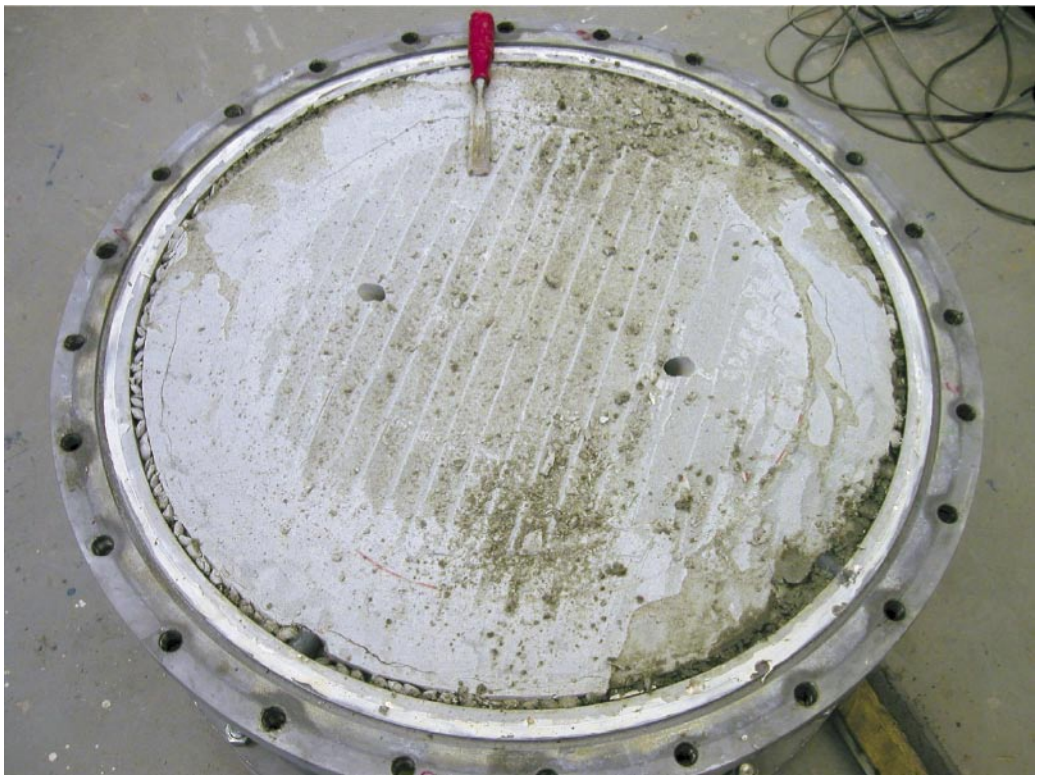

Figure 7-23. *Picture from dismantling of the test. The load cells and the frame with the supporting ring have been removed. The tool shows the upwards direction. The pellets on the right side are wet.*

8 Modelling

8.1 Introduction

Several different types of modelling and theoretical evaluations have been done, the following work being most important:

- Analytical modelling of the interaction between the bentonite blocks and the perforated deposition container for optimisation of the hole size and understanding of the penetration of bentonite through the holes and behind the container.
- Modelling of the temperature evolution for design purpose.
- Finite element modelling of THM evolution in the small scale test.
- Finite element modelling of the water saturation process for evaluation of the saturation time.
- Conceptual modelling of the water inflow and piping scenarious for design purpose

The work with these models will be described in this chapter.

8.2 Interaction between the bentonite and the perforated deposition container

The bentonite will swell at first radially through the holes in the perforated steel cylinder and then tangentially between the steel and the rock surface (see Figure 8-1). It is desired that the swelling pressure from the bentonite inside the steel cylinder σ_0 can be transferred to the rock with a swelling pressure σ_1 and further through the gap behind the steel with a swelling pressure σ_2, which are high enough to yield good sealing

The geometry of the circular holes are shown in Figure 8-2, which is derived from the assumption that the "degree of perforation" (that is area of holes divided to total area) is $\mu = 0.6$, that all holes have equal dimension and that the distribution is symmetric with an offset of half a hole.

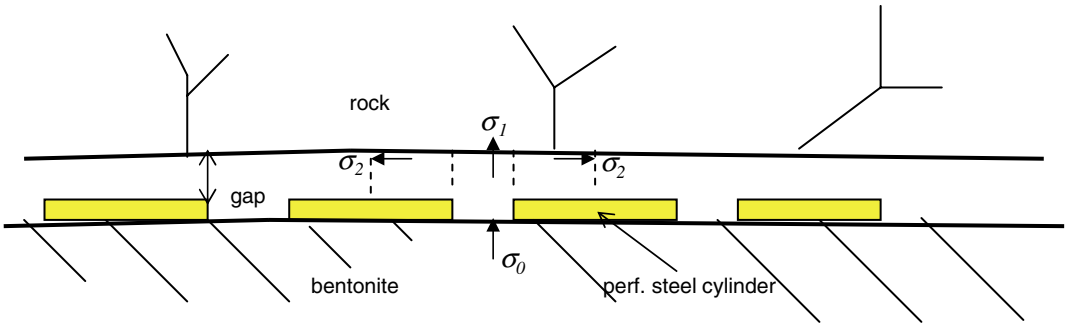

Figure 8-1. *The original swelling pressure of the bentonite σ_0 is reduced to σ_1 when it swells through the holes to the rock and further to σ_2 when it swells behind the steel cylinder.*

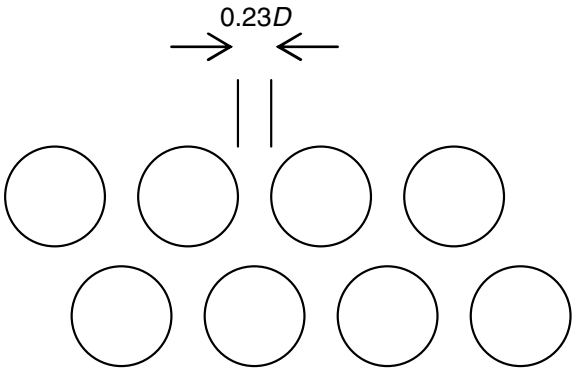

Figure 8-2. *Geometry of the circular holes.*

The swelling and the reduction in density and swelling pressure is a function of the geometry. In order to find the best geometry of the perforation of the steel cylinder a theoretical derivation of the swelling pressures σ_1 and σ_2 have been done. σ_1 is in these formulas assumed to be the average swelling pressure between the steel tube and the rock, i.e. the swelling pressure half way between the steel tube and the rock.

For the chosen degree of perforation 60% the distance between the holes will be 0.23D (0.459r) while the longest distance that the buffer must swell between the holes will be 0.42r.

The analytical solution of the swelling is derived from equilibrium considerations after completed swelling and is described in Appendix 1. Only the stage after completed swelling and homogenisation is considered. The calculation is made in two steps. The first step regards the stresses after swelling through the holes and considers a state of equilibrium in only the axial direction. The second step regards the stresses after swelling into the gap between the container and the rock and considers a state of equilibrium in only the radial direction.

An equilibrium equation of the axial forces from σ_0 to σ_1 as a result of the axial swelling through the holes yields Equation 8-1, while the radial swelling derived from equilibrium of forces in radial direction from σ_1 to σ_2 yields Equation 8-2 (Appendix 1).

$$\sigma_1 = \sigma_0 \cdot e^{\frac{-2(d+z/2)\tan\phi}{r_1}} \tag{8-1}$$

$$\ln\sigma_2 = \ln\sigma_1 + K\ln\frac{r_2}{r_1} - \frac{r_2 - r_1}{z}\cdot 2\tan\phi \tag{8-2}$$

where

r_1 = hole radius
r_2 = radius at σ_2
d = container thickness
z = gap between the container and the rock

$$K = \left(\frac{\nu}{1-\nu} - 1 \right)$$

ν = Poisson's ratio
φ = friction angle

For the steel container we assume that

d = 0.008 m
z = 0.0425 m
σ_0 = 10,000 kPa
φ = 20 º

r_2/r_1 = 1.42

The minimum swelling pressure σ_2, which occurs between the holes at the radius 1.42r_1 is plotted as a function of the hole radius in Figure 8-3. K = 0 (isotropic swelling pressure) and K = –1 are considered.

Figure 8-3 shows that the radius 5 cm is optimal for the container perforation. Figure 8-4 shows the decrease in swelling pressure with increased distance from the hole for the hole radius 5 cm. The figure shows that the pressure drops rapidly if there are parts of the container without holes (e.g. at the lids or at possible feet).

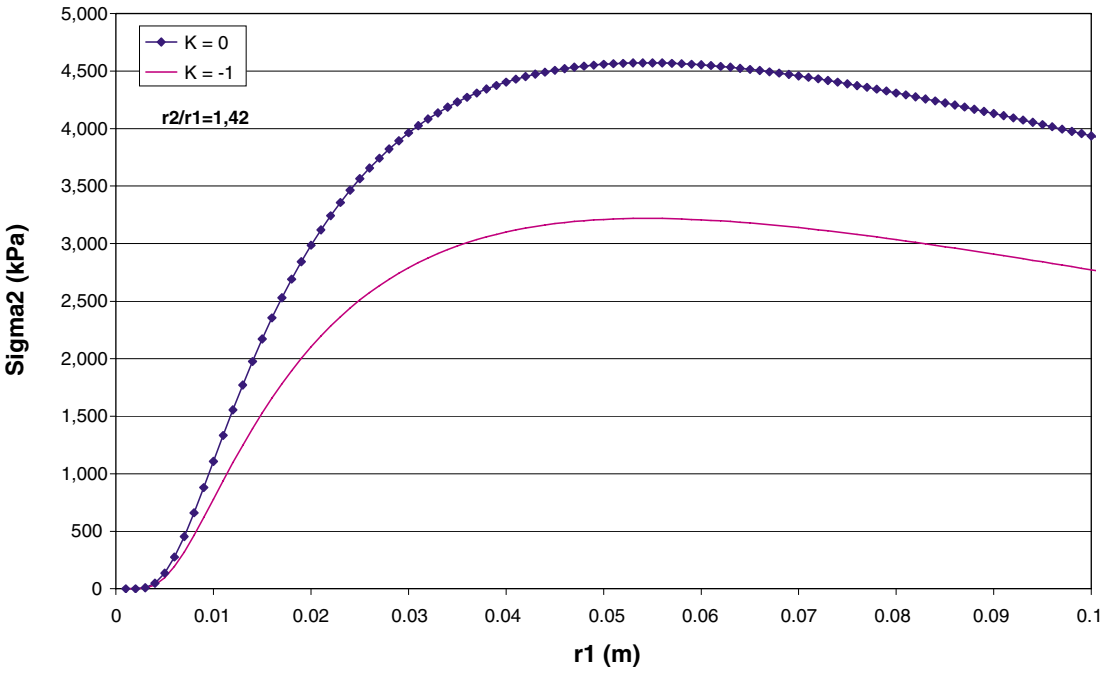

Figure 8-3. *Degree of perforation μ = 0.6. Minimum swelling pressure between the rock and the container as a function of the radius of the holes in the steel container for two cases, where K = 0 corresponds to isotropic swelling pressure.*

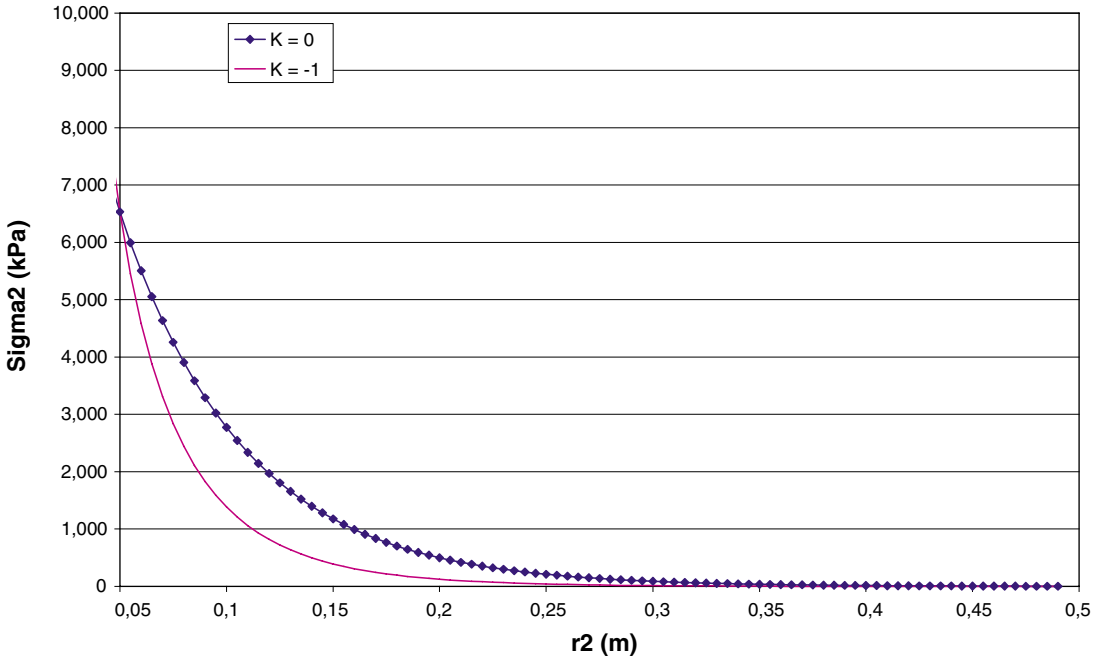

Figure 8-4. *Swelling pressure as a function of the distance from the centre of the holes in the container for the optimum hole radius 5 cm.*

8.3 Modelling of the temperature evolution for design purpose

The required distance between canisters and the influence of different factors such as thermal conductivity of the rock and the wetting of the buffer have been investigated by finite element calculations. A report considering both KBS-3H and KBS-3V has been issued /Hökmark and Fälth, 2003/.

8.4 FEM-modelling of the HM evolution in the small scale test

8.4.1 General

A preliminary modelling of the scale test has been done with a finite element calculation with simplified boundary and initial conditions (no account taken of the perforated steel cylinder or the swelling of the bentonite blocks). The buffer in the model has thus been assumed to fill the entire space between the canister and the rock from start.

The finite element modelling has been done with the FEM program ABAQUS with modelling of all relevant hydro-mechanical processes. The technique and the material models for this calculation have been developed for modelling of KBS-3V. The program, the processes and the material data are described by /Börgesson and Hernelind, 1999/ and will not be shown in this report.

8.4.2 Buffer material properties

The properties of the buffer at start calculations are

- dry density: ρ_d = 1,570 kg/m^3 and
- water ratio: w = 0.10

which yield

- void ratio: e = 0.77 and
- degree of saturation: S_r = 0.361.

The water ratio after complete water saturation is for this void ratio w = 0.277 and the density at saturation is ρ_m = 2,010 kg/m^3.

The data used for the processes describing the behaviour of the buffer are identical to the data used for the KBS-3V calculation /Börgesson and Hernelind, 1999/ with exception of the data for a process called "moisture swelling", which had to be changed due to the difference in initial water content of the buffer used in KBS-3H compared to the buffer intended for KBS-3V (where w = 17% is planned)

The shortcomings of the effective stress theory are compensated in ABAQUS by this procedure "moisture swelling". The procedure changes the volumetric strain ε_v by adding a strain that can be made a function of the degree of saturation S_r:

$\Delta\varepsilon_v = f(S_r)$

The new data for this process is compiled in Table 8-1.

Table 8-1. Change in volumetric strain ε_v as a function of the degree of saturation S_r used in the "moisture swelling" procedure (selection of curtailed data).

S_r	$\Delta\varepsilon_v$
0.1	–0.135
0.2	–0.0214
0.3	–0.00113
0.361	0
0.4	–0.00149
0.5	–0.00963
0.6	–0.0209
0.7	–0.0331
0.8	–0.0452
0.9	–0.0566
0.91	–0.0577
0.925	–0.0608
0.95	–0.0728
0.975	–0.0990
0.99	–0.125
0.998	–0.134
1.0	–0.135

The data for this procedure has been settled so that there is a linear relation between the suction (negative pore water pressure) and the total stress when the buffer is confined without possibility to change volume. Figure 8-5 shows the results of a verification simulation.

8.4.3 Element mesh

The element mesh used in the calculation is shown in Figure 8-6. The mesh is axi-symmetric around the centre of the canister. The cylindrical part of the perforated steel container is not included in the model but the two end parts are included. The filters on the periphery are modeled by applying a constant water pressure in the nodes marked with rings in the figure.

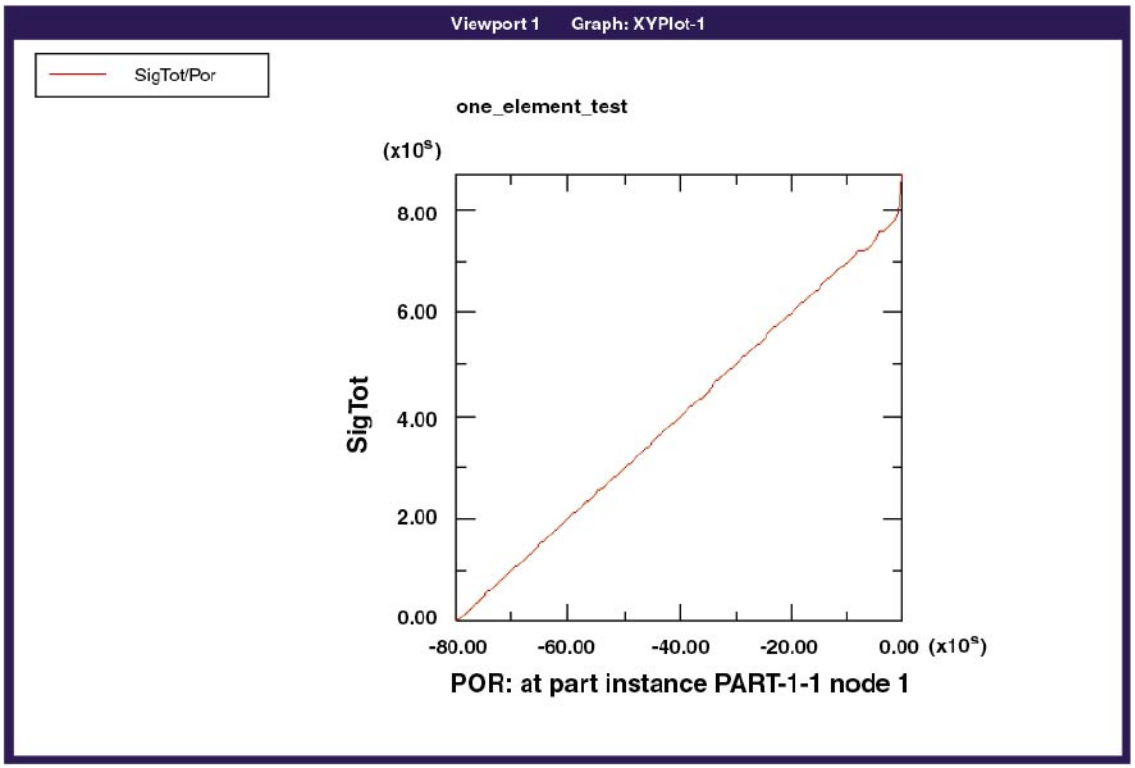

Figure 8-5. *Development of total stress (kPa) by the confined buffer as a function of the pore water pressure (kPa). Results of a verification calculation.*

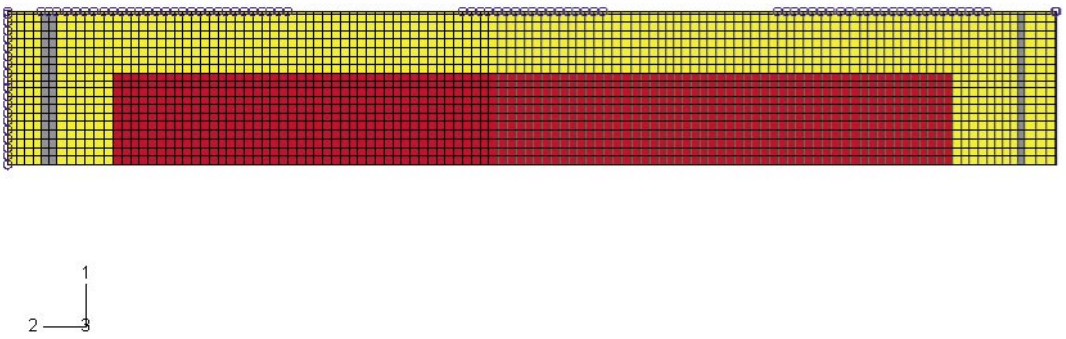

Figure 8-6. *Element mesh for the finite element calculation. Axial symmetry around the lower boundary. Red = canister. Yellow = bentonite buffer. Grey = steel lids of the container. ◦ = filter*

8.4.4 Initial conditions and boundary conditions

The start value of the basic variables of the buffer must be defined as well as the boundary conditions. The following initial conditions are applied:

e = 0.77 (void ratio)

S_r = 0.361 (degree of saturation)

which yields

w = 0.169 (water ratio)

ρ_d = 1,570 kg/m^3 (dry density)

ρ_m = 2.01 (density at saturation)

Two more initial conditions are required:

u = –31,000 kPa (pore pressure)

p = 18,910 kPa (average effective stress)

which yields

p_{tot} = 0 kPa (total pressure)

The following boundary conditions are applied and kept during the calculation:

Mechanically all boundaries of the buffer have been locked so no deformations of these boundaries can take place. Since all nodes of the canister and the steel lids are locked the mechanical properties of those materials are meaningless.

Hydraulically all boundaries of the buffer, except the boundaries to the filter mats, are free, which means that no water can pass the boundaries and that also the hydraulic properties of the other materials are meaningless. The nodes of the filter mats are hydraulically locked at 0 kPa, which means that water is freely accessible from the filters.

8.4.5 Results

The results of the modeling are shown in Appendix 2 and compared with the measurements as history plots of the total stress and relative humidity in the points where these variables are measured. Examples of contour plots of results after 4 and 24 weeks are shown in Figures 8-7 and 8-9. The results show that the model predicts a rather fast saturation in spite of that the increased water pressure in the filters was not included. The model is almost completely water saturated after 24 weeks. A comparison with the measured results as shown in Appendix 2 reveals that the real saturation is slower. The predicted time to reach full saturation was about 100 days while the measurements indicate that more than 140 days was required. The difference is probably caused by a combination of three factors:

1. The delaying effect of the perforated container is not included in the model.
2. The model overestimates the wetting rate at high degree of saturation.
3. Clogging of parts of the filters by entrapped air and penetrating bentonite may have delayed the wetting.

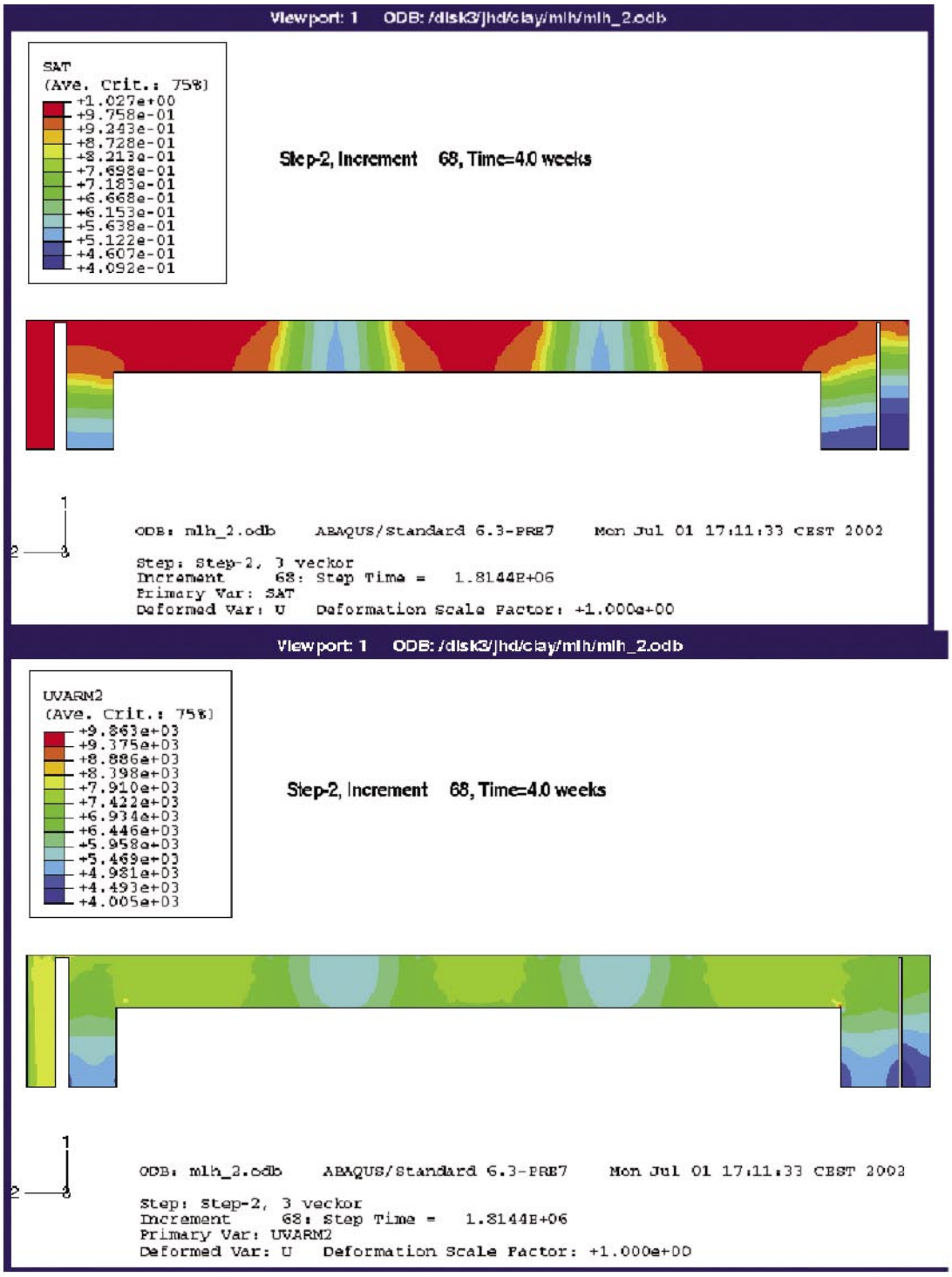

Figure 8-7. *Predicted degree of saturation (upper figure) and total stress (kPa) after 4 weeks.*

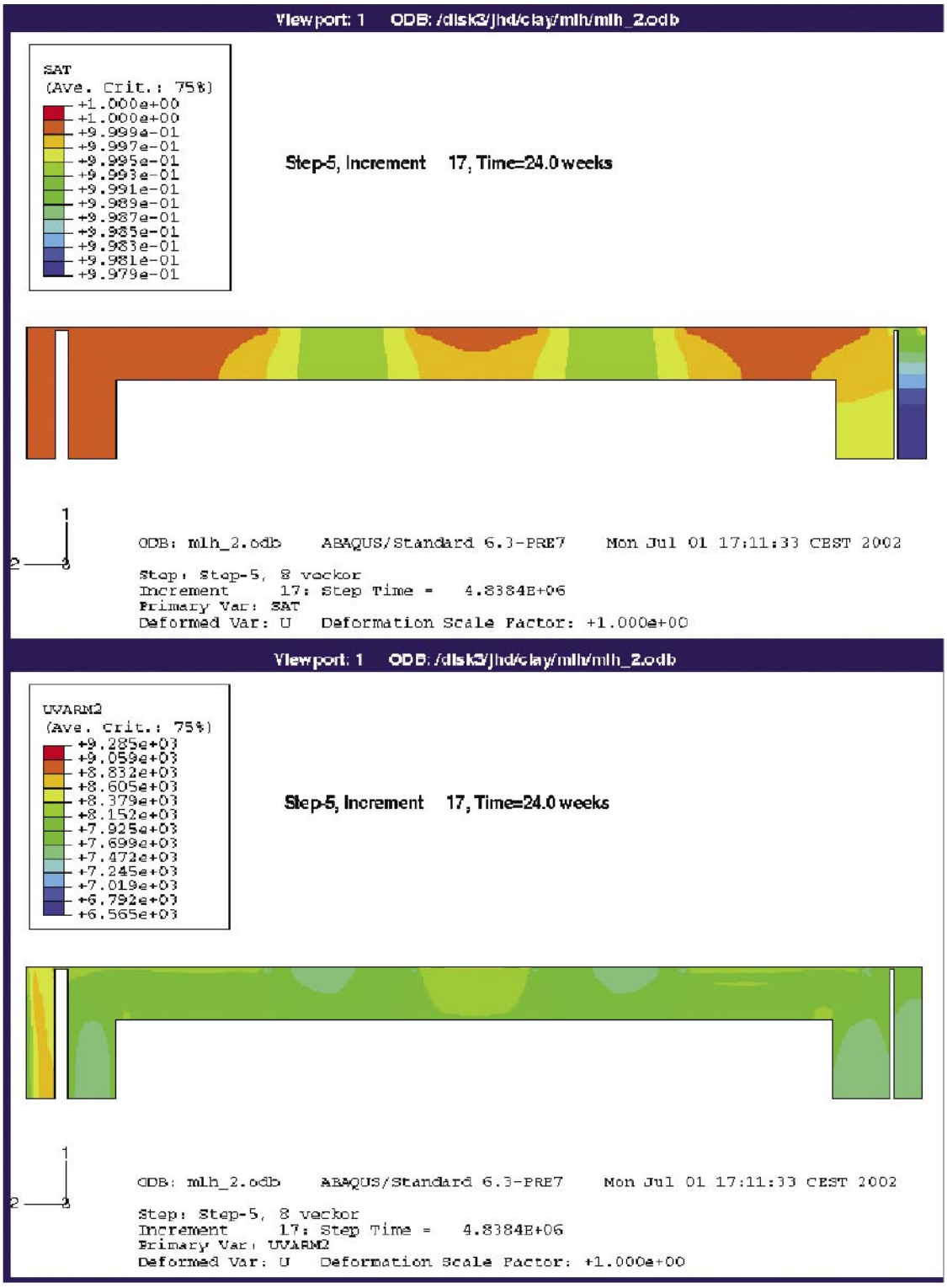

Figure 8-8. *Predicted degree of saturation (upper figure) and total stress (kPa) after 24 weeks.*

8.5 FEM-modelling of the saturation time of a KBS-3H repository

8.5.1 Model geometry and data

General

The modelling work was performed with the finite element program, Code_Bright version 2.2. For the specific problem, an axi-symmetric 2D geometry was applied. Moreover, the thermo-hydraulic processes were analysed. The gas pressure was held constant, although vapour transport was allowed.

The chosen hydraulic conditions consisted of an initial draw-down around the tunnel and a constant boundary pressure at a radius of 25 m. In analogy, thermal condition consisted of an initial temperature, a decaying heat-load from the canisters and a temperature boundary at a radius of 3 m.

Minor differences between the presuppositions in Sweden and Finland led to the treatment of these conditions as two different cases, henceforth denoted the SKB and the Posiva case, respectively. Calculations were made for six different host rock hydraulic conductivities: 10^{-8}, 10^{-10}, 10^{-11}, 10^{-12}, 10^{-13} and 10^{-15} m/s.

Geometry

The 2D axi-symmetric model geometries used are shown in Figure 8-9. The gap between the steel cylinder and the rock was 32.5 mm. The perforated envelope of the steel cylinder was 10 mm thick, while the impermeable end was 20 mm. The perforated envelope was treated as a special material, see below.

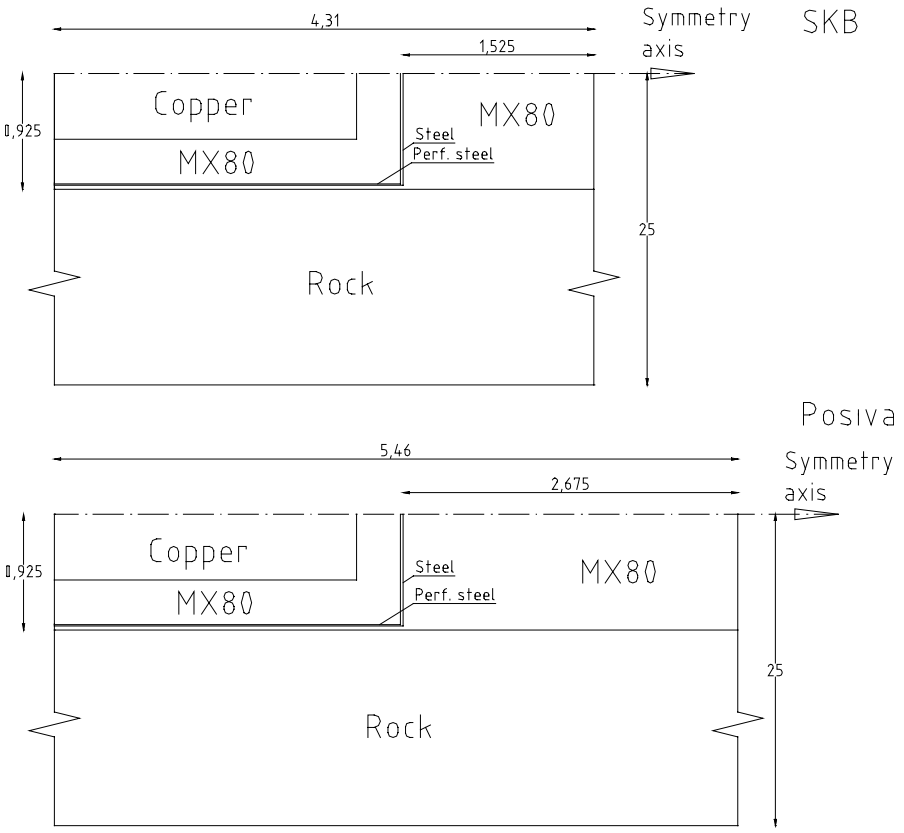

Figure 8-9. *Model geometry. SKB and Posiva case.*

The gap between the steel cylinder and the rock was handled as if the buffer had swelled into it from the inside of the cylinder. This operation implies that the void ratio and the saturation degree are adjusted, in order to keep the total void volume and water ratio constant. In this case, the void ratio was defined on the basis of a final saturated density, see below.

Initial and boundary conditions

The water pressure in the undisturbed rock was assumed to be 5 MPa. This pressure was applied as a boundary condition at the radius 25 m from the symmetry axis. The initial condition was obtained though keeping the water pressure in the tunnel at

0.1 MPa for 10 years. In this way an initial draw-down was achieved (see Figure 8-10). In all cases, except for the lowest rock conductivity assumption, i.e. 10^{-15} m/s, a steady state condition was reached within that time. After this phase of drainage the initial water pressure in the buffer material was set to –117.4 MPa to represent emplacement of the unsaturated bentonite buffer.

The undisturbed rock temperature was assumed to be 15°C. The heat-load from the canister was modelled as:

$$P = P_0 \times e^{-\lambda_e \times t} \tag{8-3}$$

where P_0 is the canister heat power at the time of deposition, t is time and λ_e is a time constant. Different parameter values were use for different time periods in order to follow the decay described by a sum of exponential terms /Hökmark and Fälth, 2003/. The employed heat load was treated as a spent fuel with an age averaging 30 and 40 years, respectively and is shown in Figure 8-11. The heat load was applied as a nodal surface boundary throughout the whole canister cylinder in Code_Bright.

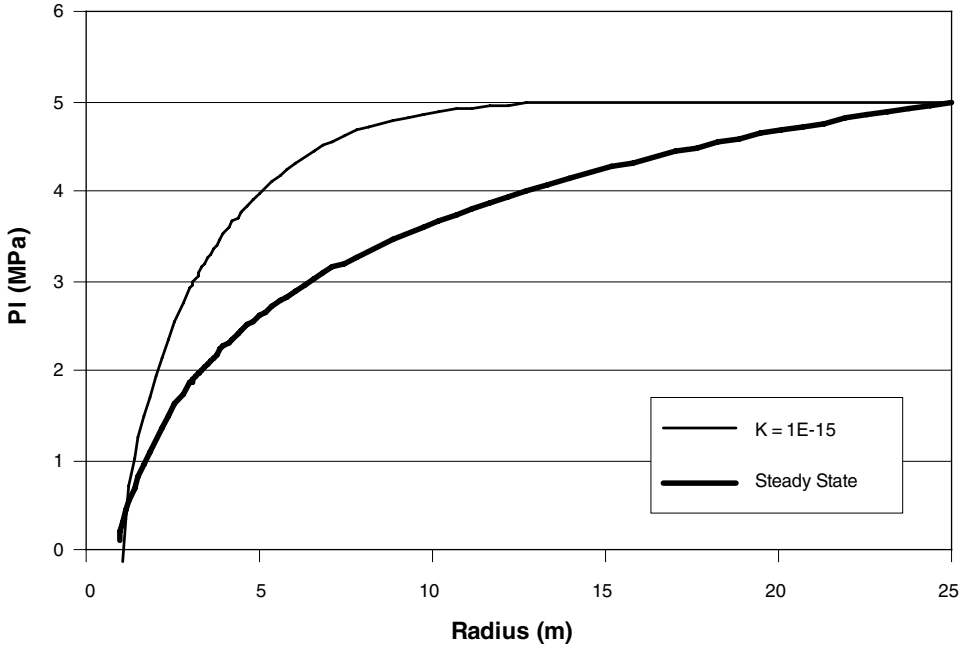

Figure 8-10. *Initial water pressure distribution in rock obtained from draw-down after 10 years with the rock hydraulic conductivity 10^{-15} m/s.*

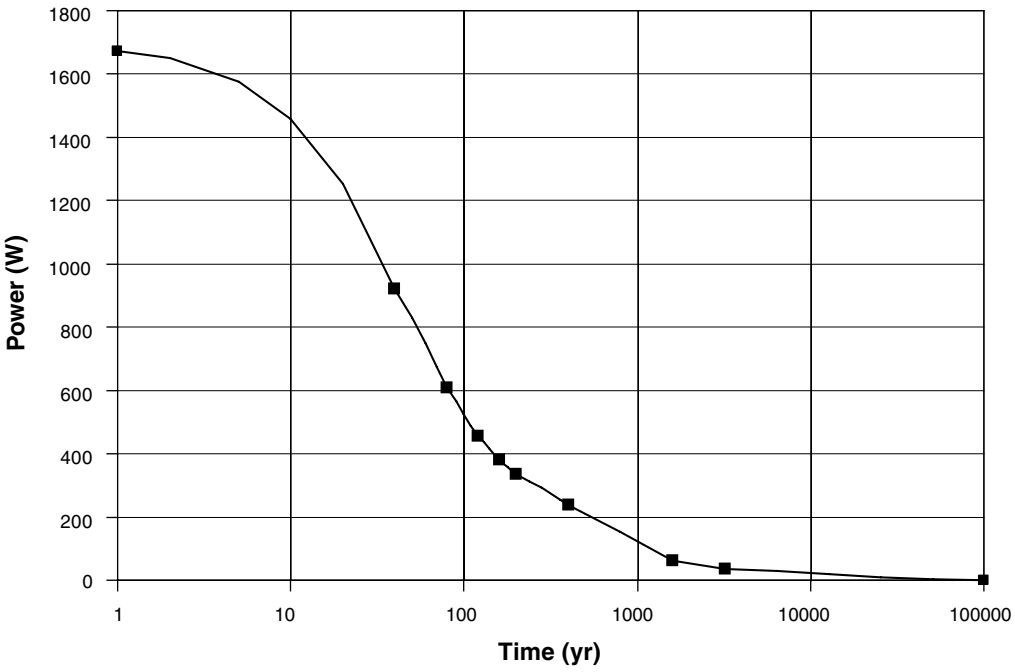

Figure 8-11. *Heat load decay.*

A temperature boundary was applied at the radius 3 m from the symmetry axis. This was in order to account for the heat conduction beyond the model geometry as well as the heat contribution from all tunnels. The temperature increase was calculated analytically through addition of a large number of line sources, each described by the expression:

$$T(r,z,t) = \frac{1}{\rho \cdot c \cdot (\sqrt{4\pi \cdot a})^3} \cdot \int_0^t \frac{u(t)}{(\sqrt{t-t'})^3} \int_{-H}^{H} \exp\left(-\frac{r^2 + (z-z')^2}{4a(t-t')} \right) dz'\, dt' \qquad (8\text{-}4)$$

where 2H is the length of each line source, u(t) = Q(t)/2H is the time-dependant unit length power, a = λ/(ρc) is the thermal diffusivity /Hökmark and Fälth, 2003/. In this calculation, a tunnel distance of 40 m was assumed.

The applied temperature boundaries are shown in Figure 8-12 and a compilation of initial condition is presented in Table 8-2.

The basic assumption for the initial conditions of the buffer was that the average density of the buffer after saturation and swelling was ρ_m = 2.000 kg/m^3 and an initial water ratio of 10%. The average density corresponds to a void ratio (e) of 0.77, according to:

$$e = \frac{\rho_s - \rho_m}{\rho_m - \rho_w} \qquad (8\text{-}5)$$

where ρ_s and ρ_w are the solid and water density, respectively. For this void ratio, the water ratio of 10% corresponds to an initial degree of saturation of 0.361 (see Equation 7 in Appendix 3a). With the applied retention properties (see below), this saturation degree corresponds to an initial suction value of 117.5 MPa.

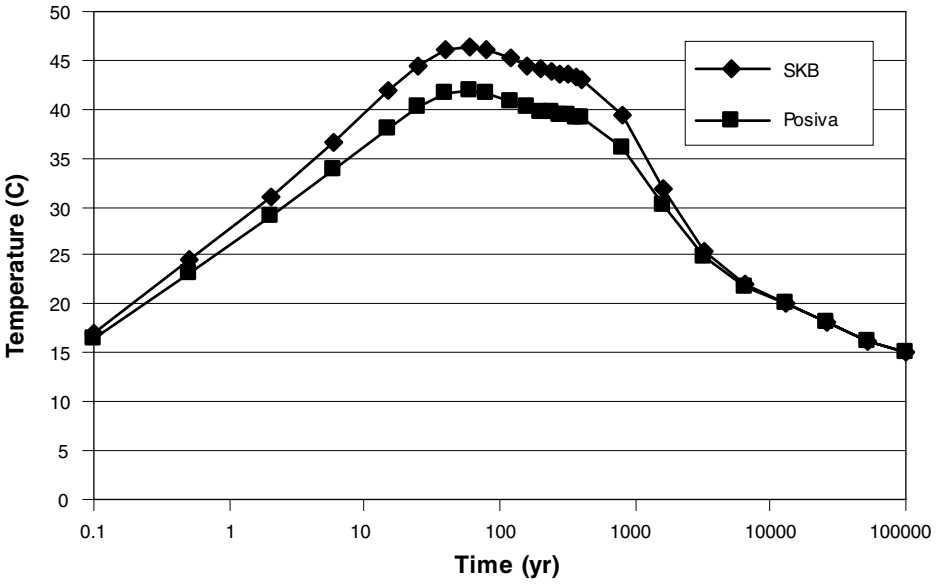

Figure 8-12. *Applied temperature boundary at radius 3 m. SKB and Posiva case.*

Material data

Compilations of applied retention, thermal and hydraulic properties and initial conditions are presented in Tables 8-2 to 8-4. Retention curves are shown in Figure 8-13.

The perforated steel was treated as a mixture of MX-80 and steel. The properties were calculated as weighted averages (MX-80 : Steel = 60%:40%) for porosity, density, intrinsic permeability, specific heat and thermal conductivity.

The impermeable materials steel and copper were given low porosity and hydraulic conductivity and the same initial water pressure as the bentonite in order to make them not interact hydraulically with the buffer.

Table 8-2. Initial conditions.

Material	Temperature	Liquid pressure	Porosity
MX-80		–117.4 MPa	0.435
Perforated steel			0.265
Rock	15°C	(see Figure 8-10)	0.005
Copper		–117.4 MPa	0.01
Steel			0.01

Table 8-3. Retention properties.

Material	Law	P_0	λ	P_m	λ_m
MX80	$S_r = \left\{1+\left(\frac{P_g - P}{P_0 \cdot \left(\frac{\sigma}{\sigma_0}\right)}\right)^{\frac{1}{1-\lambda}}\right\}^{-\lambda} \left\{1-\frac{P_g - P}{P_m}\right\}^{\lambda_m}$	14	0.25	500	1.1
Perforated steel		14	0.25	500	1.1
Rock	$S_r = \left\{1+\left(\frac{P_g - P}{P_0 \cdot \left(\frac{\sigma}{\sigma_0}\right)}\right)^{\frac{1}{1-\lambda}}\right\}^{-\lambda}$	4	0.65	–	–
Copper		500	0.3	–	–
Steel		500	0.3	–	–

Table 8-4. Thermal and hydraulic properties.

Material	Solid phase density (kg/m³)	Intrinsic permeability (m/s)	Liq rel perm $k_{rl} = S_r^{\delta l}$ δ_l	Vap tourt	Solid phase spec heat (J/kgK)	Heat cond (W/mK) $\lambda = \lambda_{dry}(1 - S_r) + \lambda_{sat} S_r$ λ_{dry}	λ_{sat}
MX80	2,800	5.7×10^{-21}		0.6	900	0.367*	1.3
Perforated steel	4,800	3.42×10^{-21}		0.6	614	18	18
Rock	2,600	10^{-15}–10^{-22}		10^{-5}	800	3.0† 2.6‡	3.0† 2.6‡
Copper	8,930	10^{-30}		10^{-10}	390	390	390
Steel	7,800	10^{-30}	3	10^{-10}	460	45	45

† SKB –case; ‡ Posiva-case; * see Appendix 3b.

8.5.2 Results

Calculated time-scales of total saturation are presented as a function of the rock hydraulic conductivity in Figure 8-14. It can be noted that the time is independent on the conductivity above the level of 10^{-11} m/s. The time-scale for saturation is approximately 10 years in this domain. The time-scales at conductivities below the level of 10^{-12} m/s are, on the other hand, strongly dependent on the conductivity.

A small difference can be noted between the SKB and the Posiva case. The time-scales in the Posiva case is approximately 10% longer than the SKB case.

A more comprehensive presentation of results is given in Appendix 3b in the form of scan-lines and point-analyses. Among these results a few observations can be noted:

- For cases with high rock hydraulic conductivity, the time of saturation varies along the tunnel. Buffer in the cylinder saturates more rapidly than in the distance block (see Figures A3-3 and A3-8 of Appendix 3b). The time to saturate the buffer between the canister and the rock is approx. 4 years for a host rock with a hydraulic conductivity in the range of 10^{-8} to 10^{-11} m/s.

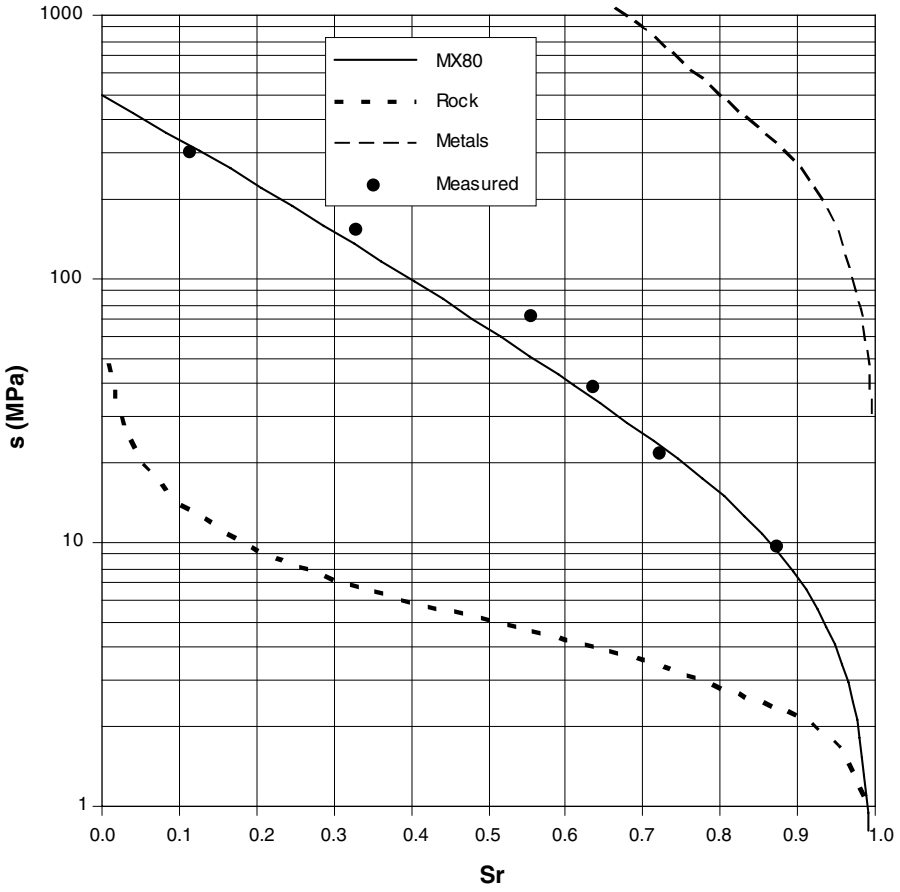

Figure 8-13. *Retention curves for applied materials.*

- For cases with low rock hydraulic conductivity, the rock de-saturates during the process (see Figures A3-6, A3-7, A3-11 and A3-12 of Appendix 3b)

8.5.3 Conclusions and discussion

The results demonstrate that the saturation process exhibits two domains, one determined by the buffer at higher rock conductivities and one determined by the rock at lower conductivities. The transition zone between these two domains appears to occur between 10^{-11} and 10^{-12} m/s.

In can be noted that the calculated time-scales correspond fairly well with the reported results form ABAQUS models of the KBS-3V method /Börgesson and Hernelind, 1999/.

The bedrocks in question hardly exhibit a uniform, well-defined, hydraulic conductivity. It is therefore possible that different parts of a repository would saturate several decades apart. However, the occurrence of fractured zones around the tunnels could lead to an axial redistribution of ground water. This would limit the time differences between different parts, and probably enhance the process in parts with low hydraulic conductivity of the rock. Such an approach has not been addressed in this study.

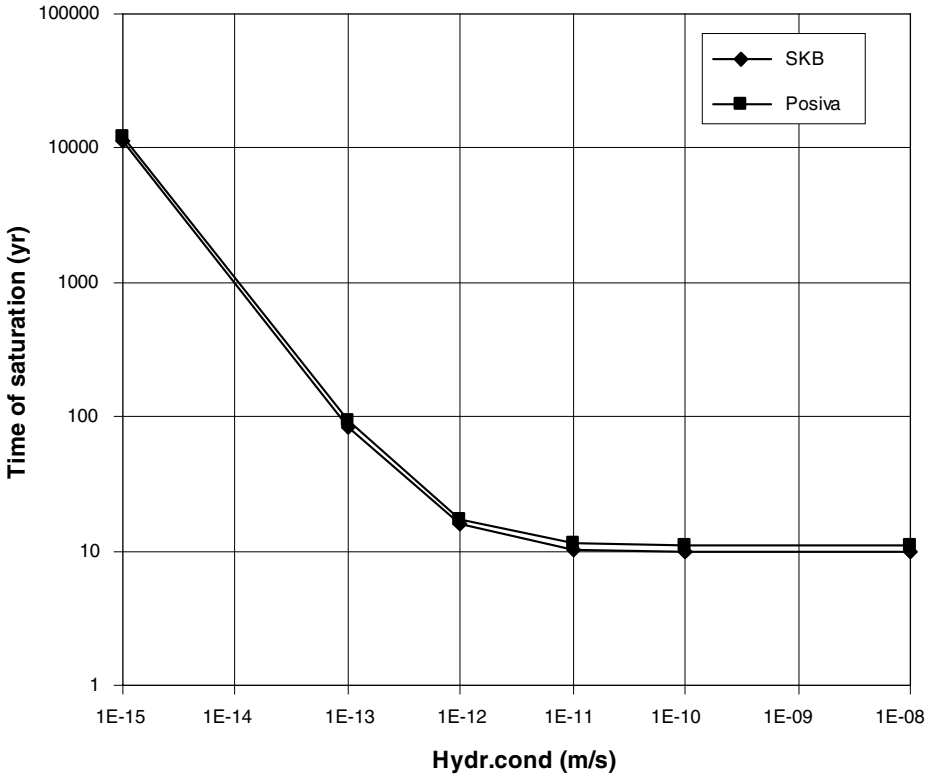

Figure 8-14. *Time to saturation for different hydraulic conductivities of the rock. SKB and Posiva case.*

The assumption made here of a low (atmospheric) pressure and constant total amount of gas may contribute to overestimate the vapour diffusivity, and consequently the time-scale of saturation. However the assumption is usually considered to be reasonably justified for up to at least 100°C. Another possible effect is a saturation delay, due to the entrapment of gas within the tunnel pore volume. The diffusion of dissolved gas could in this case extend the time-scale of saturation. This effect is probably most important at high rock hydraulic conductivities.

Applied temperature boundaries in this study were calculated with an assumed tunnel distance of 40 m. It should be noted that any significant alteration of this distance would change the temperatures and in the end change the time-scale of saturation, at least in the cases with high rock hydraulic conductivities.

Finally, while some of the properties of the rock are fairly well known, such as the thermal conductivity and the retention properties, others were in this study based on initiated guesses, such as values for porosity and vapour tortuosity. Realistic alternative values to these choices are expected to have a marginal effect on the final time-scale, but could readily be analysed in detail if required.

8.6 Conceptual modeling for design purpose

See Chapter 9.

9 Tight distance block scenario

9.1 Introduction

A solution for handling the water inflow into the deposition drift in the KBS-3H concept is to make the distance block come in contact with the water, swell and thereby seal the gap between the block and the rock surface. The idea is to not let any water flow between the container sections. The concept is called “tight distance block”. This chapter contains a preliminary analysis of the function of that concept. It consists of the following parts:

- Presumptions and design.
- Scenario descriptions.
- Foreseen processes and problems.
- Consequences.
- Conclusions.

9.2 Presumptions and design

The two proposed design alternatives of a distance block section in the tight distance block concept are shown in Figure 9-1. The gap between the block and the rock is either be very small (a few mm) or filled with sealing material (bentonite pellets is proposed) in order to prevent piping when the water pressure increases. According to investigations performed in both scale 1:10 and large scale the distance block needs to be supported by a ring fixed to the rock wall for both alternatives (bolted).

In the final repository, the hydraulic situation at the container positions is going to vary between no inflow at all (fracture free rock) and a large inflow from several fractured zones of several liters per minute. Since the other piping/erosion phenomena have been studied with the assumption of 0.1 l/min for one canister position this will be the inflow assumed also for the tight distance block scenario. This is probably non-conservative and stronger inflow will also be considered but for simplicity mainly the base case will be treated.

The following basic data is settled:

- Inflow: 0.1 l/min for one container section.
- One container section (total length and volume) = supercontainer + one distance block section.
- Pressure increase rate at stopped inflow: 100 kPa/h.
- 300 m tunnel: 30–40 container sections.
- Installation of one container section per day.
- 30–60 days until closure.

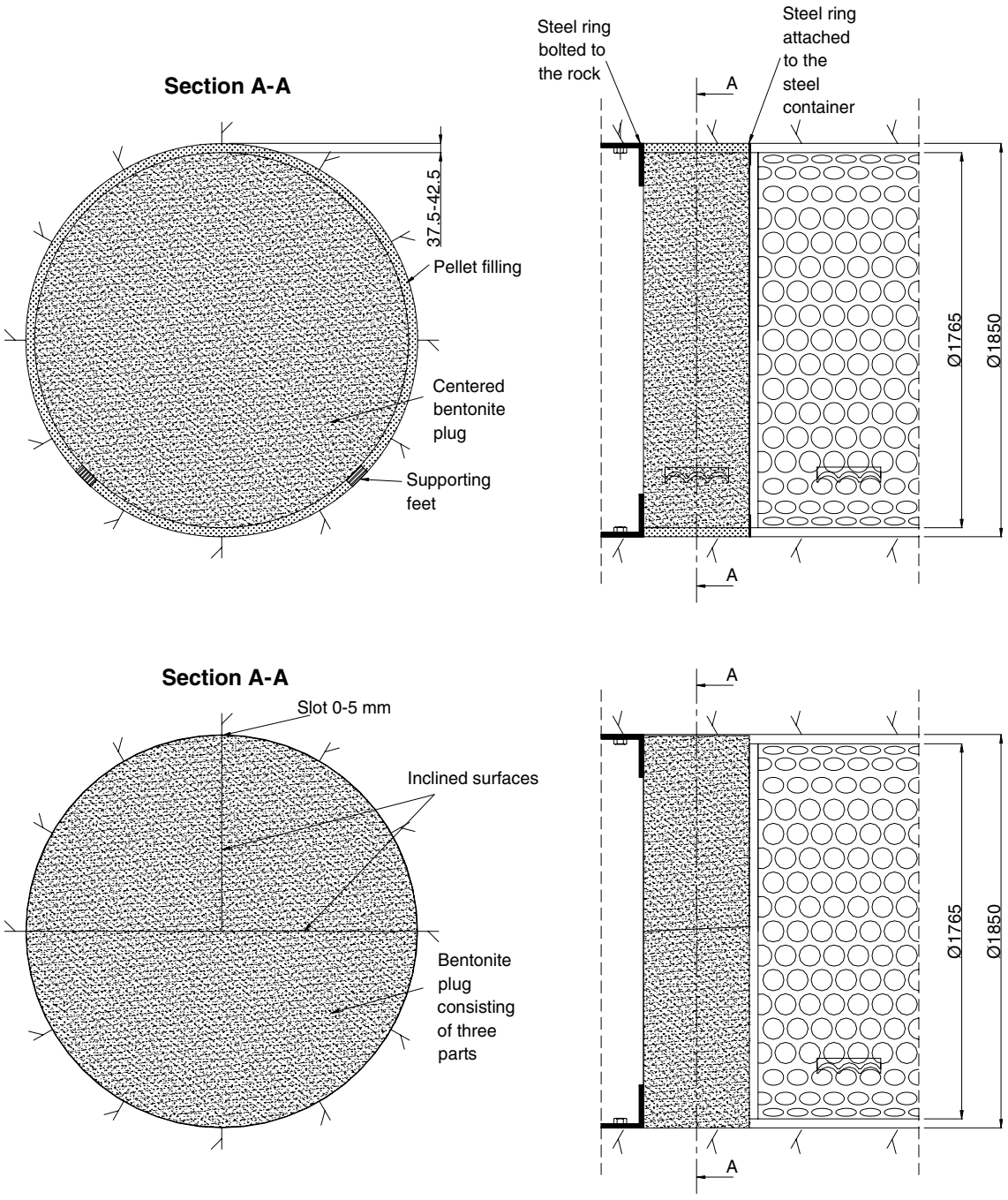

Figure 9-1. *Two proposed design alternatives of the tight distance block concept. See Chapter 9.3.*

These figures yield:

- The total empty volume that needs to be filled between two distance blocks surrounding a perforated container is 1.54 m^3.
- Theoretical time until a container section is filled with water is 10–11 days.

9.3 Scenario descriptions and foreseen processes and problems

The following is an example of a conceptual model of the inflow and piping scenario:

Inflow takes place in one point above the package with the perforated steel container and the buffer and canister in the centre of the package with the inflow rate 0.1 l/min. Water pressure builds up to 2,000 kPa in the fracture if water inflow is stopped. The rate of water pressure increase is 100 kPa/h. This case is the reference case.

After 1 day	4 m^2 of the floor is filled with water and gel.
After 2 days	the water reaches the distance block.
After 3 days	the entire bottom is filled (to 2 m width). The water level will rise 0.2–0.4 mm/min either on one side a time or simultaneously.
After 10 days	the entire void is filled.

The maximum amount of water absorbed by the buffer periphery by the buffer inside the super container is ~ 0.01 l/min.

The slow filling of the gap between the container and the rock yields that the gap between the distance block and the rock will be sealed with a gel that is tight enough to prevent water from flowing past the block. The water pressure is low when the water table rises since the gel in the pellets filled gap (or very small gap, depending on which design alternative is chosen) is formed within minutes and the water table increase rate is less than a mm/min. This means that piping will not occur during filling if the block does not move. In some tests there has been a leakage due to such a block displacement, but the leakage has eventually stopped (treated later in the text). The distance block will thus prevent water from leaving the container section. The last part to be sealed is the top of the distance block. Then the gap and all empty spaces in the container section are filled with water and the water pressure will rise due to that the water flowing from the rock is stopped and

- if there is no unfilled space left to reduce the water pressure increase and the rate of water pressure increase is too high for sealing there will be piping. Once piping has occurred there is a large risk that the water flow rate is too high for sealing to appear,
- if the rate of water pressure increase is low enough there will not be piping.

The scenario is likely to be the same independently of where the inflow takes place and if it takes place in many spots instead of in one spot. The main parameters that are important are the inflow rate and the rate of water pressure increase. If the distance block is equipped with a ring according to Figure 9-1 there will be no piping at the reference case, which has been shown with tests both in the scale 1:10 and in large scale.

If there is no piping the water pressure will continue to rise with the rate 100 kPa/h according to the scenario description until full water pressure has been reached. This means that the water pressure will act on the distance block, which thus must be strong enough to withstand this pressure.

The wetting of the bentonite inside the perforated container may cause local gelling especially if water drips on the bentonite. Under certain conditions unfilled parts, which are isolated by the gel, may occur. In such a case the water filling may be faster since the volume is smaller and the pressure increase thus starts earlier. However, the low density of the gel originating from the inner part of the container means that piping should occur in that gel before it may occur at the distance block. There will thus probably be internal piping until the entire space is filled. The difference from the base case is thus that the pressure will start to increase earlier but the pressure will not be high until the entire section is filled because of the low inner resistance to piping in that gel (this lack of piping resistance is why the distance block is needed).

There is however another process that may occur during the water filling. When water penetrates the narrow opening between the distance block and the rock surface in the bottom of the tunnel (or into the pellets) the block may heave due to the swelling of the bentonite. This process has been observed in some scale tests. If the block heaves when a large part of the empty space between the super container and the rock has been filled with water, there is a risk that there will be an open fracture in the gel below the distance block. Since the water pressure in that case will be several meters of water head, there may be a water leakage through that fracture. The leakage may stop due to the self-healing of the bentonite but it may also continue since it was observed in the basic tests that a water pressure of that size in combination with a high flow rate is not easily stopped. However, in the scale tests and the full scale tests this leakage has stopped.

This process and piping at the top of the distance block entail probably the highest risk for piping. A way to minimize the risk of heave is to use well-compacted pellets in the gap above the block because the pellets will hinder the heave. The concept with pellets is thus preferential and the heave can be further prevented if feet or spacers are applied not only in the bottom but also on the top of the block.

9.4 Consequences

When the distance block has sealed and no water can pass, the increase in water pressure behind the distance block will yield the following consequences:

There will be an axial force from the water pressure in the container section acting on the distance block. This axial force on the distance block needs to be taken by the steel ring. The total force can be calculated as the pressure multiplied with the active pressurized area. The larger the active area the higher is the force. The crucial question is thus how deep radially into the bentonite (or in between the distance block and the container) the water pressure penetrates.

If there is a swelling pressure between the distance block and the rock surface, the friction between the bentonite and the rock surface will resist part of the axial force. The bolted steel ring must take the rest of the force. In addition to the water pressure there may be a swelling pressure from the wetted bentonite. However, this pressure is in the beginning low compared to the high water pressure that rapidly increases.

The resulting force and the required swelling pressure between the distance block and the rock surface in order to be able to resist that force are calculated in Appendix 7. The calculations show that the influence of how deep the water pressure penetrates is of course very strong.

The contact area between the distance block and the rock surface that has a swelling pressure is also of course vital for the resistance. The laboratory scale tests have shown that the total area of the block that swells and resists the force is small (i.e. the axial depth of water penetration), which means that we probably cannot count on this effect but must assume that the entire force needs to be taken by the supporting ring.

Tests on how deep in radial direction between the block and the super container the water pressure penetrates have been done. The conclusion is that the penetration is not very deep (a couple of cm) if the distance block is in good axial contact with the end of the container. If there is a slot between the container and the block the penetration will be deeper. In all tests, both scale tests and full scale tests, the penetration has not exceeded 5 cm even with a slot between the distance block and the container of 7 mm. However, after 45 days the scale tests have shown that the effect penetrates to 10 cm.

A special scenario is if the water pressure acting on the ring via the distance block yields a small movement of the block e.g. due to breakage or deformations. If the slot that appears at such a movement is 1 mm wide in the entire cross section it will be filled rather fast (~ 30 minutes) and the water pressure may thus act on the entire cross section with a very high force that cannot be taken by the bolted ring. This is a severe scenario that must be prevented. A strong safety margin must thus be set. Tests of such a scenario may also be required.

An original axial slot should be avoided, but if it is small it is unlikely that the water pressure will penetrate into such a slot since the sealing capacity of the bentonite is strong when the slot is small and the filling rate is low (as shown in the piping tests).

The total force F1 that needs to be taken is thus (see Appendix 7):

$$\mathrm{F1} = \left[\pi \left(\frac{D}{2} \right)^2 - \pi \left(\frac{D - 2\delta}{2} \right)^2 \right] u \qquad (9\text{-}1)$$

where

u = water pressure (kPa)
δ = radial distance from rock surface of increased water pressure (m)
$\underline{D}$ = tunnel diameter (1.85 m)

The radial gap between the bentonite blocks inside the perforated container and the rock surface is in average 5.5 cm and this is the minimum space where the water pressure can be assumed to prevail. The measured radial penetration of the water is small due to the slow wetting, should be less than 5 cm according to the tests. The consequence is that the water pressure may act on an area reaching radially from the rock surface 11 cm in. The total force from a water pressure of 2,000 kPa will thus be

$F1 = 0.60 \times 2000 = 1{,}200$ kN

At the water pressure 5,000 kPa the total force will be

$F1 = 0.60 \times 5{,}000 = 3{,}000$ kN

An additional safety margin may be required. Figure 9-2 shows the force F1 plotted as a function of the radial distance d for three different water pressures.

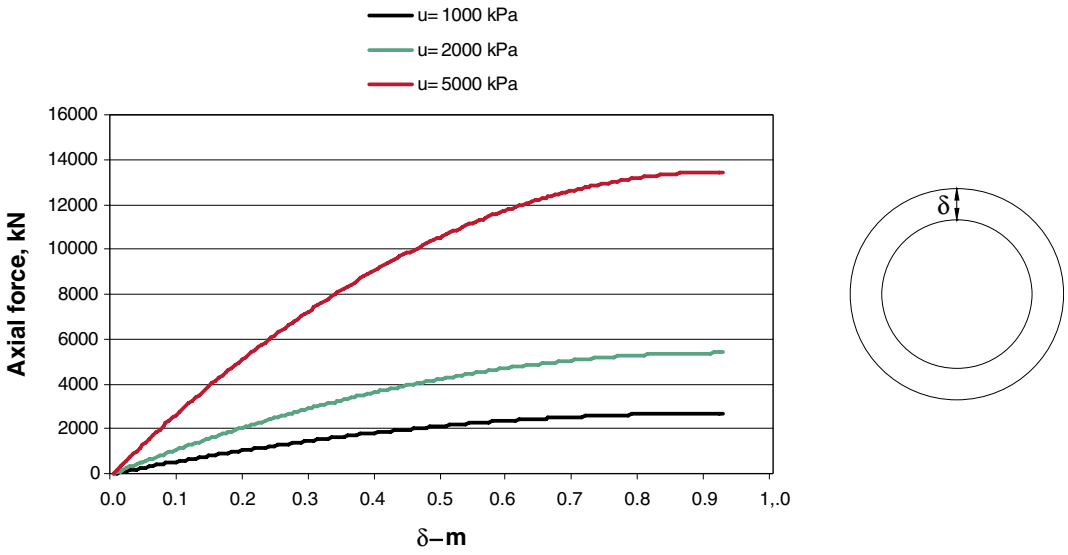

Figure 9-2. *The total force that needs to be taken by the supporting ring as a function of δ (radial distance from rock surface of increased water pressure) at three different water pressures.*

9.5 Preliminary conclusions

The conclusions from these analyses in combination with the tests shown in Chapter 7 are thus that the bolted ring can work as intended for the reference scenario and prevent piping and displacement of the distance block with one of the suggested designs. The ring must be fixed to the rock surface with bolts that are so strong and undeformable that the total force can be resisted without deformation. The real danger consists of a sudden small displacement of the block so that the water pressure is applied on the entire cross section area of the tunnel.

The scenario description mainly refers to the base case. The consequence of higher water pressure (up to 5 MPa), faster pressure build-up (up to 1,000 kPa/h) and faster water inflow rate (up to 1.0 l/min) has also been investigated. The results indicate that 5 MPa and 1,000 kPa/h. and 1.0 l/min inflow cannot be accepted. 0.2 l/min inflow was barely handled in a scale test (together with 1,000 kPa/h and 5 MPa).

The length of the distance blocks is probably influencing the function in a positive way. If the reference case is considered unacceptable additional large scale tests for investigation of this effect should be done in order to extend the limits.The following further tests are thus suggested:

- Tests of the consequences of a sudden displacement of the supporting ring.
- Tests in large scale to look at the influence of the length of the distance blocks.

10 Open tunnel scenario

10.1 Introduction

If the distance blocks cannot be proven to function properly during the initial stage of the repository before the end plug has been applied, an alternative solution is to keep the tunnel open by placing the distance blocks on feet, thereby letting the water flow freely on the bottom of the tunnel. Due to the inclination of the tunnel the water will be transported out of the tunnel. A preliminary analysis of the function of such a system will be done in this chapter. The analysis consists of the following parts:

- Presumptions.
- Scenario descriptions.
- Foreseen processes and problems.
- Estimated consequences.
- Improved solutions.
- Conclusions.

10.2 Presumptions

In the final repository the hydraulic conditions at the container positions are going to vary between no inflow at all (fracture free rock) and a large inflow from several fractured zones of several liters per minute. Since the other piping/erosion phenomena have been studied with the assumption of 0.1 l/min for one canister position this will be the reference inflow assumed also for the open tunnel scenario. This is probably non-conservative so as "compensation" all positions have been assumed to yield 0.1 l/min.

The following basic data is selected:

- Inflow: 0.1 l/min, container section.
- Pressure increase rate: 100 kPa/h.
- 300 m tunnel: 30–40 container sections.
- Installation of one container section per day.
- 90 days until closure.

These figures yield:

- Total inflow in entire tunnel: 3–4 l/min.
- Total inflow until closure: ~ 450 m^3 water.
- Relative humidity in unventilated tunnel RH = 100%.

10.3 Scenario descriptions and foreseen processes and problems

10.3.1 General

The scenario will differ somewhat between the case that the water flows in so many points or at such positions that no liquid water comes in contact with the bentonite and the case that water is dripping or flowing on the bentonite.

10.3.2 No water dripping on the buffer:

Scenario

0.1 l/min is rather evenly distributed along the rock surface. This yields *RH* = 100% that condenses on the rock surface and flows along the rock surface down to the bottom of the tunnel and then flows out from the inclined tunnel section. Example: for container No 15 about 1.5 l of water enters the tunnel section and 1.6 l leaves it.

The water level will not reach the buffer since the flow is not large enough compared to the tunnel inclination. The buffer will only swell due to the high *RH*.

How fast does the buffer swell?

The water uptake is a factor of 10 slower when *RH* = 100% is applied in contact with a confined bentonite sample compared to when liquid water is applied according to preliminary tests. The reason is probably that the water transport is not limited by the bentonite but by the vapour transport rate in air.

Scoping calculation

The buffer must swell and fill the gap to come in contact with the rock. It must absorb about the same amount of water that is required to fill the gap. If the gap is 2 cm (at the distance block) 2 g/cm^2 (20,000 g/m^2) must thus be absorbed. This amount of water must be transported by diffusion in air (assuming no air-movements, an assumption that is non-conservative). If one assumes that the buffer takes all the humidity from the air and reaches the water ratio 30% *RH* at the buffer surface will be about 95% and at the rock surface 100%. This gradient will transport water through the air by diffusion. The gradient will be increased with time since the gap will decrease due to the swelling. In order to compensate for this *RH* = 90% has been used for the bentonite surface.

The diffusion coefficient of water vapour transport in air is

D = 3E–5 m^2/s.

The driving force is the gradient in *RH* recalculated to the gradient in vapour mass content m (g/m^3) over the gap width Δl: $\Delta m/\Delta l$

The rate of vapour mass transportation q (g/m^2, s) is thus according to Equation 10-1:

$$q = D \times \Delta m/\Delta l. \qquad (10\text{-}1)$$

At 20°C air can hold 17.3 g water per m^3 air (RH = 100%). The difference in RH = 10% thus corresponds to Δm = 1.73 g/m^3 water.

The required mass of water transport during the time t is

$q = 20{,}000/t$ (g/m^2 s) (10-2)

Equations 10-1 and 10-2 yield

$t = (\Delta l \times 20{,}000/(D \times \Delta m)$ (10-3)

t = 0.02×20,000/(3E–5×1.73) = 7.7E6 seconds = 89 days

According to this simple approach it would thus take about 3 months until so much water has diffused that the entire gap is filled. *This is a very rough estimation, since the process is more complicated.* The process will probably be faster since the assumption that the only transport mechanism is diffusion is very questionable due to possible air movements in the tunnel. If the gap is wider than 2 cm the time will be accordingly longer since the gradient is smaller.

Simple tests with bentonite samples placed over a free water surface have been made and they confirmed the rate of diffusion. However, the tests also showed that the bentonite samples cracked and small pieces fell down.

10.3.3 Water dripping on the buffer

If water cannot be prevented from dripping on the buffer, the buffer will immediately swell at the contact and absorb the water (see Figure 10-1). The rate of swelling and the rate of the amount of water that can be absorbed increase with the salt content of the water and decrease with time. If the bentonite cannot absorb all the water, it will flow along the bentonite surface and swell at other places. Rather soon the buffer will have swelled 2 cm and come into contact with the rock wall and the piping erosion phenomena will start. The rate of erosion is mainly a function of the flow rate, the flow length and the salt content. Some erosion tests have been done. The results are shown in Figure 10-2. If the flow rate in the dripping point is 0.01 l/min (1/10 of the water in the container section) the erosion will according to Figure 10-2 be about 0.01 g/min in tap water. In salt water (1.1%) the erosion will be 10 times higher according to these preliminary tests, i.e. 0.1 g/min.

1.1% salt in eroding water

The total amount of erosion will thus be 14 g/day (or 140 g/day in salt water). If the tunnel is open for 60 days the total amount of eroded material will thus be 864 g (8,640 g in salt water) or roughly 1–10 kg.

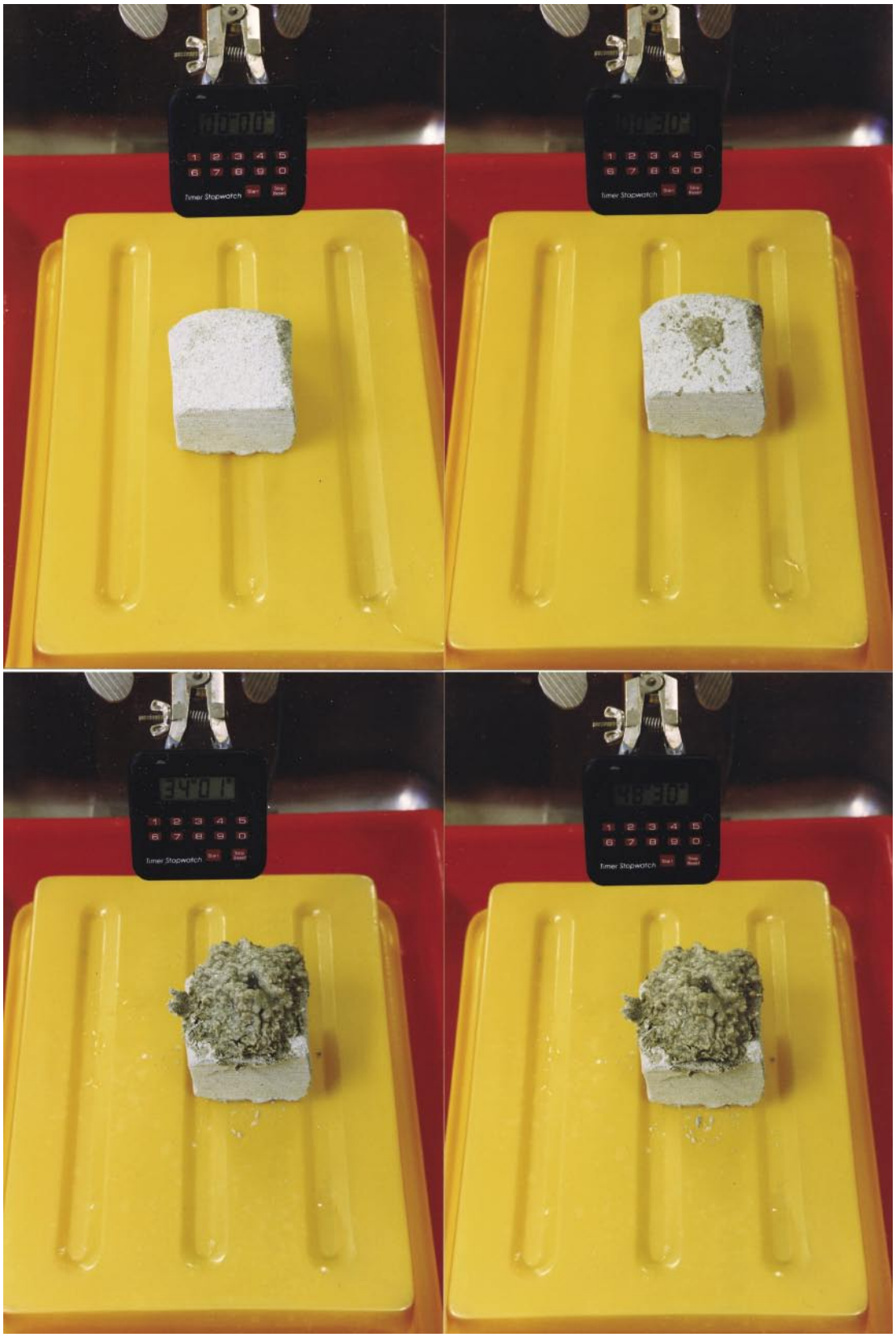

Figure 10-1. *Tap water dripping on a bentonite sample. From left to right: 0 min, 0.5 min, 34 min and 48 min after start.*

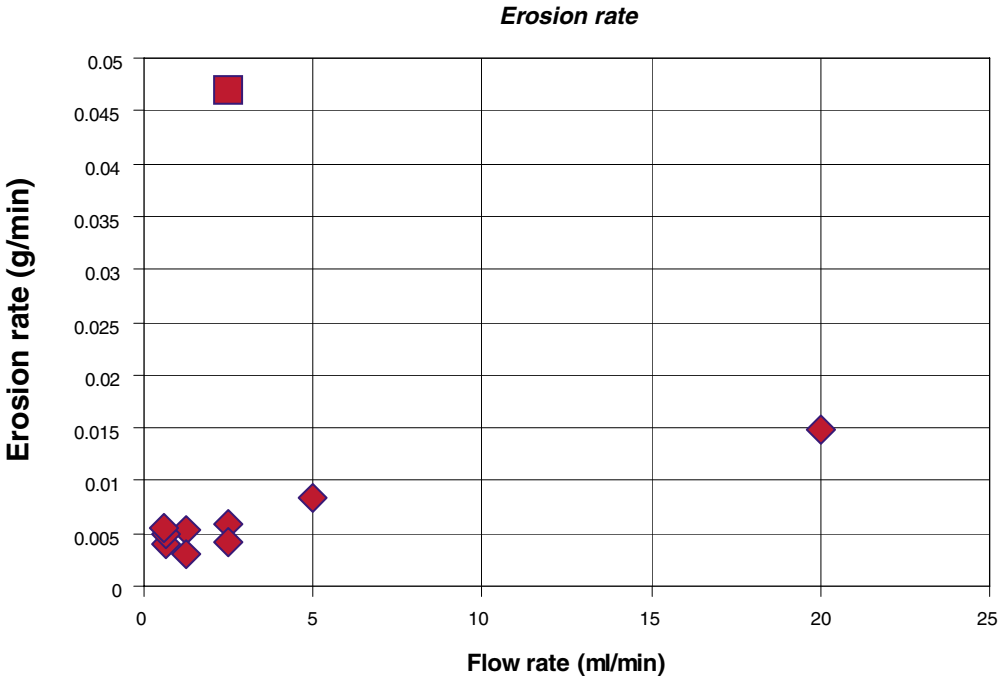

Figure 10-2. *Erosion rate as a function of flow rate for 10 cm long samples with a 2 mm diameter hole with tap water as eroding water (taken from the tests shown in Chapter 6).*

10.4 Consequences

The consequence of RH = 100% on the tunnel walls and homogeneous moisture uptake is not an issue provided that the buffer does not crack and pieces do not drop to the floor. If it takes 3 months for the buffer to swell enough to fill all gaps the tunnel will be plugged before this process is completed. If water is dripping on the bentonite the erosion will according to the estimation done be 1–10 kg for 2 months, which probably is not devastating for the buffer.

However, these calculations have been done with very simplified assumptions. Water dripping on the bentonite will as seen in Figure 10-1 yield a very fast swelling and a gel in contact with the rock surface within hours. Although the calculation yields erosion that may be acceptable it cannot be disregarded that the gel may be formed on the bottom where it will come in contact with the running water from inner sections, which means more swelling and more erosion. In addition, the erosion rate is calculated from tests on samples with the length 10 cm and no account has been taken to the influence of the length of the flow path, which may increase the erosion substantially.

Another very severe consequence is that the bentonite blocks will crack on the surface when exploited to high RH. Such cracking leads to that parts of the block fall into pieces and the pieces will be gathered on the floor with increased swelling and erosion. Preliminary tests showed that cracking and degradation of the buffer occur rather fast in high RH.

In summary the consequences are very difficult to foresee but there is a high risk of severe damage. The simple calculations indicate that even if the consequences of swelling and subsequent erosion are acceptable the cracking and degradation of the buffer probably will be devastating.

10.5 Improved solutions

10.5.1 Ventilation

One idea to reduce the wetting of the buffer is ventilation i.e. to blow dry air through the tunnel from a cross-hole in the end of the tunnel. The theoretical total amount of airflow required in order to dry all inflowing water can be calculated. If air with *RH* = 0% enters the tunnel and air with *RH* = 100% leaves the tunnel 1 m^3 of air may have consumed 17.3 g water at 20°C. Since the total water inflow is 4 l/min the entire flow of air in order to absorb all water is 231 m^3/min. However, air with RH less than about 60% cannot be used since it will dry the bentonite blocks with cracking as a possible consequence. Air with *RH* = 60% means that 580 m^3/min or about 10 m^3/s must be forced through the tunnel, which of course is impossible since it implies an air velocity of more than 100 m/s through the 2 cm wide gap (cross section area 0.12 m^2).

Ventilation can thus not dry all the inflowing water but only about 10%. On the other hand ventilation may function as a "protection" of the bentonite. If the air transport is fast enough *RH* in the flowing air may stay rather unchanged due to the short time in the tunnel. If e.g. the air velocity is 10 m/s the air will stay for less than 30 seconds, which could be a too short time to significantly increase RH in the air.

This scenario can be calculated. Moisture flux from a water surface exposed to an air stream can be expressed according to Equation 10-4 /see e.g. Wadsö, 1993/.

$$F = k_p \times \Delta p_a \qquad (10\text{-}4)$$

where

F = moisture flux (kg/m^2s)
k_p = mass transfer coefficient (kg/m^2 s Pa)
Δp_a = difference in vapour pressure between the water surface and the air flow (Pa)
k_p is a function of the air velocity /Wadsö, 1993/ and for the chosen air velocity 10 m/s
$k_p = 350 \times 10^{-9}$ kg/m^2 s Pa.

The moisture absorbed from the water surface into the air stream can thus be calculated. If *RH* = 60% is used in the air the average initial vapour pressure p_a is

p_a = 1,400 Pa.

In free water p_a = 2,300 Pa, which yields Δp_a = 900 Pa. Since the vapor pressure in the air stream will increase with time due to the absorbed water we assume an average Δp_a = 450 Pa. This yields

$F = 350 \times 10^{-9} \times 450 = 0.158 \times 10^{-3}$ kg/m^3s = 0.158 g/m^2s

0.158 g vapour will thus be absorbed by the air stream per second per m^2 rock surface. The total time until the air stream leaves the tunnel is 30 seconds which means that

F = 4.74 g/m^2

vapour will be absorbed. Since the thickness of the gap is only 2 cm 0.02 m^3 air will absorb 4.74 g vapour, which yields 237 g vapour per m^3. This is not possible since only $0.4 \times 17.3 =$ 6.9 g/m^3 water per m^3 air can be absorbed at RH = 60%. The air will thus be saturated with vapour after about one second!

These simple calculations indicate that ventilation does not help. Instead it may enhance the water flux from the rock surface to the bentonite blocks.

10.5.2 Degradable cover

One idea is to cover the bentonite blocks with a protection sheet that is water repelling in RH = 100% for several months but degrading in a predictable trace. The thickness could then be adapted to the degradation rate so that the protection disappears after a few months. A preliminary study has been done by the institution for Fiber and polymer technology at KTH. According to this study there are such materials and the potential for such a concept to function is large. However, further studies must be done and the consequences of e.g. ruptures in the plastic occurring during installation must be investigated.

10.6 Conclusions

Although the analyses and calculations done are very rough the conclusions is that the open tunnel concept does not work unless the bentonite is protected during installation. The swelling of the buffer due to the high RH in the air and the dripping of water on the buffer obviously leads to degradation and erosion of the buffer. The use of degradable plastic cover or other protection materials should therefore be further investigated.

11 Conclusions

The function of the buffer in the KBS-3H concept has been investigated by laboratory tests in both small scale and full scale, by modeling and by scenario analyses. These investigations have yielded that the concept is feasible but also that there still are some critical questions that need to be further investigated. Some general conclusions are the following:

Scale test

The scale test simulating the saturation and maturation of two canister sections in scale 1:10 showed that the interaction between the buffer and the perforated container is complicated but acceptable from a safety point. The following main observations were done:

- The bentonite had swelled through the holes of the container and between the container and the simulated rock and covered the entire gap.
- The measured swelling pressure outside the container and the measured average buffer density were in the same range as the expected without container.
- The axial hydraulic conductivity of the buffer in the gap outside the container was measured and found to be about 10^{-12} m/s or a higher than expected from the density and swelling pressure measurements but still low enough for fulfilling the demands of the buffer.
- The perforated container was expanded by the inside swelling of the buffer and ruptured at a few locations near the end parts.
- The expansion of the container is believed to be the reason for the high swelling pressure and density outside the container.
- The increased hydraulic conductivity in the gap outside the container is judged to be caused by the uneven swelling behind the container as shown by the theoretical calculations.

Big Bertha large scale test

The actual large scale test was postponed, since the equipment has been used for testing the function of the distance blocks, and is planned to be started in 2005.

Basic sealing tests

The basic sealing tests have revealed the problems for bentonite to seal flowing water and how vulnerable the buffer is when the water pressure is rapidly increased after sealing. The tests lead to the following observations:

- Very low water pressure is sufficient to hinder sealing and cause permanent piping and erosion at constant water pressure (2–4 kPa).
- Very little water flow is required to hinder sealing and to cause permanent piping and erosion (less than 0.001 l/min) when the water pressure increase rate after sealing is high.
- The processes are complicated with many variables and dependent variables.

- The length of the piping channel is one parameter that influences. The longer it is the better the ability to seal.
- Salt in the ground water improves the possibility for the bentonite to seal but increases the erosion rate strongly.
- The values 2–4 kPa and 0.001 l/min are probably conservative since they are combined with either high water pressure or high water flow rate.
- The hydraulic function of the rock is very important.

After long time the sealing is helped from other wetting parts and is expected to tighten all leaks if the swelling pressure is higher than the water pressure. The distance plug is thus expected to function if the water flow is not so high that the erosion reduces the density but it may take a long time for it to seal. One conclusion from these tests is also that more realistic flow and pressure control should be used in further testing and that the complexity of included parameters calls for scenario simulations.

Reference scenario

The basic tests led to the selection of a reference scenario was settled for the subsequent tests. The reference scenario was the following:

- Water inflow of 0.1 l/min per canister section.
- The rate of water pressure increase of 100 kPa /hour.

Most tests were done with these assumptions but other cases were tested as well.

Tests in scale 1:10 of the function of the distance block

The complex process and geometry called for scale tests with simulation of mainly the basic scenario for further understanding of the processes and for development of the technique for making the distance block function properly. The following main conclusions were drawn from the tests of the distance block in scale 1:10:

- The filling rate and the water pressure increase rate are very important for the sealing ability. With the basic inflow scenario the distance plug seems to seal in the scale 1:10 when the gap between the rock and the plug is 2–4 mm but not for larger gaps.
- If the distance block seals and prevents leakage the water pressure build up behind the block must be taken by the block.
- A supporting ring that captures part of the force arising from water pressure behind the distance block is required.
- The sealing of the distance block works very well for the reference scenario with the suggested solution.
- The sealing did not work for higher water pressure.
- The water pressure reaches 15–50 mm radially into the block at the applied scale and geometry.
- The sealing function worked well during at least 90 days although the force was doubled during the first 60 days and then remained constant.
- A gap between the container and distance block should be avoided as far as possible since it increases the force on the ring although the sealing ability works well also in radial direction if the gap is not too wide.

Large scale tests of the function of the distance block

Since some design parameters could not be properly tested in the scale 1:10 and since the effect of the scale might be important, several tests were performed in large scale in the test equipment designed for the Big Bertha experiment.

The conclusions of the full scale sealing tests were the following:

- The scale effects are strong.
- It is possible to seal according to the desires for the reference scenario if engineering solutions with a supporting ring and either pellets in the gap or a very small gap of a few mm is used.
- The measured total force caused by a high water pressure inside the distance block was not very high since the radial distance from the rock surface that the water pressure acted on was only 10–15 mm.
- The results also show that it is important to avoid a slot between the bentonite blocks and between a bentonite block and the container although a slot of 7 mm could be handled as shown in the scale tests.

Another conclusion is that piping and erosion and proof of sealing cannot be scaled but need to be confirmed in full scale for the worst case.

Modelling

A lot of modelling work for simulation and prediction of different processes has also been performed, analytical, numerical as well as conceptual. The following modelling studies were done:

The swelling of the bentonite through and behind the perforated container has been modelled analytically. The model describes the state after full maturation. The results yield that the optimal hole diameter is 10 cm when the present container design is used and that the loss in swelling pressure behind the container furthest away from the holes is about 60%.

The hydro-mechanical evolution of the scale test has been predicted by FEM-modelling of the test. The model was simplified in the sense that the perforated container was not included. Comparison with measured results showed that the general behaviour was fairly well predicted but also that the measured wetting was considerably slower than predicted, partly due to the influence of the container and partly due to some general shortcomings in the late stage of the water saturation phase.

An imaginary KBS-3H repository has also been modelled both regarding the temperature evolution for design purpose and the saturation rate for safety assessment. The saturation modelling showed that the time until complete water saturation is about 10 years if the rock has an average hydraulic conductivity higher than 10^{-11} m/s while the hydraulic conductivity of the rock determines the hydration rate if it is lower than 10^{-12} m/s. The time to full saturation is e.g. according to these calculations 100 years if $K = 10^{-13}$ m/s.

Scenario analyses of the tight distance block concept

The investigations have mainly concerned the alternative with a distance block that is supposed to seal and prevent all water flow past the block during the installation phase either by a tight fitting block or with a slot that is filled with pellets. A scenario analysis of this concept called the tight distance block concept has also been done.

The conclusions from this scenario analyses in combination with other investigations are that the bolted ring can work as intended for the reference scenario and prevent piping and displacement of the distance block with one of the suggested designs. The ring must be fixed to the rock surface with bolts that are so strong and undeformable that the total force can be resisted without deformation. The real danger consists of a sudden small displacement of the block so that the water pressure is applied on the entire cross section area of the tunnel.

The scenario description mainly refers to the reference scenario. The consequence of higher water pressure (up to 5 MPa), faster pressure build-up (up to 1,000 kPa/h) and faster water inflow rate (up to 1.0 l/min) has also been investigated. The results indicate that 5 MPa and 1,000 kPa/h. and 1.0 l/min inflow cannot be accepted. 0.2 l/min inflow was barely handled in a scale test (together with 1,000 kPa/h and 5 MPa).

The length of the distance blocks is probably influencing the function in a positive way. If the reference case is considered unacceptable additional large scale tests for investigation of this effect should be done in order to extend the limits. The following additional tests are thus suggested:

- Tests of the consequences of a sudden displacement of the supporting ring.
- Tests in large scale to look at the influence of the length of the distance blocks.

Scenario analyses of the open tunnel concept

An alternative solution is to keep the tunnel open by leaving a gap between the distance block and the rock surface so that the water can pass the block without interference. Although the analyses and calculations done are very rough, the conclusion is that the open tunnel concept does not work unless the bentonite is protected during installation. The swelling of the buffer due to the high RH in the air and the dripping of water on the buffer obviously leads to degradation and erosion of the buffer. The use of degradable plastic cover or other protection materials should therefore be further investigated.

References

Börgesson L, Johannesson L-E, Sandén T, Hernelind J, 1995. Modelling of the physical behaviour of water saturated clay barriers. Laboratory tests, material models and finite element application. SKB Technical Report TR 95-20, SKB, Stockholm.

Börgesson L, Hernelind J, 1999. Coupled Thermo-Hydro-Mechanical calculations of the water saturation phase of phase of a KBS-3 hole. SKB TR-99-41. Svensk Kärnbränslehantering AB.

Hökmark H, Fälth B, 2003. Thermal dimensioning of the deep repository. SKB TR-03-09. Svensk Kärnbränslehantering AB.

Wadsö L, 1993. Studies of Water Vapor Transport and Sorption in Wood. Doctoral Thesis, Report TVBM-1013, Building Materials, Lund University, Sweden.

Appendix 1

Theoretical model of the swelling of bentonite through the holes of the perforated container and behind its walls

Theoretical modelling

Round holes are considered. Only the stage after completed swelling and homogenisation is considered. The calculation is made in two steps. The first step regards the stresses after swelling through the holes and considers a state of equilibrium in only the axial direction. The second step regards the stresses after swelling into the slot between the container and the rock and considers a state of equilibrium in only the radial direction.

Step 1. Equlibrium after swelling through the holes:

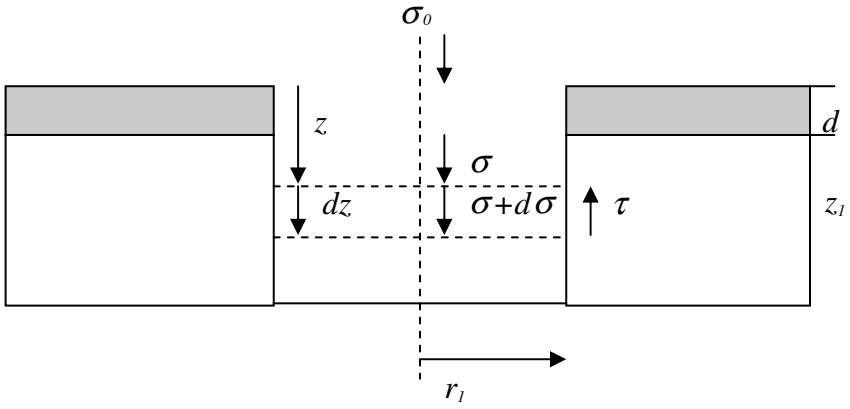

d = container thickness
z_1 = distance between container and the rock
r_1 = hole radius
σ_0 = swelling pressure at z = 0

Force equilibrium in axial direction:

$$-d\sigma \cdot \pi r_1^2 = \sigma \tan\phi \cdot 2\pi r_1 \cdot dz$$

$$-\frac{d\sigma}{\sigma} = \frac{2\tan\phi}{r_1} \cdot dz$$

$$dz = -\frac{r}{2\tan\phi} \cdot \frac{d\sigma}{\sigma}$$

Integrating:

$$\int_0^z dz = -\frac{r_1}{2\tan\phi}\int_{\sigma_0}^{\sigma}\frac{d\sigma}{\sigma}$$

$$z = -\frac{r_1}{2\tan\phi}\left(\ln\sigma - \ln\sigma_0\right)$$

σ_1 = average swelling pressure in the slot (at $z = d+z_1/2$)

$$e^{\left(\ln\sigma_1 - \ln\sigma_0\right)} = e^{-\frac{2z\tan\phi}{r_1}}$$

$$\sigma_1 = \sigma_0 \cdot e^{\frac{-2\left(d+z_1/2\right)\tan\phi}{r_1}} \qquad (8\text{-}1)$$

Step 2a. Equilibrium after swelling into the slot without considering in-plane stresses:

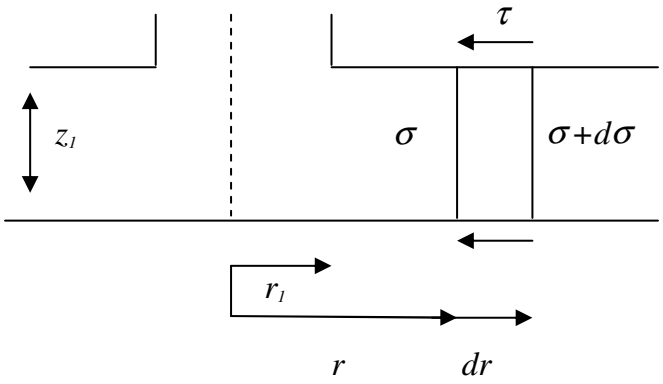

Force equilibrium in radial direction:

$$\sigma\cdot 2\pi r z_1 - \left(\sigma+d\sigma\right)2\pi\left(r+dr\right)z_1 = \left[\pi\left(r+dr\right)^2 - \pi r^2\right]\left(\sigma+\frac{d\sigma}{2}\right)\cdot\tan\phi\cdot 2$$

$$-\sigma dr - r d\sigma = \sigma r dr\cdot\frac{2\tan\phi}{z_1}$$

$$-\frac{dr}{r} - \frac{d\sigma}{\sigma} = dr\frac{2\tan\phi}{z_1}$$

Integrating from r_1 to a specified maximum distance between the holes r_2:

$$-\int_{\sigma_1}^{\sigma_2}\frac{d\sigma}{\sigma}=\int_{r_1}^{r_2}\frac{dr}{r}+\frac{2\tan\phi}{z_1}\int_{r_1}^{r_2}dr$$

$$\ln\sigma_1-\ln\sigma_2=\ln\frac{r_2}{r_1}+(r_2-r_1)\frac{2\tan\phi}{z_1}$$

$$\ln\sigma_2=\ln\sigma_1-\ln\frac{r_2}{r_1}-\frac{r_2-r_1}{z_1}\cdot 2\tan\phi \qquad (8\text{-}2)$$

Step 2b. Equilibrium after swelling into the slot (general case):

$$-(\sigma_r+\Delta\sigma_r)(r+\Delta r)\Delta\varphi\cdot\Delta z+\sigma_r\cdot r\Delta\varphi\Delta z+\tau_{r\varphi}\cdot\Delta r\cdot\Delta z-(\tau_{r\varphi}+\Delta\tau_{r\varphi})\cdot\Delta r\Delta z+\cdot$$
$$(\sigma_\varphi+\sigma_\varphi+\Delta\sigma_\varphi)\cdot\Delta r\cdot\Delta z+\frac{\Delta\varphi}{2}+[(\tau_{rz}+\Delta\tau_{rz})-\tau_{rz}]\cdot\Delta\varphi\cdot\left[\tfrac{(r+\Delta r)^2}{2}-\tfrac{r^2}{2}\right]=0$$

$$-\sigma_r r\Delta\varphi\Delta z-\sigma_r\Delta r\Delta\varphi\Delta z-\Delta\sigma_r r\Delta\varphi\Delta z-\Delta\sigma_r\Delta r\Delta\varphi\Delta z+\sigma_r r\Delta\varphi\Delta z-\Delta\tau_{r\varphi}\Delta r\Delta z+\sigma_\varphi\Delta r\Delta z\Delta\varphi+$$
$$\Delta\sigma_\varphi\,\Delta r\tfrac{\Delta\varphi}{2}\cdot\Delta z+\Delta\tau_{rz}\cdot\Delta\varphi\left(r\cdot\Delta r+\tfrac{\Delta r^2}{2}\right)=0$$

$$(\sigma_\varphi-\sigma_r)-\Delta\sigma_r\left(\tfrac{r}{\Delta r}+1\right)+\Delta\sigma_\varphi/2-\frac{\Delta\tau_{r\varphi}}{\Delta\varphi}+\frac{\Delta\tau_{rZ}}{\Delta z}\left(r+\frac{\Delta r}{2}\right)=0$$

$$\Delta\sigma_\varphi=0$$
$$\frac{\Delta\tau_{r\varphi}}{\Delta\varphi}=0$$
$$\Delta\tau_{rZ}=-2\sigma_r\cdot\tan\phi$$

$\Rightarrow$

$$(\sigma_\varphi-\sigma_r)-\Delta\sigma_r\frac{r}{\Delta r}-\frac{2\sigma_r\tan\phi}{\Delta z}\cdot r=0 \qquad (8\text{-}3)$$

Assuming isotropic swelling pressure:

$$\sigma_r = \sigma_\varphi$$

$$\Rightarrow$$

$$-\Delta\sigma_r \frac{r}{\Delta r} - \frac{2\sigma_r \tan\phi}{\Delta z} \cdot r = 0$$

$$-\frac{d\sigma_r}{\sigma_r}\Delta z = 2\tan\phi \cdot \Delta r$$

$$-\left(\ln\frac{\sigma_2}{\sigma_1}\right) \cdot h = 2\tan\phi\left(r_2 - r_1\right)$$

$$\sigma_2 = \sigma_1 \cdot e^{-\frac{2\tan\phi\left(r_2 - r_1\right)}{h}} \qquad (8\text{-}4)$$

Assuming anisotropic swelling pressure:

$$\sigma_\varphi / \sigma_r = \nu/(1-\nu) \Rightarrow$$

$$\sigma_\varphi - \sigma_r = \sigma_r\left(\frac{\upsilon}{1-\upsilon} - 1\right)$$

$$K = \left(\frac{\nu}{1-\nu} - 1\right) \Rightarrow$$

$$\sigma_\varphi - \sigma_r = \sigma_r \cdot K$$

into Equation 8-3 yields

$$-\Delta\sigma_r \frac{r}{\Delta r} + \sigma_r\left(+K - \frac{2\tan\phi}{\Delta z} \cdot r\right) = 0$$

$$\frac{d\sigma_r}{\sigma_r}\Delta z = \left(K\frac{dr}{r}\Delta z - 2\tan\phi\, dr\right)$$

$$\left(\ln\frac{\sigma_2}{\sigma_1}\right) h = K \cdot h \cdot \ln\frac{r_2}{r_1} - 2\tan\phi\left(r_2 - r_1\right)$$

$$\frac{\sigma_2}{\sigma_1} = \cdot e^{K\ln\left(\frac{r_2}{r_1}\right) - 2\tan\phi\left(\frac{r_2 - r_1}{h}\right)}$$

$$\ln\sigma_2 = \ln\sigma_1 + K\ln\frac{r_2}{r_1} - \frac{r_2 - r_1}{z_1} \cdot 2\tan\phi \qquad (8\text{-}5)$$

v	*K*
0	–1
0.3	–0.57
0.5	0

Thus ν = 0 in Equation 8-5 yields Equation 8-2 and ν = 0.5 yields Equation 8-4.

Appendix 2

Results from predictions of the small scale test and comparison with measured results

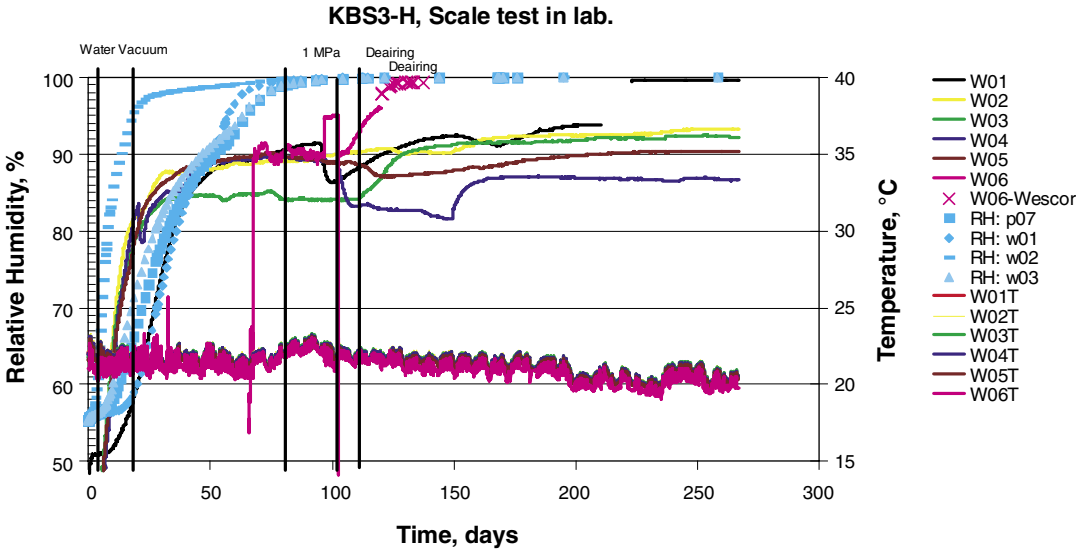

Figure A2-1. Predicted relative humidity (blue dots) and measured relative humidity (W01–W06).

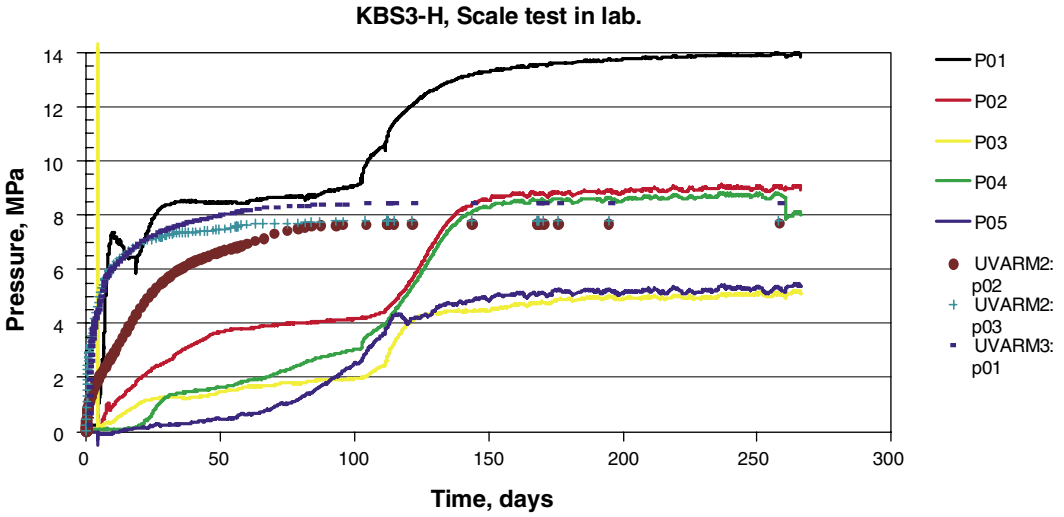

Figure A2-2. Predicted total pressure (dots) and measured total pressure (P01–P05).

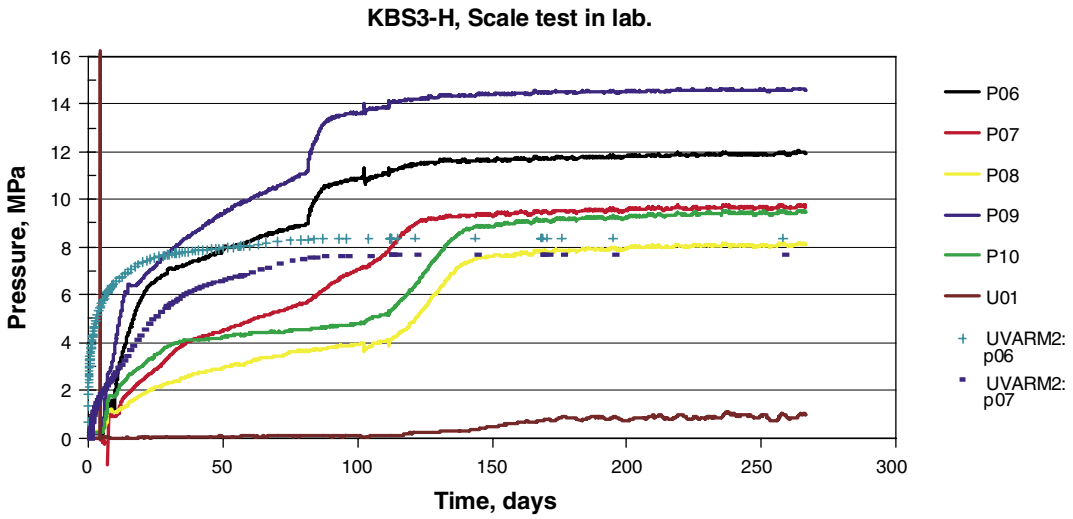

Figure A2-3. *Predicted total pressure (dots) and measured total pressure (P06–P10).*

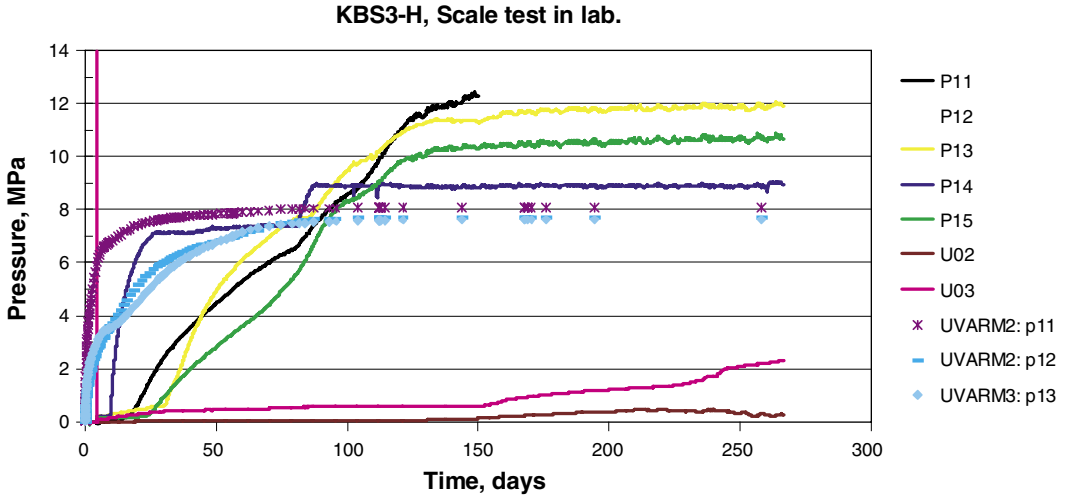

Figure A2-4. *Predicted total pressure (dots) and measured total pressure (P11–P15).*

Appendix 3

Some assumptions and results of the saturation modelling in Chapter 8-5

A. Equivalent effective thermal conductivity of space between canister and rock

The thermal conductivity (λ) of the bentonite is normally calculated as a linear function of the degree of saturation:

$$\lambda = \lambda_{dry}\,(1-S_r) + \lambda_{sat}\,S_r \qquad (4)$$

where S_r is the degree of saturation. According to existing data, the parameter values are: $\lambda_{dry} = 0.3$; $\lambda_{sat} = 1.3$.

No gap between the cylinder and the rock was explicitly modelled, since such a task would require the inclusion of the mechanical processes. Instead, the buffer was modelled as if it from start had swelled into this gap. Since the main concern of the work was to calculate the saturation process, it was important to model a correct initial water ratio. But for a given initial water ratio, the initial degree of saturation of a buffer expanded into the gap is lower than for the actual buffer within the cylinder. As a consequence, the initial thermal conductivity of the buffer would be incorrect. The lower end point λ_{dry} was therefore adjusted in order to compensate for this effect as well as the thermal conductivity of the actual gap (see Figure A3-1).

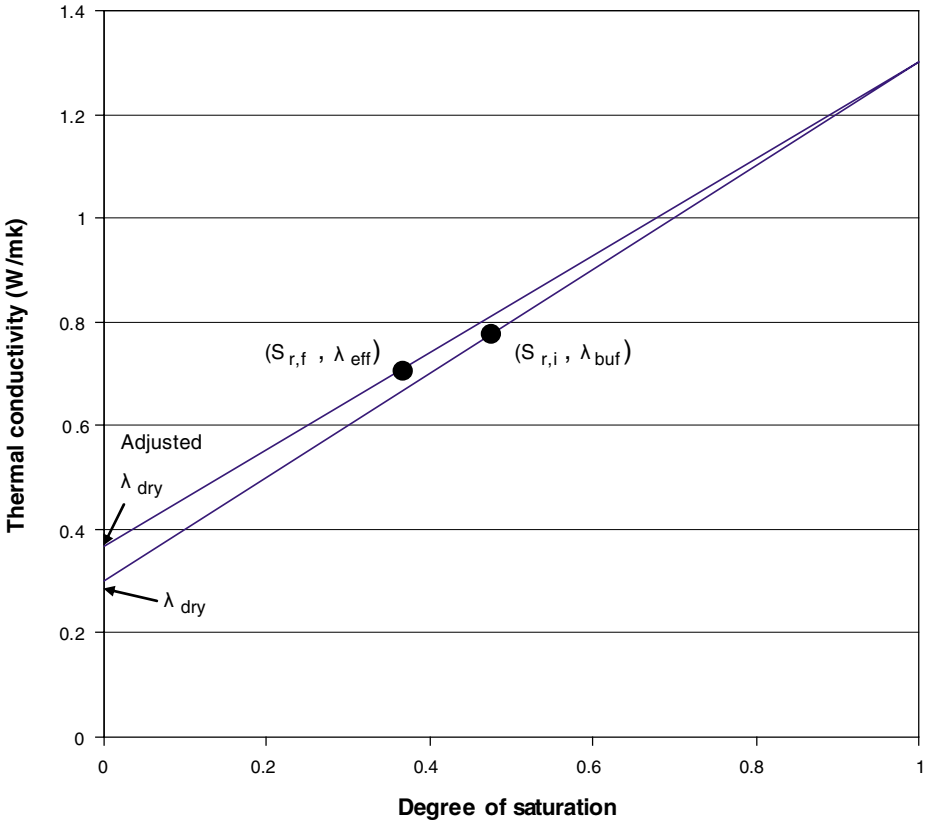

Figure A3-1. *Actual thermal conductivity (λ_{buf}) and degree of saturation for non expanded buffer ($S_{r,i}$), and effective conductivity (λ_{eff}) and degree of saturation for expanded buffer ($S_{r,f}$).*

The section area of the buffer and the gap are calculated as (Figure A3-2):

$$A_{buffer} = \pi \left(R_1^2 - R_0^2\right) \qquad A_{gap} = \pi \left(R_3^2 - R_2^2\right) \tag{5, 6}$$

The ratio between the initial buffer area and the final total area is:

$$r_A = \frac{A_{buffer}}{A_{buffer} + A_{gap}} = 0.895 \tag{7}$$

The final void ratio e_f is 0.77. The initial void ratio e_i is calculated as:

$$e_l = r_A(e_f + 1) - 1 = 0.584 \tag{8}$$

The ratio between the solid density and the water density r_ρ is 2.78. The water ratio is 0.10. The initial and final degree of saturation ($S_{r,i}$ and $S_{r,f}$) is calculated as:

$$S_{r,i} = \frac{r_\rho \cdot w}{e_i} = 0.476 \quad S_{r,f} = \frac{r_\rho \cdot w}{e_f} = 0.361 \tag{9, 10}$$

The initial thermal conductivity of the buffer λ_{buf} is calculated with Equation 4 to 0.776 W/mK. The thermal conductivity of the gap is assumed to be 0.3 W/mK /Hökmark and Fälth, 2003/. The effective thermal conductivity of the buffer and the gap is given by sum of the thermal resistivety of the buffer and the gap, respectively:

$$\frac{\ln\left(\frac{R_1}{R_0}\right) + \ln\left(\frac{R_3}{R_2}\right)}{\lambda_{eff}} = \frac{\ln\left(\frac{R_1}{R_0}\right)}{\lambda_{buf}} + \frac{\ln\left(\frac{R_3}{R_2}\right)}{\lambda_{gap}} \tag{11}$$

In this case, λ_{eff} is 0.704 W/mK.

Finally, the λ_{dry}-value in Equation 4 can be adjusted so that saturation degree of the expanded buffer $S_{r,f}$ corresponds to the effective conductivity λ_{eff}. The adjusted λ_{dry}-value is thus 0.367 W/mK.

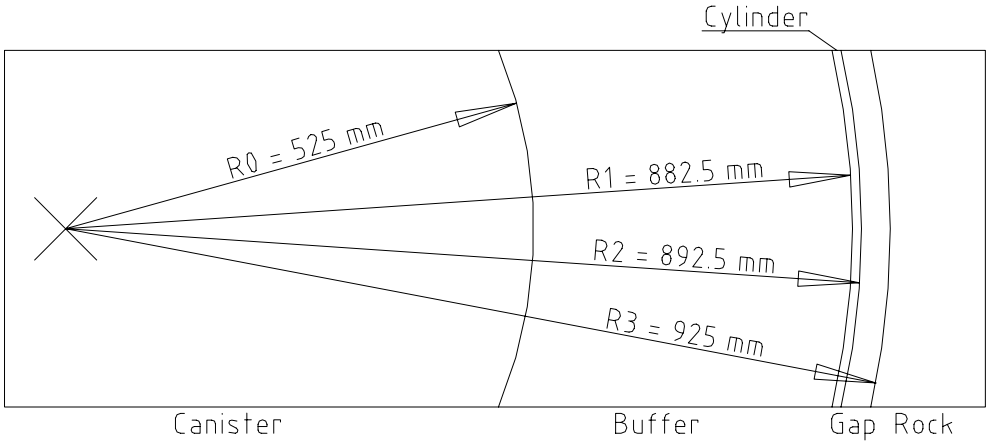

Figure A3-2. *Tunnel section.*

B. Modelling results. Point analyses and scan-lines

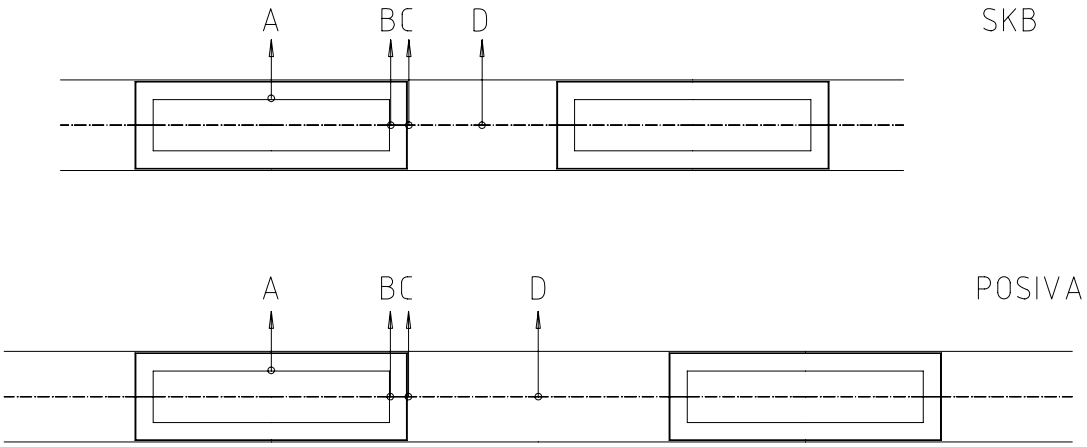

Figure A3-3. *Points and scan-lines. SKB and Posiva case.*

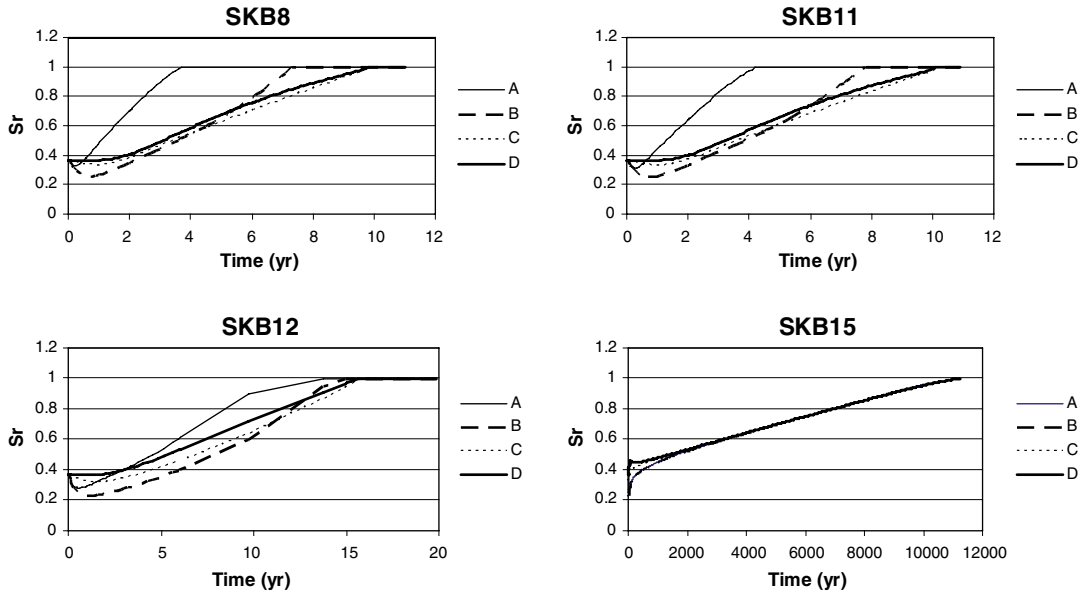

Figure A3-4. *Degree of saturation. Point analyses (A–D). SKB-case. Hydraulic conductivities: 10^{-8}, 10^{-11}, 10^{-12} and 10^{-15} m/s.*

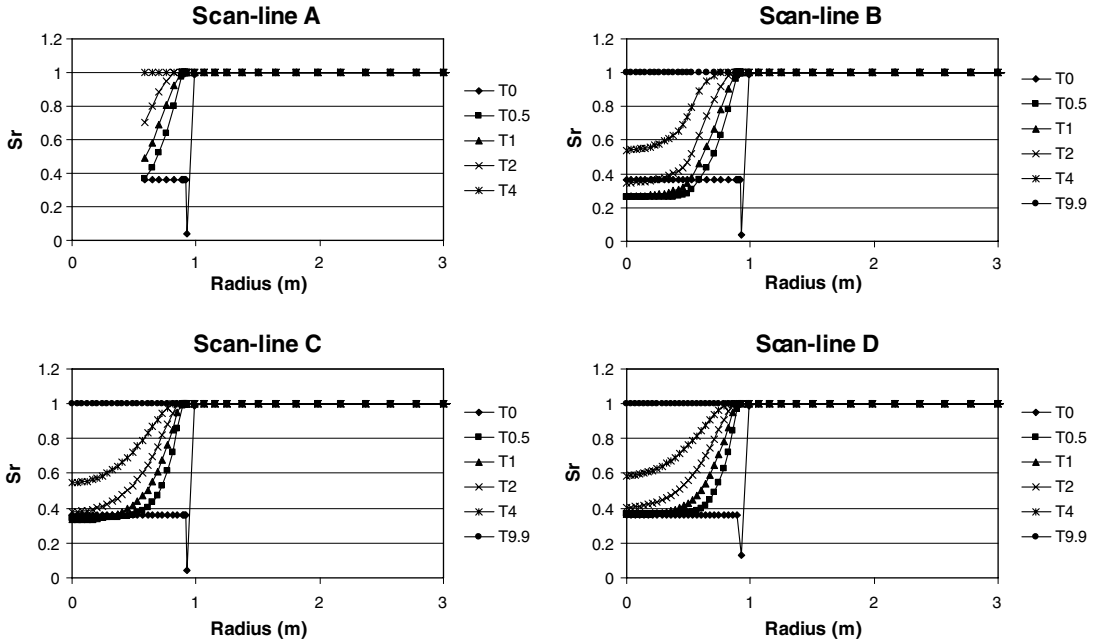

Figure A3-5. *Degree of saturation. Scan-lines (A–D). SKB-case. Hydraulic conductivity: 10^{-8} m/s.*

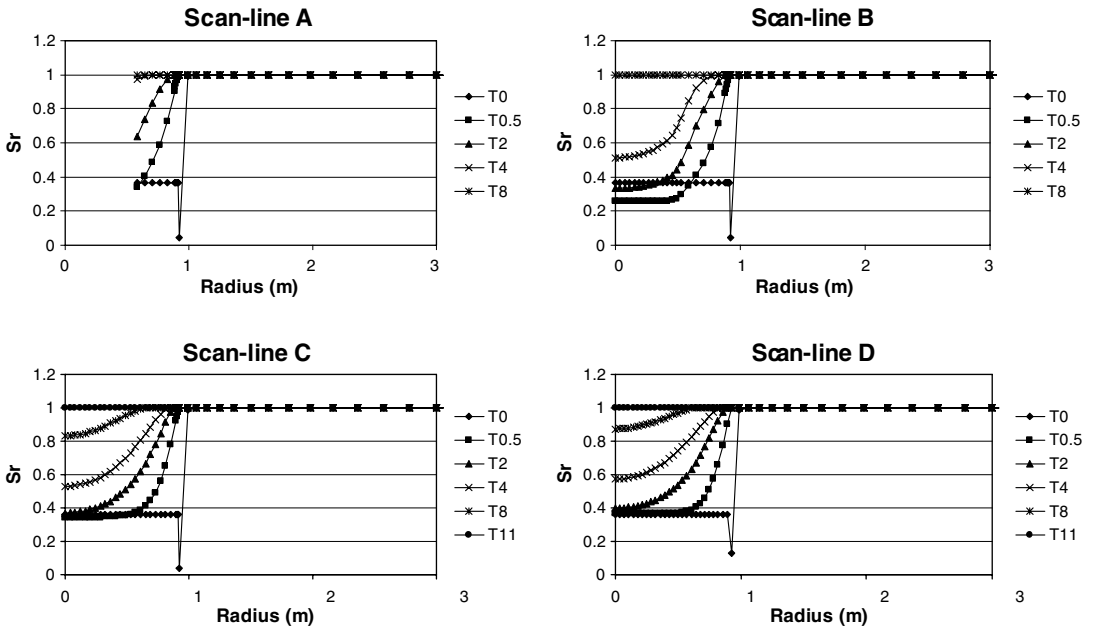

Figure A3-6. *Degree of saturation. Scan-lines (A–D). SKB-case. Hydraulic conductivity: 10^{-11} m/s.*

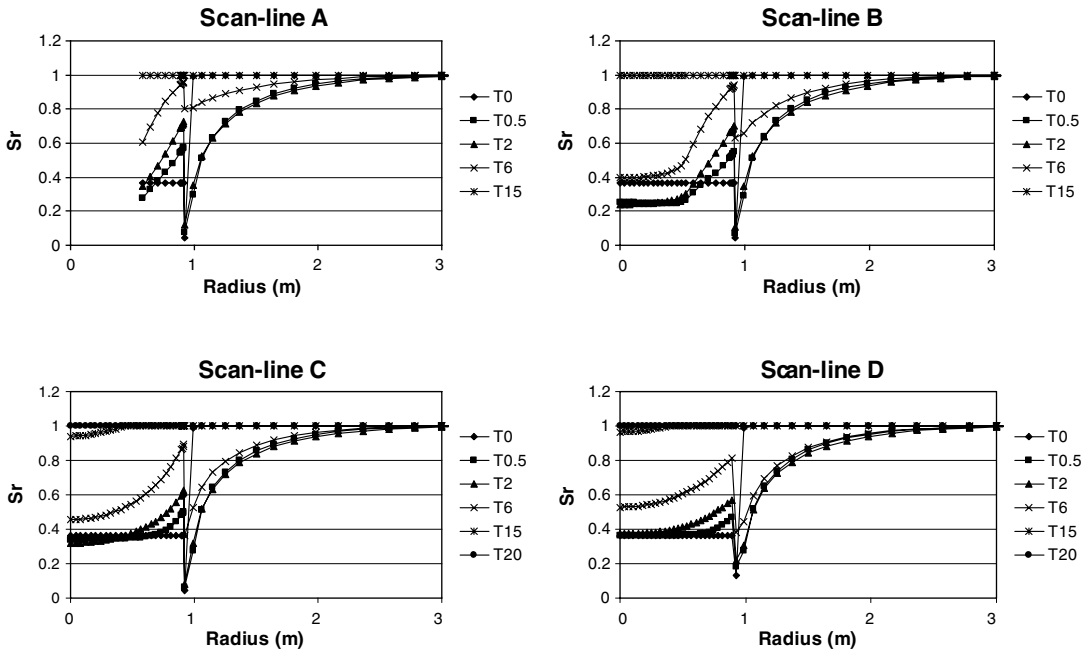

Figure A3-7. *Degree of saturation. Scan-lines (A–D). SKB-case. Hydraulic conductivity: 10^{-12} m/s.*

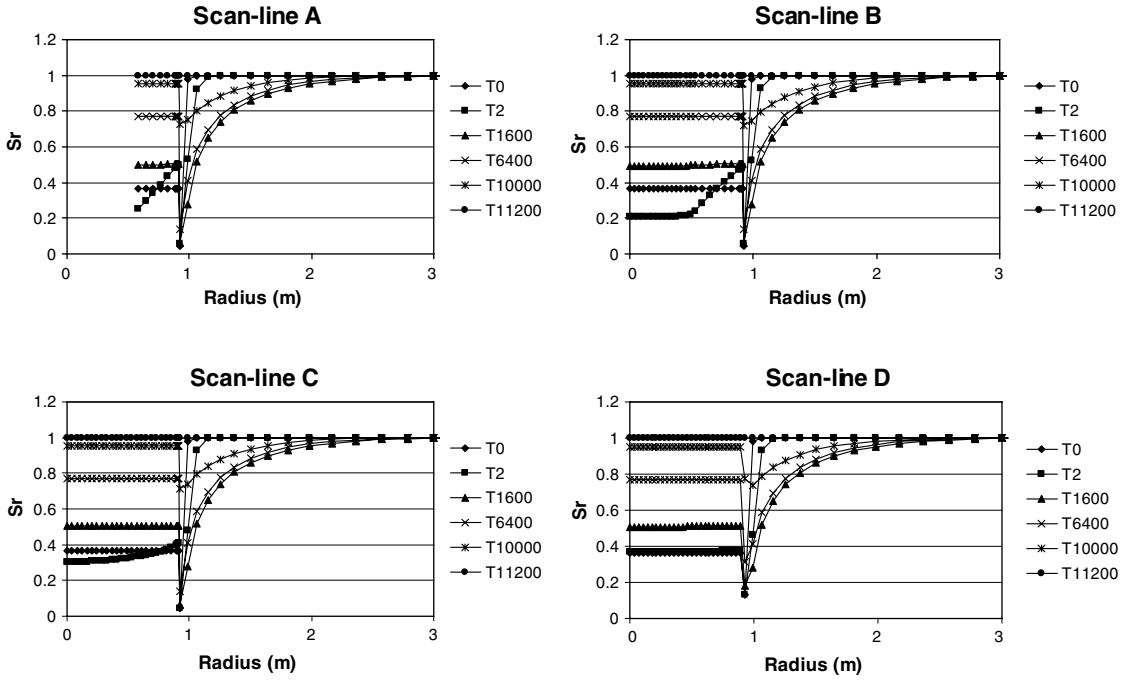

Figure A3-8. *Degree of saturation. Scan-lines (A–D). SKB-case. Hydraulic conductivity: 10^{-15} m/s.*

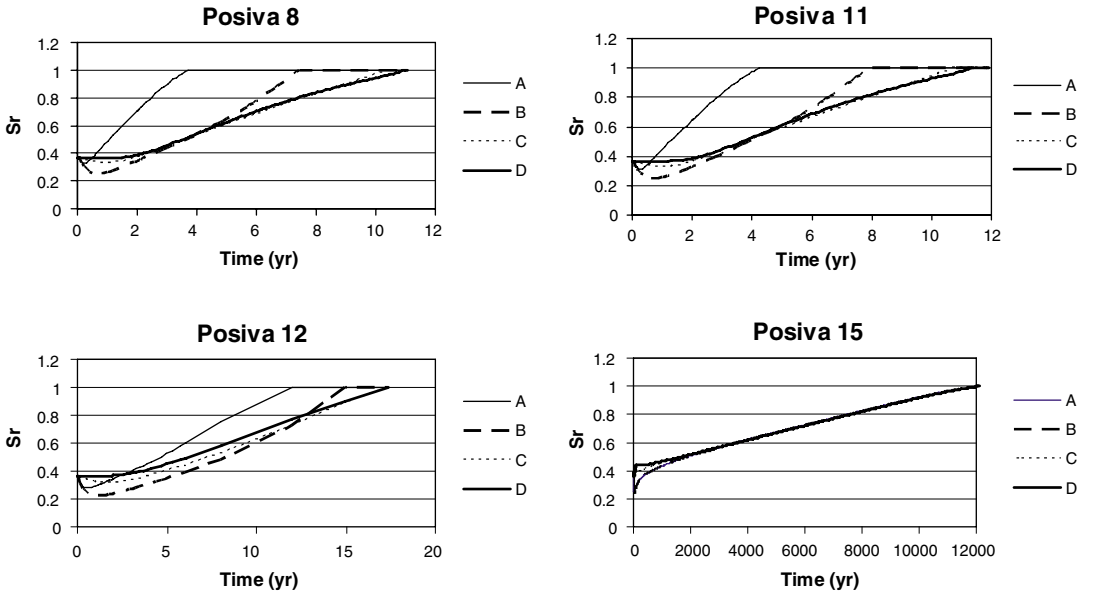

Figure A3-9. *Degree of saturation. Point analyses (A–D). Posiva-case. Hydraulic conductivities: 10^{-8}, 10^{-11}, 10^{-12} and 10^{-15} m/s.*

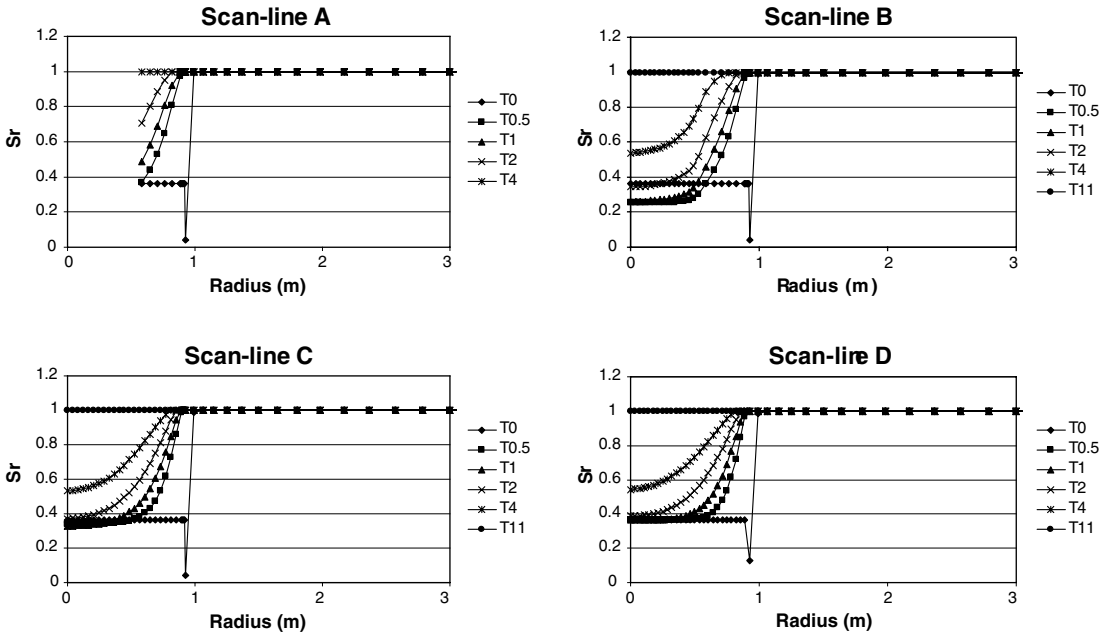

Figure A3-10. *Degree of saturation. Scan-lines (A–D). Posiva-case. Hydr. conductivity: 10^{-8} m/s.*

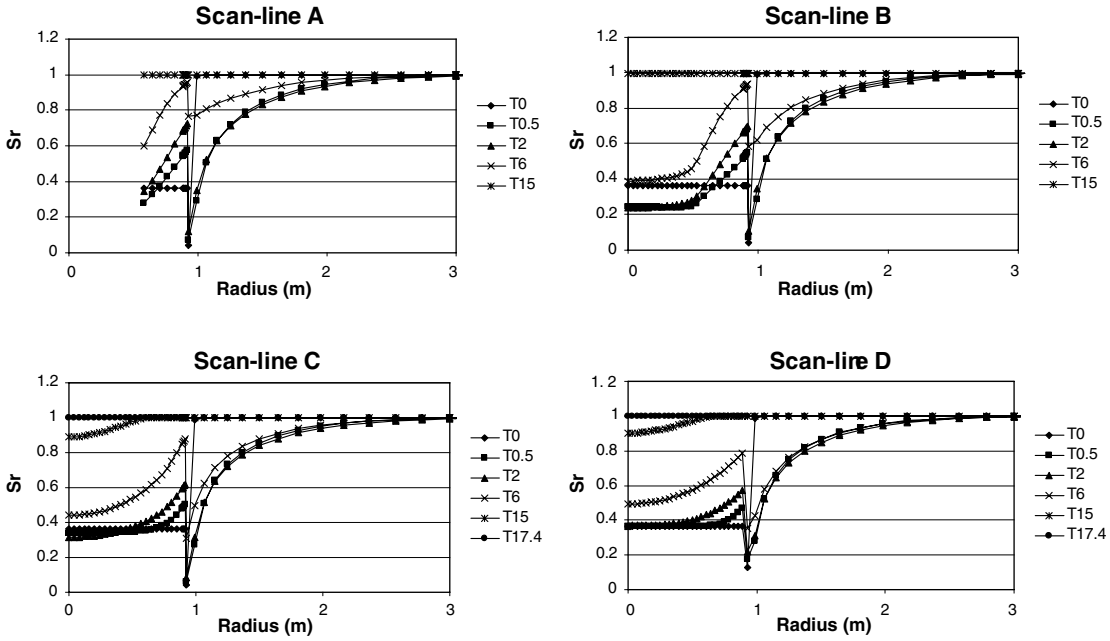

Figure A3-11. *Degree of saturation. Scan-lines (A–D). Posiva-case. Hydr. conductivity: 10^{-11} m/s.*

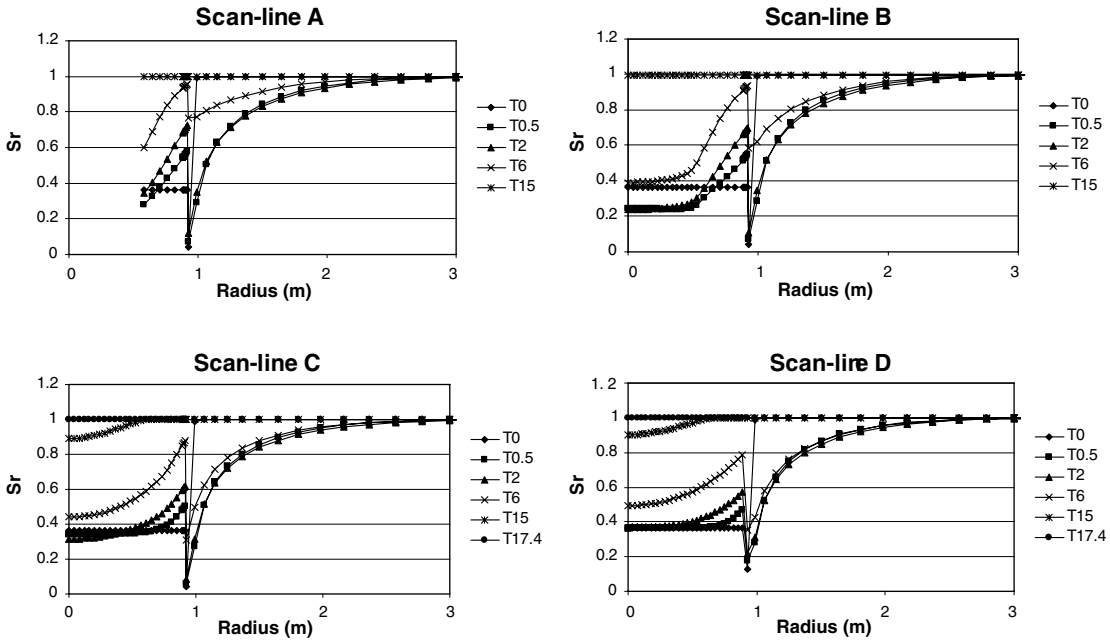

Figure A3-12. *Degree of saturation. Scan-lines (A-D). Posiva-case. Hydr. conductivity: 10^{-12} m/s.*

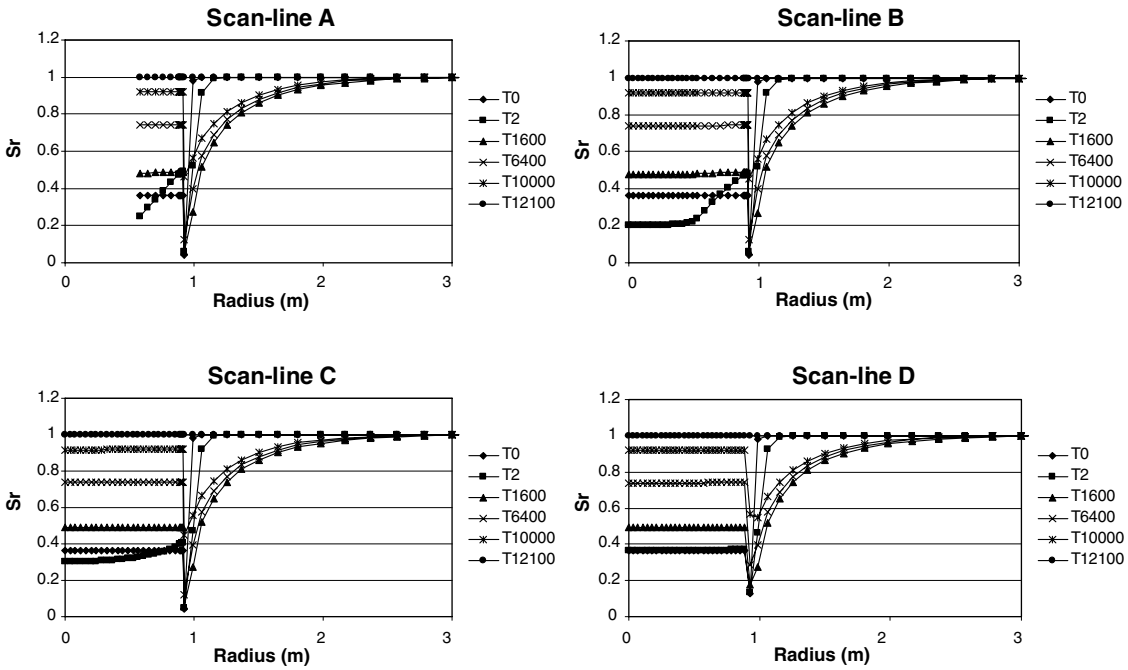

Figure A3-13. *Degree of saturation. Scan-lines (A-D). Posiva-case. Hydr. conductivity: 10^{-15} m/s.*

Appendix 4

Scale tests, Series I

Test I-1

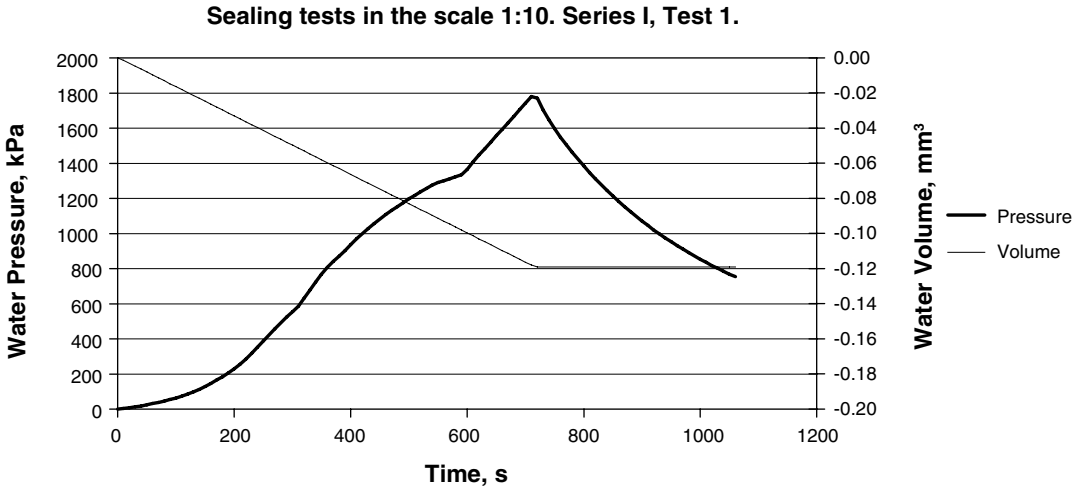

Water pressure increase and inflow volume as a function of time. The sample rested 62h before test start.

Test I-2

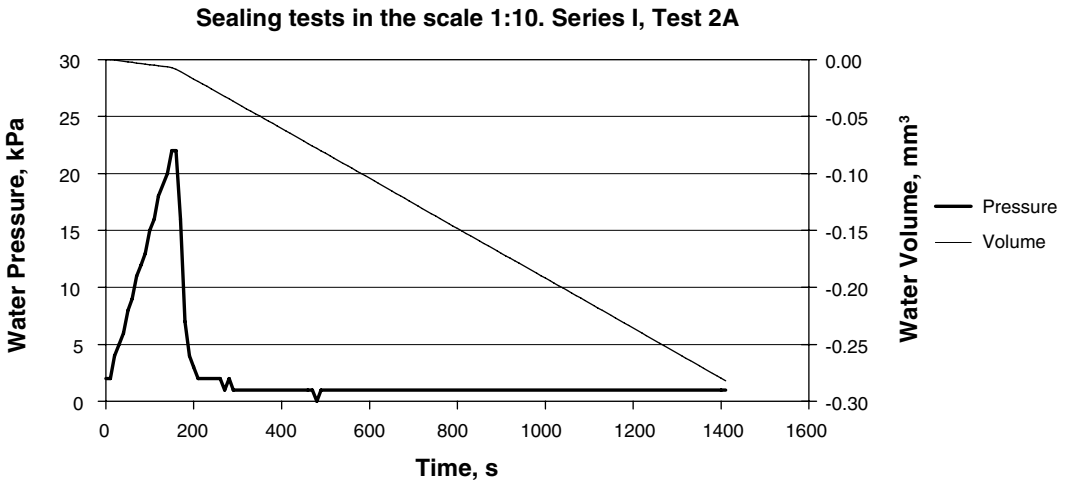

Test 2A. Water pressure increase and inflow volume as a function of time. The water pressure increase was very high 500 kPa/h and piping occurred at very low pressure.

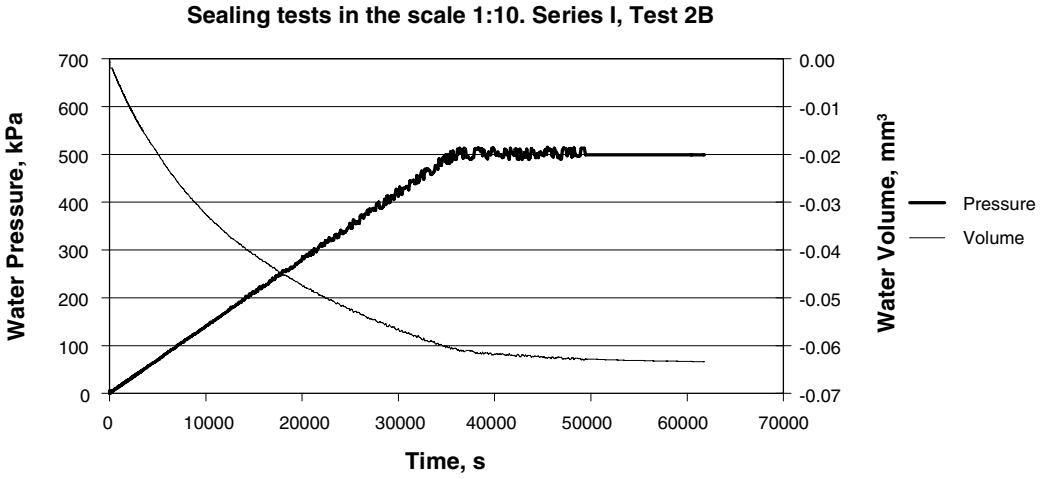

Test 2B. Water pressure increase and inflow volume as a function of time. The sample was left for about 20 minutes and the water pressure increase was reduced to 50 kPa/h.

Test I-3

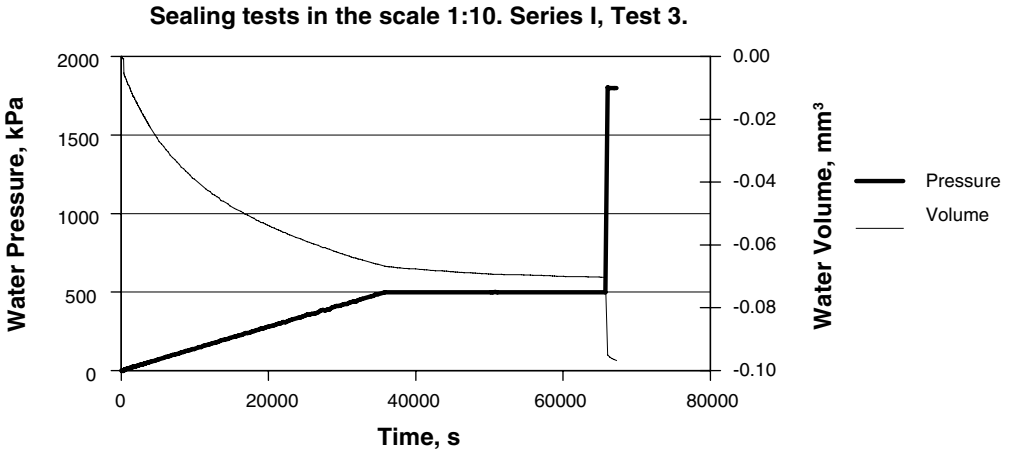

Water pressure increase and inflow volume as a function of time. The water pressure increase was 50 kPa/h. No breakthrough.

Test I-4

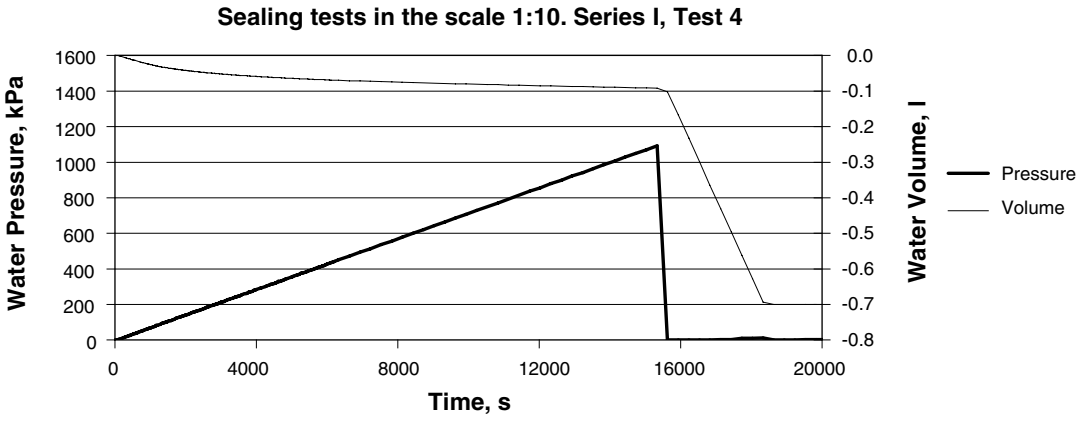

Water pressure increase and inflow volume as a function of time. The water pressure increase was 250 kPa/h.

Test I-5

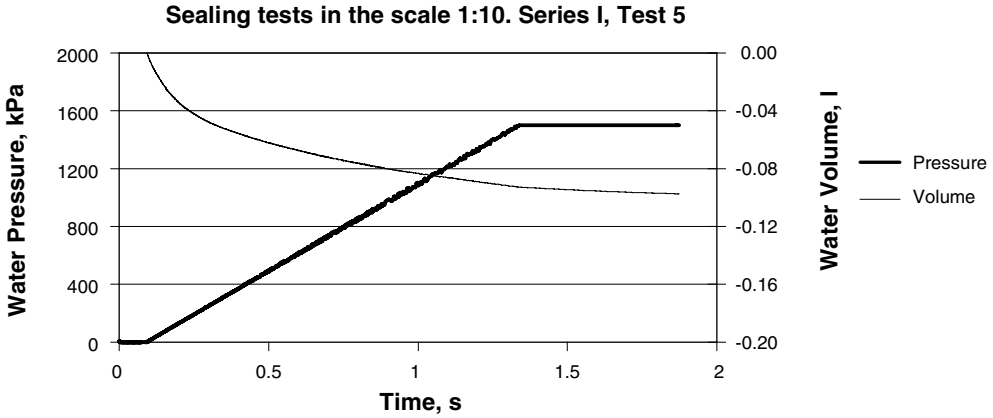

Water pressure increase and inflow volume as a function of time. The water pressure increase was 50 kPa/h. No breakthrough.

Test I-6

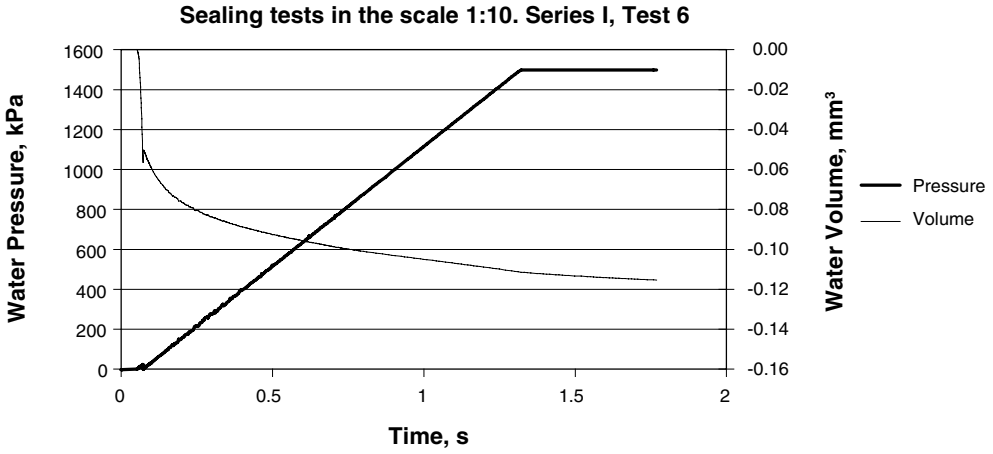

Water pressure increase and inflow volume as a function of time. The water pressure increase was 50 kPa/h. There was no axial slot in this test. No breakthrough.

Test I-7

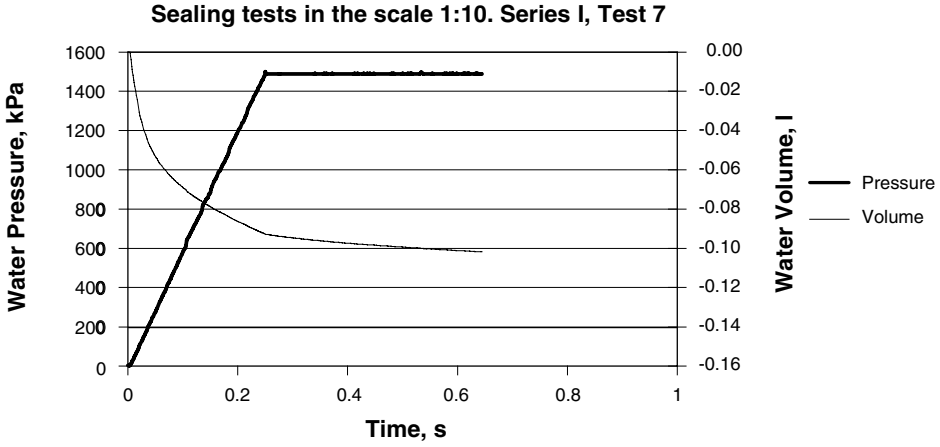

Water pressure increase and inflow volume as a function of time. The water pressure increase was 250 kPa/h. The filling rate was in this test set to 0.001 l/min (0.01 l/min in the other tests in this series). No breakthrough.

Appendix 5

Scale tests, Series II

Test II-1

The test started by applying an inflow of 0.01 l/min i.e. the flow was scaled 1:10, but the filling rate of the volume behind the plug was about 200 times greater than in the real case (1.25 hours compared to 10 days). The test was run for about 8 days and during this time it was not possible to fill the empty space behind the block because of a continuous leakage past the plug as shown in the picture below. The erosion of bentonite during this time was considerable. During the test the plug moved about 5 mm axially. A radial swelling pressure was build up in the top to about 250 kPa. The high inflow rate in combination with a block that moved, made it impossible for the distance block to seal.

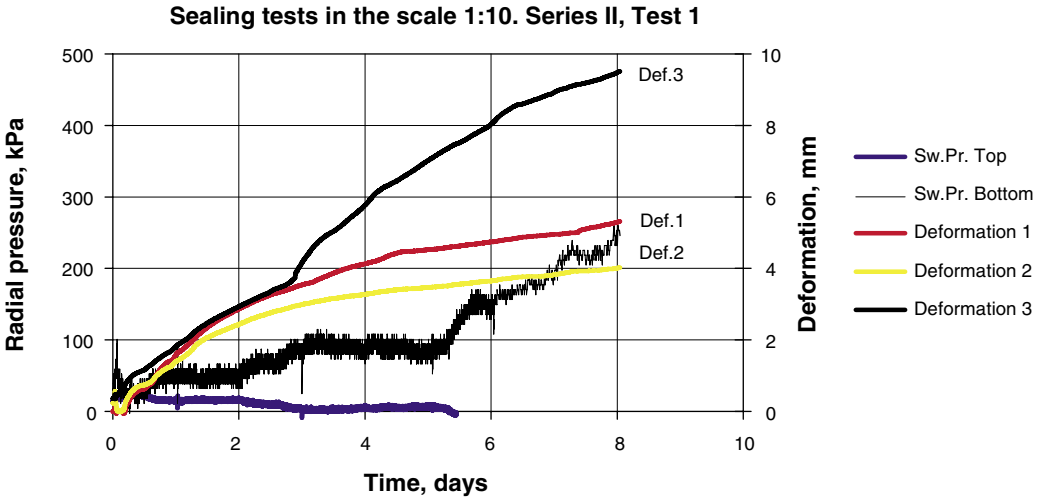

Test II-1. Displacement of the plug and radial swelling pressure as a function of time.

Test II-1. Picture taken outside the plug during the test. The leakage of water and the bentonite erosion is very strong.

Test II-2

In test number 2 the inflow was adjusted in order to fill the slot behind the plug in about 3 days. A ring was attached to the distance block outside the block. The ring was free to move in this test but in contact with the displacement sensors. When the slot was filled, a pressure ramp of 100 kPa/h was applied. At 55 kPa piping occured. The block had moved about 10 mm during the filling time and when the pressure ramp was applied the movement increased considerably. When the block was examined after interrupting the test, a large crack was observed as seen in the picture below.

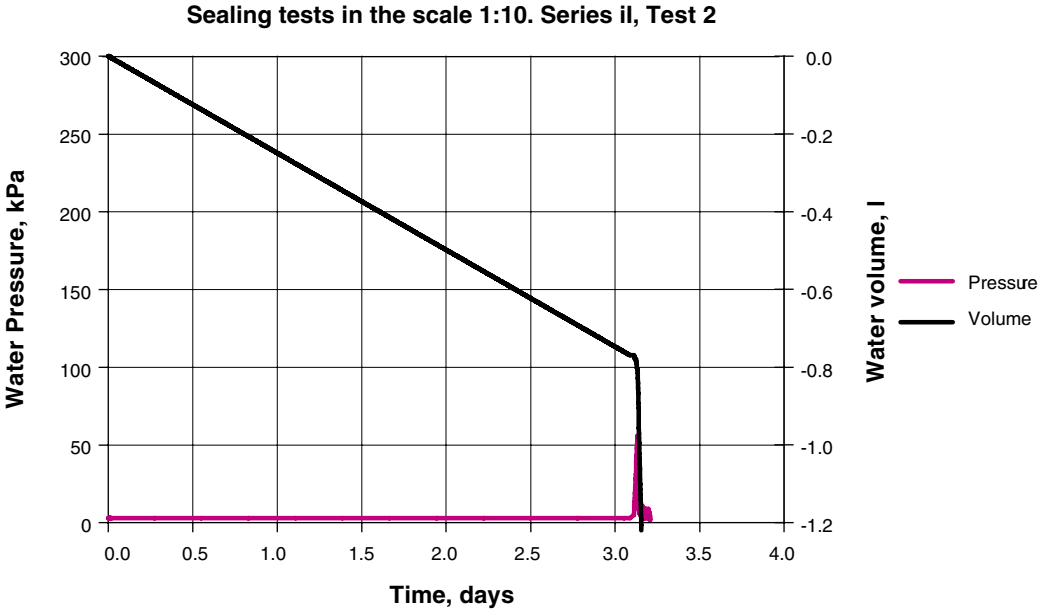

Test II-2. Water pressure increase and inflow volume as a function of time.

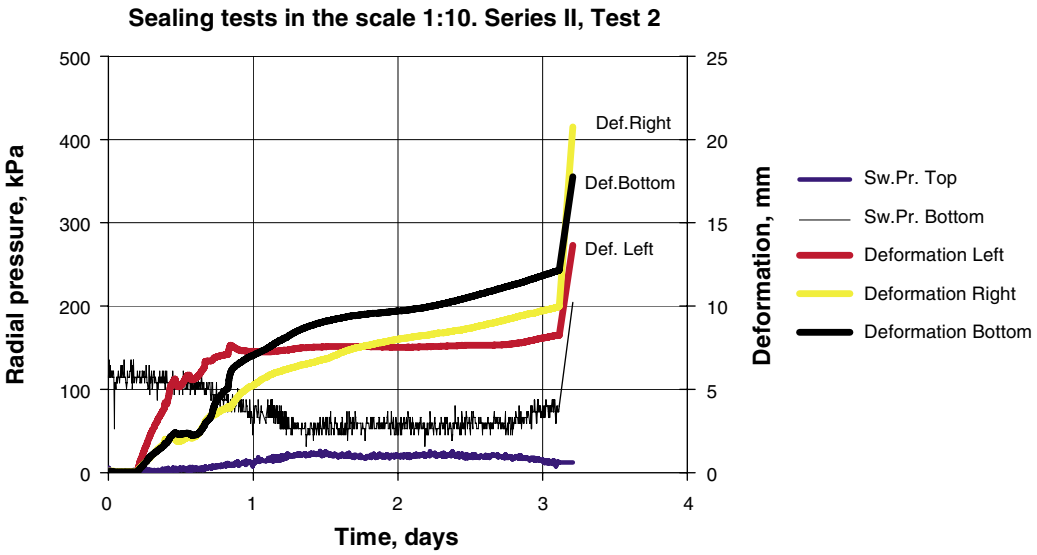

Test II-2. Displacement of the plug and radial swelling pressure as a function of time.

Test II-2. Picture taken outside the plug after removing the displacement sensors and the steel ring. The inflow was about 60 times lower than in Test II-1, but still the leakage and bentonite erosion was very strong.

Test II-3

In this test and the following the displacement sensors was exchanged to load cells. This means that the bentonite block was locked in the axial position and thus the force measured instead of diplacements. After test 1 and 2 it was obvious that a supporting ring fixed to the "rock" was required.

The filling time in this test was about 6.5 days. When the slot volume was filled a pressure ramp of 144 kPa/h was applied, with a maximum pressure of 2 MPa. The distance block could take this without any leakages. The axial force measured with three load cells reached during the filling time between 4 and 6 kN and about 10 kN during the pressure ramp.

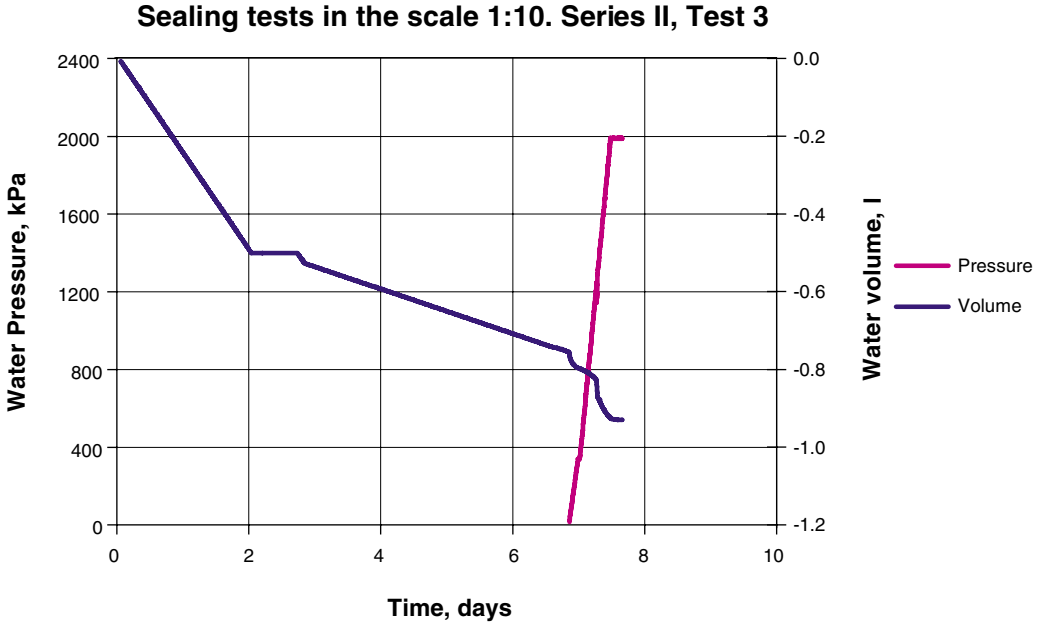

Test II-3. Water pressure increase and inflow volume as a function of time.

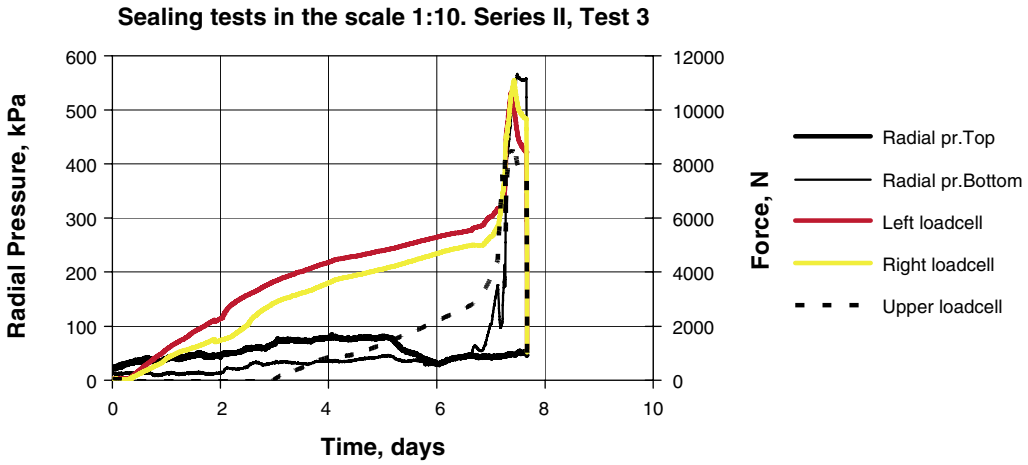

Test II-3. Axial load on the bentonite plug and radial swelling pressure as a function of time.

Test II-3. Picture showing a part of the distance block after dismantling of test 3. The left side faced the PVC dummy. The picture shows that only a small part of the block was active in the sealing process.

Test II-4

Test 4 was one of the tests where salt water was used (the other one was test number 9). The salt content was 3.5% NaCl/$CaCl_2$. The filling rate was adjusted in order to fill up the slot volume in 5 days. After this time, a pressure ramp of 100 kPa/h was applied. The maximum pressure was 2 MPa.

There was a small leakage pass the plug during the filling, about 150 cl, witch self sealed. The sample could take the water pressure without any leakages.

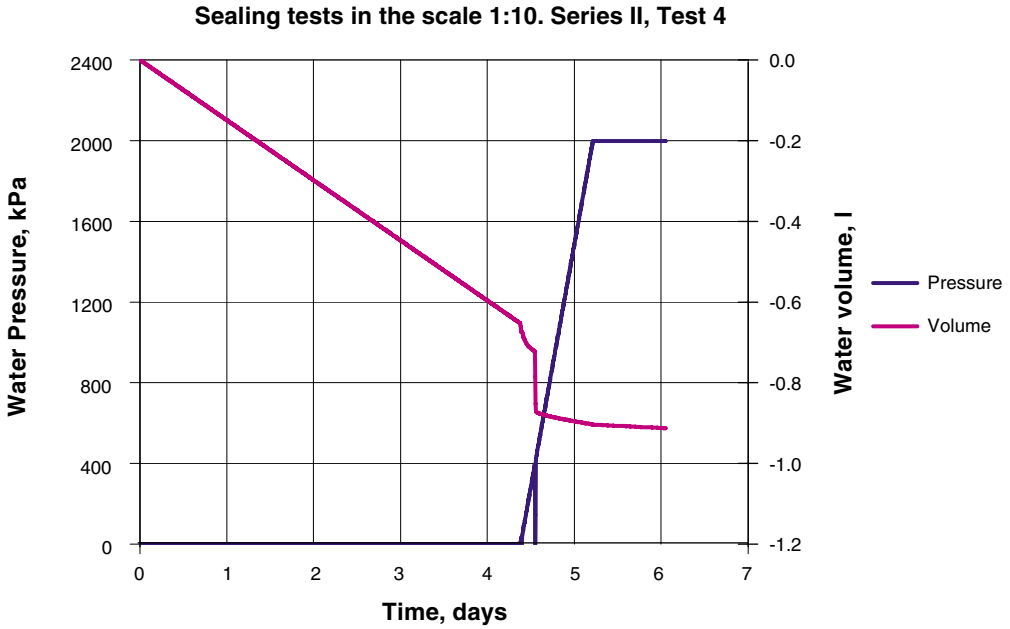

Test II-4. Water pressure increase and inflow volume as a function of time.

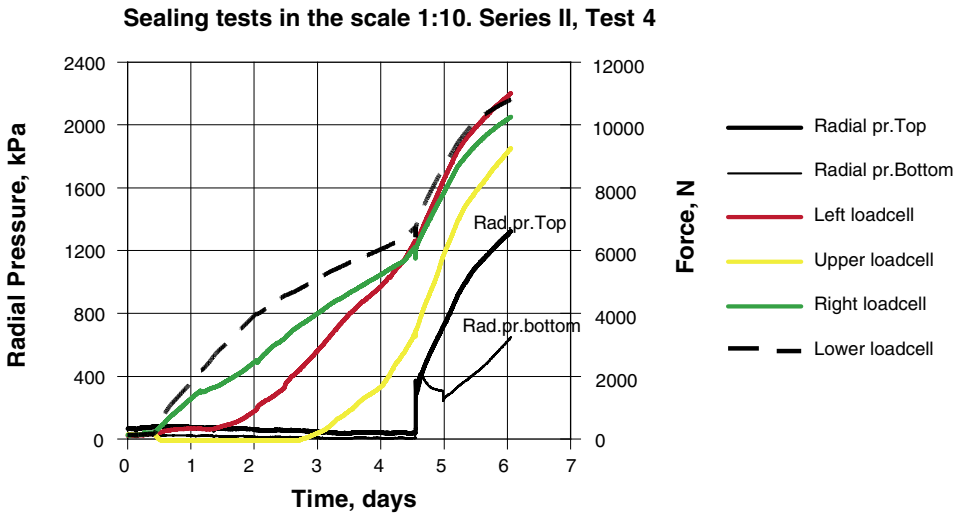

Test II-4. Axial load on the bentonite plug and radial swelling pressure as a function of time.

Test II-4. Picture taken from inside after removal of the PVC dummy. The end of the bentonite block is shown. The "active area" that was wetted is very clearly seen.

Test II-5

In Tests 5 to 9 the distance block was placed 7 mm from the container by use of a small plastic disc mounted on the container. The axial slot has been made with the purpose to study the influence of such an unfavorable situation. The filling time in this test was 5 days. When the slot volume had been filled a pressure ramp of 100 kPa/h was applied. The maximum pressure was 2MPa. There was no leakage past the plug during filling and pressurizing.

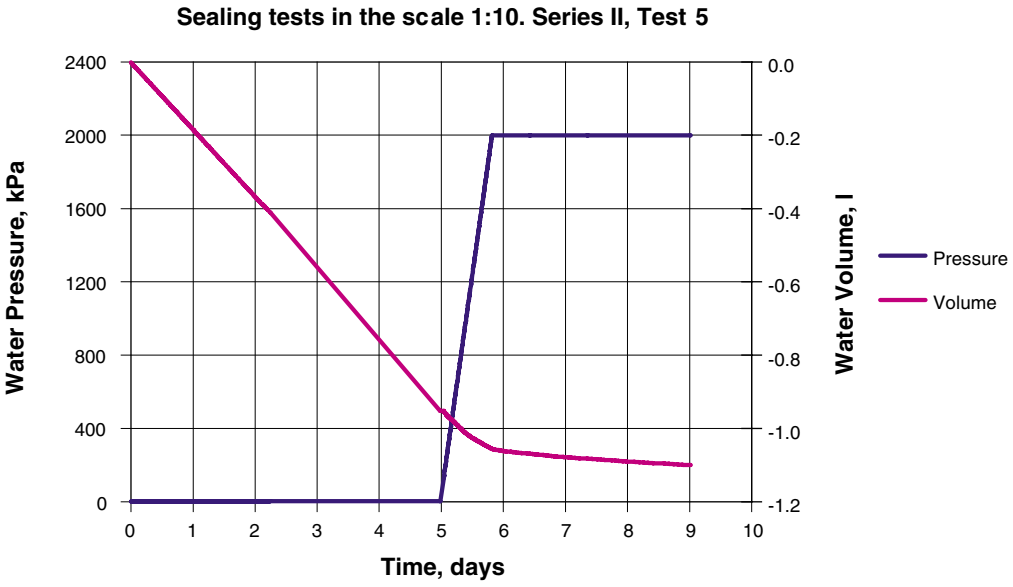

Test II-5. Water pressure increase and inflow volume as a function of time.

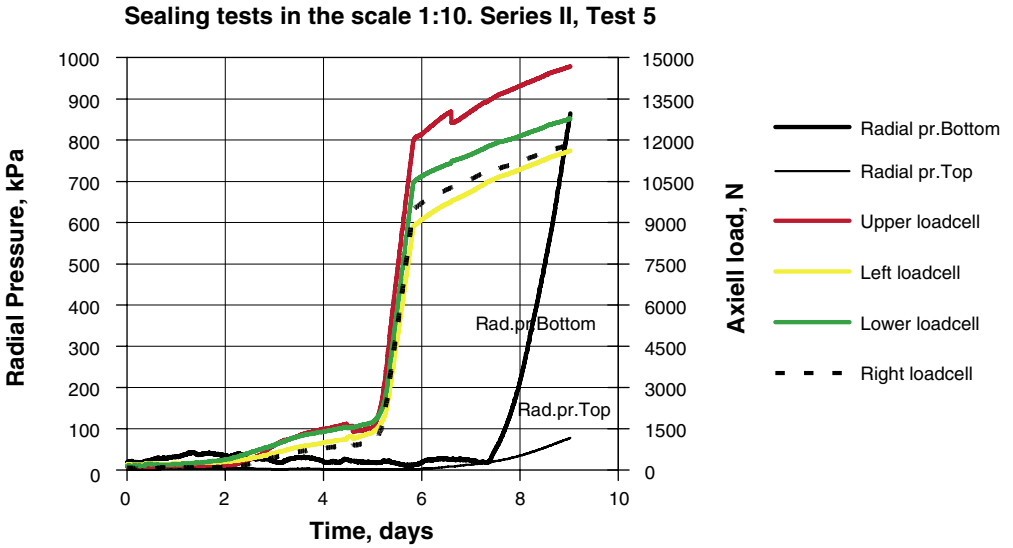

Test II-5. Axial load on the bentonite plug and radial swelling pressure as a function of time.

Test II-6

The arrangement in this test was the same as in test 5 but the limits regarding filling rate, increase of water pressure and the maximum applied pressure were tested. The filling time in this test was 1 day. An attempt to apply a pressure ramp after this time was done but it was not possible. A new attempt was done after 2 days. After this time a pressure ramp of 1,000 kPa/h was applied. The pressure increased to 300 kPa and then piping occurred. After 4 days recovery time a new pressure ramp was applied. This time the sample take 5 MPa. The "active area " was in the same range as in test 5.

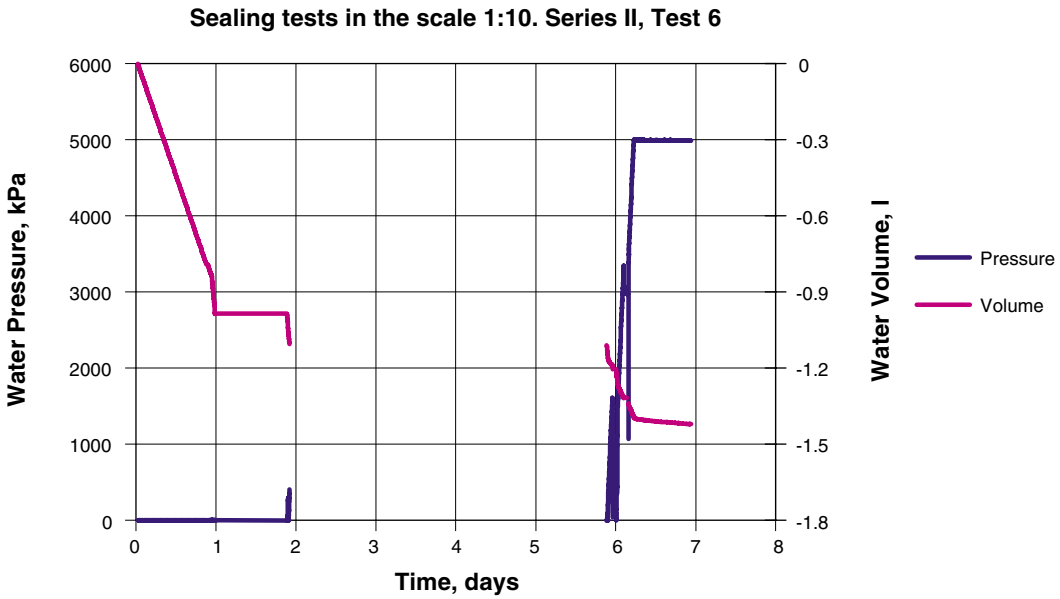

Test II-6. Water pressure increase and inflow volume as a function of time.

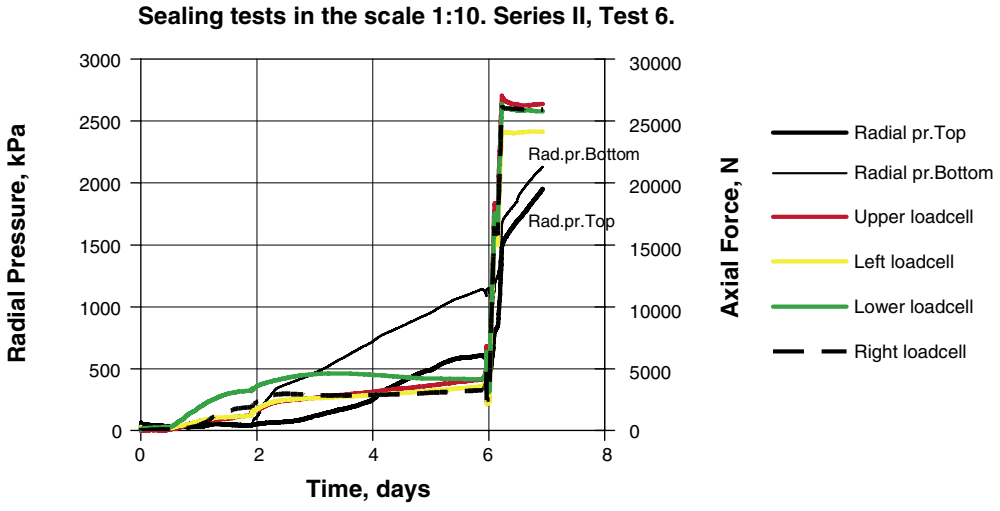

Test II-6. Axial load on the bentonite plug and radial swelling pressure as a function of time.

Test II-6. Picture of half the distance block and the PVC dummy taken after dismantling. When the PVC dummy was removed from the test cylinder the block was split in two parts. The sealing and the swelling into the slot along the PVC dummy is clearly seen.

Test II-7

The conclusion from Test 6 was that the reason for the early piping was the fast filling rate. In Test 7 the filling rate was changed to 5 days. After this time a pressure ramp of 100 kPa/h was applied. The plan was to increase the pressure up to 5 MPa, but at 2.5 MPa there was a breakthrough due to that the block cracked. Besides the demands on the sealing ability of the bentonite blocks, there must also be demands on the mechanical strength of the blocks.

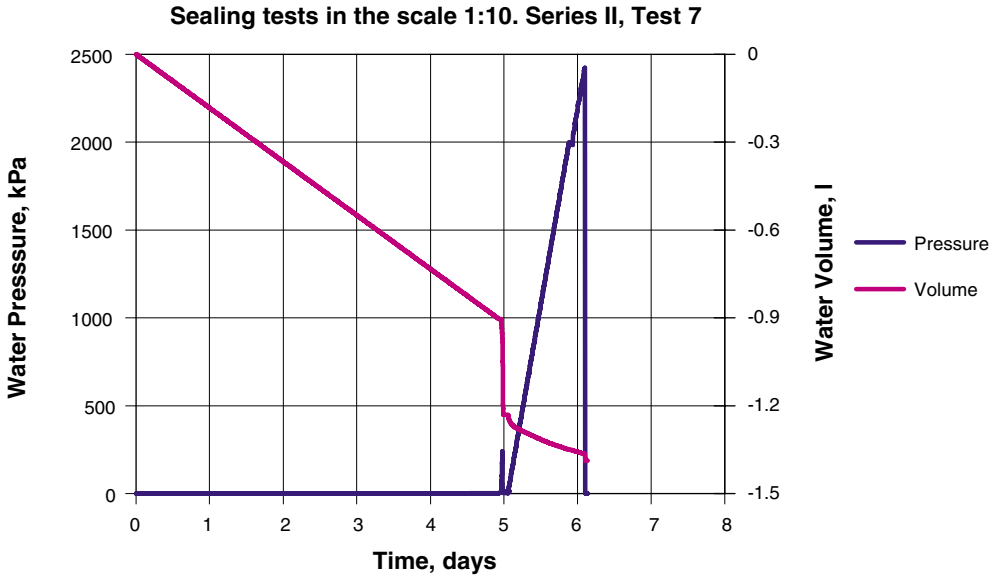

Test II-7. Water pressure increase and inflow volume as a function of time.

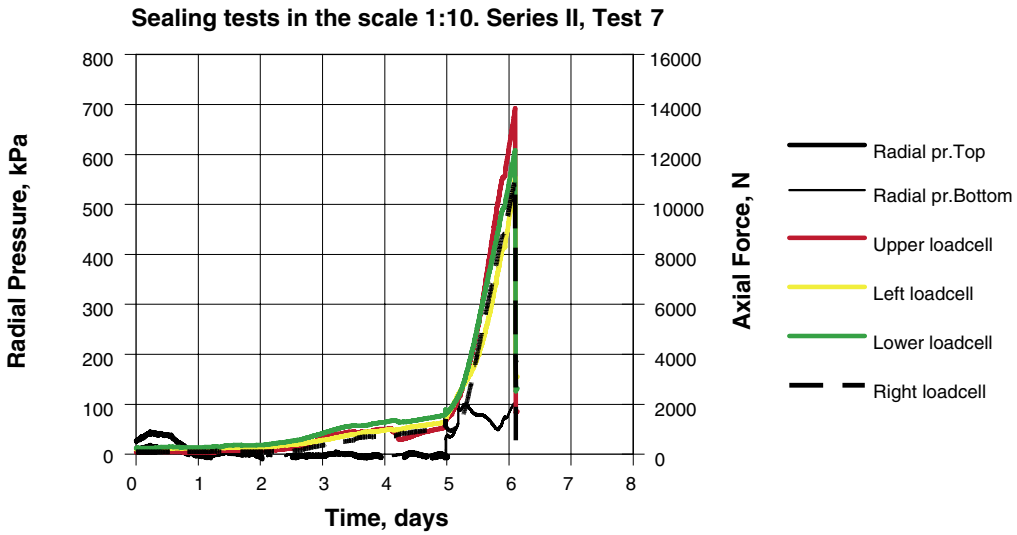

Test II-7. Axial load on the bentonite plug and radial swelling pressure as a function of time.

Test II-7. Picture from test II-7 showing the outside of the block after removal of the load cells and the steel ring. When the inner water pressure reached 2.5 MPa a central part of the distance block cracked.

Test II-8

In this test an additional attempt was done to find the limits of the filling rate. The filling rate was set to 2 days. After this time a pressure ramp of 100 kPa/h was applied. Piping occurred at about 140 kPa. After 2 hours recovery time a new ramp was applied. The maximum applied pressure was 2 MPa. There were no leakages during the pressurizing.

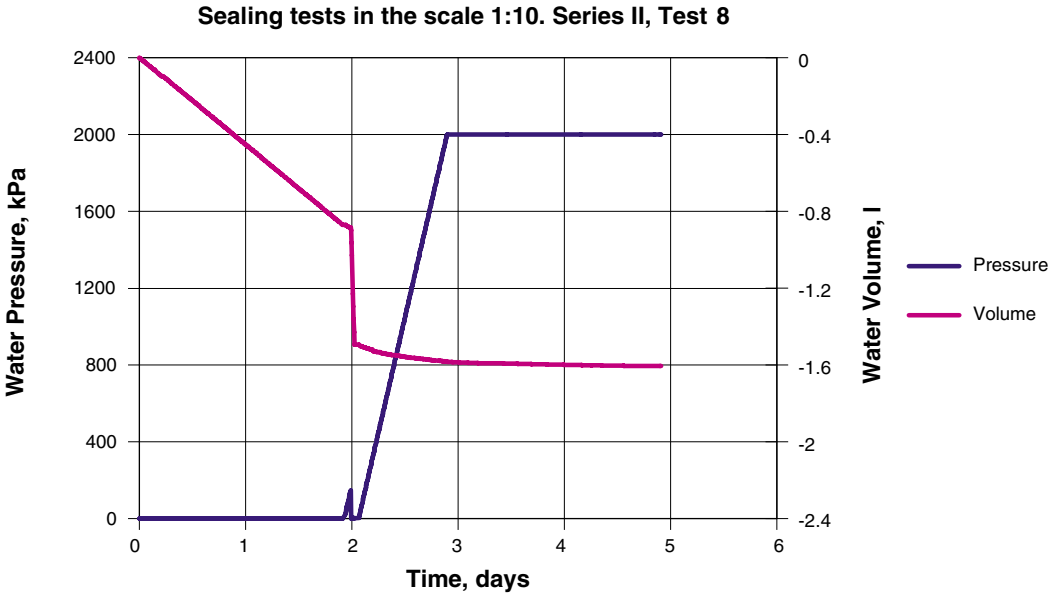

Test II-8. Water pressure increase and inflow volume as function of time.

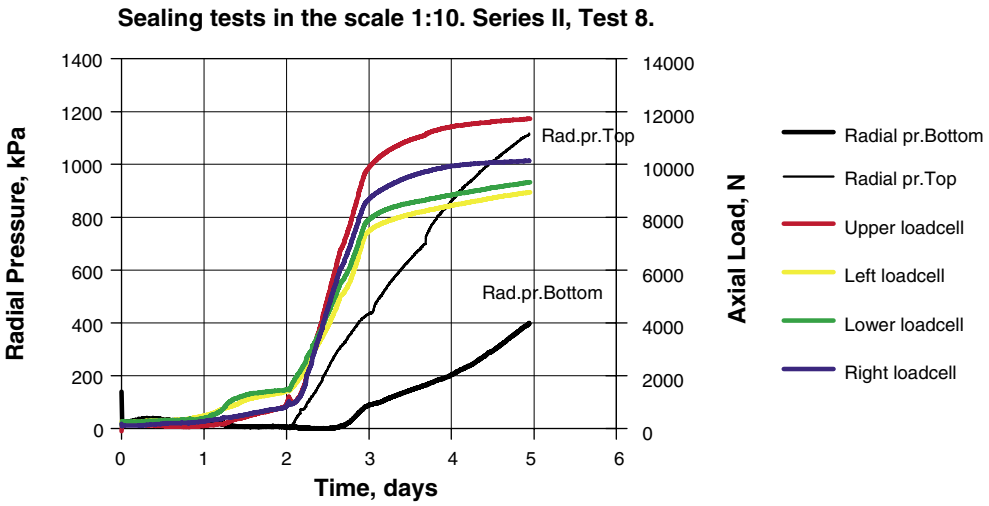

Test II-8. Axial load on the bentonite plug and radial swelling pressure as a function of time.

Test II-8. Picture of the wetted peripheral surface of the distance block.

Test II-9

This test was a long term test and was left for about 3 months. The water used in the test contained 2% $NaCl/CaCl_2$. In order to increase the mechanical strength of the plug, two bentonite blocks were installed. The slot volume was filled during 36 hours and a pressure ramp of 100 kPa/h was applied. The maximum pressure was set to 2 MPa. The bentonite managed to seal and there were no leakages during the filling, the pressurizing or the 3 months test (except for a few cl initially).

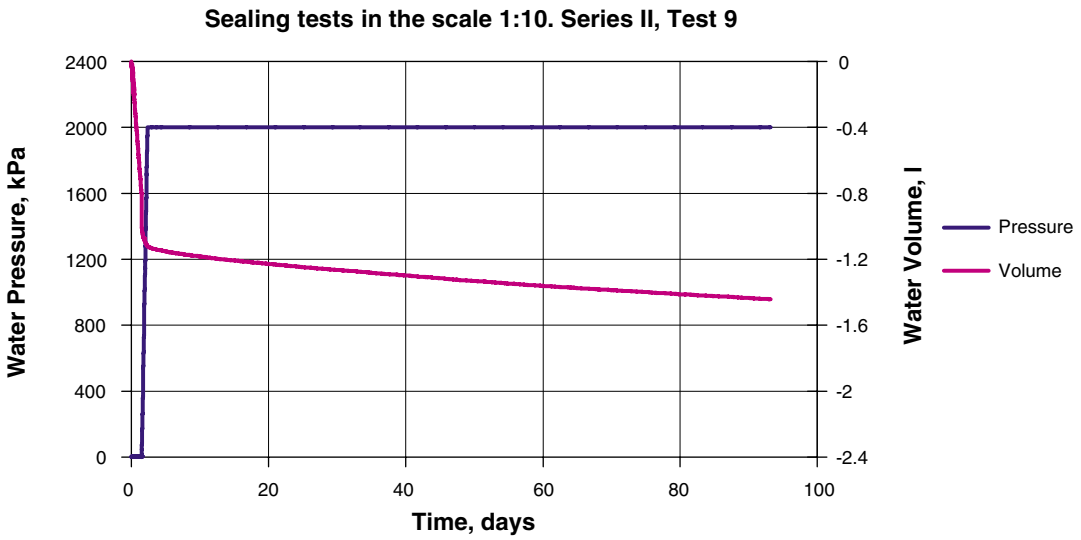

Test II-9. Water pressure increase and inflow volume as a function of time.

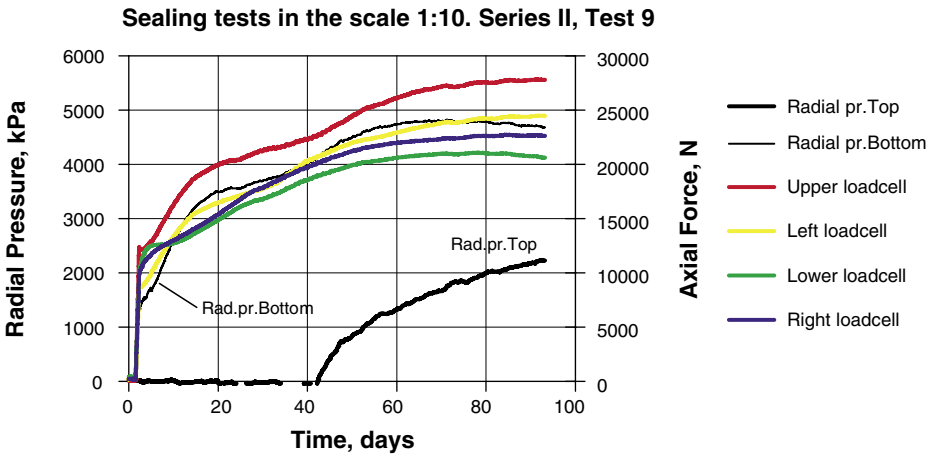

Test II-9. Axial load on the bentonite plug and radial swelling pressure as a function of time.

Test II-9. Picture of the bentonite blocks after dismantling. The inner block (lower in the picture) is wet all around the periphery, but the outer block is only wet on the bottom part.

Appendix 6

Full scale tests

Test BB1

The layout of test BB1 is shown in Figure BB1-1. In similarity with the 1:10 scaled test 8 outlet holes were used for water outflow and a peripheral slot on the lid, connecting the eight holes, was used to simulate the slot on the neighboring perforated container. The design was probably favorable for the sealing since the real slot will be larger than the simulated and the construction may be regarded to simulate a supporting ring that is not water tight.

The test started and water was filled with a rate that would correspond to a filling time of about a week, which is expected for the reference case. It turned out that the leakage was very strong and the filling rate had to be rather high. After about 8 days no more water could be filled and the pressure increase started. The progress of the test is shown in Figures BB1-2 and BB1-3.

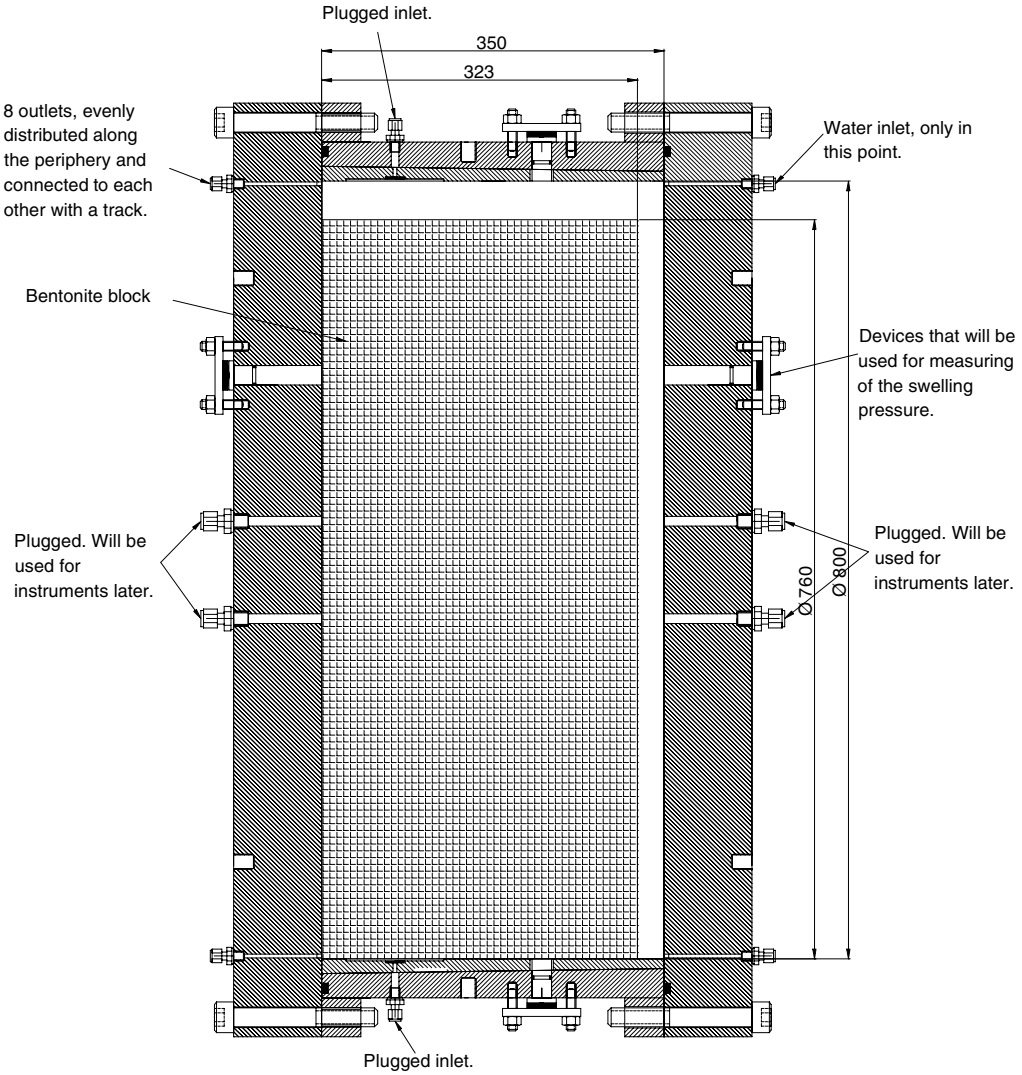

Figure BB1-1. *Layout of sealing test BB1. Dimensions in mm.*

Figure BB1-2 shows that the leakage before no more filling was possible was very high. 110 liters of water had leaked through when the pressure build up test could start. At first the pressure increase rate 50 kPa/h was tried. After about 1.5 days these tests had to be interrupted because piping occurred over and over again. Then the rate was decreased with a factor 10 to 5 kPa/h. This rate worked until after 10 days there was piping at the pressure 1,200 kPa.

Figures BB1-4 to BB1-7 show the water ratio distribution at different radiuses for samples taken after dismantling. Figures BB1-8 and BB1-9 show pictures taken after dismantling.

The conclusion from this test was thus that the scale effect was very strong. The slot, which was 10 times larger than the slot at the test in the scale 1:10, could hardly handle the pressure increase rate that was 10 times lower. The distance plug did thus not work for the reference case in full scale.

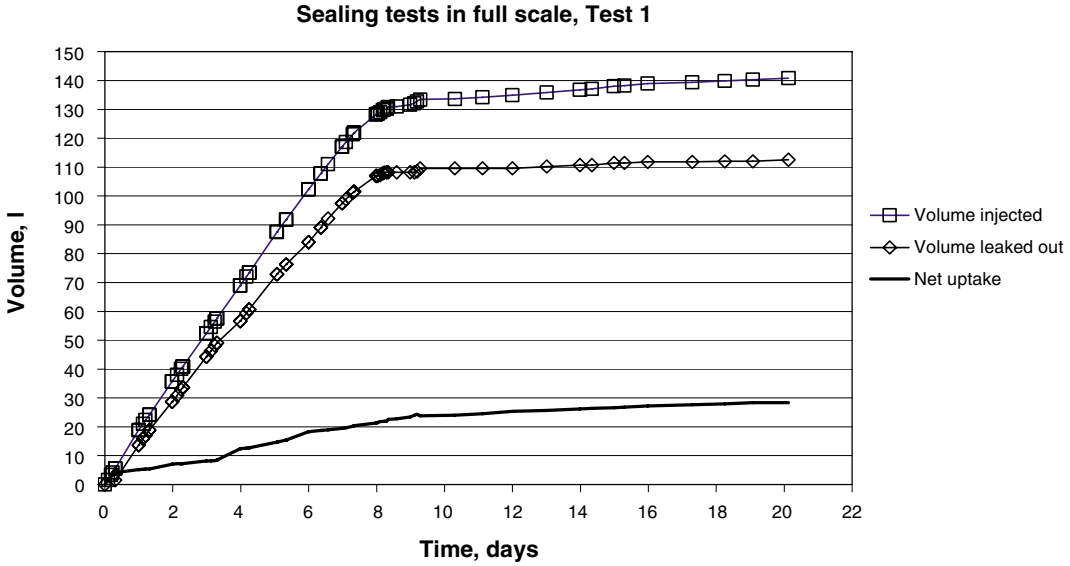

Figure BB1-2. *In and outflow of water as a function of time during the filling and pressure increase.*

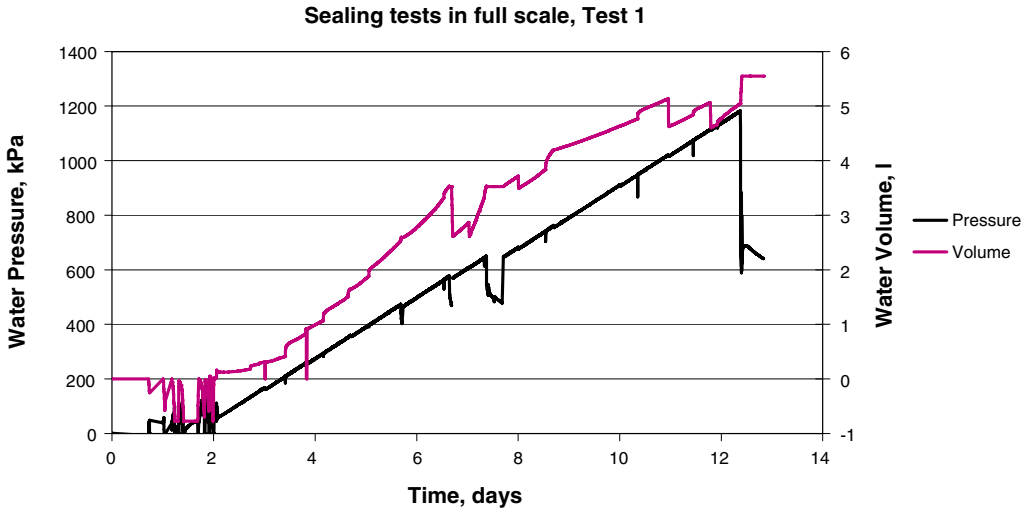

Figure BB1-3. *Water pressure increase and inflow volume as a function of time.*

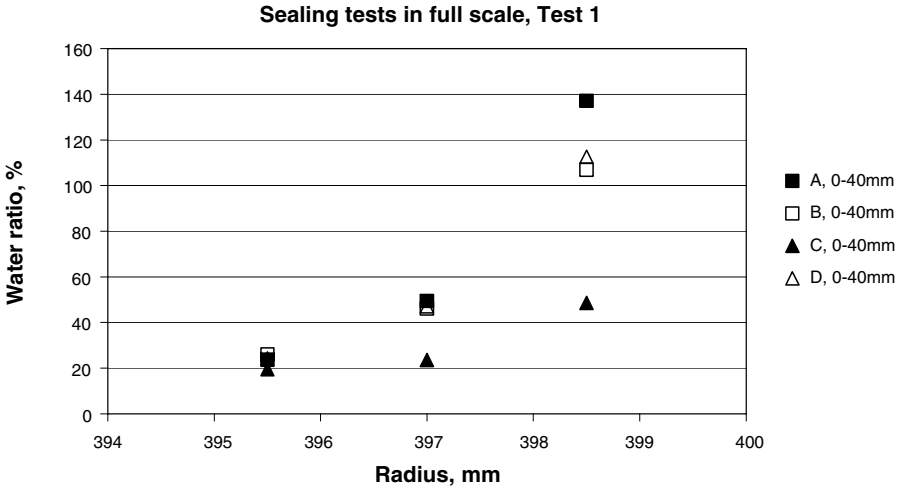

Figure BB1-4. *Diagram showing the water ratio distribution in the former slot on the upper level (0–40 mm). Samples have been taken in four directions: A, B, C and D, where A is up and D is down.*

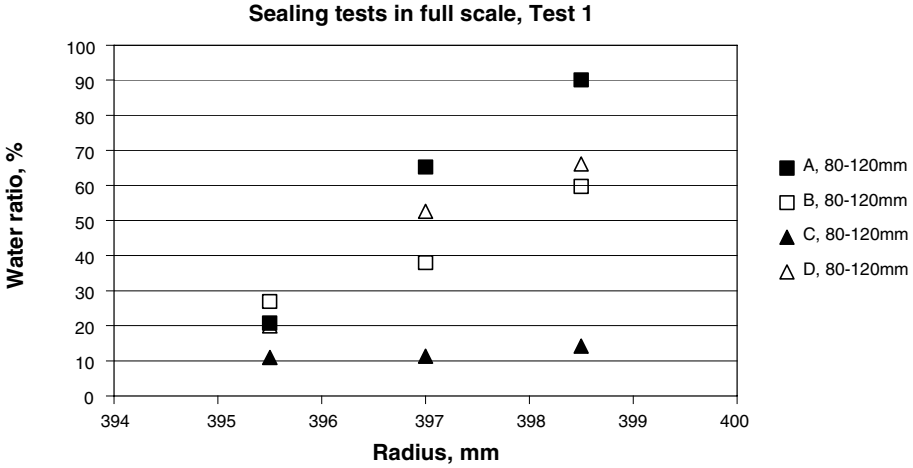

Figure BB1-5. *Diagram showing the water ratio distribution in the former slot on the middle level (80–120 mm). Samples have been taken in four directions: A, B, C and D, where A is up and D is down.*

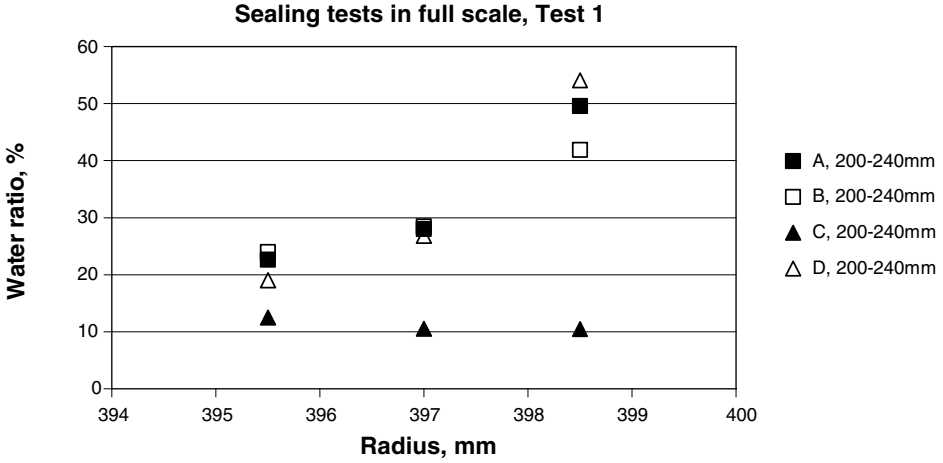

Figure BB1-6. *Diagram showing the water ratio distribution in the former slot on the lower level (200–240 mm). Samples have been taken in four directions: A, B, C and D, where A is up and D is down.*

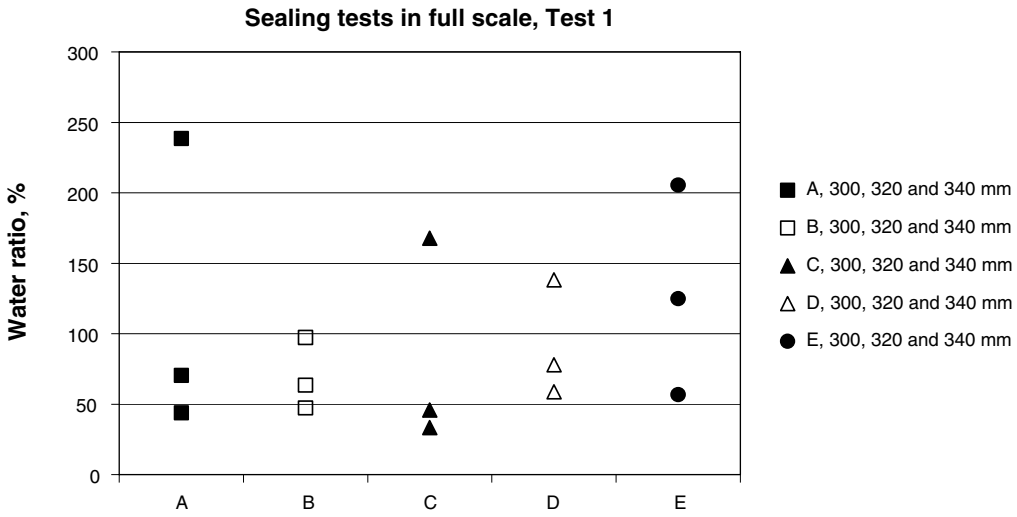

Figure BB1-7. *Diagram showing the water ratio distribution in the bottom of the sample against the axial slot. Samples have been taken in four directions: A, B, C and D, where A is up and D is down but also in position E which is in the centre.*

Figure BB1-8. *Picture showing the low pressure side after interruption of the Test 1. The pen is placed on top of the block. BB1.*

Figure BB1-9. *Picture showing the radial slot filled with clay. BB1.*

Test BB2

Since test BB1 showed that either an engineering solution or a decreased slot must be used a second test was performed with the following idea:

The reason for the malfunction of the sealing is that too much bentonite needs to swell before the density in the slot has increased to such a high value that the swelling pressure can handle the water pressure without piping. A way to reduce the required swelling is to either reduce the slot width or to seal the slot. An engineering technique could then be to fix a steel ring on the rock surface and put it in contact with the distance block. If the distance block is centered and the ring is made as a collar that goes several cm inside the block periphery, the sealing can be accomplished between the collar and the block instead of between the rock and the block. The test was thus designed according to this principle. The layout of test 2 is shown in Figure BB2-1.

Since the inner vertical slot was skipped the block was thicker and the slot volume smaller, see Table 7-3.

The filling rate was adapted so that the slots should be filled after 3 days. Then the water pressure was increased with the rate 50 kPa/h. The progress of the test is shown in Figures BB2-2 and BB2-3.

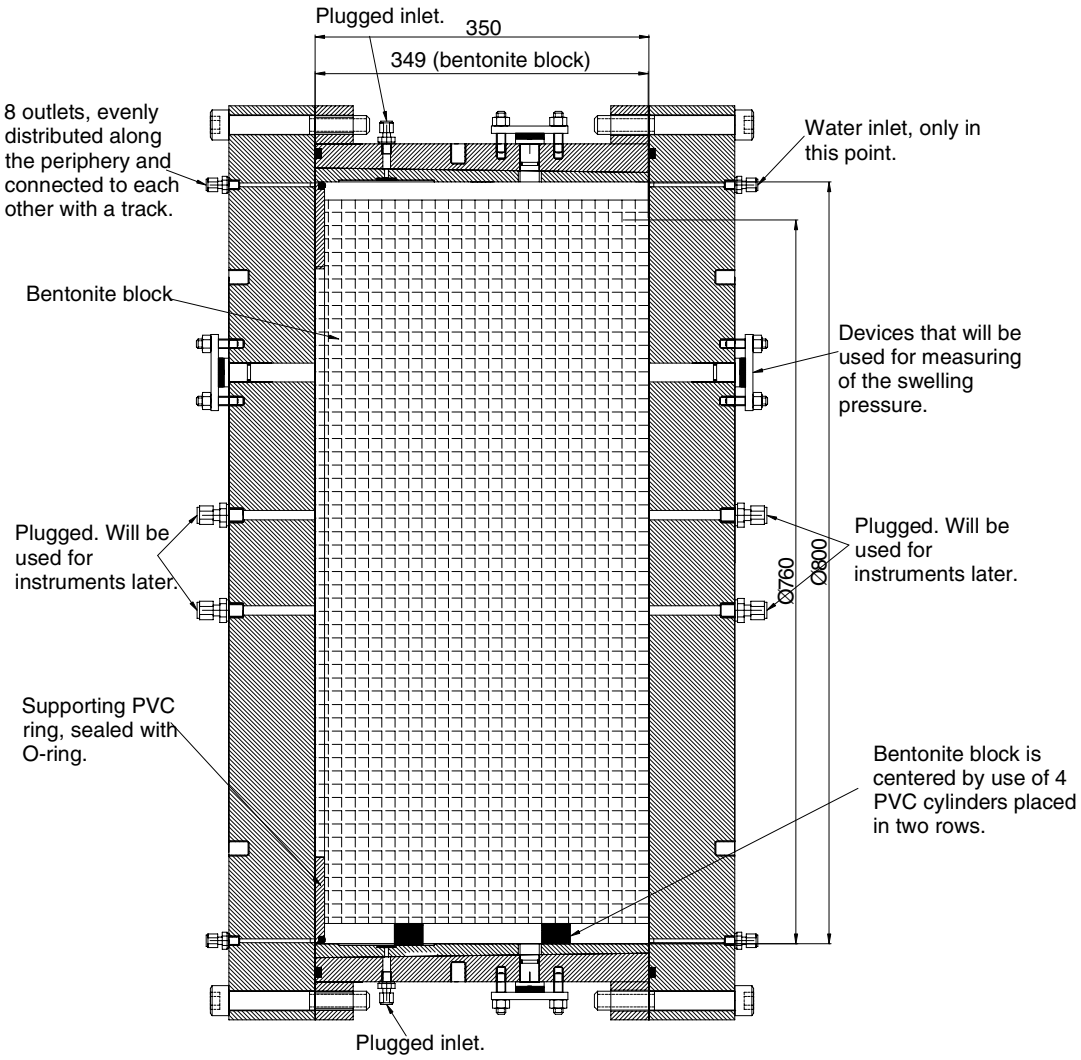

Figure BB2-1. *Layout of sealing test BB2. Dimensions in mm.*

The diagram presenting the water filling and increase of water pressure shows that there was no leakage during filling, but some leakage appeared at the beginning of the pressure increase. The net inflow during the pressure increase is mainly caused by filling up the air pockets. For the pressure increase the GDS was supplemented with a rubber bladder in order to increase the available water volume before the test had to be interrupted for refilling of the GDS. Unfortunately the bladder broke at 500 kPa so the GDS and frequent filling had to be practiced again. However, subsequently the pressure could be raised until 1,500 kPa with the intended rate and no piping occurred. After a few hours rest the pressure was increased to 2 MPa without piping.

Figure BB2-4 shows the water ratio distribution in the periphery of the distance block determined on samples taken after dismantling of the test. Figures BB2-5 and BB2-6 show pictures taken during the dismantling.

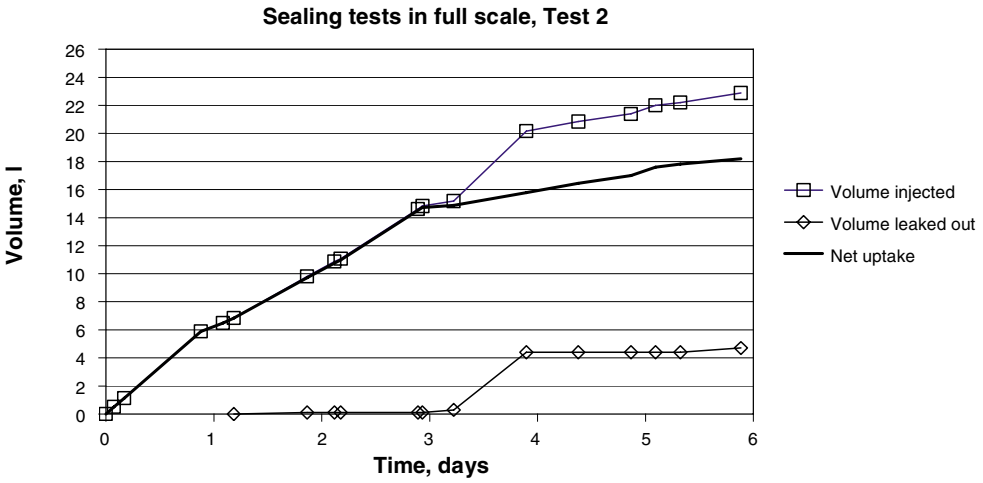

Figure BB2-2. *In and outflow of water as a function of time during water filling and pressure increase of BB2.*

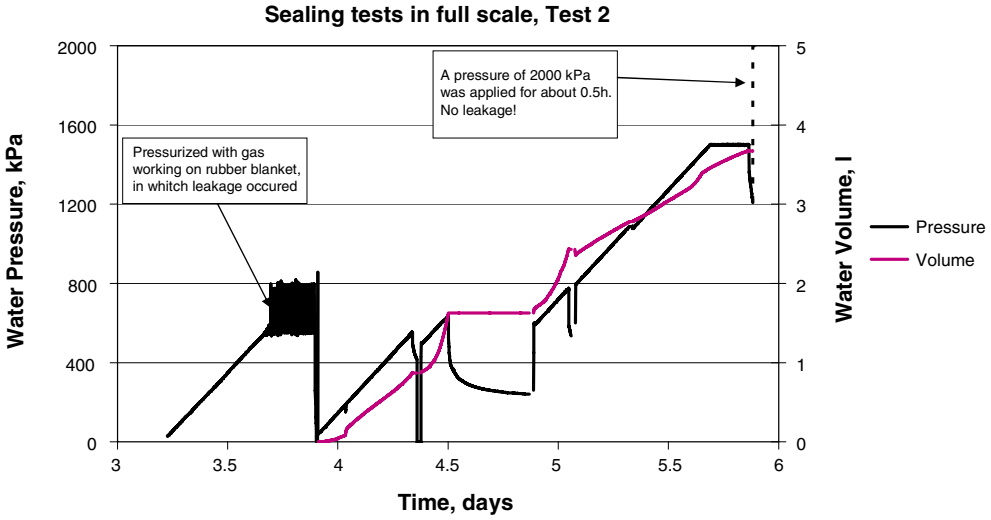

Figure BB2-3. *Water pressure increase and inflow volume as a function of time.*

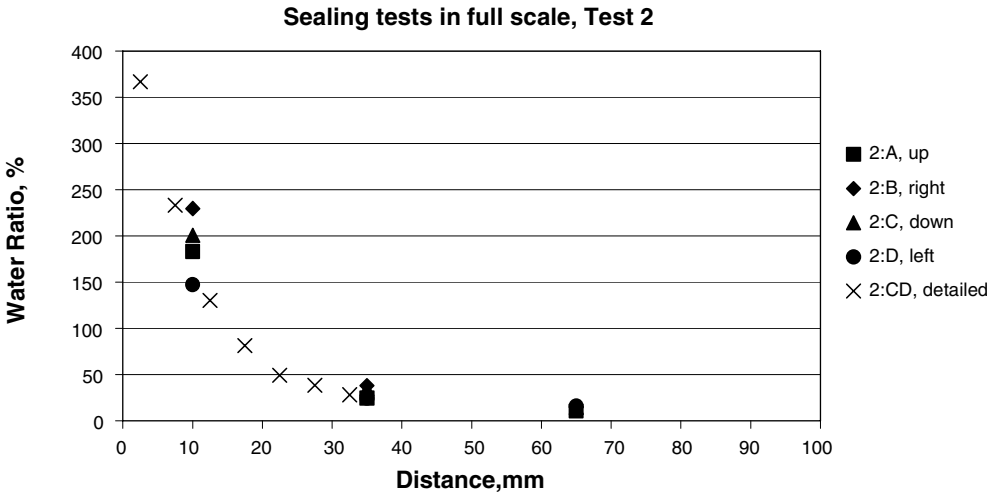

Figure BB2-4. *Diagram showing the water ratio distribution in the former slot against the collar ring. Samples have been taken in four directions: A, B, C and D, where A is up and D is down.*

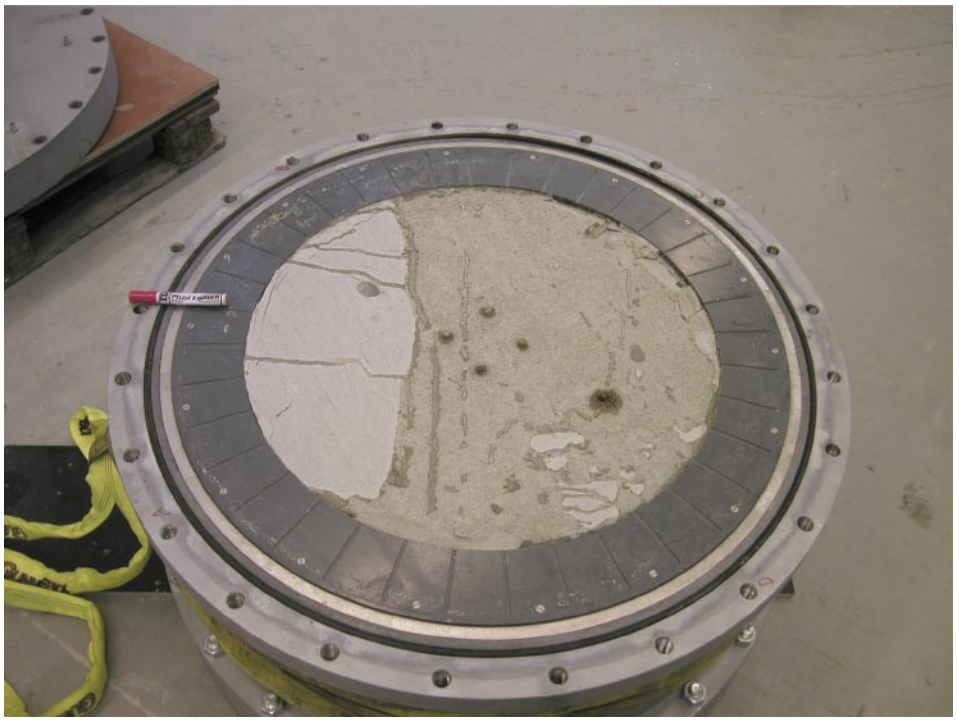

Figure BB2-5. *Dismantling of BB2. The collar ring is not yet removed.*

Figure BB2-6. *The wetting and sealing of the zone behind the collar ring.*

Test BB3

An alternative design in order to get a fast sealing between the bentonite plug and the rock, is to have very small gaps from the start. The emplacement of such a block can be very difficult in reality. In order to facilitate the installation, the bentonite block must probably be divided in three parts, each with inclining faces. This design was tested in BB3 (except for the division in three parts). The layout of the test is shown in Figure BB3-1.

The filling rate was adapted in order to fill the slots in about 3 days. After filling, the water pressure was increased with the rate 100 kPa/h to a maximum pressure of 2 MPa. The progress of the test is shown in Figure BB3-2.

The diagram presenting the water filling and increase of water pressure shows that at 700 kPa there was a drop in pressure. There was no leakage which means that there probably was an internal piping i.e. the water reached a space with air in the slot. A new pressure ramp, 50 kPa/h was applied 15 h later. The pressure rose to 900 kPa where a new internal piping occurred and a pressure drop occurred again. A small leakage about 0.5 dl was detected. The sample then had a recovery time of about 48 hours and a pressure of 2 MPa was applied. A small leakage was detected, about 2.5 dl.

Figures BB3-4 shows a picture taken during dismantling. The results of sampling is shown in Table BB3-1.

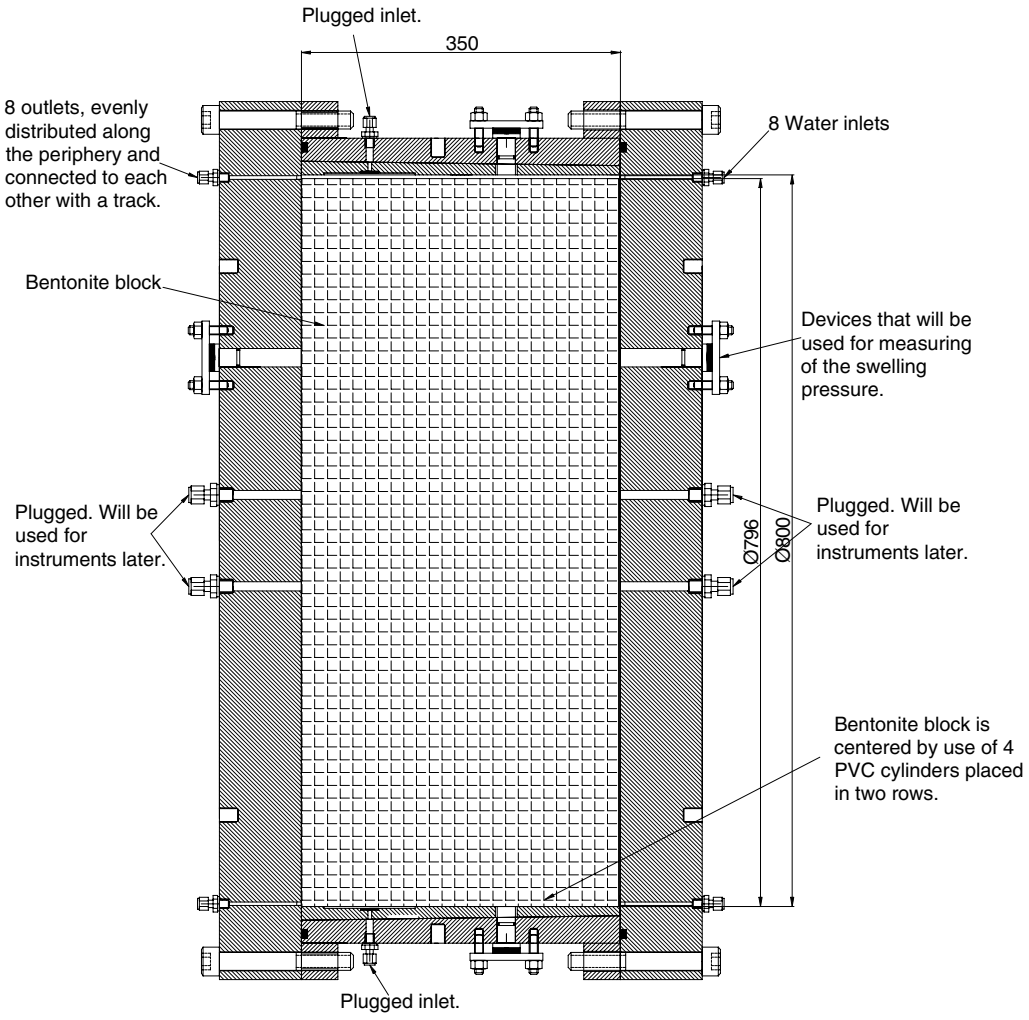

Figure BB3-1. *Layout of sealing test BB3. Dimensions in mm.*

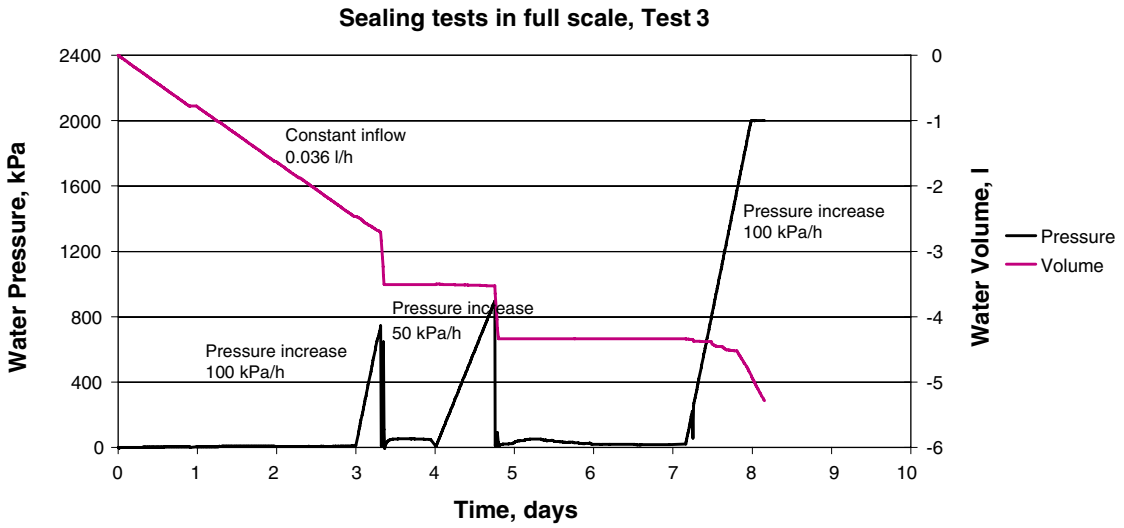

Figure BB3-2. *Water pressure increase and inflow volume as a function of time for BB3.*

Figure BB3-3. *Picture showing the sealed slot.*

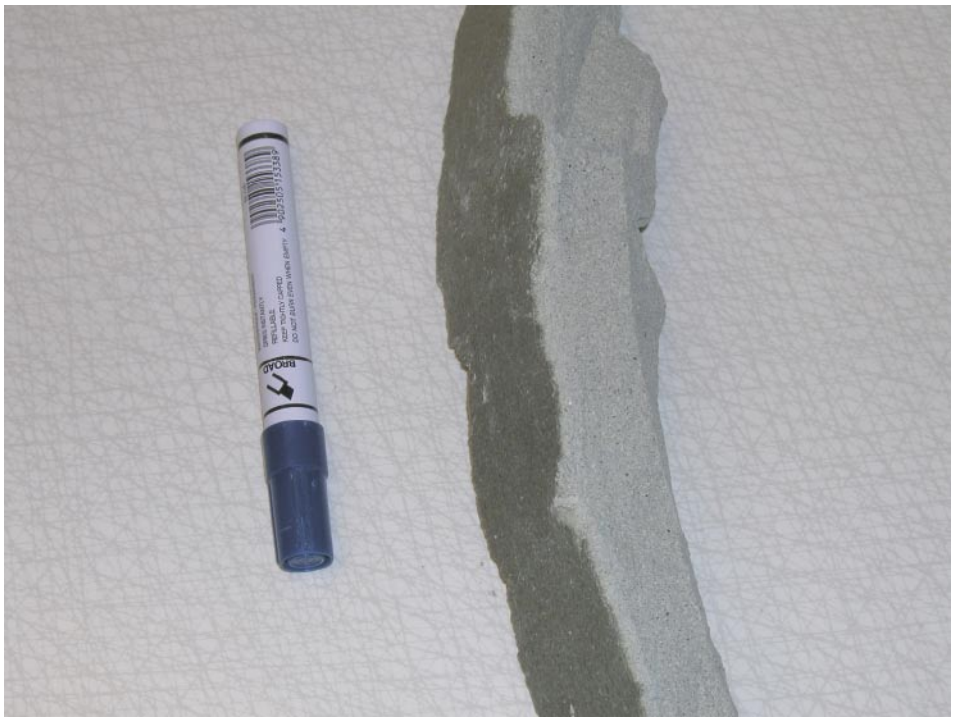

Figure BB3-4. *Picture showing bentonite excavated at the upper slot in BB3.*

Table BB3-1. Results of sampling after dismantling test BB3.

Sampling in the slot connecting the ”leakage holes”				
	mb g	m+mb g	ms+mb g	w %
Top	0.820	4.510	3.063	64.5
Bottom	0.760	3.580	2.349	77.5
Sampling in the low pressure side, 0-20 mm down, in the outermost slot				
	mb g	m+mb g	ms+mb g	w %
Top	0.800	4.040	3.340	27.6
Bottom	0.830	3.230	2.694	28.8
Left	0.840	2.570	2.210	26.3
Right	0.840	3.030	2.600	24.4
Sampling 140-160 mm down from the low pressure side, in the outermost slot				
	mb g	m+mb g	ms+mb g	w %
Top	0.813	11.066	9.500	18.0
Bottom	0.818	4.036	3.601	15.6
Left	0.821	4.788	4.255	15.5
Right	0.845	5.426	4.745	17.5
Sampling on high pressure side, in the outermost slot				
	mb g	m+mb g	ms+mb g	w %
Top	0.838	10.262	7.772	35.9
Bottom	0.814	8.439	6.388	36.8
Left	0.807	8.445	6.677	30.1
Right	0.844	9.671	7.203	38.8

Test BB4

In test BB4 another design with bentonite in the slot was used (Figure BB4-1). The block had an outer diameter of 770 mm and was centered in the "tunnel" by use of small feet made of PVC. After positioning of the block the slot was filled with bentonite pellets. The test simulated that there was a "leaking supporting ring". Water was filled with a constant flow of 0.006 l/min, see Figure BB4-2. The theoretical time to fill the pore volume with this flow is about 8 days. The sample couldn't take the fast pressurizing which was depending on the constant flow. During this time there were small leakages through the pellet, totally about 5 dl. After 9 days a pressure ramp of 100 kPa/h was applied. The pressure was raised to 2 MPa and was held here for about 3 days.

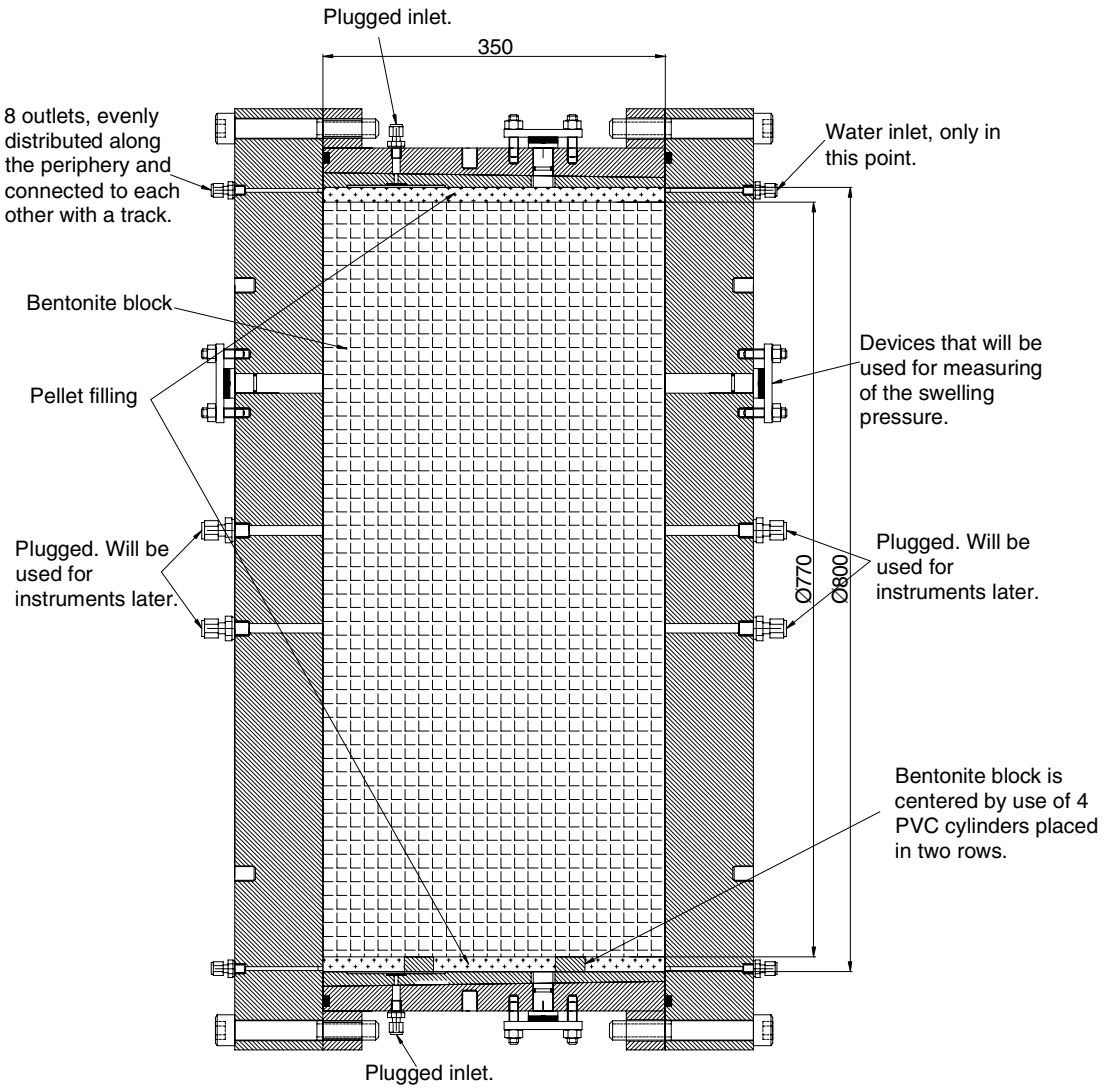

Figure BB4-1. *Layout of sealing test BB4. Dimensions in mm.*

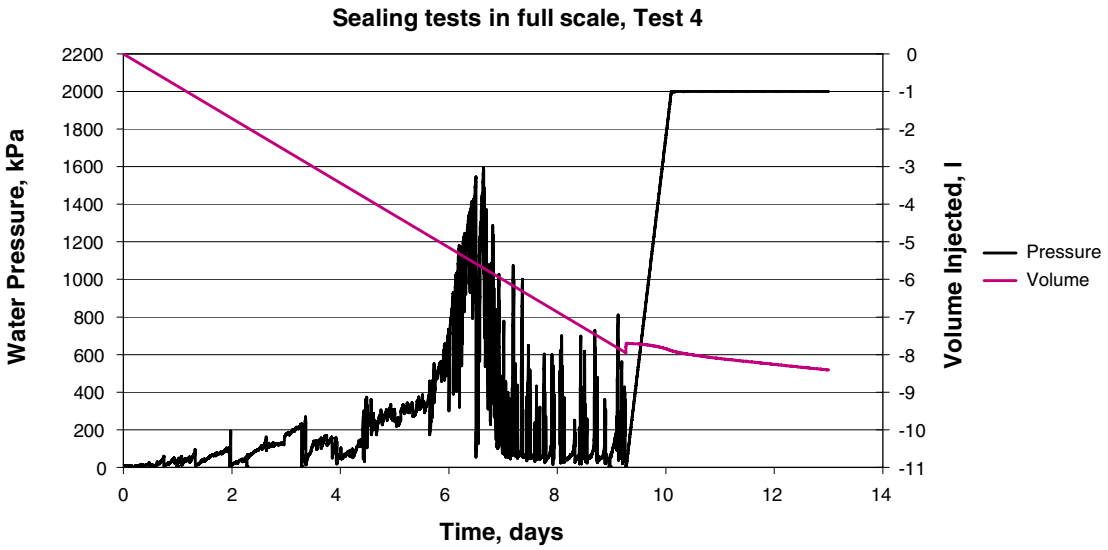

Figure BB4-2. *Water pressure increase and inflow volume as a function of time for BB4.*

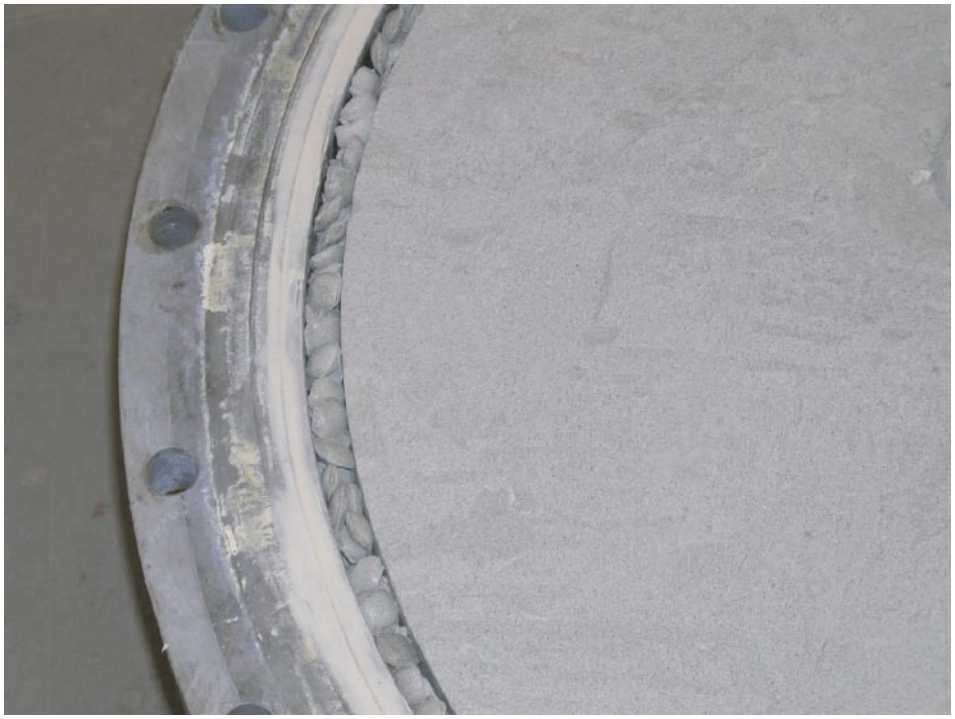

Figure BB4-3. *Picture showing the pellet filled slot during installation.*

Figure BB4-4. *Picture from the pellet filled slot after interruption.*

Table BB4-1. Results of sampling after dismantling test BB4.

Sampling in Test 4.
Sampling only in the pellet filled slot.

Low pressure side	mb g	m+mb g	ms+mb g	w %
Top	0.850	8.430	4.750	94.4
Bottom	0.850	6.850	5.180	38.6
Left	0.8401	3.150	9.600	40.5
Right	0.850	9.160	6.080	58.9
100 mm down from low pressure side	**mb g**	**m+mb g**	**ms+mb g**	**w %**
Top	0.8302	3.4202	0.440	15.2
Bottom	0.8402	6.9302	2.050	23.0
Left	0.8502	4.9701	9.710	27.9
Right	0.8402	4.8301	9.890	25.9
High pressure side	**mb g**	**m+mb g**	**ms+mb g**	**w %**
Top	0.850	8.960	4.780	106.4
Bottom	0.840	15.430	10.590	49.6
Left	0.830	15.200	9.860	59.1
Right	0.840	16.110	10.660	55.5

Test BB5

Test 5 was similar to Test 4 with one exception, a dummy made of PVC, simulating the next super container, was placed on the inlet side, against the bentonite block. This was made in order to better simulate the filling of water i.e. the rise of the water level with time. A perforated steel plate keeps the pellet in place around the block, Figure BB5-1.

Water was filled up with a constant flow of 0.006 l/min, as shown in Figure BB5-2. The theoretical time to fill the pore volume with this flow rate is about 10 days. The water pressure started to rise after 10 days and reached about 1,000 kPa. At this point the pressure device broke and the pressure decreased to about 600 kPa. After about 24 hours the device was exchanged and a new pressure ramp applied. Since the pressure increase had been interrupted it was decided to apply 2 MPa in 1 hour. The distance block could take this pressure and the pressure was kept for about 24 hours. There were no leakages during this test.

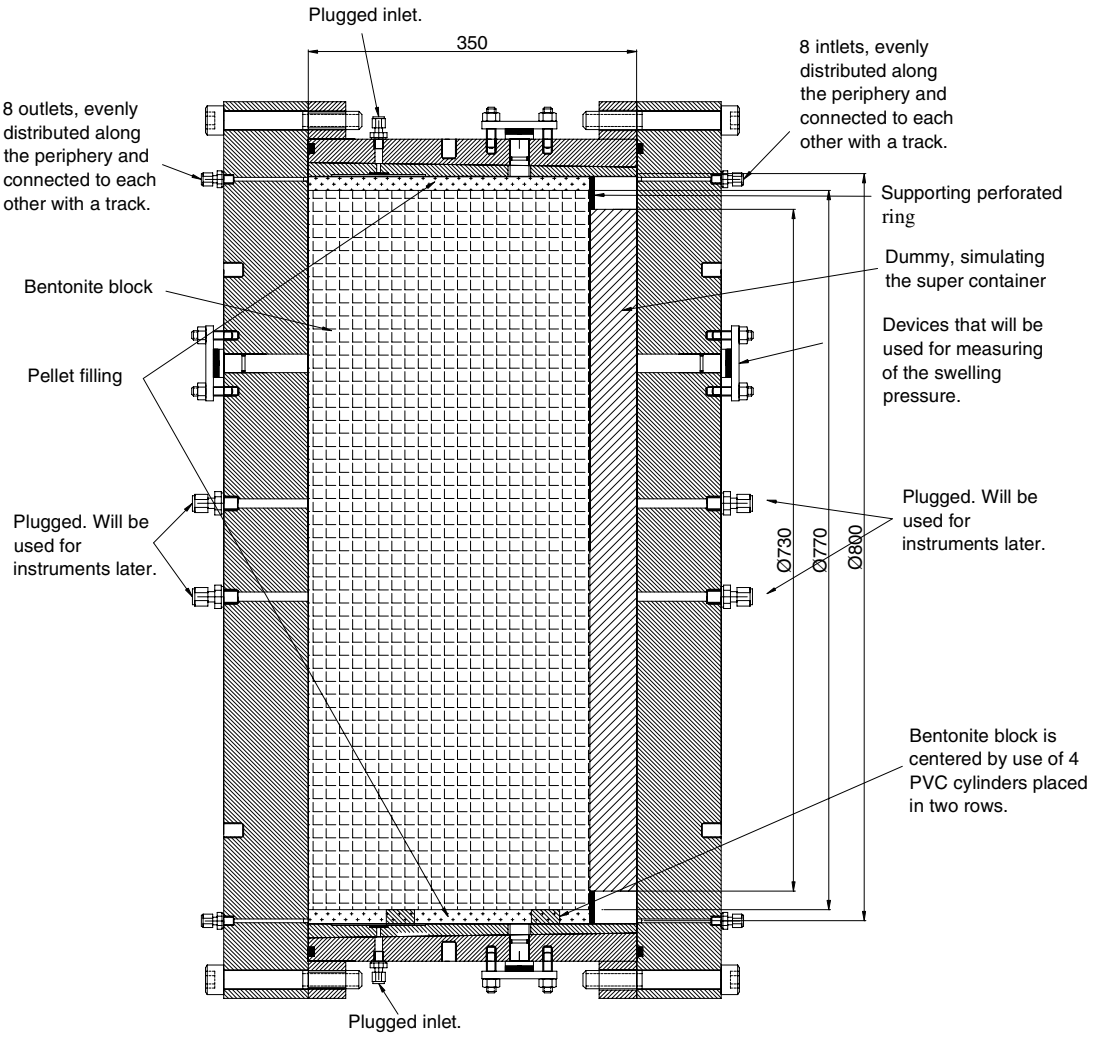

Figure BB5-1. *Layout of sealing test BB5. Dimensions in mm.*

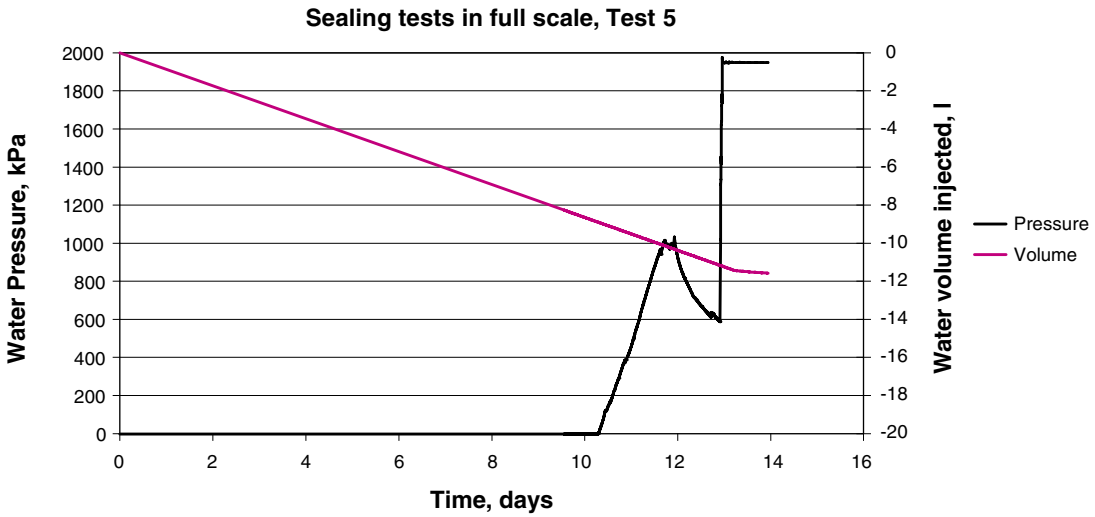

Figure BB5-2. *Water pressure increase and inflow volume as a function of time for BB5.*

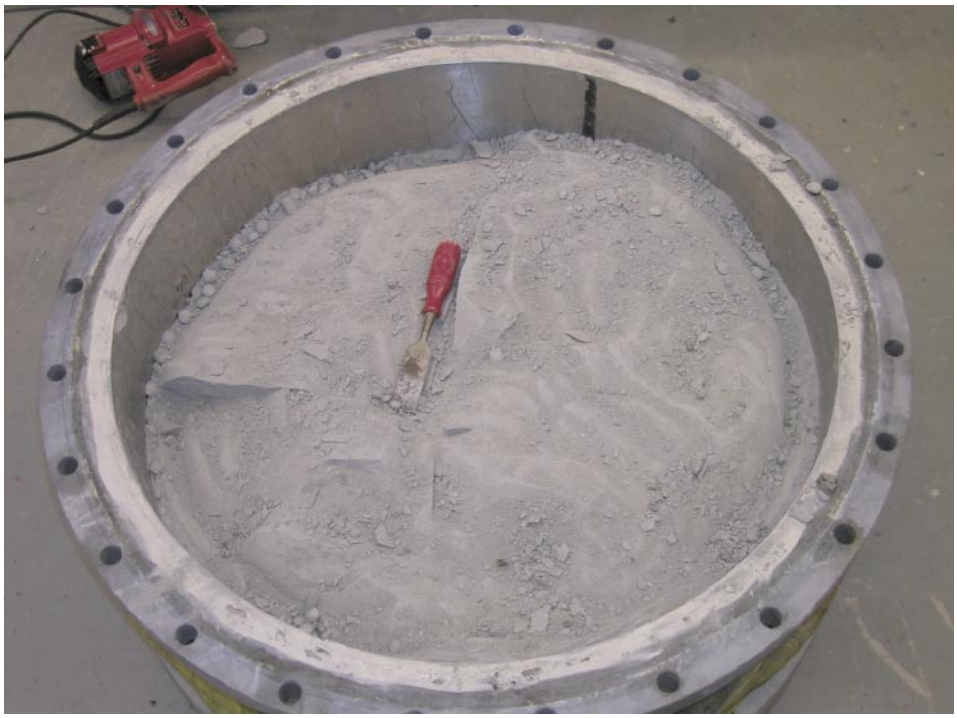

Figure BB5-2. *Picture showing the sample during the excavation. The pellet is still dry after excavation of half the block.*

Table BB5-1. Results of sampling after dismantling test BB5.

Sampling in Test 5.
Sampling only in the pellet filled slot.

Low pressure side

	mb g	m+mb g	ms+mb g	w %
Top	0.850	12.410	10.930	14.7
Bottom	0.840	18.180	13.480	37.2
Left	0.820	17.980	16.060	12.6
Right	0.860	20.900	18.760	12.0

100 mm down from low pressure side

	mb g	m+mb g	ms+mb g	w %
Top	0.810	28.230	25.330	11.8
Bottom	0.870	19.530	16.360	20.5
Left	0.840	22.370	20.000	12.4
Right	0.840	22.950	20.180	14.3

High pressure side, 20-50 mm from perforated sheet

	mb g	m+mb g	ms+mb g	w %
Top	0.850	21.460	16.750	29.6
Bottom	0.840	20.630	14.640	43.4
Left	0.820	16.970	12.470	38.6
Right	0.810	28.620	20.940	38.2
Middle	0.800	33.010	26.300	26.3

Test BB6 (measurement of load)

The large scale tests show that the sealing seems to work for the reference case if a supporting ring that does not need to be water tight at the rock surface is used. In order to study the problem with the pressure on the distance block in large scale two tests with measurement of forces against the supporting ring were performed (BB6 and BB7).

These tests correspond to test series II of the scale tests. The scale tests showed that in spite of the existence of a deliberate slot between the distance block and the container the pressure from the water inside the distance block acted on a ring at the rock surface reaching radially only about 5 cm from the rock surface.

A special frame was constructed in which four load cells were mounted, see Figure BB6-1. The lid was mounted outside the steel ring and fixed with bars and the load cells mounted on the lid.

Water was filled up with a constant flow of 0.006 l/min. The theoretical time to fill the pore volume with this flow was about 10 days. After 9 days the system was filled and a pressure ramp of 100 kPa/h applied. Internal piping occured at three different occasions: at 480, at 950 and at 1,300 kPa. At these internal pipings there was a total leakage of about 1 dl. At the fourth pressure ramp the sample could withstand 2 MPa. This pressure was applied for about 48 hours.

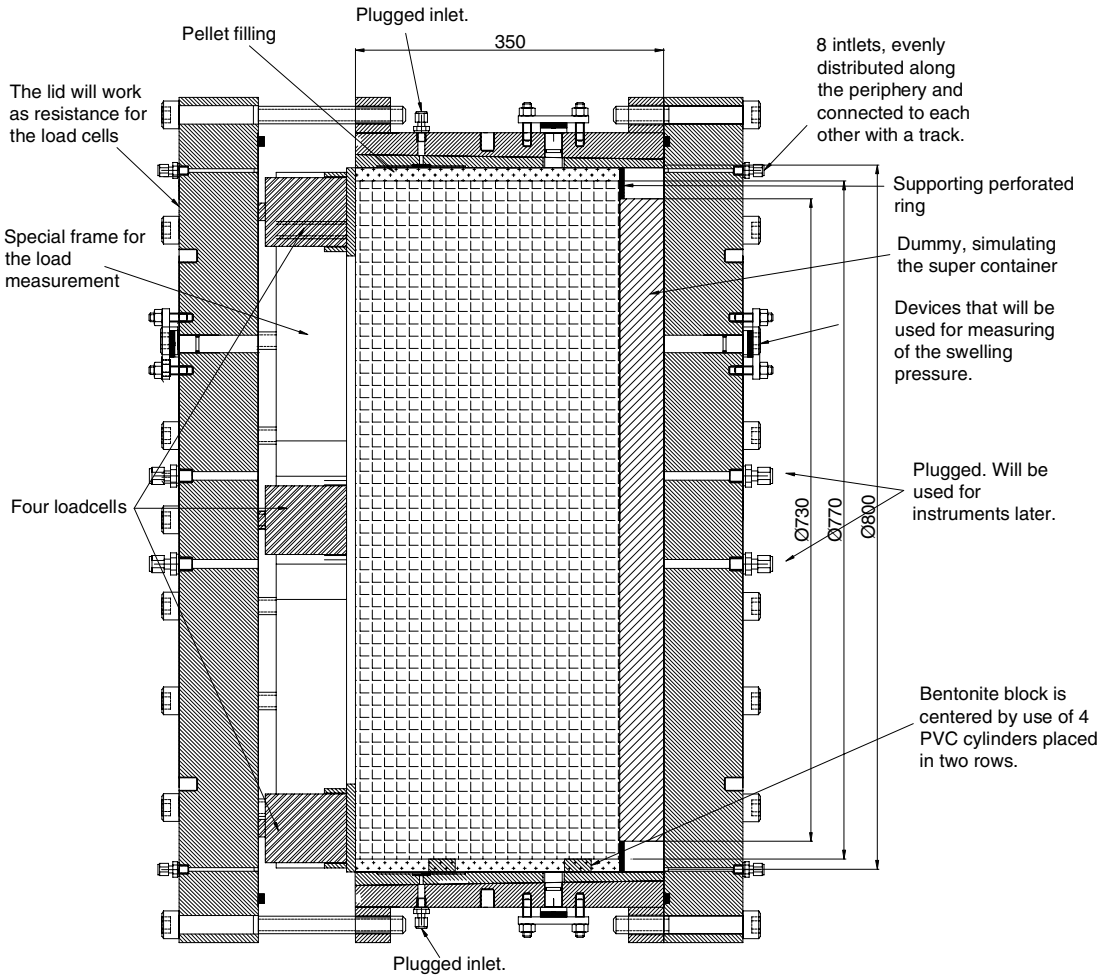

Figure BB6-1. *Layout of sealing test BB6. Dimensions in mm.*

The history plots of applied water pressure and the total volume of inflow water is shown in Figure BB6-2 while the forces measured by the four force transducers are shown in Figure BB6-3. Test BB7 was intended to be identical to BB6 with the only difference that the distance block was larger, without pellets and the gap only in average 2 mm. The results were similar, showing that the water pressure 2,000 kPa could be resisted without piping. Unfortunately water penetrated behind the dummy container and the back lid at the water pressure 1,200 kPa so the test had to be interrupted. The test was continued after removal of the force transducers.

The results of the sampling after dismantling are shown in Table BB6-1.

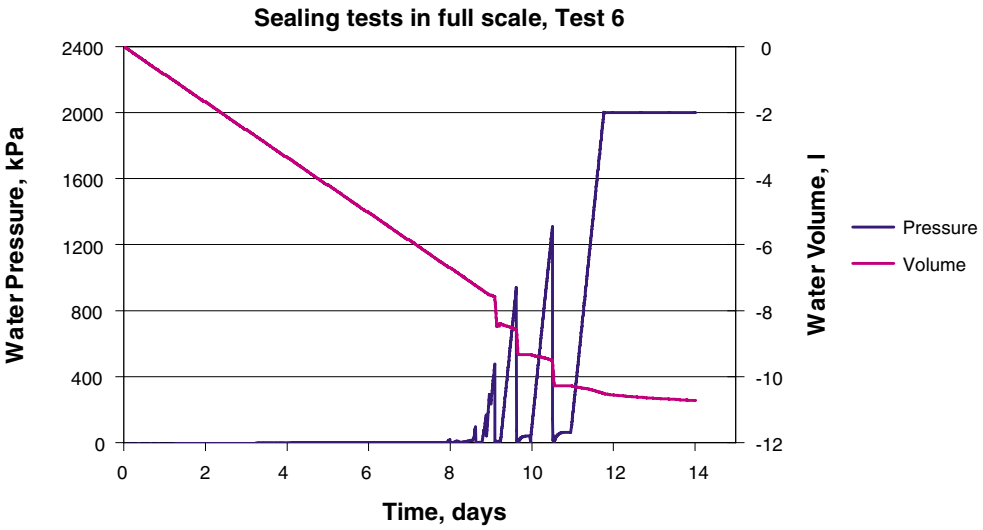

Figure BB6-2. *Water pressure increase and inflow volume as a function of time for BB6.*

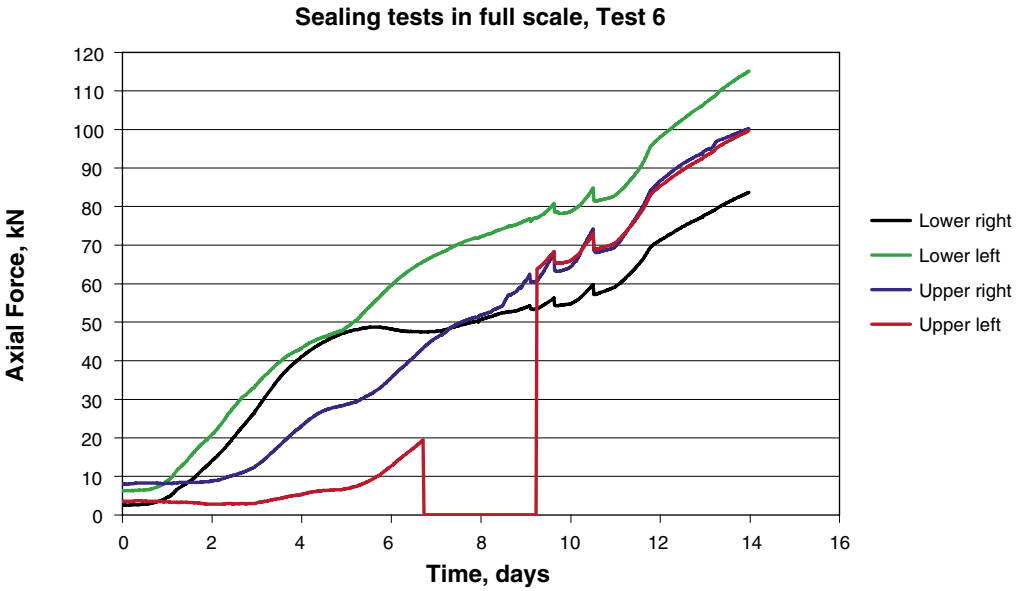

Figure BB6-3. *Diagram showing the axial force as a function of time for BB6.*

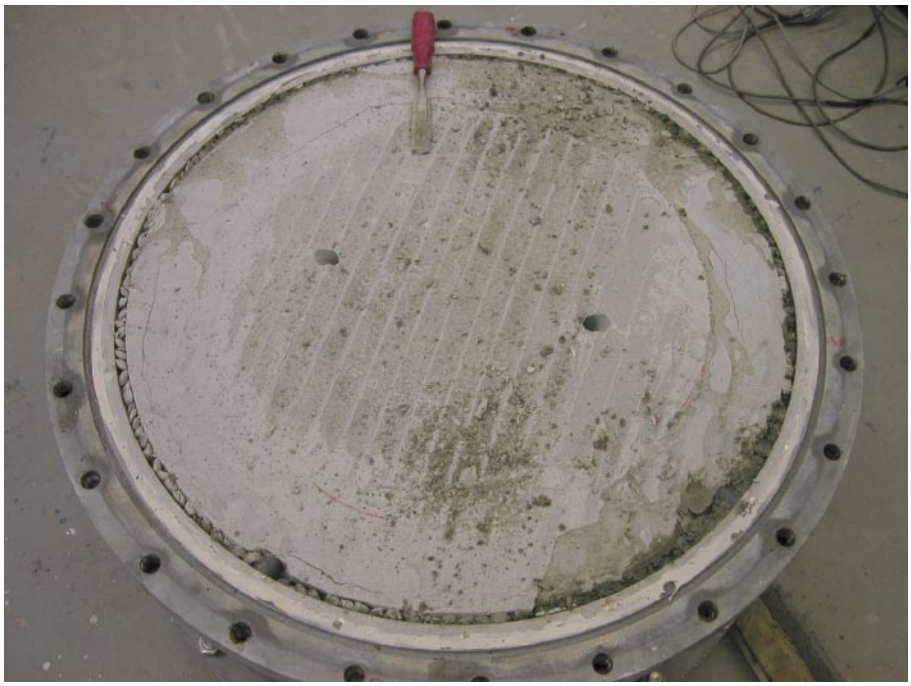

Figure BB6-4. *Picture from dismantling of the test. The loadcells and the frame have been removed. The tool shows the upper direction. The pellets on the right side are dark (wet).*

Table BB6-1. Results of sampling after dismantling test BB6.

Sampling in Test 6.
Sampling only in the pellet filled slot.

Low pressure side

	mb g	m+mb g	ms+mb g	w %
Bottom	0.800	16.760	12.780	33.2

100 mm down from low pressure side

	mb g	m+mb g	ms+mb g	w %
Top	0.800	18.360	14.220	30.8
Bottom	0.830	13.880	11.400	23.5
Left	0.830	16.760	13.890	22.0
Right	0.840	11.540	9.220	27.7

200 mm down from low pressure side

	mb g	m+mb g	ms+mb g	w %
Top	0.830	26.350	22.130	19.8
Bottom	0.830	22.790	19.870	15.3
Left	0.820	12.280	9.630	30.1
Right	0.820	11.270	9.440	21.2

High pressure side, 0-20 mm from perforated sheet

	mb g	m+mb g	ms+mb g	w %
Top	0.870	16.440	10.900	55.2
Bottom	0.860	14.190	8.900	65.8
Left	0.840	18.150	12.770	45.1
Right	0.850	26.400	18.370	45.8

Test BB7

Test BB7 was intended to be identical to BB6 with the only difference that the distance block was larger, without pellets and the gap only in average 2 mm. The test was also a repetition of BB3, completed with the PVC dummy and measurement of the axial force. The test set-up is shown in Figure BB7-1.

Water was filled up with a constant flow of 0.0048 l/min, see Figure BB7-2. The theoretical time to fill the empty space with this flow was about 10 days. After about 8 days is the system was filled and the water pressure increased (still running with constant flow). Internal piping occured at about 1,100 kPa. A new pressure ramp was with 100 kPa/h was applied starting at 800 kPa. After a number of internal pipings, suddenly the axial force starts to increase very fast. The explanation for this was that water had leaked in between the PVC dummy and the lid, which was discovered after interruption of the test. The dummy was bolted to the lid and sealed of with a rubber gasket. The construction was not strong enough and the water pressure could act on the whole area. Depending on the limited range of the load cells it was necessary to dismount the load cells and the frame. When this was done, a new pressure ramp was applied. The sample could stand 2 MPa and this pressure was kept for about 6 days.

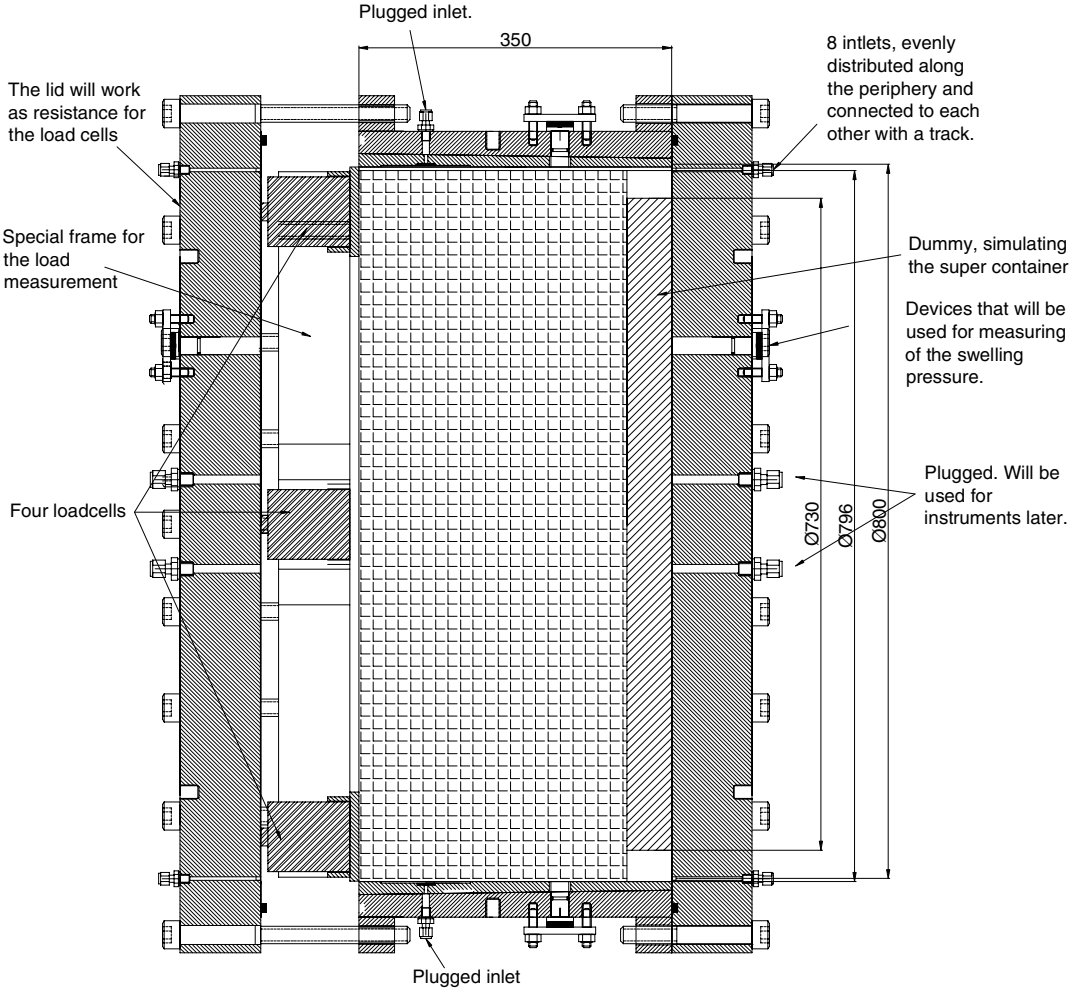

Figure BB7-1. *Layout of sealing test BB7. Dimensions in mm.*

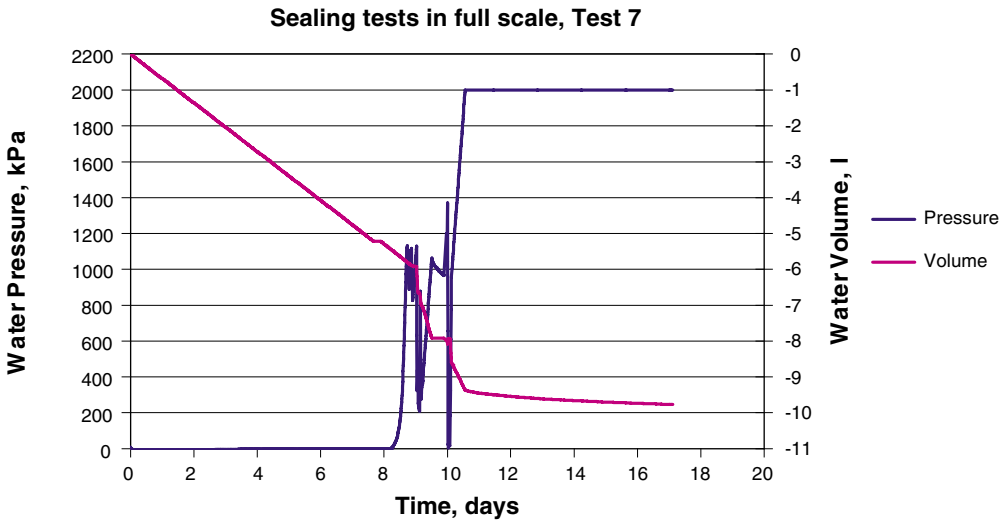

Figure BB7-2. *Water pressure increase and inflow volume as a function of time for BB7.*

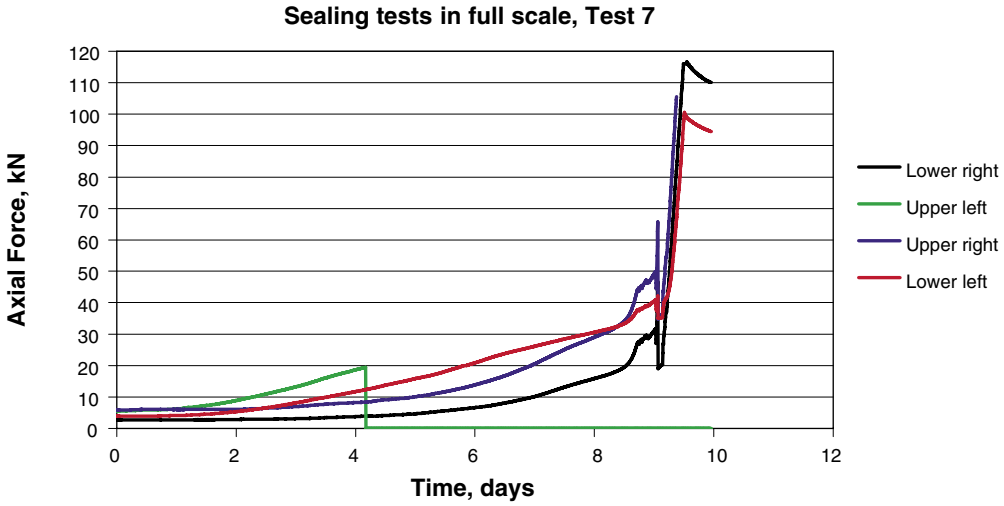

Figure BB7-3. *Diagram showing the axial force as a function of time for BB7.*

Figure BB7-4. *Picture showing the PVC dummy and the slot which at excavation was filled with bentonite. As shown only a very small part of the bentonite block took part in the sealing. About 5 cm radial from the edge of the dummy the bentonite is dry.*

Figure BB7-5. *Picture from the dismantling and excavation. Half the block is removed. Everything is dry.*

Table BB7-1. Results of sampling after dismantling test BB7.

Sampling in Test 7.
Sampling only in the slot and in the nearest parts.
The block is dry except for a small part near the slot.
The slot is completely filled with gel.

Sample	mb g	m+mb g	ms+mb g	w %
Up, 5cm from edge of PVC dummy	0.790	27.480	24.980	10.3
Up, 2cm from edge of PVC dummy	0.790	49.450	40.190	23.5
Up, upper part of slot	0.810	31.430	20.560	55.0
Up, lower part of slot	0.810	11.700	3.720	274.2
Down, upper part of slot	0.800	19.840	9.760	112.5
Down, lower part of slot	0.800	16.110	4.190	351.6
Right, upper part of slot	0.800	18.540	9.630	100.9
Right, lower part of slot	0.810	18.650	3.630	532.6
Left, upper part of slot	0.810	26.040	15.520	71.5
Left, lower part of slot	0.820	23.700	6.180	326.9

The results were similar, showing that the water pressure 2,000 kPa could be resisted without piping. Unfortunately water penetrated behind the dummy container and the back lid at the water pressure 1,200 kPa so the test had to be interrupted. The test was continued after removal of the force transducers.

Appendix 7

Forces on the distance block

The following forces are acting axially on the distance block:

1) Driving force from the water pressure (u) inside the distance block acting on a ring-shaped surface of the distance block between the rock surface and the radial distance δ from the rock surface (see Figure 1):

$$\mathrm{F1} = \left[\pi\left(\frac{D}{2}\right)^2 - \pi\left(\frac{D-2\delta}{2}\right)^2\right]u \tag{1}$$

2) Resistance force from the weight of the distance block (from friction):

$$\mathrm{F2} = \pi\left(\frac{D}{2}\right)^2 \rho g l \tan\phi \tag{2}$$

3) Resistance from the friction between the distance block (having the swelling pressure s acting on the rock surface) and the rock surface:

$$\mathrm{F3} = s\pi D \tan\phi \tag{3}$$

4) The force taken by the supporting ring:

F4

Force equilibrium:

$$\mathrm{F1} - \mathrm{F2} = \mathrm{F3} + \mathrm{F4} \tag{4}$$

Yields if no supporting ring is used ($F4 = 0$)

$$\left[\pi\left(\frac{D}{2}\right)^2 - \pi\left(\frac{D-2\delta}{2}\right)^2\right]u - \pi\left(\frac{D}{2}\right)^2 \rho g l \tan\phi = s\pi D l \tan\phi \tag{5}$$

which yields

$$\left[\frac{D}{4} - \frac{(D-2\delta)^2}{4D}\right]u - \frac{D}{4}\rho g l \tan\phi = s l \tan\phi \tag{6}$$

which yields

$$s = \frac{u}{l\tan\phi}\delta\left(1 - \frac{\delta}{D}\right) - \rho g \frac{D}{4} \tag{7}$$

where

s = required radial swelling pressure between the distance plug and the tunnel rock surface (kPa)
u = water pressure (kPa)
l = plug length (1.5 m)

φ = friction angle between rock and buffer (20º)
δ = radial distance from rock surface of increased water pressure (m)
D = tunnel diameter (1.85 m)
ρ = density of distance block (2.0 g/cm^3)
g = acceleration of gravity (9.81 m/s^2)

Figure A7-1 shows the required swelling pressure as a function of δ (radial distance from rock surface of increased water pressure) at three different water pressures. The swelling pressure is assumed to act on the entire surface and length of the distance block.

However, the tests accounted for in Chapter 7 show that the resistance from the swelling pressure and friction may be very small and if *F2* and *F3* are neglected the entire force *F1* needs to be taken by the supporting ring.

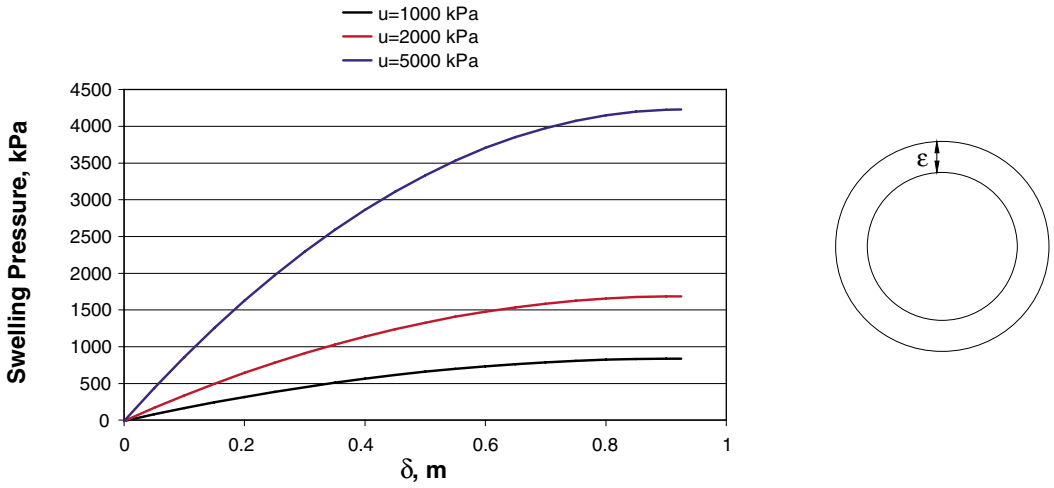

Figure A7-1. *Required swelling pressure from the distance plug on the rock for avoiding displacements at different water pressure.*